

**Development and Application of Methods for Sensitive and Specific Detection
of SARS-CoV-2 and Variants in Clinical and Environmental Samples**

by

Teresa Kumblathan

A thesis submitted in partial fulfillment of the requirements for the degree of

Doctor of Philosophy

in

Analytical and Environmental Toxicology

Department of Laboratory Medicine and Pathology
University of Alberta

© Teresa Kumblathan, 2024

Abstract

The COVID-19 pandemic, caused by SARS-CoV-2, had far-reaching global health consequences, with the virus spreading rapidly via respiratory droplets and aerosols. Accurate and timely diagnostic testing became critical for guiding public health policies and preventing the spread of infections. The standard clinical testing of SARS-CoV-2 RNA involves nasopharyngeal swabs (NPS) sample collection and reverse transcription quantitative polymerase chain reaction (RT-qPCR) detection. Clinical testing for public health surveillance quickly became overwhelmed due to constraints on available diagnostic supplies and human resources. Therefore, testing became restricted to specific patients. To complement standard clinical testing and alleviate some of these testing constraints, I designed and developed alternative approaches.

SARS-CoV-2 is present in oral fluids, but viral detection has proven challenging due to the heterogenous and viscous matrix of these fluids, which hinders subsequent analysis, and the limited resources pose obstacles for large-scale community biomonitoring. This led to my first proposed project with my colleagues as part of the pandemic preparedness team to develop new sampling and testing methods for monitoring SARS-CoV-2 in oral fluids. To achieve sensitive and reliable analysis of viral RNA in oral fluids, I integrated viral inactivation, RNA release and preservation, and subsequent direct detection of SARS-CoV-2 on magnetic beads. The unique formulation of the viral inactivation and RNA preservation (VIP) buffer enabled patients to self-collect samples, minimizing the need for healthcare professionals and transmission of infection. The VIP buffer also enabled sample stability for at least 3 weeks. This method offered a limit of detection of 25 RNA copies per 200 μ L of sample and 9-111x higher sensitivity than the Centers for Disease Control and Prevention recommended kit. This new integrated method successfully analyzed more than 200 patient samples and was also used for pooled sample analysis.

Due to the overwhelming strain on clinical testing resources, wastewater surveillance (WS) was promoted as an alternative for community biomonitoring of SARS-CoV-2 because viral particles were proven to enter wastewater via stools of infected patients. My comprehensive literature evaluation on SARS-CoV-2 WS highlighted challenges such as complex matrices, lack of standardized procedures, and poor and irreproducible recoveries. To overcome these challenges and address my second objective of implementing WS to complement clinical testing, I developed a robust method for highly sensitive wastewater detection of SARS-CoV-2. Viral particles and free RNA were captured from both phases of wastewater using an electronegative membrane (EM), followed by incubation in the VIP-Mag buffers, and direct RT-qPCR detection. My method's capability of detecting trace and diverse concentrations of SARS-CoV-2 in wastewater is attributed to the enhanced recovery (80%) and efficient removal of PCR inhibitors. I analyzed 120 wastewater samples and consistently detected higher levels of RNA than the provincial reference lab.

To expand the capacity of detecting the rapidly evolving SARS-CoV-2 variants, I proposed my third objective to develop multiplex RT-qPCR assays for the early detection VOCs in wastewater. To address this objective, I developed three multiplex assays using naturally selected mutations capable of differentiating Alpha, Beta, Delta, and Omicron sub-variants. These assays have excellent efficiencies (90–104%) for all targets and LODs of 4-28 RNA copies per reaction. Analysis of 294 wastewater samples revealed that the trends of Alpha, Beta, Gamma, Delta, and Omicron sub-variants aligned with clinical trends, and suggested early wastewater detection of certain variants prior to reported clinical cases.

Finally, to establish a universal platform for the detection of various co-circulating viruses, my fourth objective was to demonstrate that my WS protocol can be easily adapted for

other viruses. To address this objective, I used the enveloped Omicron and the non-enveloped Norovirus (NoV) as examples of structurally different, but clinically significant viruses. My WS protocol successfully quantified NoV (genotypes I and II) and Omicron subvariants in the same sets of 94 wastewater samples with high recovery (72% and 80%, respectively). The results showed seasonal trends of NoV and Omicron variants in the same wastewater systems which matched clinical trends and revealed an inverse relationship between the presence of these viruses.

Overall, my methods and strategies highlight the importance of robust platforms for clinical testing and community surveillance of enveloped and non-enveloped viruses. These techniques demonstrate the adaptability of platforms for future biomonitoring of community infections such as COVID-19, and beyond.

Preface

This thesis is an original work by Teresa Kumblathan. The research project, of which this thesis is a part, received research ethics approval from the University of Alberta Research Ethics Board, project name “Saliva and gargle test for COVID-19”, No. Pro00117059, April 1 2020, and project name “CL3 Viral Infectivity Models”, No. UAP3885, June 1 2020.

Parts of Chapter 1 of this thesis have been reprinted from *Trends in Anal. Chem.*, 117107, Liu Y, Kumblathan T, Tao J, Xu J, Feng W, Xiao H, Hu J, Huang C, Wu Y, Zhang H, Li XF, Le XC, Recent advances in RNA sample preparation techniques for the detection of SARS-CoV-2 in saliva and gargle, Copyright 2023, with permission from Elsevier. Liu Y wrote the primary manuscript. I helped draft, revise, and edit all parts of the primary manuscript. Tao J, Xu J, Feng W, Xiao H, Hu J, Huang C, Wu Y, Zhang H, Li XF, and Le XC contributed to editing the manuscript.

Parts of Chapter 1 of this thesis have also been published as Kumblathan T, Liu Y, Uppal GK, Hrudey SE, Li XF. Wastewater-based epidemiology for community monitoring of SARS-CoV-2: progress and challenges. *ACS Environ. Au.* **2021**, 1(1), 18-31. Accessed on 21 Nov 2023 from: <https://doi.org/10.1021/acsenvironau.1c00015>. I drafted, revised, and edited all sections of the primary manuscript. I also made all the tables and figures. Liu Y and Uppal GK helped with drafting of the primary manuscript. Hrudey SE and Li XF contributed to editing the manuscript. Copyright 2021 American Chemical Society (ACS). Further copyright permissions requests are to be directed to ACS.

Chapter 2 of this thesis has been published as Liu Y, Kumblathan T, Feng W, Pang B, Tao J, Xu J, Xiao H, Joyce MA, Tyrrell DL, Zhang H, Li XF. On-site viral inactivation and RNA preservation of gargle and saliva samples combined with direct analysis of SARS-CoV-2 RNA

on magnetic beads. *ACS Meas. Sci. Au.* **2022**, 2 (3), 224-32. Accessed on 21 Nov 2023 from: <https://doi.org/10.1021/acsmesuresciau.1c00057>. I conceptualized experimental design, performed the experiments, data collection and analysis, text, and schematic composition, and revised the overall manuscript. Liu Y and I contributed equally. Feng W, Pang B, Tao J, Xu J, Xiao H, Joyce MA, Tyrrell DL, Zhang H, and Li XF contributed to editing the manuscript. Copyright 2022 ACS. Further copyright permissions requests are to be directed to ACS.

Chapter 3 of this thesis has been reprinted from *J. Environ. Sci.*, 130, Kumblathan T, Liu Y, Qiu Y, Pang L, Hrudehy SE, Le XC, Li XF, An efficient method to enhance recovery and detection of SARS-CoV-2 RNA in wastewater, Copyright 2023, with permission from Elsevier. I conceptualized experimental design, performed the experiments, data collection and analysis, text and schematic composition, and revisions of the overall manuscript. Liu Y contributed to experimental design and manuscript revisions. Qiu Y, Pang L, Hrudehy SE, Le XC, and Li XF contributed to editing the manuscript.

Parts of Chapter 4 of this thesis have been published as Liu Y, Kumblathan T, Joyce MA, Tyrrell DL, Tipples G, Pang X, Li XF, Le XC. Multiplex Assays Enable Simultaneous Detection and Identification of SARS-CoV-2 Variants of Concern in Clinical and Wastewater Samples. *ACS Meas. Sci. Au.* **2023**, 3 (4), 258–268. Accessed on 21 Nov 2023 from: <https://doi.org/10.1021/acsmesuresciau.3c00005>. Liu Y conceptualized experimental design, performed the multiplex optimization and clinical experiments, data collection and analysis, text, and schematic composition, and revised the primary manuscript. I performed the multiplex optimization and wastewater experiments, data collection and analysis, and helped revise the primary manuscript. Joyce MA, Tyrrell DL, Tipples G, Pang X, Li XF, and Le XC contributed to

editing the manuscript. Copyright 2023 ACS. Further copyright permissions requests are to be directed to ACS.

Parts of Chapter 4 of this thesis have also been published as from Kumblathan T, Liu Y, Pang X, Hrudey SE, Le XC, Li XF. Quantification and Differentiation of SARS-CoV-2 Variants in Wastewater for Surveillance. *Environ. Health*. **2023**, 1 (3), 203-213. Accessed on 21 Nov 2023 from: <https://doi.org/10.1021/envhealth.3c00089>. I conceptualized experimental design, performed the experiments, data collection and analysis, text and schematic composition, and revised the overall manuscript. Liu Y contributed to experimental design and manuscript revisions. Pang X, Hrudey SE, Le XC, and Li XF contributed to editing the manuscript. Copyright 2023 ACS. Further copyright permissions requests are to be directed to ACS.

Chapter 5 of this thesis has been reprinted from *Sci. Total Environ.*, 920, Kumblathan T, Liu Y, Crisol M, Pang XL, Hrudey SE, Le XC, Li XF. Enhanced Quantification of Noroviruses and Omicron Subvariants in Wastewater Revealing the Co-Circulating Viral Trends, Copyright 2024, with permission from Elsevier. I conceptualized experimental design, performed the experiments, data collection and analysis, text and schematic composition, and revised the overall manuscript. Liu Y contributed to experimental design and manuscript revisions. Crisol M contributed to some multiplex optimization experiments. Pang XL, Hrudey SE, Le XC, and Li XF contributed to editing the manuscript.

Acknowledgements

I would like to express my sincere gratitude to my supervisor, Dr. Xing-Fang Li, for all the support, guidance, and faith in me from the very beginning and in my future.

Thank you to my supervisory committee members, Dr. Hongquan Zhang and Dr. Andrei Drabovich, as well as Dr. Chris Le for all the helpful suggestions and encouragement throughout my graduate program. I would also like to thank Dr. Yanming Liu for all the invaluable technical advice. Special thanks to Dr. Lorne Tyrrell, Dr. Michael Joyce, Dr. Lilly Pang, and Dr. Judy Qiu for all the collaborative support which made my research projects possible.

I am also very grateful to Dr. Jelena Holovati, Ms. Lisa Purdy, Ms. Kristi Lew, and Dr. Monika Keelan for all the words of wisdom and warmth during all the ups and downs of grad school! You all have been such an inspiration for me since I started the MLS program as an undergraduate student. I would also like to thank Ms. Katerina Carastathis and Ms. Cheryl Titus for all the administrative and personal support! To all the AET and LMP students who I have had the pleasure of making many memories with, thank you for making grad school fun. Thank you especially to Caley, Kristin, Nic, Yasmine, Tetiana, Camille, Di, and Jenny!

My success and completion of my PhD would not have been possible without the support of my parents, Paul and Alka. Appa and Amma, thank you for all the love and prayers throughout my academic career. Thank you to my husband, Nelson, for being my companion and encouraging me to shoot for the stars! A special hug for my dearest friends, Jicelle and Natsumi, for always being a ray of sunshine on the hard days and unconditionally being there for me!

Lastly, I am grateful to all the funding agencies mentioned in the research chapters for supporting my work.

Table of Contents

Chapter One: Introduction to Challenges of SARS-CoV-2 Clinical Testing and Alternative Solutions	1
1.1 Impact of COVID-19 Pandemic on Public Health	2
1.2 Basics to Understanding Virology	2
1.3 Severe Acute Respiratory Syndrome Coronavirus 2 (SARS-CoV-2)	3
1.4 SARS-CoV-2 Diagnostic Biomarkers	6
1.5 Sample Collection, Viral Inactivation, and RNA Extraction	8
1.6 Detection of Viral RNA Using Reverse Transcriptase Quantitative Polymerase Chain Reaction (RT-qPCR)	10
1.7 Challenges with Standard Clinical Testing of SARS-CoV-2	12
1.8 Alternative Approaches to the Standard Clinical Testing Standard of SARS-CoV-2	15
1.8.1 Oral Fluid Testing for SARS-CoV-2	15
1.8.2 Wastewater Testing for SARS-CoV-2	19
1.9 Rationale and Scope of Thesis	23
1.10 References	25
Chapter Two: Development of a Method for the Detection of SARS-CoV-2 in Saliva and Gargle Samples	44
2.1 Introduction	45
2.2 Experimental	51
2.2.1 Sample Collection	51
2.2.2 VIP Buffer Preparation	52
2.2.3 Mag Beads Buffer Preparation and Sample Processing	53
2.2.4 Pooled Oral Fluids Preparation	54
2.2.5 Spiking of Saliva and Gargle Samples with Pseudo-Virus	54
2.2.6 RT-qPCR Detection of Concentrated RNA Directly from Magnetic Beads	55
2.3 Results and Discussion	55
2.3.1 Development of a VIP Buffer for the Self-Collection of Gargle and Saliva Samples	55
2.3.2 Concentration of Viral RNA onto Magnetic Beads and Direct RT-qPCR Detection	58
2.3.3 Recovery of Viral RNA from Gargle and Saliva Samples	62
2.3.4 Stability and Preservation of Viral RNA in the VIP Buffer	63
2.3.5 Sensitivity and Reproducibility of the VIP-Mag-RT-qPCR Method	66
2.3.6 Comparison of Tap Water and Saline Used for Collecting Gargle Samples	67

2.3.7 Comparison of the VIP-Mag Method with the CDC-Recommended Kit	68
2.3.8 Detection of SARS-CoV-2 in Patients' Gargle and Saliva Samples Collected from the Onset of Clinical Symptoms through Recovery	70
2.3.9 Application of the VIP-Mag-RT-qPCR Method to the Analysis of Pooled Samples	75
2.4 Conclusion	76
2.5 References	78
Chapter Three: Development of a Method for Enhanced Wastewater Surveillance of SARS-CoV-2 in the Community	84
3.1 Introduction	85
3.2 Experimental	91
3.2.1 Wastewater Sample Collection	91
3.2.2 Capture of SARS-CoV-2 from Wastewater Samples	91
3.2.3 Extraction of RNA from Wastewater Samples using the VIP Buffer and Concentration onto Magnetic Beads Followed by Direct RT-qPCR Detection	92
3.2.4 Determination of Wastewater Recovery	93
3.2.5 Statistical Analysis	94
3.3 Results and Discussion	94
3.3.1 Development of an EM-VIP-Mag-RT-qPCR Method for Enhanced Detection of SARS-CoV-2 in Wastewater	94
3.3.2 VIP-Mag-RT-qPCR for Efficient Removal of RT-qPCR Inhibitors and Ultra-Sensitive In-Situ Amplification on Beads	100
3.3.3 Improved RNA Recovery	103
3.3.4 Blind Test of Composite Wastewater Samples with Diverse SARS-CoV-2 RNA Concentrations	105
3.3.5 Detection of SARS-CoV-2 in 120 Wastewater Samples Using EM-VIP-Mag-RT-qPCR and Comparison with APL Reference Lab	107
3.4 Conclusion	110
3.5 References	111
Chapter Four: Multiplex RT-qPCR Assays for the Early Detection of Variants of Concern (VOCs) in Wastewater	121
4.1 Introduction	122
4.2 Experimental	126
4.2.1 Wastewater Sample Collection	126

4.2.2 SARS-CoV-2 RNA Used for the Development and Validation of Multiplex RT-qPCR Assays	126
4.2.3 Wastewater Viral Particle Concentration and RNA Extraction Protocol: EM-VIP-Mag	128
4.2.4 Determination of Total SARS-CoV-2 RNA Directly on Magnetic Beads Containing Concentrated Viral RNA via CDC N1 Gene RT-qPCR	128
4.2.5 Singleplex RT-qPCR Assays for the Alpha, Beta, Gamma, and Delta Variants	129
4.2.6 Multiplex RT-qPCR Assays for the Alpha, Beta, and Delta Variants	131
4.2.7 Multiplex RT-qPCR Assays for the Delta Variant	132
4.2.8 Dynamic Range, Efficiency, Analytical Sensitivity, Specificity, and Reproducibility of the ABG and Delta Multiplex RT-qPCR Assays	133
4.2.9 Singleplex RT-qPCR Assays for the Omicron Variants	135
4.2.10 Triplex RT-qPCR Assay for the Omicron Variants	137
4.2.11 Dynamic Range, Efficiency, Analytical Sensitivity, and Validation of the Omicron Triplex Assay	138
4.2.12 Application of the ABG, Delta, and Omicron Multiplex RT-qPCR Assays for Monitoring SARS-CoV-2 Variants of Concern in Wastewater Samples	140
4.2.13 Application of the ABG and Delta Multiplex RT-qPCR Assays for Investigating Distribution of Variants in Mouse Tissues	141
4.3 Results and Discussion	145
4.3.1 Development and Assessment of ABG and Delta Multiplex Assays	145
4.3.2 Wastewater Surveillance using ABG Multiplex Assay	149
4.3.3 Wastewater Surveillance using Delta Multiplex Assay	151
4.3.4 Development and Assessment of Omicron Multiplex Assay	152
4.3.5 Wastewater Surveillance using Omicron Triplex Assay	156
4.3.6 Application of Multiplex Assays for Investigating Distribution of Variants in Mouse Tissues	162
4.4 Conclusion	165
4.5 References	167
Chapter Five: Advances in Wastewater Analysis Revealing the Co-Circulating Viral Trends of Noroviruses and Omicron Subvariants	173
5.1 Introduction	174

5.2 Experimental	177
5.2.1 Wastewater Collection from Two Wastewater Treatment Plants from July 2022 - June 2023	177
5.2.2 Simultaneous Concentration, Extraction, and Preservation of RNA of Structurally Different Viruses	177
5.2.3 Determination of the Recovery of Norovirus from Wastewater using a Surrogate (Murine Norovirus)	178
5.2.4 Norovirus GI and GII Primer, Probe, and Target Sequence Design	180
5.2.5 Norovirus GI and GII Singleplex RT-qPCR Assay Optimization	181
5.2.6 Norovirus GI and GII Multiplex RT-qPCR Optimization	182
5.2.7 Dynamic Range, Efficiency, Analytical Specificity, Sensitivity, and Reproducibility of NoV Multiplex Assay	182
5.2.8 Application of the Norovirus Multiplex RT-qPCR Assays and Omicron Triplex RT-qPCR Assay for Monitoring Norovirus and Omicron in Wastewater Samples	184
5.2.9 Statistical Analysis	185
5.3 Results and Discussion	185
5.3.1 Simultaneous Capture and Extraction of Norovirus and Omicron from Wastewater Samples	185
5.3.2 Development and Assessment of a Multiplex RT-qPCR TaqMan MGB Assay for NoV GI and GII	189
5.3.3 Simultaneous Monitoring of Norovirus and Omicron Subvariants in 94 Wastewater Samples Collected from July 2022 to June 2023	193
5.4 Conclusion	200
5.5 References	202
Chapter Six: Conclusions and Future Perspectives	211
References	220
Bibliography	223

List of Tables

Table 2.1	Comparison of reported methods on inactivation, RNA release and extraction for the detection of SARS-CoV-2 in saliva and gargle samples.	46
Table 2.2	A summary of reported methods that were used to detect SARS-CoV-2 in pooled samples.	47
Table 3.1	Comparison of the concentration, extraction, and detection methods used by various studies for WS of SARS-CoV-2.	87
Table 3.2	SARS-CoV-2 RNA copies in the aqueous and solid phase of wastewater samples analyzed separately	98
Table 3.3	5x dilutions of specific bi-monthly wastewater samples to monitor for sufficient removal of RT-qPCR inhibitors	102
Table 4.1	Global Initiative on Sharing All Influenza Data (GISAID) accession numbers for the sequence of the clinical nasopharyngeal specimens used to extract Alpha, Beta, Gamma, Delta, and Omicron (BA.1, BA.2, BA.4, BQ1.1 (derivative of BA.5), and XBB.1) RNA	127
Table 4.2	Primer and probe combinations developed for the detection and discrimination of SARS-CoV-2 variants of concern	130
Table 4.3	Optimal RT-qPCR conditions for singleplex and multiplex assays for the detection of five targets: HV69-70 deletion, and K417N, K417T, T478K and P681R mutations	131
Table 4.4	Primer and probe combinations developed for the detection and discrimination of SARS-CoV-2 Omicron subvariants	137
Table 4.5	Optimal RT-qPCR conditions for the singleplex and Omicron triplex assays for the detection of three targets: HV 69-70 deletion, K417N, and L452R mutations.	138
Table 4.6	Primer and probe combinations developed for the detection of SARS-CoV-2 WT	142
Table 4.7	Performance comparison between singleplex and multiplex RT-qPCR assays for the five targets	146
Table 4.8	RT-qPCR efficiencies and LOD of ABG assay and Delta assay for the detection of SARS-CoV-2 variants of concern	146
Table 4.9	Analytical sensitivity of the ABG and Delta multiplex RT-qPCR assay for the detection of the Alpha, Beta, Gamma, and Delta variants of SARS-CoV-2.	148
Table 4.10	Performance comparison between singleplex and Omicron triplex RT-qPCR assays for the three Omicron assay targets.	153
Table 4.11	Analytical sensitivity of the Omicron triplex RT-qPCR assay for the detection of the Omicron BA.4.	154
Table 4.12	Validation of the Omicron Triplex RT-qPCR assay by examining the RNA of Omicron subvariants extracted from passaged isolates of clinical nasopharyngeal swab samples	155
Table 5.1	Sequences of primers and probes designed to detect NoV GI and GII.	181

Table 5.2	Optimized NoV GI and GII singleplex RT-qPCR conditions and NoV multiplex RT-qPCR conditions.	190
Table 5.3	Performance comparison of singleplex assay versus multiplex assay for NoV GI and GII.	191
Table 5.4	Validation of the NoV multiplex RT-qPCR assay by examining the RNA of Norovirus genogroups (GI and GII) isolated from clinical stool samples.	192
Table 5.5	Analytical sensitivity of the NoV multiplex RT-qPCR assay for the detection of NoV GI and GII.	193

List of Figures

Figure 1.1	Genome organization of SARS-CoV-2 and the relative positions of gene targets	4
Figure 1.2	Schematic of SARS-CoV-2 life cycle inside a host cell	5
Figure 2.1	The overall oral fluids method	51
Figure 2.2	Detection of SARS-CoV-2 RNA in gargle samples treated with different reagents	57
Figure 2.3	Detection of SARS-CoV-2 RNA in gargle samples treated with glycogen or carrier RNA.	57
Figure 2.4	Detection of SARS-CoV-2 RNA in saliva and gargle samples treated with either freshly prepared VIP buffer or the VIP buffer stored at room temperature for six months	58
Figure 2.5	Detection of SARS-CoV-2 RNA in the absence or the presence of commercial beads	60
Figure 2.6	Comparison of different concentrations of PEG 8000 in the beads-binding buffer for concentrating viral SARS-CoV-2 RNA.	61
Figure 2.7	Detection of 65, 390, or 3900 copies of SARS-CoV-2 RNA in saliva and gargle samples using the VIP-Mag-RT-qPCR method	62
Figure 2.8	Recovery of viral RNA from RNase-free water and pooled gargle samples	63
Figure 2.9	Evaluation of SARS-CoV-2 RNA stability	65
Figure 2.10	Determination of the sensitivity of the VIP-Mag-RT-qPCR method	66
Figure 2.11	Detection of SARS-CoV-2 RNA in tap water gargle and saline gargle samples	68
Figure 2.12	Comparison of the VIP-Mag method to the standard QIAamp Viral RNA Mini Kit	70
Figure 2.13	Standard curve from the RT-qPCR analysis of the N1 gene segment (CDC)	71
Figure 2.14	Monitoring SARS-CoV-2 RNA levels in saliva and gargle samples collected by a NPS-confirmed SARS-CoV-2 positive patient	72
Figure 2.15	Monitoring SARS-CoV-2 RNA levels in saliva and gargle samples collected by the second NPS-confirmed SARS-CoV-2 positive patient	73
Figure 2.16	SARS-CoV-2 RNA levels in saliva samples collected four times a day for five days.	74
Figure 2.17	SARS-CoV-2 RNA levels in gargle samples collected four times a day for seven days.	74
Figure 2.18	Performance evaluation of the VIP-Mag-RT-qPCR method on pooled samples	76
Figure 3.1	Performance analysis of two electronegative membranes (EMs) in deionized water and negative wastewater spiked with SARS-CoV-2 pseudoviral RNA	96
Figure 3.2	Separate analysis of the aqueous and solid phases of wastewater samples collected from two wastewater treatment plants	97
Figure 3.3	Schematic showing steps of wastewater sample processing and analysis	99
Figure 3.4	Optimization of the previously developed VIP-Mag method for wastewater samples by increasing the wash step	101
Figure 3.5	Monitoring wastewater samples for the presence of RT-qPCR inhibitors	102

Figure 3.6	Recovery of viral RNA from wastewater samples	104
Figure 3.7	Dilution validation study where a previously determined wastewater sample was diluted by a negative wastewater sample by 10, 100, and 1000 times and processed by this study and the reference lab.	106
Figure 3.8	Pearson correlation analysis of results obtained using the EM-VIP-Mag-RT-qPCR method with the results provided by the reference laboratory	107
Figure 3.9	120 wastewater samples analyzed from May 2021 to February 2022	108
Figure 4.1	Standard curves of targets HV69-70 deletion, and K417N and K417T mutation using singleplex RT-qPCR assays and using the ABG multiplex RT-qPCR assay	134
Figure 4.2	Standard curves of targets T478K and P681R using singleplex RT-qPCR assays and using the Delta multiplex RT-qPCR assay	135
Figure 4.3	Standard curves of targets HV69-70 deletion, K417N, and L452R mutation using singleplex RT-qPCR assays and using the Omicron triplex RT-qPCR assay	139
Figure 4.4	Standard curves of target D614D using the singleplex RT-qPCR assay	143
Figure 4.5	Changes in the percentage weight of mice infected with different doses of VOC and routes of infection.	144
Figure 4.6	Detection and monitoring of Alpha, Beta, Gamma, and Delta in wastewater using multiplex RT-qPCR from May 16 th 2021 – January 23 rd 2022	150
Figure 4.7	Detection and monitoring of Omicron sub-lineage in Calgary wastewater using multiplex RT-qPCR from January 25 th 2022 – March 20 th 2023	159
Figure 4.8	Detection and monitoring of Omicron sub-lineage in Edmonton wastewater using multiplex RT-qPCR from January 25 th 2022 – March 20 th 2023	160
Figure 4.9	Overall detection trend of SARS-CoV-2 Variants of Concern in wastewater samples collected from Calgary and Edmonton from May 2021 to March 2023.	161
Figure 4.10	Distribution of VOCs found in different mouse tissues after being infected either oropharyngeally, intranasally, or via transmission from an infected mouse.	164
Figure 5.1	Standard curve of Murine Norovirus	180
Figure 5.2	Standard curves of targets Norovirus GI and GII using singleplex RT-qPCR assays and the multiplex NoV RT-qPCR assay	184
Figure 5.3	Overview of wastewater protocol for Norovirus and Omicron	186
Figure 5.4	Separate analysis of the aqueous and solid phases of ten representative wastewater samples collected from two wastewater treatment plants	188
Figure 5.5	Detection and monitoring of wastewater samples collected from Calgary from July 2022 to June 2023	194
Figure 5.6	Detection and monitoring of wastewater samples collected from Edmonton from July 2022 to June 2023	195

Chapter One: Introduction to Challenges of SARS-CoV-2 Clinical Testing and Alternative Solutions*

*A portion of this chapter has been published and was modified from Liu, Y.; Kumblathan, T.; Tao, J.; Xu, J.; Feng, W.; Xiao, H.; et al. Recent advances in RNA sample preparation techniques for the detection of SARS-CoV-2 in saliva and gargle. *Trends Anal. Chem.* **2023**, 165, 117107. Liu Y wrote the primary manuscript. I helped draft, revise, and edit all parts of the primary manuscript. Tao J, Xu J, Feng W, Xiao H, Hu J, Huang C, Wu Y, Zhang H, Li XF, and Le XC contributed to editing the manuscript.

* A portion of this chapter has been published and was modified from Kumblathan, T.; Liu, Y.; Uppal, G.K.; Hrudey, S.E.; Li, X.F. Wastewater-based epidemiology for community monitoring of SARS-CoV-2: Progress and Challenges. *ACS Environ. Au* **2021**, 1, 18–31. I drafted, revised, and edited all sections of the primary manuscript. I also made all the tables and figures. Liu Y and Uppal GK helped with drafting of the primary manuscript. Hrudey SE and Li XF contributed to editing the manuscript.

1.1 Impact of COVID-19 Pandemic on Public Health

The Coronavirus Disease of 2019 (COVID-19) pandemic resulted in over 774 million cases and 7 million deaths over the last four years.¹ The virus responsible for this pandemic was the Severe Acute Respiratory Syndrome Coronavirus 2 (SARS-CoV-2). The COVID-19 pandemic severely damaged the state of global public health, economies, and societies. This damage was unprecedented and continues as new variants emerge and spread. Some of these variants have demonstrated increased transmissibility, disease severity, immune escape, and have variable response to therapeutics and vaccines.^{2,3,4} During the onset of COVID-19, the public healthcare system faced several burdens on resources to mitigate the impacts of the pandemic and prevent the spread of disease. Therefore, the COVID-19 pandemic highlighted the need for better preparedness and control of disease spread, specifically the need for rapid and accessible methods for the detection of pathogens. To develop improved alternative solutions, the SARS-CoV-2 target along with challenges associated with the gold standard of sample collection and detection will first need to be better understood. I will discuss these aspects in this chapter.

1.2 Basics to Understanding Virology

Viruses are infectious host dependent organisms. In general, viruses rely on the host for biosynthesis, are structurally smaller, infects living things, can have a deoxyribonucleic acid (DNA) or ribonucleic acid (RNA) derived genome, and transmit via viral particles called virions.⁵ DNA and RNA are examples of nucleic acids that carry genetic information for life functions.⁶ This genetic information is packaged inside virions. A virion is the infectious form of the virus and has two main purposes: 1) to protect the viral genome from the environment, and 2) to facilitate entry into the host cell. The main components of a virion are the genome and capsid. Non-enveloped viruses contain these two components. Enveloped viruses have an additional

lipid bilayer membrane that encloses the capsid and genome.⁷ For a virus to infect a host cell, the virion must attach and penetrate the host cell. Once inside, the viral genome is exposed and has access to host cellular components for gene expression and genome replication. The virus then uses the host cell to assemble the new virion. By interacting and using the host cell plasma membrane, the newly synthesized virion is then released and proceeds to infect the next host cell. This viral infection can lead to cellular injury, host immune responses, viral shedding, and transmission. In immunocompetent individuals, the innate and adaptive immunity work together to clear the viral infection, whereas further complications may occur in immunocompromised individuals.⁸

There are currently two classification systems for human viruses: the International Committee for Taxonomy of Viruses (ICTV) and the Baltimore system. The ICTV classifies viruses based on their genome type (DNA vs RNA), nature of genome (single stranded (ss) or double stranded (ds), linear, or circular), size of genome, structure of capsid (icosahedral, helical, etc.), and whether an envelope is present or not. The Baltimore system classifies viruses based on the different pathways used by the viral genome to create messenger RNA.⁹ In this chapter, I will focus on my target virus of interest, SARS-CoV-2.

1.3 Severe Acute Respiratory Syndrome Coronavirus 2 (SARS-CoV-2)

SARS-CoV-2 is classified under the family of Coronaviruses that have been responsible for other major large-scale outbreaks such as the Severe Acute Respiratory Syndrome (SARS) pandemic in 2002 and the Middle Eastern Respiratory Syndrome (MERS) epidemic in 2012. SARS-CoV-2 is the newest addition to the genus *Betacoronavirus* and is hypothesized to be a result of transmission from wild animals (i.e., bats) to humans, also known as zoonotic spillover.¹⁰⁻¹³ SARS-CoV-2 is an enveloped, positive sense single stranded RNA (+ssRNA) virus.

This means that the genetic material can be used to directly translate into proteins using the host cell's synthesis machinery.¹⁴ Coronaviruses have a long genome with the genome of SARS-CoV-2 being 29 kb (Figure 1).¹⁵ There are 14 open reading frames (ORFs) that encode 16 nonstructural proteins, 9 accessory proteins, and 4 structural proteins. The structural proteins include the spike (S), envelope (E), membrane (M), and nucleocapsid (N) proteins (Figure 2).^{15,16,17,18} The S protein is particularly important for pathogenesis and mediates SARS-CoV-2 host cell anchorage and entry. The E protein facilitates intracellular transport and viral assembly. The M protein promotes protein-protein interactions and plays a role in viral assembly. The N protein plays multifunctional roles in RNA synthesis, packaging, and stability.¹⁹

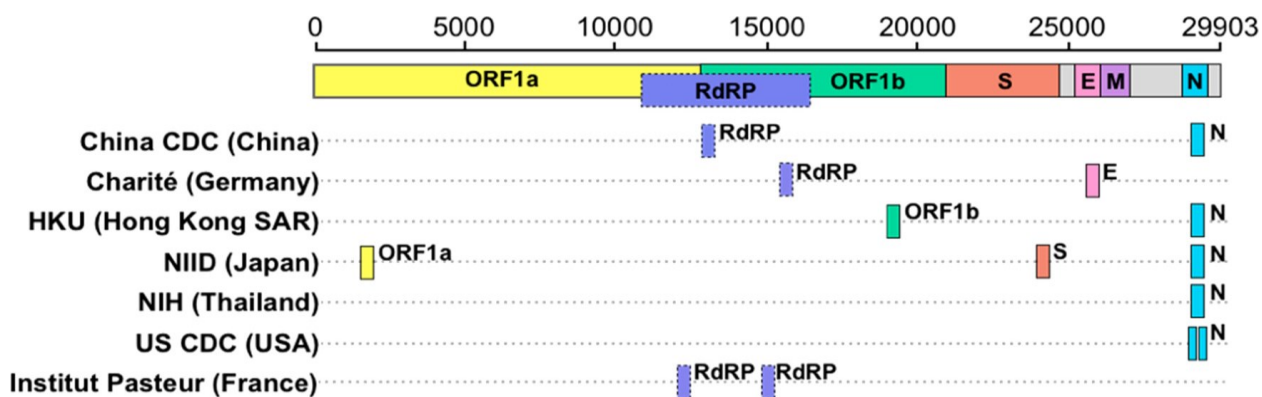


Figure 1.1 Genome organization of SARS-CoV-2 and the relative positions of gene targets. ORF, open reading frame; RdRP, RNA-dependent RNA polymerase; S, spike protein; E, envelope protein; M, membrane protein, and N, nucleocapsid protein. Figure reprinted with permission from Feng et al., 2020. Available from: <https://pubs.acs.org/doi/10.1021/acs.analchem.0c02060>

SARS-CoV-2 demonstrates tissue tropism which is the affinity of a virus for a specific tissue type. For SARS-CoV-2, the tissue tropism is towards tissues with a receptor called angiotensin-converting enzyme 2 (ACE2) and the transmembrane protease serine 2

(TMPRSS2).²⁰ In humans, the tissue tropism is highest in the upper and lower respiratory tract, but also in other areas such as the heart, kidney, liver, and gastrointestinal tract.²¹ SARS-CoV-2 is transmitted in humans mainly through respiratory droplets and aerosols, but other routes of transmission include fomites and fecal-oral.^{10,22} Once the SARS-CoV-2 virion reaches the respiratory tract, the S protein receptor binding domain binds the ACE2 receptor and TMPRSS2 cleaves the S1/S2 cleavage site. This signals for virus-cell membrane mediated fusion. Once inside, the +ssRNA is released and becomes translated into replicase proteins.¹⁵ The host's cellular components are used for biosynthesis of a new virion. After assembly, the new virion is secreted from the plasma membrane and goes onto infecting the next host cell.^{10,17}

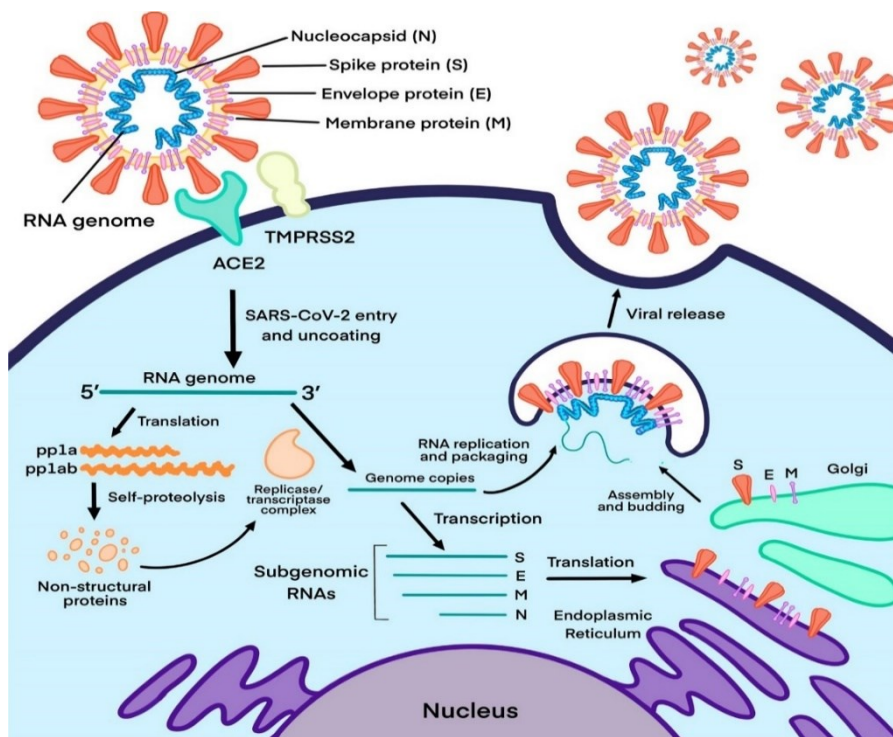


Figure 1.2. Schematic of SARS-CoV-2 life cycle inside a host cell. Figure reprinted with permission from Feng et al., 2020. Available from:

<https://pubs.acs.org/doi/10.1021/acs.analchem.0c02060>

Once a patient is infected, the time from exposure to symptom onset is approximately 2-7 days.²³ The most common COVID-19 symptoms are fever, cough, fatigue, malaise, chills, sore throat, and a runny nose.²⁴⁻²⁷ Some patients also experienced gastrointestinal symptoms such as nausea and diarrhea.²⁸ In immunocompromised patients, complications of COVID-19 could progress to acute respiratory distress, pneumonia, cardiac dysfunction, organ failure, and death.^{23,27,29} In immunocompetent patients, SARS-CoV-2 is considered a self-limiting infection with symptoms clearing after 5-12 days.²⁵ During this time of infection, it is recommended by the Centers for Disease Control and Prevention (CDC) to isolate during the symptoms and 3 days after symptom improvement to avoid transmitting the virus to others.³⁰ Therefore, to ensure patients are accurately diagnosed and can isolate to prevent the spread of disease, assays that are sensitive and specific for SARS-CoV-2 biomarkers are required for timely diagnosis.

1.4 SARS-CoV-2 Diagnostic Biomarkers

According to the Food and Drug Administration (US) and the National Institutes of Health (US), a diagnostic biomarker is a molecule that when detected suggests the presence of a disease or a condition.³¹ Diagnostic biomarkers can be used to screen, diagnose, or monitor patients. Diagnostic biomarkers are usually clinically significant biomolecules such as nucleic acids and proteins. Ideally, a diagnostic biomarker used in clinical laboratories should be present in clinical human samples where it can be detected sensitively and specifically by readily available analytical assays.^{32,33} When discussing sensitivity and specificity, it is important to distinguish the difference between the analytical and clinical use of the terms. Analytical sensitivity is used to describe the smallest amount of an analyte that can be accurately detected by the method, whereas clinical sensitivity describes the detection of all the people with a disease being accurately identified via the specific analyte as positive by the method. Analytical

specificity is used to describe the method's ability to measure a particular analyte rather than other analytes in a sample, whereas clinical specificity describes the detection of all the people without the disease being accurately identified as negative by the method.^{34,35} For the purpose of my thesis, I will use the terms specificity and sensitivity in their analytical aspects.

For the diagnosis of COVID-19 and detection of SARS-CoV-2 in a human sample, both nucleic acids and proteins can be used as diagnostic biomarkers. However, molecular diagnostic methods using RNA are the most common because of the higher availability of assays, sensitivity, and specificity. RNA detection is done via reverse transcriptase quantitative polymerase chain reaction (RT-qPCR). Low concentrations of the RNA target can be directly amplified to detectable amounts.³⁶ The details of the RT-qPCR process will be further discussed in a later section. Some gene targets for SARS-CoV-2 include the RNA encoding for the ORF, RNA dependent RNA polymerase (RdRP), S, E, M, and N proteins.¹⁵ SARS-CoV-2 proteins (i.e., S, E, M, and N) and immunoproteins (i.e., antibodies) can also be used as biomarkers, but cannot be directly amplified. Therefore, immunoassays which create a signal via enzyme labelling or substrate catalytic reactions are used, but these assays require more expensive reagents.³⁷ Other disadvantages which limit the use of immunoassays include interference from non-specific antibodies and autoantibodies, resulting in false results.³⁸ Over the last four years, tremendous work has been put into developing other novel strategies for SARS-CoV-2 biomarker detection including rapid antigen tests using lateral flow assays and point of care detection using isothermal amplification techniques.^{39,40,41} For the scope of my thesis, I will focus on discussing the gold standard for detection of SARS-CoV-2 which is RT-qPCR detection of SARS-CoV-2 RNA.

1.5 Sample Collection, Viral Inactivation, and RNA Extraction

There are several different types of human samples used for the diagnosis of SARS-CoV-2. The following samples are listed in order of most to least sensitive for SARS-CoV-2 RNA detection: bronchoalveolar lavage, sputum, nasopharyngeal swab (NPS), stool, blood, and urine.^{42,43,44} As SARS-CoV-2 is found at highest viral loads in the respiratory tract, respiratory samples are preferred for diagnosis. The recommended sample is the NPS because collection is relatively invasive and easier to collect than lower respiratory tract samples. Other disadvantages of lower respiratory tract samples include the requirement for invasive equipment, healthcare personnel for collection, needing patients to actively produce a sample by coughing, and potential contamination by commensal oral microorganisms.¹⁵ For NPS collection, a Dacron or polyester swab is inserted 2-4 cm into the nasopharynx to collect a sample and then placed in a sterile container before being transported to a clinical laboratory.⁴⁵ After samples are collected, they are shipped to a clinical laboratory at 2-8°C. The maximum storage time at this temperature is 5 days. The NPS must be stored at -80°C if there are delays in transport and sample analysis.^{45,46}

Before the NPS sample can be analyzed for the presence of SARS-CoV-2, it must undergo viral inactivation and RNA extraction. Viral inactivation is a process in which a virus' ability to replicate is inhibited, meanwhile preserving proteins and nucleic acids.⁴⁷ RNA extraction is a process that isolates high quality RNA from a sample.⁴⁸ In general, methods used for viral inactivation and RNA extraction can be classified into three categories: physical treatment (heat, radiation, sonication, or homogenization), chemical treatment (solvent based detergents or denaturants), enzymatic (proteinase K and lysozymes), or a combination of these.^{47,49,50} During the viral inactivation and RNA extraction steps, (1) the envelope and capsid

of the viral particle is broken resulting in RNA release, (2) non-RNA materials (DNA, proteins, salts, etc.) are removed, and finally (3) the RNA is concentrated, purified, and recovered using precipitation or elution methods.^{51,52}

Physical treatments are harsher as they physically break open the virion. For example, with heating techniques, high temperatures are used to alter the viral structure and degrade important proteins.⁵³ Radiation techniques, like ultraviolet (UV) and gamma, result in cleavage or crosslinking of nucleic acids, as well as the formation of reactive free radicals which inhibit viral replication pathways.⁴⁷ With sonication and homogenization, an intense sonic or physical force is used to disrupt the viral structure. Some other limitations of physical treatments include degradation of RNA and requirement of expensive analytical equipment.⁵⁴

Chemical treatments are the most used method as they are widely available through commercialized kits. They use reagents (chaotropic agents, reducing agents, detergents, or organic solvents) used in commercial lysis buffers to break open the virion and denature proteins.⁵² For example, commonly used chaotropic agents, such as guanidinium hydrochloride (GuHCl), denature viral capsids and proteins in the cell membrane, and inactivate enzymes. Reducing agents such as 2-mercaptoethanol (2-ME) and dithiothreitol (DTT), break disulfide bonds of enzymes and proteins leading to denaturation. Other reagents like detergents (sodium dodecyl sulfate (SDS), Triton X-100, and Tween 20) and organic solvents (alcohols, ether, and chloroform) cause cell disruption by penetrating the lipid membrane of the viral envelope.^{49,50} Enzymatic treatment using proteinase K and lysosomes can be used to hydrolyze virions and inactivate other enzymes.⁵² A combination of physical, chemical, and/or enzymatic methods for viral inactivation and RNA extraction is beneficial for two reasons. Firstly, it cannot be assumed that commonly available commercial kits are sufficient to completely render all human samples

as non-infectious, especially when the viral loads are variable.⁵⁵ Secondly, certain physical treatments such as prolonged heat treatment, especially in alkaline samples or in the presence of divalent cations, can result in RNA degradation. Therefore, to ensure complete inactivation and RNA stability, combinations of more gentle methods of viral inactivation and RNA extraction are recommended.

1.6 Detection of Viral RNA Using RT-qPCR

Polymerase chain reaction (PCR) is a nucleic acid amplification strategy commonly used in research and clinical laboratories to exponentially amplify nucleic acids so they can be detected and quantified.³⁶ Because of its simplicity, specificity, and sensitivity over many other assays, it is considered the most widely used detection technique in molecular biology.^{56,57} In general, the mastermix of a PCR reaction includes a forward primer, reverse primer, a heat stable polymerase (usually Taq polymerase), PCR buffer, and deoxynucleotide triphosphate (dNTPs) which are the building blocks for the amplified product. Each dNTP uses a different base (adenine (dATP), cytosine (dCTP), guanine (dGTP), and thymine (dTTP)). An instrument called a thermocycler is also required to cycle through low and high temperatures during the different steps of PCR. In the first step of PCR, high temperatures (~95°C) are used to denature double-stranded DNA (dsDNA) into single-stranded (ssDNA). Then the temperature is lowered (~60°C) allowing the forward and reverse primers to anneal. This step is followed by extension where the polymerase enzyme incorporates dNTPs and synthesizes a new strand of DNA.^{56,57}

To amplify RNA, extra steps and reagents are required. Taq polymerase, the enzyme used in PCR for DNA amplification, is relatively inefficient for RNA amplification. Therefore, an RNA-dependent DNA polymerase called reverse transcriptase is used in the first step to convert RNA to complementary DNA (cDNA). Then Taq polymerase can amplify cDNA like in a

standard PCR procedure.^{58,59} The “q” in RT-qPCR describes quantitative PCR. This means that a probe with a fluorescent tag, usually an intercalating dye or hydrolysis-based probe, is used to allow for quantification of the amplified product in real time as the reaction progresses.⁶⁰ This is advantageous over standard RT-PCR because you can see that reactions are successful in real time without needing to perform gel analysis. Therefore, RT-qPCR allows for the quantification of RNA in real time. Overall, the following reagents are required in a RT-qPCR mastermix; PCR buffer, Taq polymerase, reverse transcriptase, target-specific DNA forward and reverse primers, and a target-specific probe that contains a fluorescent dye at the 5’ end and a quencher at the 3’ end. In the first step of RT-qPCR, the mastermix containing the sample RNA is incubated at 50°C allowing the reverse transcriptase to convert RNA to cDNA. During the first denaturation step, the sample is heated to 95°C which denatures RNA, leaving only cDNA for the remaining steps. Next, the temperature is lowered to 60°C which allows the target specific primers and probes to anneal to the target. Finally, in the extension step, the Taq polymerase synthesizes a new strand and hydrolyses the probe. During probe hydrolysis, the fluorophore and quencher are separated through the 5’ exonuclease activity of the Taq polymerase, allowing for a signal to be released if the fluorophore is excited at the corresponding wavelength.⁵⁷

As the RT-qPCR cycles are ongoing, an amplification curve is created. The amplification curve has three distinct phases called the initiation, exponential, and plateau phases. In the first few cycles, there is a very low level of fluorescence, and this is used to set the baseline level of fluorescence. As the cycles continue, there is exponential growth in the amplified product and the fluorescence emitted crosses a threshold indicating that the fluorescence is now significantly higher than the baseline. When a particular sample fluorescence crosses this threshold, it is denoted a cycle threshold (Ct) value which is where quantification occurs. Eventually, the

plateau phase is reached where there is a shortage in reagents, so the amplification of the product levels off.^{59,60}

SARS-CoV-2 molecular detection from NPS is performed via RT-qPCR because of its advantages. Using the Ct values, the amount of RNA present in a sample can be quantified and this information can also be utilized to estimate viral loads in a patient. Many RT-qPCR instruments are also able to simultaneously process hundreds of samples in 1-2 hours, demonstrating excellent throughput.⁵⁷ Also, compared to other methods of molecular diagnosis, RT-qPCR is extremely sensitive and specific, giving clinicians confidence in the diagnosis. This is extremely important as there is a plethora of pathogenic and commensal microorganisms in the respiratory tract.⁶¹ Therefore, accurate and precise detection of SARS-CoV-2 is critical.

1.7 Challenges with Standard Clinical Testing of SARS-CoV-2

The gold standard for clinical diagnosis of COVID-19 involves a NPS collected by healthcare professionals followed by RT-qPCR detection of SARS-CoV-2 RNA.⁶¹ However, there are several challenges and limitations in the gold standard process of COVID-19 diagnosis. These limitations and challenges can be found in the pre-analytical, analytical, and post-analytical stages of SARS-CoV-2 clinical testing.

The pre-analytical stage of SARS-CoV-2 clinical testing includes NPS sample collection, storage, and transport. Firstly, the criteria for who can be clinically tested via NPS RT-qPCR must be met. Due to the COVID-19 burden on supplies, many healthcare jurisdictions have limited clinical testing to hospitalized patients or individuals who are considered more susceptible to infections. However, many patients can be asymptomatic, pre-symptomatic, or pseudo-symptomatic meaning that they either show no symptoms or have unusual symptoms.^{15,23}

These patients are excluded from testing which can lead to population bias when testing. Regardless, these patients are infected with SARS-CoV-2 and may go around transmitting the virus to other individuals because they have not been diagnosed. Additionally, a meticulously collected NPS is essential for accurate diagnosis and to prevent false negative results. Regardless of how sensitive an assay may be, if the NPS is not inserted into the nasopharynx adequately or collected according to the guidelines, then a false negative or falsely decreased result is possible. The timing of sample collection is also important as the viral load varies throughout the course of infection. It has been reported that upper respiratory samples, like NPS, have high viral loads earlier on in the infection when symptoms may not be fully apparent.^{43,62} NPS sample collection can be challenging as the insertion of the swab into the nasopharynx is uncomfortable and may induce sneezing and nosebleeds in patients. The sneezing can expel SARS-CoV-2 viral particles into the vicinity and infect the healthcare professional collecting the sample or any other nearby individuals. If the sample is not stored at the appropriate conditions (4-8°C for short periods) or transported to the clinical laboratory for timely analysis, it is possible for the sample to be compromised and subject to RNA degradation. Sample contamination may also be a major source of pre-analytical testing error; therefore, appropriate personal protective equipment, aseptic technique, labelling, and storage must occur.⁶³

The analytical stage of SARS-CoV-2 testing includes viral inactivation, RNA extraction, and RT-qPCR detection. Viral inactivation must be complete to prevent risk of infection to healthcare professionals or laboratory professionals working with the patient sample. Efficient RNA extraction is extremely important because human samples contain a complex matrix full of substances that inhibit RT-qPCR, collectively called RT-qPCR inhibitors.⁶⁴ If RNA is not efficiently extracted, then the presence of RT-qPCR inhibitors can lead to false negative results

or falsely decreased results. Additionally, RNA is extremely susceptible to degradation by RNases which are ubiquitous, heat-stable, and very hard to remove. Commercially available viral inactivation and RNA extraction methods for SARS-CoV-2 are labour intensive, time-consuming, and use reagents that may leave residual salts that can inhibit downstream RT-qPCR.^{15,65} Several studies have attempted to apply extraction-free techniques for ease of use, but have faced several challenges regarding inefficiency, matrix effects, and reduced assay sensitivity.⁶⁶⁻⁶⁹

The analytical sensitivity, specificity, and efficiency of the RT-qPCR assay itself is crucially important. Analytical sensitivity and specificity were discussed earlier in this chapter, but PCR efficiency describes how effective the PCR is at amplifying the target sequence during each replication cycle.⁵⁶ This is extremely important since amplification of the target is on an exponential scale, therefore small changes can lead to large differences in sensitivity and efficiency of the assay.⁷⁰ PCR efficiency should ideally be between 90-110%, but can be decreased if there is poor primer and probe designs, unoptimized reagent concentrations, formation of secondary structures, and unoptimized melting temperatures.⁷¹ Therefore, the primers and probes must be carefully designed to be 100% specific to the target sequence. All reagents, especially the enzymes used, the concentration of primers and probes, as well as the thermocycler temperatures must be adjusted for optimal performance.^{72,73,74} Additionally, the sequences of the primers must also be checked for the presence of secondary structures because these structures can impact the efficiency and sensitivity of RT-qPCR assays.⁷⁴ Sample contamination is another consideration which may cause false positive results and reduce the specificity of the assay.

The post-analytical stage of SARS-CoV-2 testing includes data analysis, reporting, and application for community monitoring. After a completed RT-qPCR run, the amplification curves must be analyzed to ensure proper reporting of whether a patient sample is positive or negative for SARS-CoV-2. With the gold standard approach (NPS based RT-qPCR), the average turnaround time from sample collection to diagnosis is around 2-5 days.⁷⁵ Additionally, during a pandemic situation, the high demand for PCR reagents, NPS, and other supplies could lead to shortages in supplies and further delays in diagnosis.⁷⁶ Additionally, it is important to consider that not all the resources may be readily available in remote communities. The extended wait times and cost of diagnosis can also make it challenging for efficient and timely diagnosis of COVID-19. Because of these limitations, NPS based RT-qPCR detection of COVID-19 for community monitoring on a larger scale for COVID-19 is also insufficient and not reasonable. Therefore, in response to these challenges, new platforms are actively being researched that have better RNA extraction, tolerance of matrix effects, and adaptability.

1.8 Alternative Approaches to the Standard Clinical Testing Standard of SARS-CoV-2

1.8.1 Oral Fluid Testing for SARS-CoV-2

Gargle and saliva samples are promising alternative sample types to NPS and have been recently explored for the detection of SARS-CoV-2. This is because SARS-CoV-2 can enter the oral cavity through the oral epithelial mucosa, salivary gland secretions, gingival crevicular fluid, blood circulation, and respiratory secretions from the lower and upper respiratory tracts.^{77,78,79} Additionally, detection of SARS-CoV-2 in the early stages of infection have shown to be more sensitive from the analysis of saliva than of NPS specimens.⁸⁰ In a study by Ott et al. 2021, it was demonstrated that SARS-CoV-2 RNA can be stable in saliva for up to 25 days at room temperature.⁸¹ Several studies have analyzed the overall agreement and clinical sensitivity of

using saliva relative to NPS. The overall concordance of saliva with NPS ranges from 89-99% and the overall clinical sensitivity ranges from 83-88%.^{77,80,82-85} A summary of recent studies investigating oral fluid testing for SARS-CoV-2 can be found in Table 2.1 in Chapter 2 of my thesis. Table 2.1 outlines the specific methods for sample collection, viral inactivation, RNA extraction, and detection utilized for each of the studies listed.

There is no standardization in terms of saliva or gargle sample collection amongst the recent studies using oral fluids for the detection of SARS-CoV-2. A longer abstention time (refraining from eating, drinking, chewing gum, or smoking) before sample collection allows individuals to accumulate more viral particles in the mouth. Thus, individuals are requested to produce a saliva sample in the morning right after waking up in some studies.^{86,87,88} Five self-collection methods for saliva samples have been reported in studies. These includes (1) repeatedly spitting into a container, (2) swirling saliva in the mouth for 30 seconds to 2 minutes and then repeatedly spitting into a container, (3) coughing up deep throat saliva (and potentially sputum) and then spitting into a container, (4) drooling saliva into a container, and finally (5) chewing a cotton swab for about 1 minute to stimulate salivation or swabbing the back of the tongue and buccal mucosa, to coat the swab with saliva, and then storing the swab in a sterile tube containing a transport medium or buffer.⁸⁹⁻⁹⁶

Because saliva samples collected with mucous are thicker and more difficult to process, additional steps are required to reduce viscosity. However, this additional sample treatment may increase the risk of cross-contamination and decrease the viral concentration of the sample.⁸⁹ Additionally, saliva collected with swabs contained less viral RNA than saliva collected by either passive drooling or spitting.⁹⁶⁻⁹⁹ This may be attributed to two reasons: (1) the saliva collected on the swab may not be representative of the entire mouth, and (2) salivary swabs containing saliva

samples are usually suspended in buffer or centrifuged to release viruses, which may lower the viral concentration due to dilution by the buffer or incomplete release of viruses.^{96,100} Therefore, a clear saliva sample collected via passive drooling is the best saliva sample.

Gargle specimens are typically obtained by gargling with saline or water, which is convenient for those who have difficulty generating enough saliva. Overall, a gargling solution using ≤ 5 mL of saline, and a gargling time of > 10 seconds is recommended for gargle collection because it has a higher overall clinical sensitivity than other combinations of gargle mediums and times.¹⁰¹ Gargle samples were found to have poorer clinical and analytical sensitivity when compared to saliva.^{88,91,99} This is most likely because viral particles are diluted with the gargling solution. A lower volume of gargle solution (1–2 mL) might limit dilution of viral particles in the gargle sample.

Overall, the use of oral fluids such as gargle and saliva has several advantages: (1) the method of collection is non-invasive, (2) convenient self-collection avoids overcrowding of testing centers and need for health professionals, (3) the competing demand for swabs, reagents (e.g., viral transport media), and personal protective equipment required for NPS sample collection is alleviated, and (4) increased ease of repeated sample collection for assessing viral concentration changes.

Regardless of these advantages, the use of gargle and saliva samples for SARS-CoV-2 detection has encountered several challenges. Firstly, infectious viral particles collected in oral fluids pose a transmission risk to those who deliver, handle, and analyze these samples. On-site inactivation of virus-containing samples during self-collection is necessary to avoid potential transmission risks. Secondly, the released viral RNA is prone to digestion by enzymes present in the oral fluid samples. Methods for inactivation and RNA extraction must maintain the stability

of the released viral RNA. Thirdly, oral fluid samples contain viscous materials, that vary with individuals and sampling protocols. The viscous sample matrix can hinder downstream processing, pipetting, and lower the efficiency of RNA extraction.⁸⁹ Commercial RNA extraction kits widely used for NPS samples may not be suitable for gargle and saliva samples. The kits used in recent studies are listed in Table 2.1 (Chapter 2 of my thesis).

There is also some discrepancy in the literature about relative viral concentrations in oral fluids vs NPS. Chau et al., 2020 and Jamal et al., 2021 reported similar amounts of viral RNA detected in NPS and saliva from symptomatic patients.^{102,103} However, some studies have reported that the viral load in saliva was higher than in NPS.^{86,104-106} Other studies have shown that viral load in saliva was lower than in NPS and that the detection of SARS-CoV-2 in saliva gave higher false negative results.^{107,110} These conflicting results could be due to both biological differences of the sample used and analytical discrepancy from the techniques or methods used. Differences in sampling procedures, viral inactivation, and RNA extraction approaches, as well as different RNA targets and RT-qPCR detection assays used can all lead to analytical discrepancy. Therefore, an improved analytical protocol is required to efficiently implement the usage of oral fluids for SARS-CoV-2 diagnostic testing.

Even with the implementation of oral fluids-based testing, individual and community testing is subject to continuously evolving local and regional policies that can be restricted by the availability and accessibility. When the COVID-19 cases rose sharply, clinical testing was often limited to symptomatic patients and close contacts to manage the demand for testing and shortages in diagnostic resources. Furthermore, some individuals were unwilling to undergo testing.¹¹¹ Presymptomatic, asymptomatic, and mild cases significantly contributed to the spread of SARS-CoV-2 and were mostly undetected during clinical surveillance. As a result, clinical

testing for SARS-CoV-2 underestimates and inconsistently estimates the true scale of the pandemic in a community.¹¹² This leads to my discussion on wastewater surveillance for community biomonitoring.

1.8.2 Wastewater Surveillance of SARS-CoV-2

Wastewater surveillance (WS) can overcome some of these limitations of clinical testing by capturing data from most individuals in the community.¹¹³⁻¹¹⁷ WS is a concept where wastewater is monitored for genetic signals of SARS-CoV-2 to gain understanding of the presence and scale of COVID-19 cases in a community.^{112,115} WS is feasible because wastewater is a composite biological sample representative of the entire community. When gastrointestinal epithelial cells are infected with SARS-CoV-2, infectious virions can be released into stool.¹¹⁸ Thus, studies have estimated that 27–89% of infected patients have viral particles shed into their stool.^{62,119} Domestic wastewater also contains bath, shower, and laundry wastewater, meaning that respiratory secretions will also be present. Wastewater can also be sampled directly from sewers to isolate a population from a specific building or area within a sewer network.^{120,121} Over 20 countries around the world have reported the presence of the SARS-CoV-2 RNA in wastewater systems including untreated wastewater, treated wastewater, and sludge (Table 3.1, Chapter 3 of my thesis), but no infectious SARS-CoV-2 viral particles have been detected in wastewater and no case of SARS-CoV-2 transmission via contact with sewage or sewage-contaminated water has been reported.^{122,123} Additionally, several studies have reported the occurrence of local community transmission of SARS-CoV-2 using wastewater analysis before the first notified SARS-CoV-2 case was clinically reported.^{124,125,126} Thus, testing SARS-CoV-2 RNA in wastewater can provide an early indication about the presence of SARS-CoV-2 in a community.

The overall process for WS of SARS-CoV-2 includes wastewater sampling, virus concentration, RNA extraction and detection, and data interpretation. There is no standardized procedure for the collection or analysis of wastewater samples. In the following paragraphs, I will briefly describe examples of the different methods that can be used for each step of the WS process.

Two types of wastewater samples are suitable for surveillance of SARS-CoV-2: untreated wastewater and primary sludge. Untreated wastewater is wastewater sampled from wastewater treatment plants (WWTPs) prior to any primary treatment. Primary sludge is sampled after the sedimentation process and contains more biological solids. It has been reported that the concentration of SARS-CoV-2 could be 2–3 orders of magnitude higher in primary sludge than in untreated wastewater.^{117,127,128} Although the use of primary sludge samples may potentially reduce the sample volume required to concentrate and detect the virus, biological solids contain many RT-qPCR inhibitors and can inhibit the detection of SARS-CoV-2 RNA. For sample collection, grab and composite samples are commonly used. Grab samples represent the wastewater conditions at the exact time of collection and are highly influenced by daily fluctuations in wastewater flow and composition. Composite samples are collected by pooling multiple grab samples at a specified frequency over a set period (typically 24h). Because composite samples represent the average wastewater characteristics, they are more commonly used (Table 3.1, Chapter 3 of my thesis). Sampling frequency depends on the purpose of WS. For monitoring presence of viruses, once per week is sufficient, but if for monitoring trends of infection and detection for early warning, then daily sampling is required.^{112,117} After sample collection, samples are kept at 4°C for short term storage or –80°C for long term storage.^{129,130,131}

Wastewater contains complex chemical and biological compounds, which can cause low viral recovery with poor reproducibility, hindering efficient concentration and detection of SARS-CoV-2. Therefore, it is critical to selectively concentrate viruses and effectively reduce nontarget materials. Commonly used concentration methods and reported recoveries for WS include polyethylene glycol (PEG) precipitation (0.1-63.7%), aqueous two-phase partitioning (PEG-dextran system) (recovery not reported), filtration with electronegative membranes (EM) (0.9-65.7%), ultrafiltration (28.0-73.0%), and ultracentrifugation (~12%). PEG mediates the aggregation and precipitation of biomolecules out of solution based on their molecular weights. PEG precipitation is relatively simple, inexpensive, and can handle large volumes of wastewater (~1 L) to concentrate viruses. However, it is time-consuming (4–6 hours) and may co-concentrate RT-qPCR inhibitors, hampering subsequent detection.¹³² The PEG-dextran aqueous two-phase system includes a PEG rich upper phase and a dextran rich lower phase. The phases can provide a protective environment for the biological activity of biomolecules and allow for selective partitioning of viruses.¹³³ EMs have been widely used and concentration is relatively simple, rapid (<40 minutes), and relatively cheaper with less co-concentration of RT-qPCR inhibitors.¹³⁴ Ultrafiltration is based on size exclusion and is performed using widely available small centrifuges. However, centrifugal ultrafiltration units may become costly especially when needing to process many samples. Other drawbacks include being limited to small volumes of samples, co-concentration of RT-qPCR inhibitors, and clogging due to the turbidity of wastewater samples.¹³⁵ Ultracentrifugation at 100 000 g is another concentration method, but its application in WS is limited due to requirements of an expensive ultracentrifuge, operator training, and low recovery.¹³⁶

After the viral particles have been concentrated, the next step is to separate RNA from any non-nucleic acid substances in wastewater. Two purification methods using phenol-chloroform or solid phase extraction have been used to purify SARS-CoV-2 RNA from wastewater. Then, SARS-CoV-2 RNA can be specifically and sensitively detected using exponential amplification approaches. RT-qPCR is the most used molecular detection method, and the Ct value can be converted to RNA copies per volume of wastewater sample based on a lab-generated standard curve. For the comparison of samples collected at different times and locations, the SARS-CoV-2 concentration in the samples must be normalized using a human fecal control because viral titers in sewage samples are subject to a variety of factors (concentration of fecal matter, sewage flow rate, stormwater, etc.).^{137,138} Based on the calibrated viral genomic copies per liter of wastewater, the viral copies/person/day or the number of infected individuals in the community can be estimated.¹³⁹

Although WS has the potential to be a powerful and effective early warning tool for community-wide monitoring of viruses for public health surveillance, several challenges remain, providing opportunities for future research. Firstly, there is no standardization of procedures or methods used in WS of SARS-CoV-2 that ensure high recovery and reproducibility. Current studies used different sample types, concentration, extraction, and detection procedures, and thus results cannot be directly compared. Furthermore, many studies generally lack recovery controls and details on recovery experiments. The use of surrogate viruses as controls for determining recovery is necessary to verify consistent performance of methods across different samples and over time.¹⁴⁰ Most of the methods I discussed previously are not optimized for wastewater samples, thus have low viral recoveries due to RT-qPCR inhibition from the complex wastewater matrix. This is especially important at the start of a community outbreak when the concentrations

of viruses and/or viral components are very low. Secondly, COVID-19 case prevalence and monitoring in previous studies was limited to retrospective analysis. Real time advanced warning can only be obtained by frequent wastewater sampling, rapid wastewater analysis, and result reporting to public health authorities. Accurate estimation of population infection depends upon knowledge about numerous factors that are not known, including rate of viral shedding, daily production of stool per capita, as well as percentage of SARS-CoV-2 patients who shed virus into their stool.¹⁴¹ Therefore, for reliable and meaningful application of WS for SARS-CoV-2, there is an urgent need for efficient and sensitive protocols for wastewater sample collection, viral particle concentration, RNA extraction, and detection.

1.9 Rationale and Scope of Thesis

The commonly used gold standard process for sample collection and detection of SARS-CoV-2 has several challenges and limitations. The goal of my research was to develop new analytical methods for sensitive and robust detection of SARS-CoV-2 in clinical and wastewater samples. I hypothesized that the integration of viral inactivation, RNA release and preservation, followed by direct detection in a simplified protocol can provide sensitive detection of viral pathogens in clinical and wastewater samples. To achieve this goal, my research focused on four specific objectives: (1) to develop a new method by integrating viral inactivation, RNA release and preservation, and subsequent direct detection of SARS-CoV-2 in oral fluids, (2) to develop a robust method for the enhanced and sensitive detection of SARS-CoV-2 in wastewater for community surveillance of infections, (3) to develop multiplex RT-qPCR assays for the early detection of variants of concern (VOCs) in wastewater, and (4) to extend these developed methods and demonstrate that these assays are adaptable for monitoring other clinically

significant and co-circulating viral pathogens in wastewater. In this thesis work, I introduce novel strategies to analyze viral pathogens in both clinical and environmental samples.

This thesis consists of six chapters. Chapter 1 reviews the basics of virology, introduces SARS-CoV-2 and the gold standard for detection, introduces the standard approaches for oral fluid and wastewater sample analysis as well as the associated challenges. Chapter 2 introduces a unique method and formulation for simultaneous viral inactivation and RNA preservation followed by detection of SARS-CoV-2 in saliva and gargle samples. Chapter 3 introduces an efficient method for enhanced wastewater surveillance of SARS-CoV-2 in the community. Chapter 4 discusses the development of multiplex RT-qPCR assays for the early detection of SARS-CoV-2 VOCs in wastewater. Chapter 5 focuses on the application of the wastewater protocol for the monitoring of SARS-CoV-2 Omicron sub-variants and Norovirus in wastewater. Chapter 6 summarizes the conclusions, significance, and fundamental contributions to biology of my research work, and possible future directions.

References

1. World Health Organization. *Coronavirus (COVID-19) Dashboard*, 2023. Available from <https://covid19.who.int/> (accessed 2023-09-06).
2. Tang, J.W.; Tambyah, P.A.; Hui, D.S. Emergence of a new SARS-CoV-2 variant in the UK. *J. Infect.* **2021**, *82* (4), e27–e28.
3. Wang, P.; Casner, R.G.; Nair, M.S.; Wang, M.; Yu, J.; Cerutti, G.; et al. Increased resistance of SARS-CoV-2 variant P. 1 to antibody neutralization. *Cell Host Microbe.* **2021**, *29* (5), 747–751.
4. Zhou, D.; Dejnirattisai, W.; Supasa, P.; Liu, C.; Mentzer, A.J.; Ginn, H.M.; et al. Evidence of escape of SARS-CoV-2 variant B. 1.351 from natural and vaccine-induced sera. *Cell.* **2021**, *184* (9), 2348–2361.
5. Pellett, P.E.; Mitra, S.; Holland, T.C. Basics of virology. *Handb. Clin. Neurol.* **2014**, *123*, 45-66.
6. Minchin, S.; Lodge, J. Understanding biochemistry: structure and function of nucleic acids. *Essays Biochem.* **2019**, *63* (4), 433-456.
7. Prasad, B.V.; Schmid, M.F. Principles of virus structural organization. *Adv. Exp. Med. Biol.* **2012**, *724*, 17-47.
8. Takeuchi, O.; Akira, S. Innate immunity to virus infection. *Immunol. Rev.* **2009**, *227* (1), 75-86.
9. International Committee on Taxonomy of Viruses Executive Committee. The new scope of virus taxonomy: partitioning the virosphere into 15 hierarchical ranks. *Nat. Microbiol.* **2020**, *5*, 668–674.

10. Harrison, A.G.; Lin, T.; Wang, P. Mechanisms of SARS-CoV-2 transmission and pathogenesis. *Trends Immunol.* **2020**, 41(12):1100-15.
11. Zhou, P.; Yang, X.L.; Wang, X.G.; Hu, B.; Zhang, L.; Zhang, W.; et al. A pneumonia outbreak associated with a new coronavirus of probable bat origin. *Nature* **2020**, 579 (7798), 270-273.
12. Ellwanger, J.H.; Chies, J.A. Zoonotic spillover: Understanding basic aspects for better prevention. *Genet. Mol. Biol.* **2021**, 44.
13. Peiris, J.S.; Lai, S.T.; Poon, L.L.; Guan, Y.; Yam, L.Y.; Lim, W.; et al. Coronavirus as a possible cause of severe acute respiratory syndrome. *Lancet* **2003**, 361 (9366), 1319-1325.
14. Payne S. Introduction to RNA viruses. *Viruses* **2017**, 97–105.
15. Feng, W.; Newbigging, A.M.; Le, C.; Pang, B.; Peng, H.; Cao, Y.; et al. Molecular diagnosis of COVID-19: challenges and research needs. *Anal. Chem.* **2020**, 92 (15), 10196-10209.
16. Coronaviridae Study Group of the International Committee on Taxonomy of Viruses (CSG of ICTV). The species Severe acute respiratory syndrome-related coronavirus: classifying 2019-nCoV and naming it SARS-CoV-2. *Nat. Microbiol.* **2020**, 5, 536–554.
17. Lu, R.; Zhao, X.; Li, J.; Niu, P.; Yang, B.; Wu, H.; et al. Genomic characterization and epidemiology of 2019 novel coronavirus: implications for virus origins and receptor binding. *Lancet* **2020**, 395 (10224), 565-574.
18. Zhang, Y.Z.; Holmes, E.C. A genomic perspective on the origin and emergence of SARS-CoV-2. *Cell* **202**, 181 (2), 223-227.

19. Gorkhali, R.; Koirala, P.; Rijal, S.; Mainali, A.; Baral, A.; Bhattarai, H.K. Structure and function of major SARS-CoV-2 and SARS-CoV proteins. *Bioinform. Biol. Insights*. **2021**, *15*, 11779322211025876.
20. Hoffmann, M.; Kleine-Weber, H.; Schroeder, S.; Krüger, N.; Herrler, T.; Erichsen, S.; et al. SARS-CoV-2 cell entry depends on ACE2 and TMPRSS2 and is blocked by a clinically proven protease inhibitor. *Cell* **2020**, *181* (2), 271-280.
21. Hamming, I.; Timens, W.; Bulthuis, M.L.; Lely, A.T.; Navis, G.V.; van Goor, H. Tissue distribution of ACE2 protein, the functional receptor for SARS coronavirus. A first step in understanding SARS pathogenesis. *J. Pathol.* **2004**, *203* (2), 631-637.
22. Mukhra, R.; Krishan, K.; Kanchan, T. Possible modes of transmission of Novel coronavirus SARS-CoV-2: a review. *Acta Biomed.* **2020**, *91* (3), e2020036.
23. Li, Q.; Guan, X.; Wu, P.; Wang, X.; Zhou, L.; Tong, Y.; et al. Early transmission dynamics in Wuhan, China, of novel coronavirus–infected pneumonia. *N. Engl. J. Med.* **2020**, *382* (13), 1199-1207.
24. Wang, D.; Hu, B.; Hu, C.; Zhu, F.; Liu, X.; Zhang, J.; et al. Clinical characteristics of 138 hospitalized patients with 2019 novel coronavirus–infected pneumonia in Wuhan, China. *J. Am. Med. Assoc.* **2020a**, *323* (11), 1061-1069.
25. Wiersinga, W.J.; Rhodes, A.; Cheng, A.C.; Peacock, S.J.; Prescott, H.C. Pathophysiology, transmission, diagnosis, and treatment of coronavirus disease 2019 (COVID-19): a review. *J. Am. Med. Assoc.* **2020**, *324* (8), 782-793.
26. Richardson, S.; Hirsch, J.S.; Narasimhan, M.; Crawford, J.M.; McGinn, T.; Davidson, K.W.; et al. Presenting characteristics, comorbidities, and outcomes among 5700 patients

- hospitalized with COVID-19 in the New York City area. *J. Am. Med. Assoc.* **2020**, 323 (20), 2052-2059.
27. Huang, C.; Wang, Y.; Li, X.; Ren, L.; Zhao, J.; Hu, Y.; et al. Clinical features of patients infected with 2019 novel coronavirus in Wuhan, China. *Lancet* **2020**, 395 (10223), 497-506.
28. Mao, R.; Qiu, Y.; He, J.S.; Tan, J.Y.; Li, X.H.; Liang, J.; et al. Manifestations and prognosis of gastrointestinal and liver involvement in patients with COVID-19: a systematic review and meta-analysis. *Lancet Gastroenterol. Hepatol.* **2020**, 5 (7), 667-678.
29. Chan, J.F.; Yuan, S.; Kok, K.H.; To, K.K.; Chu, H.; Yang, J.; et al. A familial cluster of pneumonia associated with the 2019 novel coronavirus indicating person-to-person transmission: a study of a family cluster. *Lancet.* **2020a**, 395 (10223), 514-523.
30. Centers for Disease Control and Prevention. *Symptom-based strategy to discontinue isolation for persons with COVID-19*, 2020. Available from <https://stacks.cdc.gov/view/cdc/88537> (accessed 2023-09-08).
31. FDA-NIH Biomarker Working Group. *BEST (Biomarkers, EndpointS, and other Tools) Resource*, 2016. Available from www.ncbi.nlm.nih.gov/books/NBK326791/ (accessed 2023-09-08).
32. Holland, R. L. What Makes a Good Biomarker? *Adv. Precis. Med.* **2016**, 1, 66.
33. Califf, R.M. Biomarker definitions and their applications. *Exp. Biol. Med.* **2018**, 243 (3), 213-221.
34. Saah, A.J.; Hoover, D.R. "Sensitivity" and "specificity" reconsidered: the meaning of these terms in analytical and diagnostic settings. *Ann. Intern. Med.* **1997**, 126 (1), 91-94.

35. Swift, A.; Heale, R.; Twycross, A. What are sensitivity and specificity? *Evid. Based Nurs.* **2020**, 23, 2-4.
36. Mullis, K.; Faloona, F.; Saiki, R.; Horn, G.; Erlich, H.; Scharf, S. Specific enzymatic amplification of DNA in vitro: The polymerase chain reaction. *Symp. Quant. Boil.* **1986**, 51, 263–273.
37. Lequin, R. M. Enzyme immunoassay (EIA)/Enzyme-linked immunosorbent assay (ELISA). *Clin. Chem.* **2005**, 51, 2415–2418.
38. Hoofnagle, A.N.; Wener, M.H. The fundamental flaws of immunoassays and potential solutions using tandem mass spectrometry. *J. Immunol. Methods.* **2009**, 347, 3-11.
39. Mak, G.C.; Cheng, P.K.; Lau, S.S.; Wong, K.K.; Lau, C.S.; Lam, E.T.; et al. Evaluation of rapid antigen test for detection of SARS-CoV-2 virus. *J. Clin. Virol.* **2020**, 129, 104500.
40. Dinnes, J.; Sharma, P.; Berhane, S.; van Wyk, S.S.; Nyaaba, N.; Domen, J.; et al. Rapid, point-of-care antigen tests for diagnosis of SARS-CoV-2 infection. *Cochrane Database Syst. Rev.* **2022**, (7).
41. Xiao, H.; Hu, J.; Huang, C.; Feng, W.; Liu, Y.; Kumblathan, T.; et al. CRISPR techniques and potential for the detection and discrimination of SARS-CoV-2 variants of concern. *Trends Anal. Chem.* **2023**, 161, 117000.
42. Wang, W.; Xu, Y.; Gao, R.; Lu, R.; Han, K.; Wu, G.; Tan, W. Detection of SARS-CoV-2 in different types of clinical specimens. *J. Am. Med. Assoc.* **2020b**, 323 (18), 1843– 1844.
43. Zou, L.; Ruan, F.; Huang, M.; Liang, L.; Huang, H.; Hong, Z.; et al. SARS-CoV-2 viral load in upper respiratory specimens of infected patients. *N. Engl. J. Med.* **2020**, 382 (12), 1177– 1179.

44. Loeffelholz, M.J.; Tang, Y.W. Laboratory diagnosis of emerging human coronavirus infections - the state of the art. *Emerging Microbes Infect.* **2020**, 9 (1), 747– 756.
45. World Health Organization. *Laboratory Testing for Coronavirus Disease (COVID-19) in Suspected Human Cases: Interim Guidance.* **2020**, Available from <https://apps.who.int/iris/handle/10665/331501> (accessed 2020-05-08).
46. Centers for Disease Control and Prevention. *Interim Guidelines for Collecting and Handling of Clinical Specimens for COVID-19 Testing,* **2022**, Available from: <https://www.cdc.gov/coronavirus/2019-ncov/lab/guidelines-clinical-specimens.html#:~:text=Store%20respiratory%20specimens%20at%202,70%C2%B0C%20or%20below>. (accessed 2023-09-08).
47. Elveborg, S.; Monteil, V.M.; Mirazimi, A. Methods of inactivation of highly pathogenic viruses for molecular, serology or vaccine development purposes. *Pathogens.* **2022**, 11 (2), 271.
48. Shi, H.; Bressan, R. RNA extraction. *Methods Mol. Biol.* **2006**, 323, 345-348.
49. Safiabadi Tali, S.H.; LeBlanc, J.J.; Sadiq, Z.; Oyewunmi, O.D.; Camargo, C.; Nikpour, B.; et al. Tools and techniques for severe acute respiratory syndrome coronavirus 2 (SARS-CoV-2)/COVID-19 detection. *Clin. Microbiol. Rev.* **2021**, 34 (3).
50. Ali, N.; Rampazzo, R.D.; Costa, A.D.; Krieger, M.A. Current nucleic acid extraction methods and their implications to point-of-care diagnostics. *Biomed Res. Int.* **2017**, 2017.
51. Andrews, B.A.; Asenjo, J.A. Enzymatic lysis and disruption of microbial cells. *Trends Biotechnol.* **1987**, 5 (10), 273-277.

52. Liu, Y.; Kumblathan, T.; Tao, J.; Xu, J.; Feng, W.; Xiao, H.; et al. Recent advances in RNA sample preparation techniques for the detection of SARS-CoV-2 in saliva and gargle. *Trends Anal. Chem.* **2023**, 165, 117107.
53. Wigginton, K.R.; Pecson, B.M.; Sigstam, T.; Bosshard, F.; Kohn, T. Virus inactivation mechanisms: Impact of disinfectants on virus function and structural integrity. *Environ. Sci. Technol.* **2012**, 46, 12069–12078.
54. Shehadul Islam, M.; Aryasomayajula, A.; Selvaganapathy, P.R. A review on macroscale and microscale cell lysis methods. *Micromachines (Basel)*. **2017**, 8 (3), 83.
55. Blow, J.A.; Dohm, D.J.; Negley, D.L.; Mores, C.N. Virus inactivation by nucleic acid extraction reagents. *J. Virol. Methods.* **2004**, 119 (2), 195-198.
56. Kralik, P.; Ricchi, M. A basic guide to real time PCR in microbial diagnostics: definitions, parameters, and everything. *Front. Microbiol.* **2017**, 8, 108.
57. Bustin, S.A.; Nolan, T. RT-qPCR testing of SARS-CoV-2: a primer. *Int. J. Mol. Sci.* **2020**, 21 (8), 3004.
58. Myers, T.W.; Gelfand, D.H. Reverse transcription and DNA amplification by a *Thermus thermophilus* DNA polymerase. *Biochemistry.* **1991**, 30, 7661–7666.
59. Bustin, S. Absolute quantification of mRNA using real-time reverse transcription polymerase chain reaction assays. *J. Mol. Endocrinol.* **2000**, 25, 169–193.
60. Adams G. A beginner's guide to RT-PCR, qPCR and RT-qPCR. *Biochem.* **2020**, 42 (3), 48-53.
61. Kevadiya, B.D.; Machhi, J.; Herskovitz, J.; Oleynikov, M.D.; Blomberg, W.R.; Bajwa, N.; et al. Diagnostics for SARS-CoV-2 infections. *Nat. Mater.* **2021**, 20 (5), 593-605.

62. Wölfel, R.; Corman, V. M.; Guggemos, W.; Seilmaier, M.; Zange, S.; Müller, M. A.; et al. Virological assessment of hospitalized patients with COVID-2019. *Nature* **2020**, 581, 465–469.
63. Lippi, G.; Simundic, A.M. The EFLM strategy for harmonization of the preanalytical phase. *Clin. Chem. Lab. Med.* **2018**, 56, 1660–1666.
64. Dheda, K.; Huggett, J.; Bustin, S.; Johnson, M.A.; Rook, G.; Zumla, A. Validation of housekeeping genes for normalizing RNA expression in real-time PCR. *Biotechniques* **2004**, 37, 112–119.
65. Bessetti, J. An introduction to PCR inhibitors. *J. Microbiol. Methods* **2007**, 28, 159–167.
66. Fomsgaard, A. S.; Rosenstjerne, M. W. An alternative workflow for molecular detection of SARS-CoV-2 – escape from the NA extraction kit-shortage, Copenhagen, Denmark, March 2020. *Euro. Surveill.* **2020**, 25 (14), 2000398.
67. Pan, Y.; Long, L.; Zhang, D.; Yuan, T.; Cui, S.; Yang, P.; Wang, Q.; Ren, S. Potential false-negative nucleic acid testing results for severe acute respiratory syndrome coronavirus 2 from thermal inactivation of samples with low viral loads. *Clin. Chem.* **2020**, 66 (6), 794–801.
68. Schoeber, J.P.; Schlaghecke, J.M.; Meuwissen, B.M.; van Heertum, M.; van den Brule, A.J.; Loonen, A.J. Comprehensive analytical and clinical evaluation of a RNA extraction-free saliva-based molecular assay for SARS-CoV-2. *Plos One.* **2022**, 17 (5), e0268082.
69. Gadkar, V.J.; Goldfarb, D.M.; Al-Rawahi, G.N.; Srigley, J.A.; Smailus, D.E.; Coope, R.J.; et al. Extraction-free clinical detection of SARS-CoV-2 virus from saline gargle samples using Hamilton STARlet liquid handler. *Sci. Rep.* **2023**, 13 (1), 4241.

70. Bustin, S.; Dhillon, H.S.; Kirvell, S.; Greenwood, C.; Parker, M.; Shipley, G.L.; Nolan, T. Variability of the reverse transcription step: Practical implications. *Clin. Chem.* **2015**, 61, 202–212.
71. Svec, D.; Tichopad, A.; Novosadova, V.; Pfaffl, M.W.; Kubista, M. How good is a PCR efficiency estimate: Recommendations for precise and robust qPCR efficiency assessments. *Biomol. Detect. Quantif.* **2015**, 3, 9-16.
72. Chan, J.F.W.; Yip, C.C.Y.; To, K.K.W.; Tang, T.H.C.; Wong, S.C.Y.; Leung, K.H.; et al. Improved molecular diagnosis of COVID-19 by the novel, highly sensitive and specific COVID-19-RdRp/Hel real-time reverse transcription-polymerase chain reaction assay validated in vitro and with clinical specimens. *J. Clin. Microbiol.* **2020b**, 58 (5), 10-128.
73. Corman, V.M.; Landt, O.; Kaiser, M.; Molenkamp, R.; Meijer, A.; Chu, D.K.; et al. Detection of 2019 novel coronavirus (2019-nCoV) by real-time RT-PCR. *Euro Surveill.* **2020**, 25, 2000045.
74. Wang, Y.; Kang, H.; Liu, X.; Tong, Z.-H. Combination of RT-qPCR testing and clinical features for diagnosis of COVID-19 facilitates management of SARS-CoV-2 outbreak. *J. Med. Virol.* **2020c**, 92, 538–539.
75. Udugama, B.; Kadhiresan, P.; Kozlowski, H.N.; Malekjahani, A.; Osborne, M.; Li, V.Y.; et al. Diagnosing COVID-19: the disease and tools for detection. *ACS Nano.* **2020**, 14 (4), 3822-3835.
76. D'Cruz, R.J.; Currier, A.W.; Sampson, V.B. Laboratory testing methods for novel severe acute respiratory syndrome-coronavirus-2 (SARS-CoV-2). *Front. Cell Dev. Biol.* **2020**, 8, 468.

77. Fakhruddin, K.S.; Haiat, A.; Ngo, H.C.; Panduwawala, C.; Chang, J.W.; Samaranyake, L.P. Severe acute respiratory syndrome coronavirus-2 (SARS-CoV-2) viral positivity and their burden in saliva of asymptomatic carriers—a systematic review and meta-analysis. *Acta Odontol. Scand.* **2022**, *80* (3), 182-190.
78. Huang, N.; Pérez, P.; Kato, T.; Mikami, Y.; Okuda, K.; Gilmore, R.C.; et al. SARS-CoV-2 infection of the oral cavity and saliva. *Nat. Med.* **2021**, *27* (5), 892-903.
79. Zhong, M.; Lin, B.; Pathak, J.L.; Gao, H.; Young, A.J.; Wang, X.; et al. ACE2 and furin expressions in oral epithelial cells possibly facilitate COVID-19 infection via respiratory and fecal–oral routes. *Front. Med.* **2020**, *7*, 580796.
80. Lee, R.A.; Herigon, J.C.; Benedetti, A.; Pollock, N.R.; Denkinger, C.M. Performance of saliva, oropharyngeal swabs, and nasal swabs for SARS-CoV-2 molecular detection: a systematic review and meta-analysis. *J. Clin. Microbiol.* **2021**, *59* (5), 10-128.
81. Ott, I.M.; Strine, M.S.; Watkins, A.E.; Boot, M.; Kalinich, C.C.; Harden, C.A.; et al. Stability of SARS-CoV-2 RNA in non-supplemented saliva. *Emerg. Infect. Dis.* **2021**, *27* (4), 1146.
82. Khiabani, K.; Amirzade-Iranaq, M.H. Are saliva and deep throat sputum as reliable as common respiratory specimens for SARS-CoV-2 detection? A systematic review and meta-analysis. *Am. J. Infect. Control.* **2021**, *49* (9), 1165-1176.
83. Atieh, M.A.; Guirguis, M.; Alsabeeha, N.H. Cannon RD. The diagnostic accuracy of saliva testing for SARS-CoV-2: a systematic review and meta-analysis. *Oral Dis.* **2022**, *28*, 2347-2361.

84. Bastos, M.L.; Perlman-Arrow, S.; Menzies, D.; Campbell, J.R. The sensitivity and costs of testing for SARS-CoV-2 infection with saliva versus nasopharyngeal swabs: a systematic review and meta-analysis. *Ann. Intern. Med.* **2021**, *174* (4), 501-510.
85. Butler-Laporte, G.; Lawandi, A.; Schiller, I.; Yao, M.; Dendukuri, N.; McDonald, E.G.; Lee, T.C. Comparison of saliva and nasopharyngeal swab nucleic acid amplification testing for detection of SARS-CoV-2: a systematic review and meta-analysis. *JAMA Intern. Med.* **2021**, *181* (3), 353-360.
86. Rao, M.; Rashid, F.A.; Sabri, F.S.; Jamil, N.N.; Zain, R.; Hashim, R.; et al. Comparing nasopharyngeal swab and early morning saliva for the identification of severe acute respiratory syndrome coronavirus 2 (SARS-CoV-2). *Clin. Infect. Dis.* **2021**, *72* (9), 352-356.
87. Pijuan-Galito, S.; Tarantini, F.S.; Tomlin, H.; Jenkins, H.; Thompson, J.L.; Scales, D.; et al. Saliva for COVID-19 testing: Simple but useless or an undervalued resource? *Front. Virol.* **2021**, *1*, 29.
88. Poukka, E.; Mäkelä, H.; Hagberg, L.; Vo, T.; Nohynek, H.; Ikonen, N.; Liitsola, K.; et al. Detection of SARS-CoV-2 infection in gargle, spit, and sputum specimens. *Microbiol. Spectr.* **2021**, *9* (1), e00035-21.
89. Tan, S.H.; Allicock, O.; Armstrong-Hough, M.; Wyllie, A.L. Saliva as a gold-standard sample for SARS-CoV-2 detection. *Lancet Respir. Med.* **2021**, *9* (6), 562-564.
90. Chong, C.Y.; Kam, K.Q.; Li, J.; Maiwald, M.; Loo, L.H.; Nadua, K.D.; et al. Saliva is not a useful diagnostic specimen in children with coronavirus disease 2019 (COVID-19). *Clin. Infect. Dis.* **2021**, *73* (9), e3144-5.

91. Fernández-González, M.; Agulló, V.; de la Rica, A.; Infante, A.; Carvajal, M.; García, J.A.; et al. Performance of saliva specimens for the molecular detection of SARS-CoV-2 in the community setting: does sample collection method matter? *J. Clin. Microbiol.* **2021**, 59 (4), 10-128.
92. Altawalsh, H.; AlHuraish, F.; Alkandari, W.A.; Ezzikouri, S. Saliva specimens for detection of severe acute respiratory syndrome coronavirus 2 in Kuwait: A cross-sectional study. *J. Clin. Virol.* **2020**, 132, 104652.
93. Ku, C.W.; Shivani, D.; Kwan, J.Q.; Loy, S.L.; Erwin, C.; Ko, K.K.; et al. Validation of self-collected buccal swab and saliva as a diagnostic tool for COVID-19. *Int. J. Infect. Dis.* **2021**, 104, 255-261.
94. Azzi, L.; Maurino, V.; Baj, A.; Dani, M.; d’Aiuto, A.; Fasano, M.; et al. Diagnostic salivary tests for SARS-CoV-2. *J. Dent. Res.* **2021**, 100 (2), 115-123.
95. Dogan, O.A.; Kose, B.; Agaoglu, N.B.; Yildiz, J.; Alkurt, G.; Demirkol, Y.K.; et al. Does sampling saliva increase detection of SARS-CoV-2 by RT-PCR? Comparing saliva with oro-nasopharyngeal swabs. *J. Virol. Methods.* **2021**, 290, 114049.
96. De Paula Eduardo, F.; Bezinelli, L.M.; de Araujo, C.A.; Moraes, J.V.; Birbrair, A.; Pinho, J.R.; et al. Self-collected unstimulated saliva, oral swab, and nasopharyngeal swab specimens in the detection of SARS-CoV-2. *Clin. Oral Investig.* **2022**, 26 (2), 1561-1567.
97. Rajh, E.; Šket, T.; Praznik, A.; Sušjan, P.; Šmid, A.; Urbančič, D.; et al. Robust saliva-based RNA extraction-free one-step nucleic acid amplification test for mass SARS-CoV-2 monitoring. *Molecules.* **2021**, 26 (21), 6617.
98. Li, Z.; Bruce, J.L.; Cohen, B.; Cunningham, C.V.; Jack, W.E.; Kunin, K.; et al. Development and implementation of a simple and rapid extraction-free saliva SARS-

- CoV-2 RT-LAMP workflow for workplace surveillance. *PLoS One*. **2022**, 17 (5), 0268692.
99. Kohmer, N.; Eckermann, L.; Böddinghaus, B.; Götsch, U.; Berger, A.; Herrmann, E.; et al. Self-collected samples to detect SARS-CoV-2: direct comparison of Saliva, Tongue Swab, Nasal Swab, chewed cotton pads and gargle lavage. *J. Clin. Med.* **2021**, 10 (24), 5751.
100. Aita, A.; Basso, D.; Cattelan, A.M.; Fioretto, P.; Navaglia, F.; Barbaro, F.; et al. SARS-CoV-2 identification and IgA antibodies in saliva: One sample two tests approach for diagnosis. *Clinica Chimica Acta*. **2020**, 510, 717-722.
101. Tsang, N.N.; So, H.C.; Cowling, B.J.; Leung, G.M.; Ip, D.K. Performance of saline and water gargling for SARS-CoV-2 reverse transcriptase PCR testing: a systematic review and meta-analysis. *Eur. Respir. J.* **2022**, 31 (165), 220014.
102. Chau, N.V.; Lam, V.T.; Dung, N.T.; Yen, L.M.; Minh, N.N.; Ngoc, N.M.; et al. The natural history and transmission potential of asymptomatic severe acute respiratory syndrome coronavirus 2 infection. *Clin. Infect. Dis.* **2020**, 71 (10), 2679.
103. Jamal, A.J.; Mozafarihashjin, M.; Coomes, E.; Powis, J.; Li, A.X.; Paterson, A.; et al. Sensitivity of nasopharyngeal swabs and saliva for the detection of severe acute respiratory syndrome coronavirus 2. *Clin. Infect. Dis.* **2021**, 72 (6), 1064-1066.
104. Wyllie, A.L.; Fournier, J.; Casanovas-Massana, A.; Campbell, M.; Tokuyama, M.; Vijayakumar, P.; et al. Saliva or nasopharyngeal swab specimens for detection of SARS-CoV-2. *N. Engl. J. Med.* **2020**, 383 (13), 1283-1286.

105. Teo, A.K.; Choudhury, Y.; Tan, I.B.; Cher, C.Y.; Chew, S.H.; Wan, Z.Y.; et al. Saliva is more sensitive than nasopharyngeal or nasal swabs for diagnosis of asymptomatic and mild COVID-19 infection. *Sci. Rep.* **2021**, 11 (1), 3134.
106. Herrera, L.A.; Hidalgo-Miranda, A.; Reynoso-Noverón, N.; Meneses-García, A.A.; Mendoza-Vargas, A.; Reyes-Grajeda, J.; et al. Saliva is a reliable and accessible source for the detection of SARS-CoV-2. *Int J. Infect. Dis.* **2021**, 105, 83-90.
107. Lopes, J.I.; da Costa Silva, C.A.; Cunha R.G.; Soares, A.M.; Lopes, M.E.; da Conceição Neto, O.C.; et al. A large cohort study of SARS-CoV-2 detection in saliva: A non-invasive alternative diagnostic test for patients with bleeding disorders. *Viruses* **2021**, 13 (12), 2361.
108. Landry, M.L.; Criscuolo, J.; Peaper, D.R. Challenges in use of saliva for detection of SARS CoV-2 RNA in symptomatic outpatients. *J. Clin. Virol.* **2020**, 130, 104567.
109. da Costa Fernandes, P.A.; da Conceicao Ferreira, F.A.; Morais, O.M.; Ramos, C.M.; Fernandes, É.M.; da Rocha, S.A.; et al. Performance of saliva as a specimen to detect SARS-CoV-2. *J. Clin. Virol.* **2021**, 142, 104913.
110. Williams, E.; Bond, K.; Zhang, B.; Putland, M.; Williamson, D.A. Saliva as a noninvasive specimen for detection of SARS-CoV-2. *J. Clin. Microbiol.* **2020**, 58 (8), 10-128.
111. Silverman, J.D.; Hupert, N.; Washburne, A.D. Using influenza surveillance networks to estimate state-specific prevalence of SARS-CoV-2 in the United States. *Sci. Transl. Med.* **2020**, 12, eabc1126.
112. Michael-Kordatou, I.; Karaolia, P.; Fatta-Kassinou, D. Sewage analysis as a tool for the COVID-19 pandemic response and management: the urgent need for optimized protocols

- for SARS-CoV-2 detection and quantification. *J. Environ. Chem. Eng.* **2020**, 8 (5), 104306.
113. Wigginton, K. R.; Boehm, A. B. Environmental engineers and scientists have important roles to play in stemming outbreaks and pandemics caused by enveloped viruses. *Environ. Sci. Technol.* **2020**, 54, 3736–3739.
114. Yao, L.; Zhu, W.; Shi, J.; Xu, T.; Qu, G.; Zhou, W.; et al. Detection of coronavirus in environmental surveillance and risk monitoring for pandemic control. *Chem. Soc. Rev.* **2021**, 50, 3656–3676.
115. Bivins, A.; North, D.; Ahmad, A.; Ahmed, W.; Alm, E.; Been, F.; et al. Wastewater-based epidemiology: global collaborative to maximize contributions in the fight against COVID-19. *Environ. Sci. Technol.* **2020**, 54 (13), 7754–7757.
116. Murakami, M.; Hata, A.; Honda, R.; Watanabe, T. Wastewater-based epidemiology can overcome representativeness and stigma issues related to COVID-19. *Environ. Sci. Technol.* **2020**, 54 (9), 5311.
117. Peccia, J.; Zulli, A.; Brackney, D.E.; Grubaugh, N.D.; Kaplan, E. H.; Casanovas-Massana, A.; et al. Measurement of SARS-CoV-2 RNA in wastewater tracks community infection dynamics. *Nat. Biotechnol.* **2020**, 38 (10), 1164–1167.
118. Xiao, F.; Tang, M.; Zheng, X.; Liu, Y.; Li, X.; Shan, H. Evidence for Gastrointestinal Infection of SARS-CoV-2. *Gastroenterology.* **2020**, 158 (6), 1831–1833.
119. Zhang, W.; Du, R.H.; Li, B.; Zheng, X. S.; Yang, X.L.; Hu, B.; et al. Molecular and serological investigation of 2019-nCoV infected patients: implication of multiple shedding routes. *Emerg. Microbes Infect.* **2020**, 9 (1), 386–389.

120. Betancourt, W.Q.; Schmitz, B. W.; Innes, G.K.; Prasek, S. M.; Brown, K.M.; Stark, E. R.; et al. COVID-19 containment on a college campus via wastewater-based epidemiology, targeted clinical testing and an intervention. *Sci. Total Environ.* **2021**, 779, 146408.
121. Gibas, C.; Lambirth, K.; Mittal, N.; Juel, M. A.; Barua, V. B.; Brazell, L. R.; et al. Implementing building-level SARS-CoV-2 wastewater surveillance on a university campus. *Sci. Total Environ.* **2021**, 782, 146749.
122. Westhaus, S.; Weber, F. A.; Schiwy, S.; Linnemann, V.; Brinkmann, M.; Widera, M.; et al. Detection of SARS-CoV-2 in raw and treated wastewater in Germany—suitability for COVID-19 surveillance and potential transmission risks. *Sci. Total Environ.* **2021**, 751, 141750.
123. Giacobbo, A.; Rodrigues, M.A.S.; Zoppas Ferreira, J.; Bernardes, A.M.; de Pinho, M.N.; et al. A critical review on SARS-CoV-2 infectivity in water and wastewater. What do we know? *Sci. Total Environ.* **2021**, 774, 145721.
124. La Rosa, G.; Iaconelli, M.; Mancini, P.; Bonanno Ferraro, G.; Veneri, C.; Bonadonna, L.; et al. First detection of SARS-CoV-2 in untreated wastewaters in Italy. *Sci. Total Environ.* **2020**, 736, 139652.
125. Medema, G.; Heijnen, L.; Elsinga, G.; Italiaander, R.; Brouwer, A. Presence of SARS-Coronavirus-2 in sewage. *Environ. Sci. Technol. Lett.* **2020**, 7 (7), 511–516.
126. Randazzo, W.; Truchado, P.; Cuevas-Ferrando, E.; Simón, P.; Allende, A.; Sánchez, G. SARS-CoV-2 RNA in wastewater anticipated COVID-19 occurrence in a low prevalence area. *Water Res.* **2020**, 181, 115942.

127. Graham, K.E.; Loeb, S.K.; Wolfe, M.K.; Catoe, D.; Sinnott-Armstrong, N.; Kim, S.; et al. SARS-CoV-2 RNA in wastewater settled solids is associated with COVID-19 cases in a large urban Sewershed. *Environ. Sci. Technol.* **2021**, *55*, 488–498.
128. Carrillo-Reyes, J.; Barragán-Trinidad, M.; Buitrón, G. Surveillance of SARS-CoV-2 in sewage and wastewater treatment plants in Mexico. *J. Water Process. Eng.* **2021**, *40*, 101815.
129. Centers for Disease Control and Prevention. *National Wastewater Surveillance System (NWSS)*, **2021**. Available from <https://www.cdc.gov/healthywater/surveillance/wastewater-surveillance/wastewater-surveillance.html> (accessed 2021-07-06).
130. Ahmed, W.; Bertsch, P.M.; Bibby, K.; Haramoto, E.; Hewitt, J.; Huygens, F.; et al. Decay of SARS-CoV-2 and surrogate murine hepatitis virus RNA in untreated wastewater to inform application in wastewater-based epidemiology. *Environ. Res. J.* **2020a**, *191*, 110092.
131. Chin, A.W.H.; Poon, L.L.M. Stability of SARS-CoV-2 indifferent environmental conditions—Authors’ reply. *Lancet Microbe* **2020**, *1* (4), e146.
132. Cheng, C.; Jia, J.L.; Ran, S.Y. Polyethylene glycol and divalent salt-induced DNA reentrant condensation revealed by single molecule measurements. *Soft Matter* **2015**, *11* (19), 3927–3935.
133. Diamond, A.D.; Hsu, J.T. Protein partitioning in PEG/dextran aqueous two-phase systems. *AIChE J.* **1990**, *36* (7), 1017–1024.

134. Lu, D.; Huang, Z.; Luo, J.; Zhang, X.; Sha, S. Primary concentration: The critical step in implementing the wastewater based epidemiology for the COVID-19 pandemic: A mini-review. *Sci. Total Environ.* **2020**, 747, 141245.
135. Ahmed, W.; Bertsch, P.M.; Bivins, A.; Bibby, K.; Farkas, K.; Gathercole, A. Comparison of virus concentration methods for the RT-qPCR-based recovery of murine hepatitis virus, a surrogate for SARS-CoV-2 from untreated wastewater. *Sci. Total Environ.* **2020b**, 739, 139960.
136. Wurtzer, S.; Marechal, V.; Mouchel, J.M.; Maday, Y.; Teyssou, R.; Richard, E.; et al. Evaluation of lockdown effect on SARS-CoV-2 dynamics through viral genome quantification in waste water, Greater Paris, France, 5 March to 23 April 2020. *Eurosurveillance.* **2020**, 25 (50), 2000776.
137. Wu, F.; Xiao, A.; Zhang, J.; Moniz, K.; Endo, N.; Armas, F.; et al. SARS-CoV-2 titers in wastewater foreshadow dynamics and clinical presentation of new COVID-19 cases. *Sci. Total Environ.* **2022**, 805, 150121.
138. Wu, F.; Xiao, A.; Zhang, J.; Gu, X.; Lee, W.L.; Kauffman, K.; et al. SARS-CoV-2 titers in wastewater are higher than expected from clinically confirmed cases. *mSystems* **2020**, 5 (4), e00614-20.
139. Gonzalez, R.; Curtis, K.; Bivins, A.; Bibby, K.; Weir, M. H.; Yetka, K.; et al. COVID-19 surveillance in southeastern Virginia using wastewater-based epidemiology. *Water Res.* **2020**, 186, 116296.
140. Chik, A.H.; Glier, M.B.; Servos, M.; Mangat, C.S.; Pang, X.L.; Qiu, Y.; D'Aoust, P.M.; et al. Comparison of approaches to quantify SARS-CoV-2 in wastewater using RT-qPCR:

Results and implications from a collaborative inter-laboratory study in Canada. *J. Environ. Sci.* **2021**, 107, 218–229.

141. Ahmed, W.; Bivins, A.; Bertsch, P.M.; Bibby, K.; Choi, P.M.; Farkas, K.; et al. Surveillance of SARS-CoV-2 RNA in wastewater: Methods optimization and quality control are crucial for generating reliable public health information. *Curr. Opin. Environ. Sci. Health.* **2020c**, 17, 82–93.

Chapter Two: Development of a Method for the Detection of SARS-CoV-2 in

Saliva and Gargle Samples*

*This chapter has been published and was modified from Liu, Y.; Kumblathan, T.; Feng, W.; Pang, B.; Tao, J.; Xu, J.; et al. On-site viral inactivation and RNA preservation of gargle and saliva samples combined with direct analysis of SARS-CoV-2 RNA on magnetic beads. *ACS Meas. Sci. Au* **2022**, 2, 224–232. I conceptualized experimental design, performed the experiments, data collection and analysis, text, and schematic composition, and revised the overall manuscript. Liu Y and I contributed equally. Feng W, Pang B, Tao J, Xu J, Xiao H, Joyce MA, Tyrrell DL, Zhang H, and Li XF contributed to editing the manuscript.

* The research project, of which this thesis is a part, received research ethics approval from the University of Alberta Research Ethics Board, project name “Saliva and gargle test for COVID-19”, No. Pro00117059, April 1 2020.

2.1 Introduction

As discussed previously, the gold standard method for the detection of SARS-CoV-2 involves three steps: collection of an upper respiratory specimen using a NPS, extraction of viral RNA using commercial kits, and detection of viral RNA using the RT-qPCR. The insertion of the NPS into the nasopharynx is uncomfortable, and irritation during NPS sampling may induce sneezing or coughing that expels viral particles, resulting in potential contamination and transmission of SARS-CoV-2 to healthcare personnel, other individuals, and objects in the area.¹ The detection sensitivity of the gold standard method is affected by variations in the time of collection, clinical course of infection, and NPS sampling skills.²⁻⁵

Oral fluids, such as saliva and gargle samples, have been proposed as alternatives to NPS for the detection of SARS-CoV-2.⁶⁻¹³ Respiratory viruses can enter the oral cavity from both the lower respiratory tract and nasopharynx. The viral shedding within the oral cavity can be captured in the saliva and gargle sample collected.¹⁴ During the SARS outbreak of 2003, throat wash and saliva was used for the diagnosis of SARS infection which demonstrates the applicability of oral fluids for viral detection.¹⁵ There are several advantages in using saliva and gargle samples for the detection of SARS-CoV-2. Saliva and gargle collection is fast, easy, and can be conveniently done at home. Self-collection of samples avoids the overcrowding of testing centers, minimizes the spread of disease, and reduces the need for healthcare professionals.¹⁶⁻¹⁹ Two studies have demonstrated that ~88% of patients were willing to self-collect saliva samples and ~99% were willing to self-collect gargle samples.^{17,20} Saliva and gargle collection is more comfortable and is suitable for various population groups, especially the elderly and children. The use of saliva and gargle samples can mitigate the shortage of swabs and viral transport media due to the global demand for NPS and molecular testing of COVID-19.^{1,21} SARS-CoV-2

in saliva and gargle samples has adequate stability for at least 7 days at a variety of storage temperatures, which allows ample time for sample collection and delivery to a testing laboratory.^{22,23} In addition to clinical diagnosis, saliva and gargle have been considered useful for repeated sampling, sample banking, mass testing for asymptomatic infections, testing in rural and resource-limited locations, and point-of-care testing applications. Examples of these applications have been listed below in Tables 2.1^{6-9,19} and Table 2.2¹⁰⁻¹³.

Table 2.1. Comparison of reported methods on inactivation, RNA release and extraction for the detection of SARS-CoV-2 in saliva and gargle samples.^{6-9,19} The checkmarks indicate the study addressed a certain aspect. The green color indicates aspects that have similar advantages to the VIP-Mag method (my method, details discussed later). The yellow color denotes aspects that are less advantageous than the VIP-Mag method.

Study	Sample	Inactivation/Extraction	RNA Release & Stability	Detection Method	Sensitivity
VIP-Mag Method	BOTH	✓	✓	✓	✓
	Saliva & Gargle	Single Tube Method (sample collection, inactivation, lysis, & maintains RNA stability) Heat at 55°C, 10 min	1 week at 4°C & Room Temperature Directly inputted into RT-qPCR without the need for elution/purification	RT-qPCR	25 RNA copies/200 µL of sample
Ranoa et al., 2020	Saliva	✓	✓	✓	✓
	Diluted in TE/TBE buffer to reduce viscosity	Heat at 95°C for 30 minutes TBE buffer and Tween 20	24 hours at 4°C (RNA) Directly inputted into RT-qPCR without the need for elution/purification	RT-qPCR	500-1000 viral particles/mL of saliva
Vogels et al., 2020	Saliva	✓	✓	✓	✓
		Heat at 95°C for 5 minutes Proteinase K	1 week at 30°C, 4°C & Room Temperature (SARS-CoV-2 in saliva pre-inactivation/extraction)	RT-qPCR	6-12 SARS-CoV-2 copies/µL of saliva

			Directly inputted into RT-qPCR without the need for elution/purification		
Lalli et al., 2021	Saliva	✓	✗	✓	✓
	Diluted in phosphate buffered saline (PBS) to reduce viscosity	Heat at 65 °C for 15 minutes, 95 °C for 5 minutes, and cooled to 4 °C RNAsecure & Proteinase K to each sample	RNA stability not mentioned Directly inputted into RT-qPCR and LAMP without the need for elution/purification	RT-qPCR LAMP	100 viral genomes/reaction
Yang et al., 2021	Saliva	✓	✓	✓	✓
		Heat at 95 °C for 10 minutes Saliva stabilization solution (5 mM TCEP, 2 mM EDTA, 29 mM NaOH, 100 µg/mL Proteinase K)	4 days at 4°C (RNA)	LAMP	200 virions/µL of saliva
Tilley et al., 2021	Gargle	✓	✗	✓	✗
	Saline solution	Heat at 65 °C for 20 minutes and cool to room temperature for 5 minutes	RNA stability not mentioned Directly inputted into RT-qPCR without the need for elution/purification	RT-qPCR Single-tube hemi-nested real-time-qPCR (STHN-RT-qPCR) to enhance the overall sensitivity	97.37% match to NPS positive samples (viral number or copy number not mentioned)

Table 2.2. A summary of reported methods that were used to detect SARS-CoV-2 in pooled samples.¹⁰⁻¹³ The checkmarks indicate that the study addressed certain aspects. The checkmarks indicate the study addressed a certain aspect. The green color indicates aspects that have similar advantages to the VIP-Mag method (my method, details discussed later). The yellow color denotes aspects that are less advantageous than the VIP-Mag method.

Study	Sample	Inactivation/ Extraction	RNA Stability	Detection Method	Results
VIP-Mag Method	Both	✓	✗	✓	✓
	Saliva	Single Tube Method (sample collection, inactivation, lysis,	1 week at 4°C & Room Temperature (RNA)	RT-qPCR	Positive detectable even after

		& maintains RNA stability) Heat at 55°C, 10 min	Directly inputted into RT-qPCR without the need for elution/purification		diluting by 32 times
Barat et al., 2021	Saliva	✓	✗	✓	✓
		Proteinase K, vortexed and heated for 5 min at 95°C NucliSENS easyMAG Panther Fusion Cobas 6800	Not mentioned	RT-qPCR	90-94% sensitivity in 5 pooled samples
Bokelmann et al., 2021	Gargle	✓	✗	✓	✓
	Sterile water	Lysis/binding buffer (Tris-HCl, LiCl, LiDS, EDTA, DTT) Quick extract (Lucigen)	Not mentioned	RT-qPCR capture and improved loop-mediated isothermal amplification (CAP-LAMP)	1 positive in 25 pooled samples can be detected
Kellner et al., 2022	Gargle	✓	✗	✓	✓
	Saline solution Hank's balanced salt solution	Guanidine thiocyanate KingFisher magnetic particle processor DNaseI for 15 minutes at 37°C QuickExtract DNA extraction solution (Lucigen)	Not mentioned	RT-qPCR LAMP	1 positive in 100 pooled samples can be detected
Willeit et al., 2021	Gargle	✓	✗	✓	✓
	Saline solution or a modified Hank's balanced salt solution 2 M 1,4-dithiothreitol	10 pooled samples mixed using KingFisher Flex mixer Lysis buffer (Tris, GITC, EDTA, 2% Triton	Not mentioned	RT-qPCR	This method was used to screen 10 734 participants from 245 schools in Austria.

	added to reduce viscosity	X-100, DTT) added and incubated for 10 min at room temperature KingFisher Flex Magnetic Particle Processor System Carboxylated magnetic bead CyBio Felix System			
--	---------------------------	--	--	--	--

Nevertheless, the use of saliva and gargle samples for the detection of SARS-CoV-2 faces several analytical challenges. Firstly, the viral load of SARS-CoV-2 in saliva and gargle samples may be lower than those in a properly collected NPS. Consequently, the false negative rate of SARS-CoV-2 in saliva samples may be slightly higher than that in NPS samples.²⁴ Furthermore, compared to saliva samples, the level of SARS-CoV-2 in gargle samples could be further diluted by the saline solution used for sample collection. Secondly, compared to NPS, saliva and gargle samples contain a more complicated sample matrix, affecting efficient RNA extraction and subsequent analysis. Saliva samples are heterogeneous and viscous, often containing sputum, food particles, metabolites, and various microorganisms. Commercial RNA extraction kits used for NPS samples cannot be directly used for oral fluids because it is difficult to efficiently extract RNA and remove RT-qPCR inhibitors from oral fluids, especially saliva. Researchers have attempted to dilute saliva samples prior to RNA extraction to minimize inhibitor impact, but dilution decreases detection sensitivity.^{17,25} Other studies have tried to bypass RNA extraction and attempted to detect SARS-CoV-2 directly in saliva using RT-qPCR. However, these attempts were not successful and had substantially lower positive results [60% (95% CI: 49%–70%)] than

studies which had an extraction step [89% (95% CI: 83%–94%)].²⁴ Furthermore, on-site inactivation of virus during self-collection avoids potential transmission risks during sampling. However, released viral RNA is prone to digestion by enzymes such as RNases present in saliva and gargle samples. A simple and fast approach to detect SARS-CoV-2 in saliva and gargle must maintain the stability of the released viral RNA during the inactivation and treatment of the saliva and gargle samples.

To confront these challenges and facilitate the use of saliva and gargle samples for the detection of SARS-CoV-2, I introduced an integrated sampling and analysis approach that enables simultaneous sample collection, SARS-CoV-2 inactivation, RNA preservation, and sensitive detection. I carefully formulated a viral inactivation and RNA preservation (VIP) buffer which served the dual purpose of inactivating SARS-CoV-2 and preserving the released viral RNA. The approach and reagents used for the self-collection of saliva and gargle samples are compatible with the subsequent magnetic (Mag) bead-based RNA capture to concentrate the viral RNA. Direct analysis of the viral RNA on the beads without requiring an elution step maximizes the sample input amount and enhances the sensitivity of the assay. Figure 2.1 shows the overall process and benefits of an integrated method for the sensitive detection of SARS-CoV-2 in gargle and saliva samples. The analytical strategy and integrated protocol make it feasible to achieve the objective of enhancing safety during sample collection and delivery while maintaining RNA integrity, thus enabling the efficient concentration and sensitive detection of SARS-CoV-2 in saliva and gargle samples.

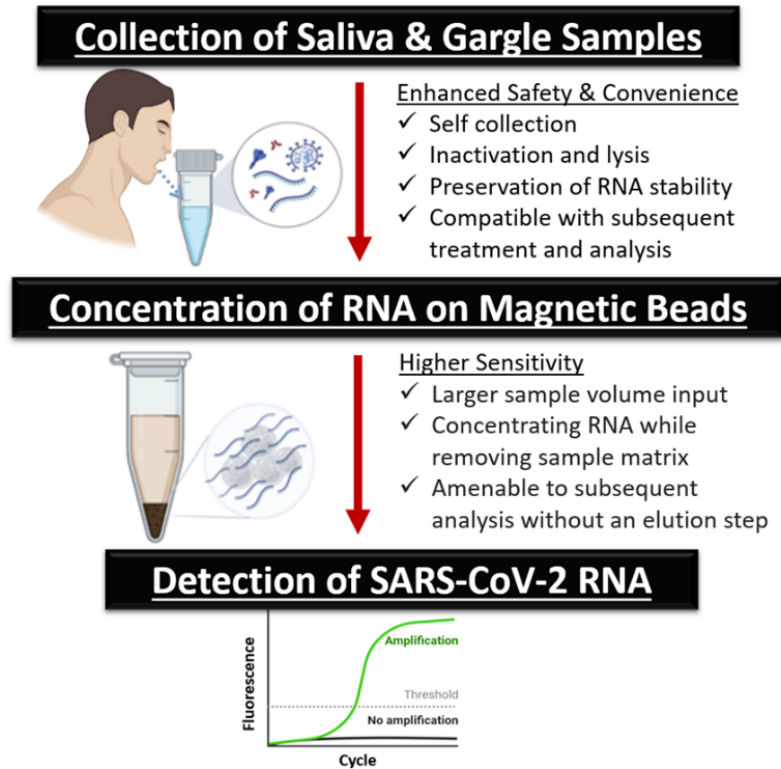


Figure 2.1 The overall method (VIP-Mag) consists of three components: (1) self-collection of gargle or saliva, with simultaneous inactivation of the virus and preservation of the viral RNA, (2) concentration of RNA onto magnetic beads, and (3) direct RT-qPCR analysis of the specific targets of SARS-CoV-2 RNA without the need for an elution step.

2.2 Experimental

2.2.1 Sample Collection

Saliva and gargle samples were collected from 23 adult volunteers. Two of these volunteers were COVID-19 patients who confirmed positive for SARS-CoV-2 using the clinical NPS RT-qPCR test. Multiple samples from the two SARS-CoV-2 positive volunteers and other SARS-CoV-2 negative volunteers were collected daily for over 4 weeks. The first SARS-CoV-2 positive volunteer collected 5 mL of saliva in sterile 50 mL conical tubes (RNase and DNase

free; Corning, Corning, NY, USA) during the first week and then collected only morning gargle samples in the following 3 weeks. During the first week, saliva samples were collected first thing in the morning, at noon, evening, and at night. Saliva was produced by actively pooling and spitting the saliva into sterile collection containers.

The second SARS-CoV-2 positive volunteer collected gargle samples first thing in the morning, at noon, evening, and at night during the first week and subsequently collected a single morning gargle sample every day for 3 weeks. An isotonic saline solution was used to collect gargle samples. Isotonic saline is the recommended by several studies for gargle samples.^{17,26} One packet of NeilMed Sinus Rinse Extra Strength (NeilMed Pharmaceuticals, Santa Rosa, CA, USA) was dissolved in 480 mL of store-bought bottled spring water (Nestlé, PureLife, Canada). Five milliliters of this saline solution were aliquoted into a sterile 50 mL conical tube (RNase and DNase free; Corning). Volunteers were instructed to pour some saline (5 mL) into their mouths, gargle, and swish for 30 s before spitting back into the same 50 mL conical tube. Then, 200 μ L of saliva or gargle sample was pipetted and mixed with 600 μ L of VIP buffer which was pre-pipetted in an eppendorf tube and stored at -20°C until time of analysis. All samples were voluntary, and consent was given for testing. Ethics approval was obtained from the University of Alberta's Research Ethics Board (No.Pro00117059).

2.2.2 VIP Buffer Preparation

The VIP buffer was prepared by adding 2-mercaptoethanol (2-ME) (final concentration 1%), Triton X-100 (2.5%), proteinase K (170 ng/ μ L), and glycogen (17 ng/ μ L) to 10mL of RLT lysis buffer. The cost of this buffer and the magnetic beads for the subsequent step was approximately \$1.1 per sample, compared to \sim \$5.6 per sample for the QIAamp Viral RNA Mini Kit from QIAGEN. To formulate a less expensive VIP buffer, I replaced the commercial RLT

buffer with guanidinium isothiocyanate (GITC). I tested various concentrations of GITC, ranging from 2M to 8M, to see which concentration was most efficient at extracting RNA. The optimized concentrations of the key ingredients of the in-house VIP buffer were 6 M guanidinium isothiocyanate, 3% 2-mercaptoethanol, 2.5% Triton X-100, 170 ng/μL of proteinase K, and 17 ng/μL of glycogen. The combined cost of this VIP buffer and the magnetic beads was ~\$0.55 per sample.

2.2.3 Mag Beads Buffer Preparation and Sample Processing

Five hundred microliters of solid phase reversible immobilization select (SPRIselect, purchased from Beckman Coulter) beads (average diameter 1 μm) were washed with RNase-free water three times and resuspended in 10 mL of bead-binding buffer (20 mM Tris-HCl pH 8.0, 2 M NaCl, 36% PEG-8000, and 2 mM EDTA). This magnetic bead suspension was stored at 4 °C (stable for at least one month). Saliva or gargle samples treated with VIP buffer on-site or mixtures freshly prepared by mixing 200 μL of saliva or gargle samples with 600 μL of VIP buffer in the lab were heated at 55 °C for 10 minutes and then centrifuged at 13,000 g for 5 min. Next, the supernatant was transferred into a new tube and then 400 μL of the magnetic beads suspension and 200 μL of pure ethanol were added into this tube and vortexed for 10 s followed by shaking at room temperature for 10 min. Centrifugation at 13,000 g for 2 minutes was followed by standing the tubes upright on a magnetic stand to collect the magnetic beads. The resulting beads were washed twice with 0.8 mL of 75% ethanol, followed by air drying for 5 min, and were resuspended in 13.5 μL of RNase-free water containing 200 ng/μL of the proteinase K inhibitor.

2.2.4 Pooled Oral Fluids Preparation

Gargle samples from 10 adult volunteers, who were previously confirmed negative for SARS-CoV-2, were combined to form a pooled negative gargle sample. This pooled negative gargle sample was used to dilute SARS-CoV-2 positive gargle samples 8, 16, and 32 times, to simulate a mass population testing scenario in which a single positive is present in a pool of 8, 16, and 32 samples, respectively. Three SARS-CoV-2 positive samples were tested for this purpose. The concentrations of SARS-CoV-2 RNA in these positive samples before dilution ranged from 120 copies/200 μ L gargle (Ct value 32.2) to 1020 copies/200 μ L gargle (Ct value 29.2). The pooled samples of each dilution factor were prepared in triplicate.

2.2.5 Spiking of Saliva and Gargle Samples with Pseudo-Virus

Saliva and gargle samples from 10 adult volunteers who were previously confirmed negative for SARS-CoV-2 were pooled to form a SARS-CoV-2 negative saliva sample and negative gargle sample, respectively. A pseudo-virus solution (purchased from SeraCare) with known RNA concentrations was added into the negative saliva or gargle pooled samples to generate synthetic samples at the indicated concentrations in the following experiments. The pseudo-virus solution contained both pseudo-virus particles and free viral RNA, and the total viral RNA copies in solution were determined as follows. The pseudo-virus solution was mixed with a QuickExtract RNA extraction solution at a 1:1 ratio in triplicates and vortexed for 10 min. Two microliters of the resulting mixture were added directly into the RT-qPCR reaction as the template because the QuickExtract RNA extraction solution itself does not inhibit RT-qPCR.²⁷ The concentration of viral RNA in the pseudo-virus solution was 13 copies/ μ L.

2.2.6 RT-qPCR Detection of Concentrated RNA Directly from Magnetic Beads

The TaqPath 1-Step RT-qPCR Master Mix (Thermo Fisher Scientific) and CDC N1 primer-probe from the 2019-nCoV RUO kit (IDT) were used according to the manufacturer's instructions. The RT-qPCR final reaction volume of 20 μL contained 13.5 μL of the resuspended magnetic bead solution obtained directly from the concentration step, 5 μL of TaqPath 1-Step RT-qPCR Master Mix, and 1.5 μL of primer-probe mix (300 nM each primer, 200 nM probe) for the N1 gene segment. The RT-qPCR thermal cycling steps were as follows: 25 °C for 2 min, 50 °C for 15 min, 95 °C for 2 min, and 45 cycles of 95 °C for 3 s and 56 °C for 30 s. RT-qPCR was performed on a QuantStudio 3 Real-Time PCR System (Applied Biosystems, Thermo Fisher Scientific) using the QuantStudio Design and Analysis Software v1.5.1.

2.3 Results and Discussion

2.3.1 Development of a VIP Buffer for the Self-Collection of Gargle and Saliva

Samples

Gargle and saliva samples are heterogeneous and viscous, often containing food remnants and proteins, including RNases that can digest free RNA. I focused on developing a VIP buffer capable of (1) inactivating SARS-CoV-2, (2) digesting viscous materials and denaturing proteins including RNases, and (3) maintaining RNA integrity in the sample (Figure 2.1). Previous research has shown that surfactants, such as Triton X-100 (2.5–10%), can destroy the envelopes of virions and that the combination of Triton X-100 with a guanidinium solution enhanced the inactivation of SARS and SARS-CoV-2.^{8,28,29} Two studies also reported that surfactants and guanidinium, such as those in the commercially available (QIAGEN) RNA extraction buffers ATL (containing 1–10% SDS), VXL (containing 30–50% GuHCl and 2.5–10% Triton X-100), and buffer RLT (containing guanidinium isothiocyanate) were able to inactivate SARS-CoV-2 at a

viral load as high as 10^6 TCID₅₀/mL (median tissue culture infectious dose per milliliter).^{29,30}

After the treatment of SARS-CoV-2 with either the RLT buffer plus mercaptoethanol or 0.5% Triton X-100 for 10 min, no infection was detectable in Vero cell cultures incubated with the treated SARS-CoV-2 sample.²⁹ However, these studies did not aim at preserving or stabilizing the released RNA from the inactivated virus.

To understand which formulation of extraction buffer was most efficient, I first tested the commercially available QuickExtract plant DNA extract solution (containing SDS) and RLT lysis buffer (containing guanidinium), as well as with the addition of 2-mercaptoethanol (2-ME), proteinase K, and Triton X-100. The analyses of gargle samples containing 3900 copies of viral RNA showed that a lower threshold cycle (Ct) was needed to achieve detection of the viral RNA when the RLT buffer was used as compared to the QuickExtract plant DNA extract solution (Figure 2.2). Guanidinium in the RLT buffer is known to reduce disulfide bonds and denature proteins. Proteinase K and 2-ME were also used to further denature proteins and digest viscous materials in oral fluids as well as RNase enzymes that would otherwise degrade RNA. Triton X-100 was used to enhance inactivation of SARS-CoV-2 by destroying envelopes of virions. I also added glycogen as an RNA carrier to enhance the recovery of low concentrations of RNA from samples.^{31,32} I compared the use of a commercially available RNA carrier and glycogen for enhancing the recovery of low amounts of RNA from gargle samples. I added 10, 20, or 40 µg of glycogen or 1 µg of carrier RNA (recommended by MagMAX viral RNA isolation kit) into 200 µL of gargle samples containing 390 or 3900 copies of viral RNA. As shown in Figure 2.3, the addition of glycogen reduced the threshold cycles (Ct) needed for the detection of 390 copies of viral RNA, suggesting a better recovery of the viral RNA for detection. The effect of carrier RNA and glycogen on the higher concentration (3900 copies) of viral RNA is minimum.

Therefore, the optimal reagent concentrations for the formulation of the VIP buffer are 1% 2-ME, 2.5% Triton X-100, 170 ng/μL proteinase K, and 17 ng/μL glycogen, supplemented in 10mL of guanidinium-containing RLT lysis buffer. I found that 600 μL of this buffer was suitable for mixing with 200 μL of gargle or saliva samples. This VIP buffer is stable for at least 6 months at room temperature (Figure 2.4).

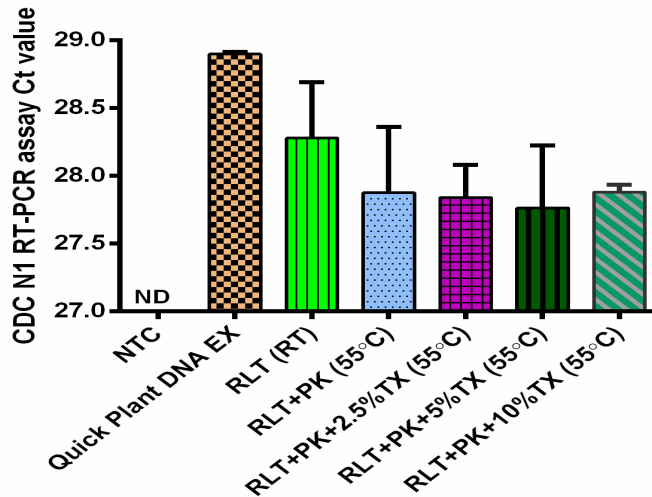


Figure 2.2. Detection of SARS-CoV-2 RNA in gargle samples treated with different reagents. Quick Plant DNA Extract, RLT lysis buffer, proteinase K (PK), and Triton X-100 were tested. The error bars represent one standard deviation of triplicate measurements. NTC (no template control) is the negative control. ND indicates no detectable SARS-CoV-2 RNA.

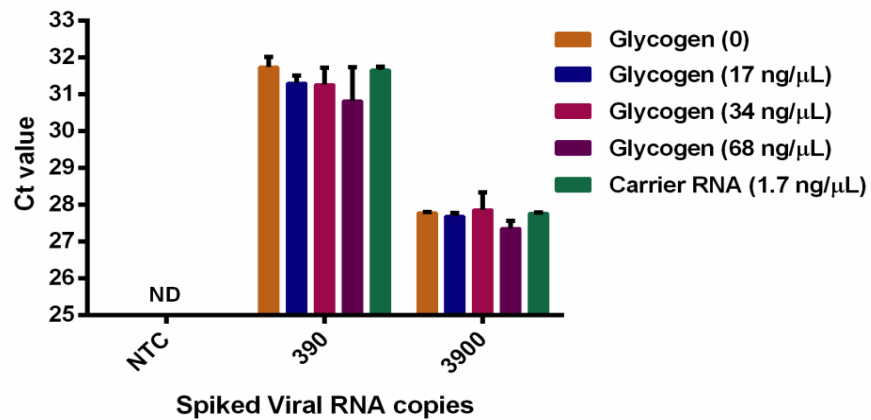


Figure 2.3. Detection of SARS-CoV-2 RNA in gargle samples treated with glycogen or carrier RNA. The gargle samples contained either 390 or 3900 copies of SARS-CoV-2 RNA. The error

bars represent one standard deviation of triplicate measurements. NTC (no template control) is the negative control. ND indicates no detectable SARS-CoV-2 RNA.

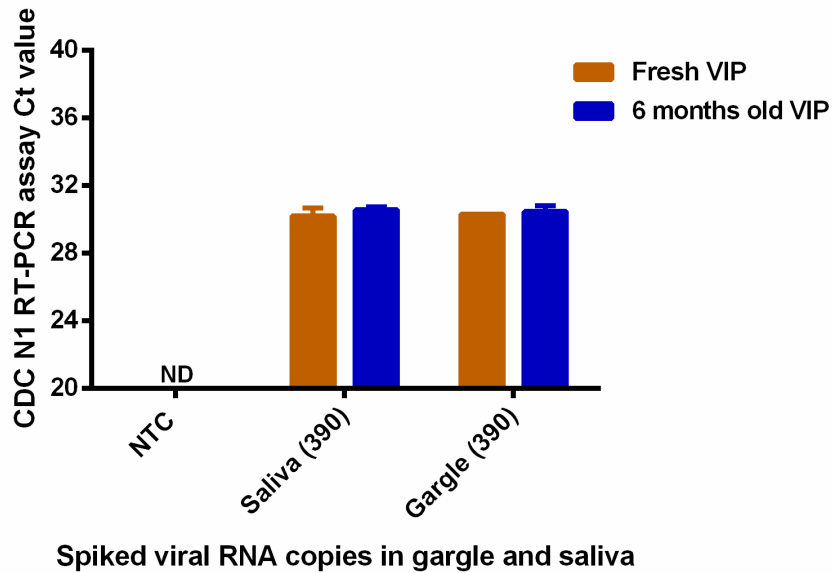


Figure 2.4. Detection of SARS-CoV-2 RNA in saliva and gargle samples treated with either freshly prepared VIP buffer or the VIP buffer stored at room temperature for six months. The saliva and gargle samples each contained 390 copies of viral RNA. The error bars represent one standard deviation of triplicate measurements. NTC stands for no template control. ND indicates no detectable SARS-CoV-2 RNA.

2.3.2 Concentration of Viral RNA onto Magnetic Beads and Direct RT-qPCR

Detection

Previous studies indicated that concentrations of viral RNA in gargle and saliva samples were lower than those in the NPS samples; consequently, the false negative rate was higher for gargle and saliva than for NPS tests.²⁴ To overcome this problem, I concentrated viral RNA on magnetic beads for the subsequent RT-qPCR detection to achieve two benefits: (1) increase the sensitivity of the assay by concentrating the target viral RNA, and (2) increase the specificity by removing sample matrix materials that could interfere with the RT-qPCR analysis. SPRIselect

beads and silica-based beads (TurboBeads) were tested. Ten or 20 μL of SPRIselect or TurboBeads were washed three times with RNase-free water and then added into an oral fluid sample containing 2000 copies of SARS-CoV-2 RNA (Figure 2.5). The samples were analyzed using RT-qPCR. After preliminary tests of various magnetic beads and volumes, I chose to use SPRIselect magnetic beads. I conducted RT-qPCR analysis of the viral RNA in the presence of magnetic beads with the final goal of conducting RT-qPCR analysis directly on the magnetic beads without the need for an RNA elution step. I found that the Ct values from the RT-qPCR analysis of 2000 copies of the SARS-CoV-2 RNA were similar in the presence and absence of the SPRIselect magnetic beads (Figure 2.5). These results indicate that the SPRIselect beads themselves do not inhibit RT-qPCR. I also optimized the concentration of PEG-8000 in the beads binding buffer for the efficient capture of RNA on the magnetic beads (Figure 2.6). The presence of PEG and Na^+ ions in the binding solution are important for the concentration of viral RNA on magnetic beads. This is because PEG removes the water surrounding the RNA, and Na^+ ions shield the negative phosphate backbones, allowing RNA to be readily adsorbed onto the magnetic beads.³³ I found that the optimal beads binding buffer consisted of 20 mM Tris-HCl at pH 8.0, 2 M NaCl, 2 mM EDTA, and 36% PEG-8000.

To simplify the assay, I conducted RT-qPCR detection of the concentrated viral RNA directly on the magnetic beads, achieving two main benefits: 1) shortening the sample preparation time, and 2) minimizing the loss of the target viral RNA. To prevent the potential problem of proteinase K unintentionally being adsorbed on the magnetic beads and inhibiting the RT-qPCR reaction, I also included a proteinase K inhibitor (tetrapeptidyl chloromethyl ketone) in the RT-qPCR reaction solution. Therefore, the magnetic beads which captured viral RNA from the gargle and saliva samples could be directly analyzed without the need for a traditional

RNA elution step. As previously mentioned, the magnetic beads themselves do not inhibit RT-qPCR.

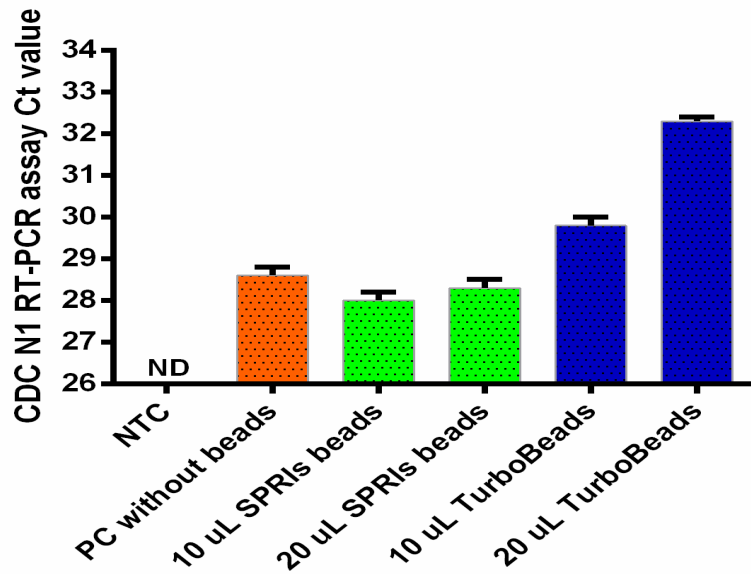


Figure 2.5. Detection of SARS-CoV-2 RNA in the absence or the presence of commercial beads (SPRIselect beads and TurboBeads). Different volumes of each were washed three times with RNase-free water and then added into a sample of 2000 copies of SARS-CoV-2 RNA. The samples were analyzed using RT-qPCR. The error bars represent one standard deviation of triplicate measurements. NTC denotes no template control. ND indicates no detectable SARS-CoV-2 RNA. PC indicates positive control.

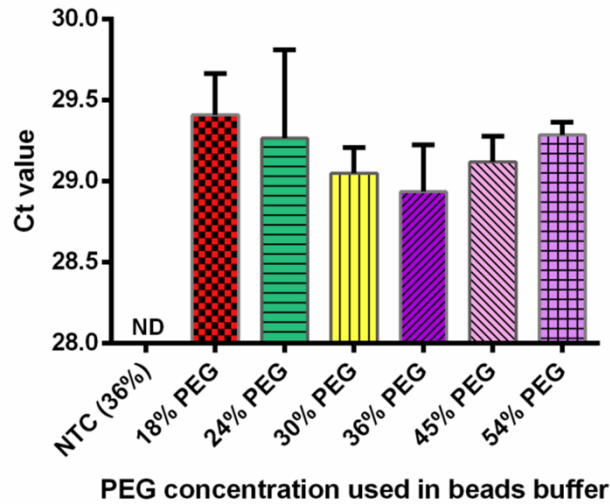


Figure 2.6. Comparison of different concentrations of PEG 8000 in the beads-binding buffer for concentrating viral SARS-CoV-2 RNA. The error bars represent one standard deviation of triplicate measurements. NTC (no template control) is negative control containing all reagents including 18% PEG. ND indicates no detectable SARS-CoV-2 RNA.

After optimizing all the reagent components, I tested the VIP-Mag-RT-qPCR method on pooled gargle samples and pooled saliva samples from 10 SARS-CoV-2 negative volunteers, as well as on the pooled samples supplemented with SARS-CoV-2 RNA at three concentrations, 65, 390, and 3900 copies per 200 μ L sample. The results show the positive detection of the N gene of SARS-CoV-2 in both the gargle and saliva samples containing as few as 65 copies of the viral RNA (Figure 2.7). For all three pairs of gargle and saliva samples containing varying concentrations of the viral RNA, the Ct values were consistent and as expected. These results demonstrate that the overall integrated VIP-Mag-RT-qPCR method is suitable for the determination of SARS-CoV-2 RNA in both gargle and saliva samples.

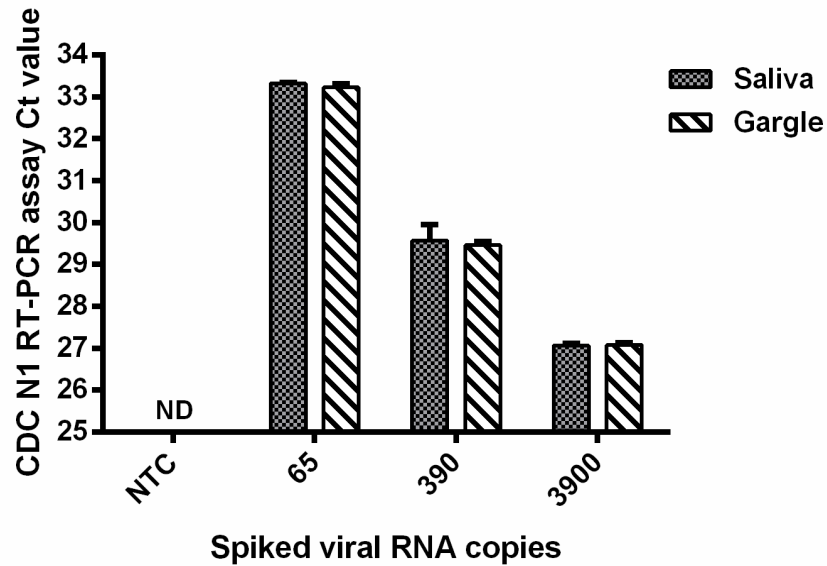


Figure 2.7. Detection of 65, 390, or 3900 copies of SARS-CoV-2 RNA in saliva and gargle samples using the VIP-Mag-RT-qPCR method. The error bars represent one standard deviation of triplicate measurements performed over three separate days. NTC (no template control) is negative control. ND indicates no detectable SARS-CoV-2 RNA.

2.3.3 Recovery of Viral RNA from Gargle and Saliva Samples

To test the overall recovery of the viral RNA, I prepared a pooled gargle sample from 10 SARS-CoV-2 negative volunteers and spiked each 200 μ L pooled sample with 65, 390, or 3900 copies of SARS-CoV-2 RNA. I determined that the overall recovery of the added SARS-CoV-2 RNA was 80–95% (Figure 2.8). For a comparison, I also added 65, 390, or 3900 copies of SARS-CoV-2 RNA into 200 μ L of RNase-free water and determined that the overall recovery of the SARS-CoV-2 RNA using my method was 93–95%. The recovery of 3900 copies of SARS-CoV-2 RNA from both the pooled gargle sample and the RNase-free water was identical (95%).

These results show acceptable overall recovery (80–95%) over a wide range of SARS-CoV-2 RNA concentrations (from 65 to 3900 copies per 200 μ L) from both gargle and water samples.

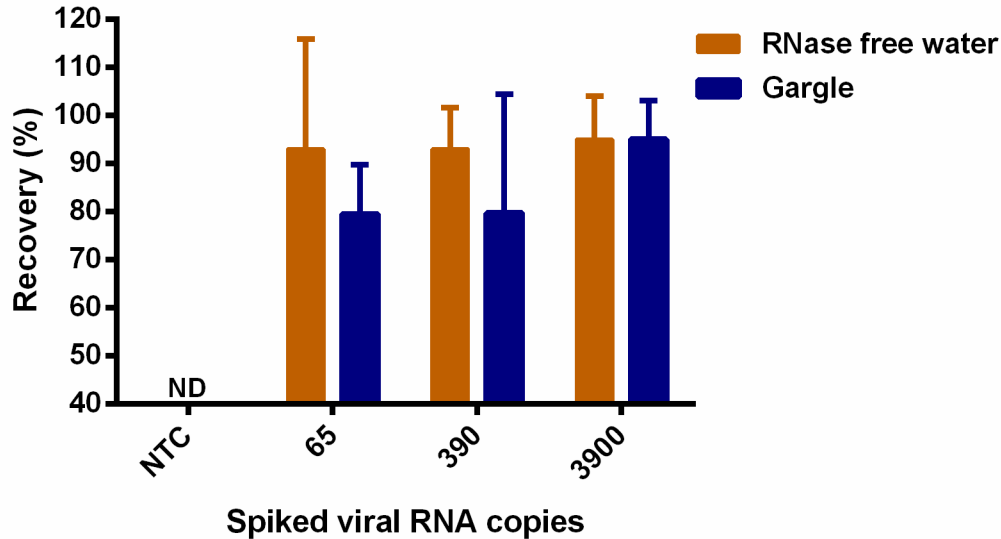


Figure 2.8. Recovery of viral RNA from RNase-free water and pooled gargle samples. RNase-free water and pooled negative gargle samples from healthy volunteers were each spiked with 65, 390, or 3900 copies of SARS-CoV-2 RNA. The samples were analyzed using the using the VIP-Mag-RT-qPCR method. The error bars represent one standard deviation of triplicate measurements. NTC (no template control) is negative control. ND indicates no detectable SARS-CoV-2 RNA.

2.3.4 Stability and Preservation of Viral RNA in the VIP Buffer

I tested the stability of SARS-CoV-2 RNA in gargle samples placed in the VIP buffer at room temperature or 4 °C for up to 8 weeks (Figure 2.9). I treated two gargle samples collected from a SARS-CoV-2 NPS-positive patient volunteer on different days. I mixed 200 μ L of each sample with 600 μ L of VIP buffer, generating nine replicate aliquots. I analyzed the first 3 aliquots on the sample collection day and stored the remaining 6 replicate aliquots for 1 week, 3 aliquots at 4 °C and the remaining 3 at room temperature. RT-qPCR analysis indicated that Ct

values are similar for all three sets of triplicates (Figure 2.9a). Therefore, SARS-CoV-2 RNA from oral fluids is stable at room temperature or 4 °C for at least 1 week when mixed with the VIP buffer. I also tested the stability of 65 and 390 copies of SARS-CoV-2 RNA added to pooled negative gargle samples (Figure 2.9b). The gargle samples containing 65 copies of viral RNA stored in VIP buffer remained positive after storage for up to 3 weeks at room temperature (Figure 2.9b). The samples containing 390 copies of viral RNA stored in VIP buffer remained positive after storage for 8 weeks at room temperature. There was no change in the Ct values between the samples stored for 1 week and 2 weeks. These results suggest that the VIP buffer is suitable for preserving samples for at least 2 weeks, which is particularly useful for testing in remote areas where the collected samples may take up to 2 weeks to be delivered to a clinical laboratory.

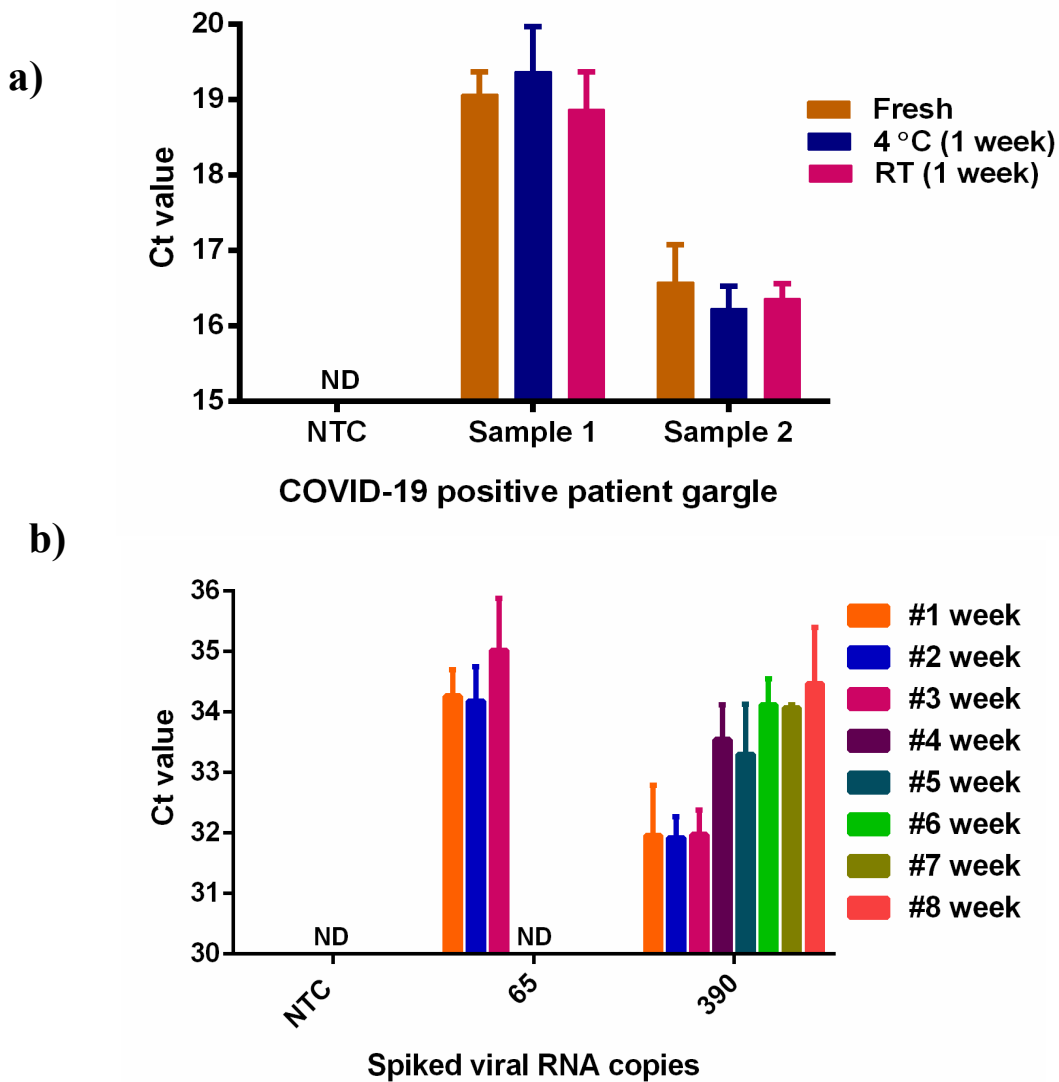


Figure 2.9. Evaluation of SARS-CoV-2 RNA stability in gargle samples collected from a) SARS-CoV-2 positive patient and b) spiked negative gargle samples and stored in VIP buffer. All the samples were treated with the VIP buffer. Triplicate aliquots of the stored samples were analyzed each week. NTC denotes no template control (negative control). ND indicates no detectable SARS-CoV-2 RNA.

2.3.5 Sensitivity and Reproducibility of the VIP-Mag-RT-qPCR Method

I tested the sensitivity of the VIP-Mag-RT-qPCR method for gargle samples prepared with known amounts of viral RNA. I added 5–200 copies of viral RNA into 200 μ L of pooled negative gargle samples. Each concentration condition was prepared in five replicates. I found that all five replicates (100%) of the gargle sample tested positive when the number of viral RNA copies was ≥ 25 (Figure 2.10). Ten RNA copies were detected in three replicates and 5 RNA copies were detected in two replicates. These results indicate that the integrated VIP-Mag-RT-qPCR method is very sensitive and capable of testing as few as 25 copies/200 μ L of gargle samples. I repeatedly tested samples containing very low concentrations of viral RNA on multiple days. I prepared 30 replicates of gargle samples containing 100 copies of viral RNA. These samples were processed and tested on 3 consecutive days (10 samples/day). The intraday coefficient variation was 1.7%, and the interday variation was 2.1%, indicating that the method yields consistent results even with only 100 copies of viral RNA is present in 200 μ L of gargle.

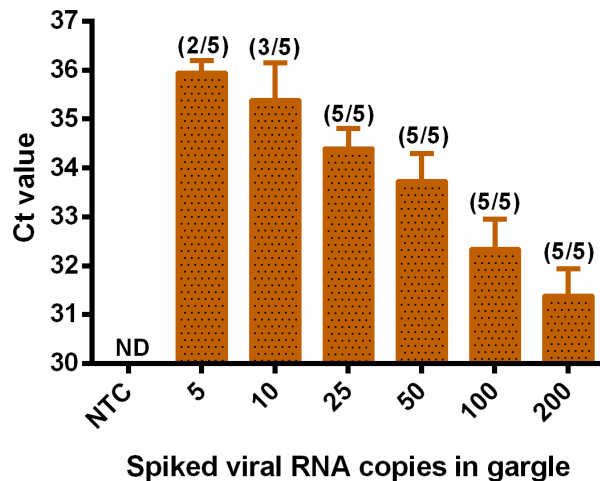


Figure 2.10. Determination of the sensitivity of the VIP-Mag-RT-qPCR method by analysis of samples containing different concentrations of SARS-CoV-2 viral RNA. The numbers on top of each bar indicate the number of samples tested positive in 5 replicates. The error bars represent

one standard deviation of Ct values from analyses of five replicate samples. NTC denotes no template control, and ND indicates no detectable SARS-CoV-2 RNA.

2.3.6 Comparison of Tap Water and Saline Used for Collecting Gargle Samples

Additionally, to explore whether tap water is suitable for collecting gargle samples, I compared the stability of SARS-CoV-2 RNA in tap water gargle and compared it to saline gargle samples. I obtained pooled tap water gargle and pooled saline gargle from SARS-CoV-2 negative volunteers. I added 65, 390, or 3900 copies of viral RNA to each type of the pooled gargle samples. I analyzed these samples after they were stored at room temperature for 2 h. The results showed that the tap water gargles containing 65 or 390 copies of the viral RNA required higher Ct to achieve detection than those for their saline gargle counterparts (Figure 2.11a). I also tested three saline gargle and three tap water gargle samples collected from a SARS-CoV-2 positive patient (Figure 2.11b). The Ct values are consistently higher for the tap water gargle samples than for the saline gargle samples. These results indicate possible degradation of viral RNA in tap water. Therefore, saline was used for the collection of all the gargle samples in this study.

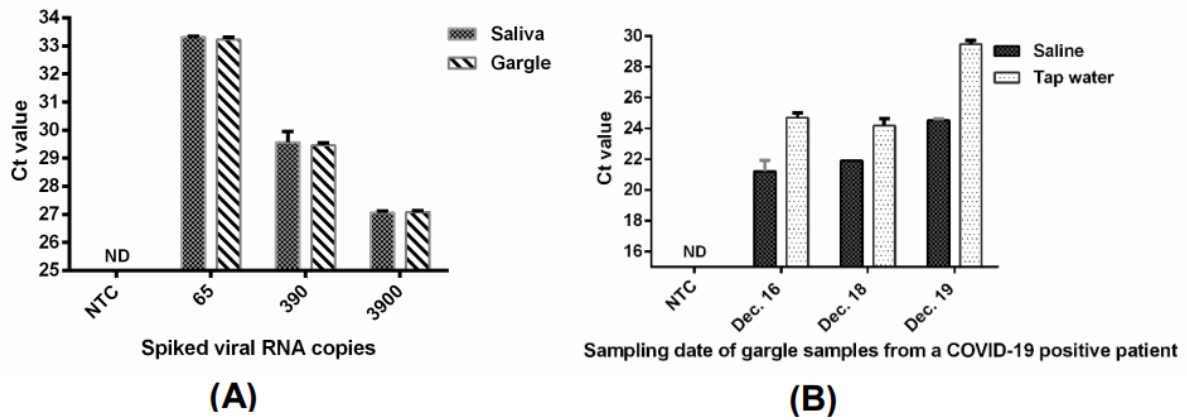


Figure 2.11. Detection of SARS-CoV-2 RNA in tap water gargle and saline gargle samples. A) Viral RNA added to tap water gargle or saline gargle samples and detected after storage at room temperature for 2 h. B) Detection of SARS-CoV-2 RNA in three tap water gargle and three saline gargle samples collected from a SARS-CoV-2 positive patient. The error bars represent one standard deviation of triplicate measurements. NTC (no template control) is negative control. ND indicates no detectable SARS-CoV-2 RNA.

2.3.7 Comparison of the VIP-Mag Method with the CDC-Recommended

Commercial Kit

I compared the VIP-Mag method with the commercial QIAamp Viral RNA Mini Kit recommended by the CDC for the detection of SARS-CoV-2. The QIAamp Viral RNA Mini Kit is widely used for extracting SARS-CoV-2 RNA from clinical NPS samples. I conducted concurrent triplicate analyses of three saliva samples and three gargle samples from SARS-CoV-2 patients. Compared to the VIP-Mag method, the method using the CDC recommended QIAamp Viral RNA Mini Kit consistently required more PCR cycles to achieve the positive detection of SARS-CoV-2 RNA (Figure 2.12). Although a similar volume (140–200 μ L) of

gargle and saliva samples was used with both methods, the QIAamp Viral RNA Mini Kit protocol required an elution step and only a fraction (5 μL recommended or 13.5 μL maximum) of the 60 μL eluted RNA could be analyzed. In contrast, the VIP-Mag method can concentrate RNA from samples and directly analyze RNA on magnetic beads without requiring an elution step. The difference in Ct values between these two methods was 3.2–6.8 cycles (Figure 2.12), corresponding to 9–111 times in analytical sensitivity. This improvement in the sensitivity of the VIP-Mag method can be attributed to a combination of the efficient concentration of RNA on magnetic beads and the elimination of PCR inhibitors from the samples. Incomplete removal of PCR inhibitors from gargle sample #2 by the QIAamp Viral RNA Mini Kit could be a reason for no difference in the Ct value (25.9) when the RNA input volume was increased from 5 to 13.5 μL (Figure 2.12). In principle, an increase of the RNA input volume would reduce Ct cycles needed for positive detection. However, if PCR inhibitors were not removed, the increase of the input sample volume would also increase the amount of PCR inhibitors affecting amplification. Thus, researchers using commercial kits to extract RNA have diluted saliva samples to lower the inhibitor concentrations, but the dilution of samples decreases the sensitivity of detection.^{17,25}

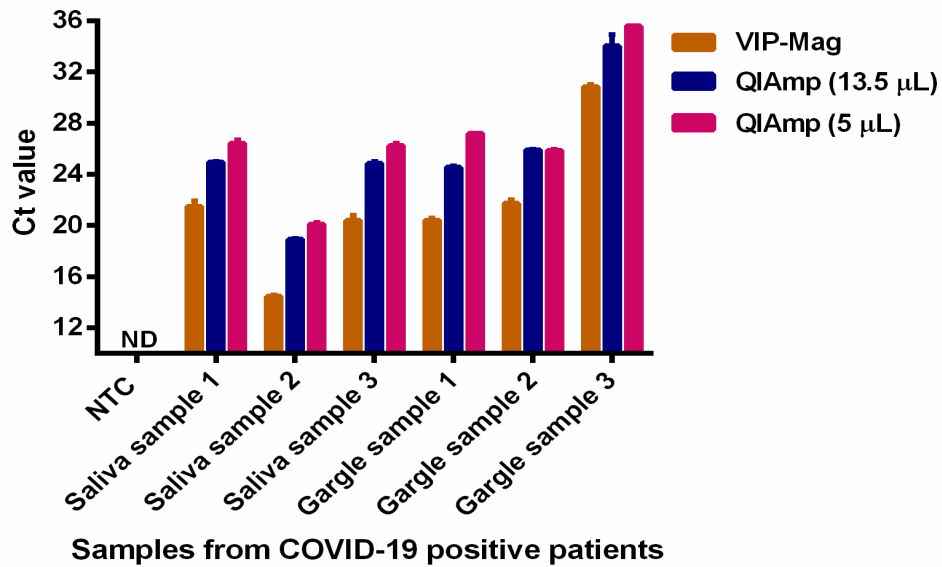


Figure 2.12. Comparison of the VIP-Mag method to the standard QIAamp Viral RNA Mini Kit used with RT-qPCR for the detection of SARS-CoV-2 positive patient’s saliva and gargle samples. The error bars represent one standard deviation from triplicate measurements. NTC indicates no template control. ND indicates no detectable SARS-CoV-2 RNA.

2.3.8 Detection of SARS-CoV-2 in Patients’ Gargle and Saliva Samples Collected from the Onset of Clinical Symptoms through Recovery

I monitored SARS-CoV-2 levels in gargle and saliva samples from two NPS-confirmed SARS-CoV-2 positive patients for about a month, covering the period of clinical symptoms and recovery. In parallel, I also tested samples from 21 volunteers, including two people who were NPS-confirmed SARS-CoV-2 negative and lived in the same house with an NPS-confirmed SARS-CoV-2 positive patient. In total, 123 samples were collected from two positive patients and 56 samples were collected from two negative volunteers.

The first patient volunteer had initial symptoms of a mild cough and fever before testing positive for SARS-CoV-2. Self-collection of saliva and gargle samples started on the fifth day after the positive NPS test and continued for 25 days. I analyzed the gargle and saliva samples and estimated the viral RNA levels by converting Ct values to viral RNA copies based on the RT-qPCR standard curve of the N1 gene segment (Figure 2.13). As shown in Figure 2.14, as many as 10^7 copies of the viral RNA were present in 200 μ L of saliva or gargle samples. All the samples collected from this patient throughout the 25 days had detectable SARS-CoV-2 RNA. Parallel analyses of saliva and gargle samples collected on the same day from two negative volunteers who lived in the same house as the patient showed no detectable SARS-CoV-2 RNA. These results confirmed that there was no false positive in the detection of SARS-CoV-2 RNA using the VIP-Mag method.

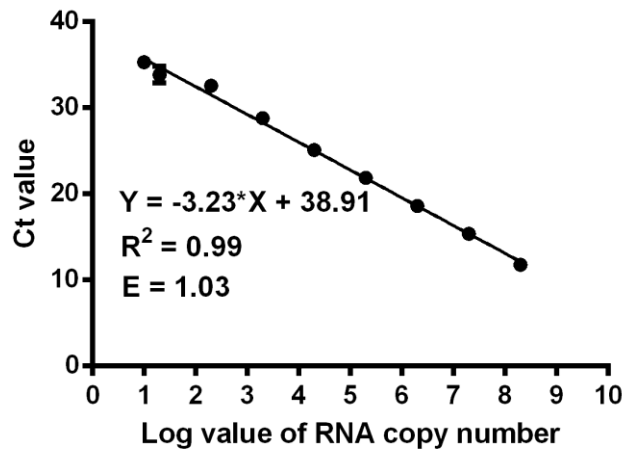


Figure 2.13. Standard curve from the RT-qPCR analysis of the N1 gene segment (CDC). The log values of the numbers of pure SARS-CoV-2 RNA are plotted against the corresponding Ct values. E represents PCR efficiency which was calculated using the equation: $E = -1 + 10^{(-1/\text{slope})}$, where slope refers to the slope of the standard curve. This standard curve was used to quantify the amounts of SARS-CoV-2 RNA in samples.

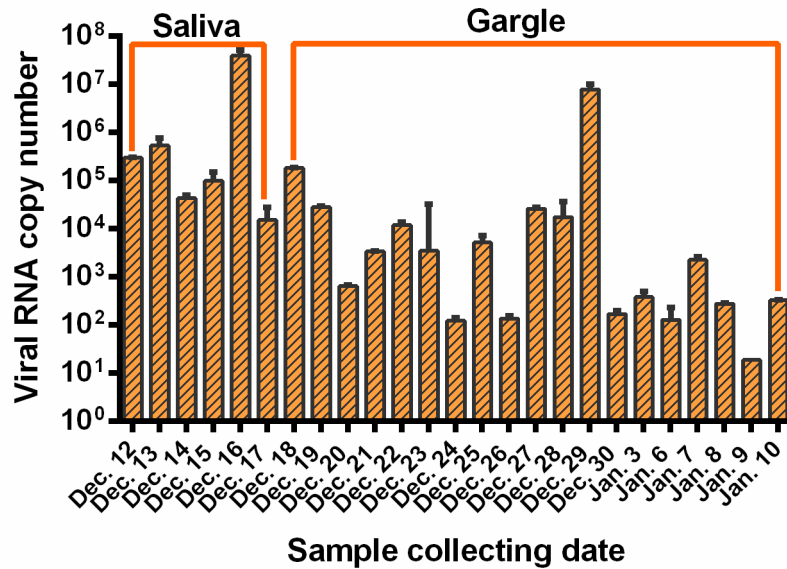


Figure 2.14. Monitoring SARS-CoV-2 RNA levels in saliva and gargle samples collected from a NPS-confirmed SARS-CoV-2 positive patient. Multiple samples were collected every day for 25 days from the onset of clinical symptoms. The error bars represent one standard deviation of duplicate measurements.

The second SARS-CoV-2 positive patient volunteer started to have a fever 2 days before the positive NPS test. The patient provided morning gargle samples daily from the 3rd day to 33rd day since the positive test and collected four gargle samples daily from the 4th day to the 11th day. The data from all the morning gargles is shown in Figure 2.15. These results show a large variation of the viral RNA levels in the gargle samples collected over time. While some samples had 10⁷ copies of viral RNA in 200 μ L gargle, several samples had viral RNA concentrations below 10² copies in 200 μ L gargle. To confirm the positive detections of these low concentrations of viral RNA, I concurrently analyzed gargle samples collected from 19 volunteers who were SARS-CoV-2 negative. All the samples from the negative volunteers had no detectable SARS-CoV-2 RNA. Interestingly, both SARS-CoV-2 positive patients had detectable SARS-CoV-2 RNA in their gargle samples for more than 2 weeks. A systematic

review of 28 studies has shown that the median duration of SARS-CoV-2 RNA shedding from respiratory sources was 18.4 days. This review demonstrated that the duration of SARS-CoV-2 RNA shedding has high heterogeneity and viral RNA was detected up to 92 days after the symptom onset.³⁴

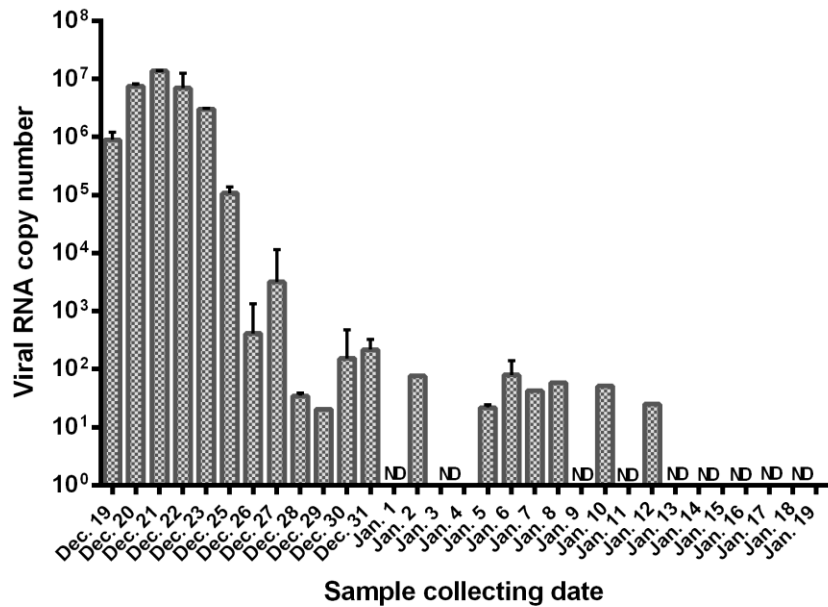


Figure 2.15. Monitoring SARS-CoV-2 RNA levels in saliva and gargle samples collected from the second NPS-confirmed SARS-CoV-2 positive patient. Multiple samples were collected every day for a month from the onset of clinical symptoms. The error bars represent one standard deviation of duplicate measurements. ND indicates no detectable SARS-CoV-2 RNA.

I also investigated whether there was any difference in viral RNA levels depending on the time of collection throughout the day. All saliva samples collected in the first 5 days from the first patient had viral RNA concentrations higher than 10⁴ copies/200 μL (Figure 2.14), but showed no temporal pattern (Figure 2.16). Four gargle samples (morning, noon, evening, and night) collected consecutively for 7 days from the second patient showed that the viral RNA concentration was the highest in the morning samples for 5 of the 7 sampling days (Figure 2.17).

These results indicate consistent detection in all samples throughout the day, however a diurnal trend cannot be identified based on the data from the samples of the two patients.

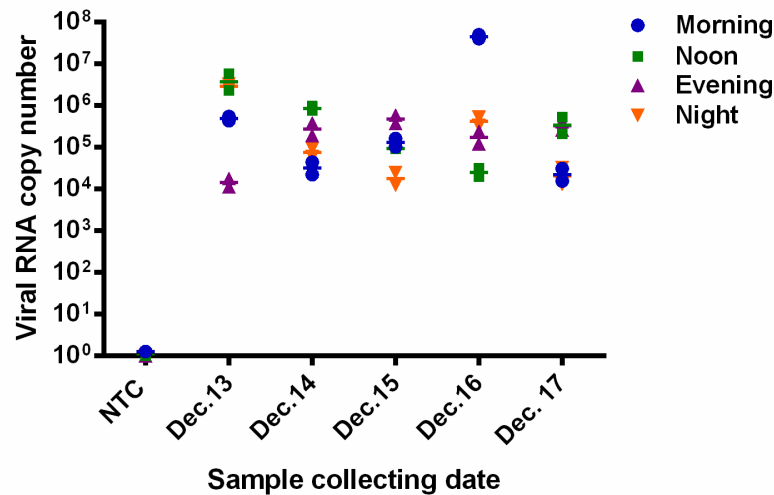


Figure 2.16. SARS-CoV-2 RNA levels in saliva samples collected four times a day for five days.

The samples were collected from the first SARS-CoV-2 positive patient volunteer from December 13 to 17, 2020. Lines represent the mean of duplicates, shown individually as symbols. NTC (no template control) is negative control.

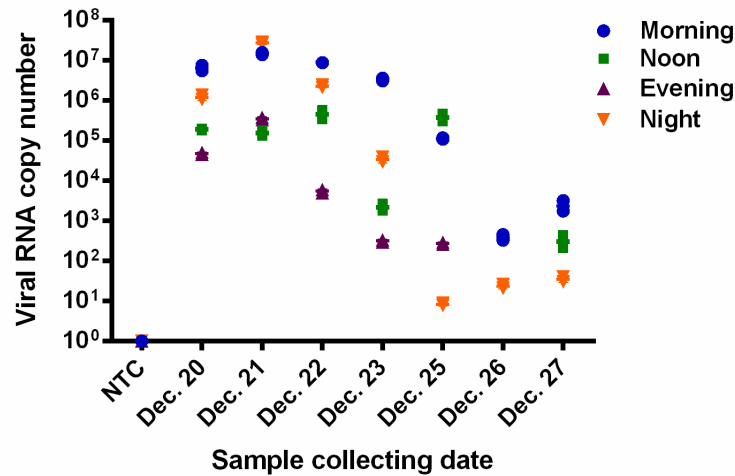
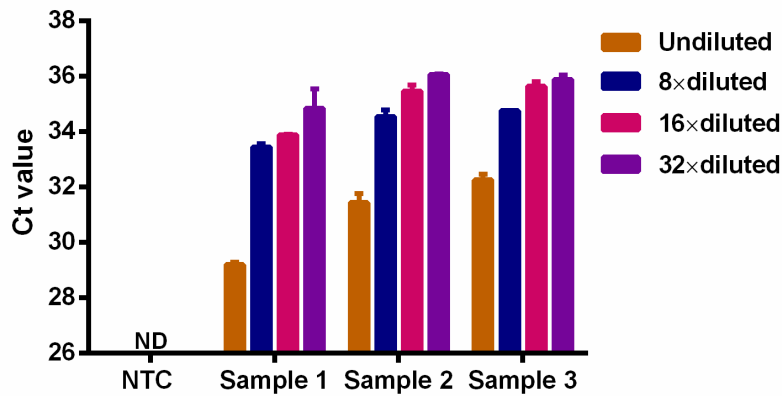


Figure 2.17. SARS-CoV-2 RNA levels in gargle samples collected four times a day for seven days. The gargle samples were collected from the second SARS-CoV-2 positive patient volunteer from December 20 to 27, 2020. Lines represent the mean of duplicates, shown individually as symbols. NTC (no template control) denotes negative control.

2.3.9 Application of the VIP-Mag-RT-qPCR Method to the Analysis of Pooled

Samples

Because the VIP-Mag-RT-qPCR method can detect as few as 25 copies of viral RNA/200 μ L gargle, such high sensitivity makes it possible to analyze pooled samples collected from multiple individuals. When the positivity rate is low, analysis of the pooled samples could save resources for mass population surveillance.^{35,38} To demonstrate application for pooled sample analysis, I first chose negative gargle samples from 10 healthy volunteers and 3 SARS-CoV-2 positive samples containing approximately 120 copies (Ct value 32.2), 210 copies (Ct value 31.4), and 1020 copies (Ct value 29.2) of SARS-CoV-2 RNA per 200 μ L gargle, respectively. To simulate a pool of 1 positive in 8, 16, or 32 samples, I diluted a positive sample with the pooled negative gargle sample 8, 16, and 32 times. The VIP-Mag-RT-qPCR analyses of these diluted samples show consistent positive detections (Figure 2.18). Thus, a single positive gargle sample pooled with 7, 15, or 31 other negative gargle samples can be detected as positive despite the dilution of the positive sample. These results demonstrate the successful application of the VIP-Mag-RT-qPCR method for the analysis of pooled gargle samples and suggest its potential for the surveillance of COVID-19 in a large population.



Gargle samples from COVID-19 positive patient

Figure 2.18. Performance evaluation of the VIP-Mag-RT-qPCR method on pooled samples. Three SARS-CoV-2 positive samples (Ct 29.2, 31.4, 32.2) were each diluted by 8, 16, and 32 times, respectively, with pooled negative gargle samples. Each diluted and undiluted samples were analyzed in triplicate using the VIP-Mag-RT-qPCR method. The error bars represent one standard deviation from the triplicate measurements. NTC indicates no template control, and ND indicates no detectable SARS-CoV-2 RNA.

2.4 Conclusion

I developed the VIP-Mag-RT-qPCR method, which includes an inexpensive solution enabling on-site sample self-collection with integrated virus inactivation and RNA preservation, magnetic bead-mediated RNA concentration, and direct analysis of the viral RNA concentrated on the magnetic beads without the need for elution. This method simplifies the procedures of sample collection and treatment of saliva and gargle samples for the detection of SARS-CoV-2. The VIP-Mag-RT-qPCR method can detect as few as 25 copies of viral RNA in 200 μ L of samples, improving the detection sensitivity 9–111 times over the QIAamp Viral RNA Mini Kit recommended by the CDC. The improved method has sufficient sensitivity to detect the diluted level of SARS-CoV-2 in pooled samples for potential large scale population surveillance. The

VIP buffer can be used for the self-collection of samples and on-site inactivation, minimizing the risks associated with viral spreading and transmission to healthcare and laboratory personnel during collection and analysis of clinical samples. Saliva and gargle samples are complementary to NPS, providing an alternative for repeated sampling, population surveillance, and point-of-care testing of SARS-CoV-2. The general strategy of viral inactivation and nucleic acid preservation could potentially be applied for the detection of other viruses and sample matrices as well.

2.5 References

1. Azzi, L.; Maurino, V.; Baj, A.; Dani, M.; d’Aiuto, A.; Fasano, M.; et al. Diagnostic Salivary Tests for SARS-CoV-2. *J. Dent. Res.* **2021**, *100*, 115– 123.
2. Wiersinga, J.W.; Rhodes, A.; Cheng, A.C.; Peacock, S.J.; Prescott, H.C. Pathophysiology, transmission, diagnosis, and treatment of coronavirus disease 2019 (COVID-19). *JAMA* **2020**, *324*, 782– 793.
3. Wölfel, R.; Corman, V.M.; Guggemos, W.; Seilmaier, M.; Zange, S.; Müller, M.A.; et al. Virological assessment of hospitalized patients with COVID-2019. *Nature* **2020**, *581*, 465– 469.
4. Zou, L.; Ruan, F.; Huang, M.; Liang, L.; Huang, H.; Hong, Z.; et al. SARS-CoV-2 viral load in upper respiratory specimens of infected patients. *N. Engl. J. Med.* **2020**, *382*, 1177– 1179.
5. Kucirka, L.M.; Lauer, S.A.; Laeyendecker, O.; Boon, D.; Lessler, J. Variation in false-negative rate of reverse transcriptase polymerase chain reaction–based SARS-CoV-2 tests by time since exposure. *Ann. Intern. Med.* **2020**, *173*, 262– 267.
6. Lalli, M.A.; Langmade, J.S.; Chen, X.; Fronick, C.C.; Sawyer, C.S.; Burcea, L.C.; et al. Rapid and extraction-free detection of SARS-CoV-2 from saliva by colorimetric reverse-transcription loop-mediated isothermal amplification. *Clin. Chem.* **2021**, *67* (2), 415-424.
7. Ranoa, D.; Holland, R.; Alnaji, F.G.; Green, K.; Wang, L.; Brooke, C.; et al. Saliva-based molecular testing for SARS-CoV-2 that bypasses RNA extraction. *Biorxiv* **2020**.
Available from: <https://doi.org/10.1101/2020.06.18.159434> (accessed 2021-12-10)
8. Tilley, P.; Gadkar, V.; Goldfarb, D.M.; Young, V.; Watson, N.; Al-Rawahi, G.N.; et al. Gargle-Direct: Extraction-free detection of SARS-CoV-2 using real-time PCR (RT-

qPCR) of saline gargle rinse samples. *MedRxiv* **2021**. Available from:

<https://doi.org/10.1101/2020.10.09.20203430> (accessed 2021-12-10).

9. Yang, Q.; Meyerson, N.R.; Clark, S.K.; Paige, C.L.; Fattor, W.T.; Gilchrist, A.R.; et al. Saliva Two Step for rapid detection of asymptomatic SARS-CoV-2 carriers. *Elife* **2021**, *10*, e65113.
10. Barat, B.; Das, S.; De Giorgi, V.; Henderson, D.K.; Kopka, S.; Lau, A.F.; et al. Pooled saliva specimens for SARS-CoV-2 testing. *J. Clin. Microbiol.* **2021**, *59* (3), e02486-20.
11. Bokelmann, L.; Nickel, O.; Maricic, T.; Pääbo, S.; Meyer, M.; Borte, S.; Riesenberger, S. Point-of-care bulk testing for SARS-CoV-2 by combining hybridization capture with improved colorimetric LAMP. *Nat. Commun.* **2021**, *12* (1), 1-8.
12. Kellner, M.J.; Ross, J.J.; Schnabl, J.; Dekens, M.P.; Heinen, R.; Grishkovskaya, I.; et al. A rapid, highly sensitive and open-access SARS-CoV-2 detection assay for laboratory and home testing. *Front. Mol. Biosci.* **2022**, *9*, 801309.
13. Willeit, P.; Krause, R.; Lamprecht, B.; Berghold, A.; Hanson, B.; Stelzl, E.; et al. Prevalence of RT-qPCR-detected SARS-CoV-2 infection at schools: First results from the Austrian School-SARS-CoV-2 prospective cohort study. *Lancet Reg. Health Eur.* **2021**, *5*, 100086.
14. Khurshid, Z.; Zohaib, S.; Najeeb, S.; Zafar, M.; Slowey, P.; Almas, K. Human saliva collection devices for proteomics: an update. *Int. J. Mol. Sci.* **2016**, *17*, 846.
15. Wang, W.K.; Chen, S.Y.; Liu, I.J.; Chen, Y.C.; Chen, H.L.; Yang, C.F.; et al. Detection of SARS-associated coronavirus in throat wash and saliva in early diagnosis. *Emerging Infect. Dis.* **2004**, *10*, 1213– 1219.

16. Wyllie, A.L.; Fournier, J.; Casanovas-Massana, A.; Campbell, M.; Tokuyama, M.; Vijayakumar, P.; et al. Saliva or nasopharyngeal swab specimens for detection of SARS-CoV-2. *N. Engl. J. Med.* **2020**, *383*, 1283– 1286.
17. Goldfarb, D.M.; Tilley, P.; Al-Rawahi, G.N.; Srigley, J.A.; Ford, G.; Pedersen, H.; et al. Self-collected saline gargle samples as an alternative to health care worker-collected nasopharyngeal swabs for COVID-19 diagnosis in outpatients. *J. Clin. Microbiol.* **2021**, *59*, e02427.
18. Kojima, N.; Turner, F.; Slepnev, V.; Bacelar, A.; Deming, L.; Kodeboyina, S.; Klausner, J. D. Self-collected oral fluid and nasal swabs demonstrate comparable sensitivity to clinician collected nasopharyngeal swabs for coronavirus disease 2019 detection. *Clin. Infect. Dis.* **2021**, *73*, e3106– e3109.
19. Vogels, C.B.F.; Watkins, A.E.; Harden, C.A.; Brackney, D.E.; Shafer, J.; Wang, J.; et al. SalivaDirect: A simplified and flexible platform to enhance SARS-CoV-2 testing capacity. *Med.* **2021**, *2*, 263– 280.
20. Hall, E.W.; Luisi, N.; Zlotorzynska, M.; Wilde, G.; Sullivan, P.; Sanchez, T.; Bradley, H.; Siegler, A. J. Willingness to use home collection methods to provide specimens for SARS-CoV-2/COVID-19 research: survey study. *J. Med. Internet Res.* **2020**, *22*, e19471.
21. Moreno-Contreras, J.; Espinoza, M.A.; Sandoval-Jaime, C.; Cantú-Cuevas, M.A.; Barón-Olivares, H.; Ortiz-Orozco, O.D.; et al. Saliva sampling and its direct lysis, an excellent option to increase the number of SARS-CoV-2 diagnostic tests in settings with supply shortages. *J. Clin. Microbiol.* **2020**, *58*, e01659.

22. Ott, I.M.; Strine, M.S.; Watkins, A.E.; Boot, M.; Kalinich, C.C.; Harden, C.A.; et al. Stability of SARS-CoV-2 RNA in non-supplemented saliva. *Emerging Infect. Dis.* **2021**, *27*, 1146– 1150.
23. Griesemer, S.B.; Van Slyke, G.; Ehrbar, D.; Strle, K.; Yildirim, T.; Centurioni, D.A.; et al. Evaluation of specimen types and saliva stabilization solutions for SARS-CoV-2 testing. *J. Clin. Microbiol.* **2021**, *59*, e01418.
24. Lee, R.A.; Herigon, J.C.; Benedetti, A.; Pollock, N.R.; Denkinger, C.M. Performance of saliva, oropharyngeal swabs, and nasal swabs for SARS-CoV-2 molecular detection: A systematic review and meta-analysis. *J. Clin. Microbiol.* **2021**, *59*, e02881.
25. Mohammadi, A.; Esmailzadeh, E.; Li, Y.; Bosch, R.J.; Li, J.Z. SARS-CoV-2 detection in different respiratory sites: A systematic review and meta-analysis. *EBioMedicine* **2020**, *59*, 102903.
26. Kandel, C.E.; Young, M.; Serbanescu, M.A.; Powis, J.E.; Bulir, D.; Callahan, J.; et al. Detection of severe acute respiratory coronavirus virus 2 (SARS-CoV-2) in outpatients: A multicenter comparison of self-collected saline gargle, oral swab, and combined oral-anterior nasal swab to a provider collected nasopharyngeal swab. *Infect. Control Hosp. Epidemiol.* **2021**, *42*, 1340– 1344.
27. Joung, J.; Ladha, A.; Saito, M.; Kim, N.G.; Woolley, A.E.; Segel, M.; et al. Detection of SARS-CoV-2 with SHERLOCK one-pot testing. *N. Engl. J. Med.* **2020**, *383*, 1492– 1494.
28. Patterson, E.I.; Prince, T.; Anderson, E.R.; Casas-Sanchez, A.; Smith, S.L.; Cansado-Utrilla, C.; et al. Methods of inactivation of SARS-CoV-2 for downstream biological assays. *J. Infect. Dis.* **2020**, *222*, 1462– 1467.

29. Welch, S.R.; Davies, K.A.; Buczkowski, H.; Hettiarachchi, N.; Green, N.; Arnold, U.; et al. Analysis of inactivation of SARS-CoV-2 by specimen transport media, nucleic acid extraction reagents, detergents, and fixatives. *J. Clin. Microbiol.* **2020**, *58*, e01713.
30. Pastorino, B.; Touret, F.; Gilles, M.; Luciani, L.; de Lamballerie, X.; Charrel, R.N. Evaluation of chemical protocols for inactivating SARS-CoV-2 infectious samples. *Viruses* **2020**, *12*, 624.
31. Andreasen, D.; Fog, J.U.; Biggs, W.; Salomon, J.; Dahslveen, I.K.; Baker, A.; Mouritzen, P. Improved microRNA quantification in total RNA from clinical samples. *Methods* **2010**, *50*, S6– S9.
32. Ramón-Núñez, L.A.; Martos, L.; Fernández-Pardo, Á.; Oto, J.; Medina, P.; España, F.; Navarro, S. Comparison of protocols and RNA carriers for plasma miRNA isolation. Unraveling RNA carrier influence on miRNA isolation. *PLoS One* **2017**, *12*, e0187005.
33. Bloomfield, V. A. DNA condensation by multivalent cations. *Biopolymers* **1997**, *44*, 269– 282.
34. Fontana, L.; Villamagna, A.H.; Sikka, M.K.; McGregor, J.C. Understanding viral shedding of SARS-CoV-2: review of current literature. *Infect. Control Hosp. Epidemiol.* **2021**, *42*, 659– 668.
35. Schulte, P.A.; Weissman, D.N.; Luckhaupt, S.E.; de Perio, M.A.; Piacentino, J.D.; Radonovich, L.J.; et al. Considerations for pooled testing of employees for SARS-CoV-2. *J. Occup. Environ. Med.* **2021**, *63*, 1– 9.
36. Cleary, B.; Hay, J.A.; Blumenstiel, B.; Harden, M.; Cipicchio, M.; Bezney, J.; et al. Using viral load and epidemic dynamics to optimize pooled testing in resource-constrained settings. *Sci. Transl. Med.* **2021**, *13*, eabf1568.

37. Grobe, N.; Cherif, A.; Wang, X.; Dong, Z.; Kotanko, P. Sample pooling: burden or solution? *Clin. Microbiol. Infect.* **2021**, *27*, 1212– 1220.
38. Deka, S.; Kalita, D. Effectiveness of sample pooling strategies for SARS-CoV-2 mass screening by RT-PCR: A scoping review. *J. Lab. Physicians* **2020**, *12*, 212– 218.

Chapter Three: Development of a Method for Enhanced Wastewater Surveillance of SARS-CoV-2 in the Community*

*This chapter has been published and was modified from Kumblathan, T.; Liu, Y.; Qiu, Y.; Pang, L.; Hruday, S.E.; Le, X.C.; Li, X.F. An efficient method to enhance recovery and detection of SARS-CoV-2 RNA in wastewater. *J. Environ. Sci.* **2023a**, 130, 139-148. I conceptualized experimental design, performed the experiments, data collection and analysis, text and schematic composition, and revisions of the overall manuscript. Liu Y contributed to experimental design and manuscript revisions. Qiu Y, Pang L, Hruday SE, Le XC, and Li XF contributed to editing the manuscript.

*A part of this chapter has also been published in Kumblathan, T.; Liu, Y.; Uppal, G.K.; Hruday, S.E.; Li, X.F. Wastewater-based epidemiology for community monitoring of SARS-CoV-2: Progress and Challenges. *ACS Environ. Au* **2021**, 1, 18–31. I drafted, revised, and edited all sections of the primary manuscript. I also made all the tables and figures. Liu Y and Uppal GK helped with drafting of the primary manuscript. Hruday SE and Li XF contributed to editing the manuscript.

3.1 Introduction

As previously mentioned in the introduction, the conventional approach for community surveillance of SARS-CoV-2 heavily relies on clinical testing using NPS sample collection followed by RT-qPCR detection. However, using the clinical diagnostic tests alone for public health surveillance can result in resources becoming overwhelmed during a pandemic situation. Furthermore, to manage the demand for testing and shortages in diagnostic resources, healthcare systems on a global scale are often limited to only testing certain populations such as symptomatic patients and close contacts. Thus, pre-symptomatic, asymptomatic, and mild symptomatic cases, that significantly contribute to the spread of SARS-CoV-2, are often undetected by clinical diagnostics and missed in community surveillance. As a result, clinical testing of SARS-CoV-2 alone underestimates the true scale of the pandemic, and public health officials must make decisions on community quarantine guidelines with limited and inadequate surveillance data. The inefficiency of NPS RT-qPCR testing in combination with waning population immunity and risk of re-infection created an urgent need for efficient community surveillance.¹

Wastewater surveillance (WS) has become a useful public health tool for assessing the status of community infections, and many organizations are adopting WS for national surveillance programs of pathogens.¹ Recently, the U.S. Centers for Disease Control and Prevention, the International Water Association, the Public Health Agency of Canada, and the Canadian Water Network have adopted WS to complement clinical testing for monitoring the status and trends of the COVID-19 pandemic in the community.²⁻⁵

Wastewater is a composite sample of the entire community, containing fecal, urine, and other biological products from individuals in the community. Several studies have demonstrated

that up to 89% of infected patients shed SARS-CoV-2 viral particles and RNA into stool as early as one-day post-infection.^{2,6-8} Additionally, SARS-CoV-2 respiratory secretions can also be captured in wastewater through bath, shower, and laundry water. Several studies have even reported successful detection of SARS-CoV-2 in wastewater up to 14 days prior to clinically reported cases.^{9,10,11} Sensitivity analysis showed that the viral RNA could be detected in wastewater at 99% probability if there were higher than on average 38 new cases per 100,000 people in the community.^{12,13}

Because of the need to respond rapidly to the COVID-19 pandemic, methods for WS of SARS-CoV-2 are based on individually accessible laboratory methods without national or international standardized procedures. WS of viruses generally involves multiple steps, including sample collection, viral particle concentration, RNA extraction, and RT-qPCR detection. To detect SARS-CoV-2 RNA accurately and sensitively in wastewater, a WS process with a high overall recovery is required. However, many studies have found poor recoveries of surrogates (structurally similar viruses) of SARS-CoV-2 from wastewater, with recoveries ranging from 0.08- 66%.¹⁴⁻¹⁸ A review of these studies and the methods used have been outlined below in Table 3.1.¹⁹⁻⁵⁵ Four major factors contribute to the poor recoveries and large variations: (1) the use of only the aqueous phase of wastewater samples while discarding the solid phase, (2) incomplete concentration of viral particles and viral RNA from wastewater, (3) inefficient RNA extraction and inadequate removal of RT-qPCR inhibitors, and (4) insufficient sample volume used for analysis, especially when viral loads are very low. The poor recoveries and reproducibility can also be attributed to sample-to-sample matrix differences. Insufficient matrix removal during the viral particle concentration and RNA extraction steps can contribute to inaccurate and inconsistent RT-qPCR results.

Table 3.1. Comparison of the concentration, extraction, and detection methods used by various studies for WS of SARS-CoV-2.

Reference	Sampling technique	Sample type (untreated/ treated wastewater or sludge)	Positive rate	Maximum concentration (genomic copies/L)	Concentration method	RNA extraction and purification method	Targeted gene by RT-qPCR
Wu et al., 2020	Grab and Composite	Untreated	10/14 (71%)	$>2 \times 10^5$	PEG ^a precipitation	TRIzol™ – chemical extraction Phenol / chloroform	CDC N1, N2, N3
Green et al., 2020	Composite	Untreated	18/22 (82%)	1.7×10^5	Ultracentrifugation	AllPrep® PowerViral® DNA/RNA Kit Spin/filter column	IP2 and IP4 of RdRp
Sherchan et al., 2020	Composite	Untreated	2/15 (13%)	7.5×10^3	Ultrafiltration & Electronegative membrane	ZR Viral RNA kit Spin/filter column	CDC N1, N2
		Treated	ND ^b				
Nemudryi et al., 2020	Composite	Untreated	7/7 (100%)	$>3 \times 10^4$	Ultrafiltration	RNeasy Mini Kit Spin/filter column	CDC N1, N2
Peccia et al., 2020	NS ^c	Primary sludge	100%	4.6×10^7	Direct RNA extraction	RNeasey PowerSoil Total RNA kit Spin/filter column	CDC N1, N2
Gonzalez et al., 2020	Composite and Grab	Untreated	98/198 (49%)	$\sim 10^5$	Electronegative membrane	NucliSENS easyMag Magnetic silica particles	CDC N1, N2, N3
Gerrity et al., 2021	Composite and Grab	Untreated	46/46	$\sim 10^6$	Ultrafiltration	Purelink viral RNA/DNA Mini kit Spin/filter column	E from Charité, CDC N1, N2 and ORF1a
		Treated	ND				
Graham et al., 2021	Composite Grab	Untreated Primary sludge	79/96 (82%)	4250 copies per g of dry weight	PEG precipitation & Ultrafiltration	Qiagen AllPrep PowerViral DNA/RNA kit	N1, N2
Ahmed et al., 2020	Grab and composite	Untreated	2/9 (22%)	1.2×10^2	Electronegative membrane & Ultrafiltration	RNeasy PowerMicrobio me kit QIAcube Connect Platform Spin/filter column	N from Charité NIID_2019-nCoV_N
Kumar et al., 2020	Composite	Untreated	2/2 (100%)	8.0×10^2	PEG precipitation	NucleoSpin® RNA Virus Spin/filter column	N, ORF1ab, and S
		Treated	ND				

Arora et al., 2021	Grab	Untreated	2/6 (33%)		PEG precipitation Centrifugation	Biospin kit (Cat# BSC77M1) Spin/filter column; KingFisher Flex System Magnetic silica beads	E, RdRp, and N
		Treated	ND	ND			
Medema et al., 2020	Composite	Untreated	N1:14/24(58%) E: 5/24(21%)	2.2×10^5	Ultrafiltration	RNeasy PowerMicrobio me kit Spin/filter column; NucliSENS kit Magnetic silica beads	CDC N1, N2, N3 and E from Charité
Trottier et al., 2020	Composite	Untreated	NS	NS	Ultrafiltration	NucleoSpin RNA Virus kit Spin/filter column	CDC N1 and N3
		Treated					
Wurtzer et al., 2020	Composite	Untreated	23/23 (100%)	$>10^{6.5}$	Ultracentrifugation	PowerFecal Pro kit by QIAGEN Spin/filter column	E from Charité
		Treated	6/8 (75%)	$\sim 10^5$			
Fongaro et al., 2021	Composite	Untreated	4/6 (66%)	5×10^6	Ultrafiltration & PEG precipitation	QIAmp viral RNA Mini kit Spin/filter column	CDC N1, S, and RdRp
Prado et al., 2020	Composite	Untreated	5/12 (42%)	NS	Ultracentrifugation	QIAmp viral RNA Mini kit Spin/filter column	CDC N2
Bar-Or et al., 2022	Composite	Untreated	10/26 (38%)	NS	PEG precipitation	RNeasy mini kit- QIAGEN Spin/filter column; NucliSENS easyMAG - bioMerieux Magnetic silica beads	E from Charité
La Rosa et al., 2020	Composite	Untreated	6/12 (50%)	NS	PEG/dextran separation	NucliSENS miniMAG Magnetic silica beads	ORF1ab, S, and RdRp from Charité
La Rosa et al., 2021	Composite	Untreated	15/40 (37.5%)	5.6×10^4	PEG/dextran separation	NucliSENS miniMAG Magnetic silica beads	E and RdRp from Charité, ORF1ab
Rimoldi et al., 2020	Grab	Untreated	3/4 (75%)	NS	Filtration	QIAMP viral RNA mini kit Spin/filter column	E from Charité, N, and ORF1ab
		Treated	ND				

Randazzo et al., 2020a	Grab	Untreated	35/42 (83%)	3.4×10^5	Aluminium flocculation – beef extract precipitation	Nucleospin RNA virus kit Spin/filter column	CDC N1, N2, N3
		Treated	11%, ND				
Randazzo et al., 2020b	Grab	Untreated	12/15 (80%)	1.0×10^5	Aluminium flocculation – beef extract precipitation	Nucleospin RNA virus kit Spin/filter column	CDC N1, N2, N3
		Treated	ND				
Balboa et al., 2021	Composite	Untreated	5/5 (100%)	1.5×10^4	Ultrafiltration PEG precipitation	STARMag 96 x 4 Universal Cartridge Kit Magnetic silica beads	N, E and RdRp
		Treated	1/4 (25%)				
		Sludge	14/34 (41%)				
Chavarria-Miró et al., 2020	Composite	Untreated	1/19 (11%)	8.3×10^2	PEG precipitations	NucliSENS miniMAG Magnetic silica beads	CDC N1, N2, IP2 and IP4 of RdRp and E from Charité
Kocamei et al., 2020	Composite	Untreated	5/7 (71%)	1.8×10^4	Ultrafiltration PEG precipitation	QIAamp cador Pathogen Mini Kit Spin/filter column	RdRp from Charité
Haramoto et al., 2020	Grab			NS	Electronegative membrane-vortex or direct extraction	QIAamp Viral RNA Mini kit in a QIAcube automated platform Spin/filter column RNeasy PowerWater Kit	N from Charité, NIID_2019-nCoV_N, CDC N1, N2
		Untreated	ND				
		Treated	1/5 (20%)				
Kitamura et al., 2021	Grab	Untreated	6/32 (19%) in supernatant 18/32 (56%) in solid	9.2×10^3	Ultrafiltration PEG precipitation Electronegative membrane	QIAamp Viral RNA kit RNeasy Microbiome kit QIAamp UltraSens Virus kit RNeasy PowerSoil kit	NIID 2019-nCoV_N, CDC N1, N2
Hata et al., 2021	Grab	Untreated	7/27 (26%)	4.4×10^4	PEG precipitation	RNeasy mini kit- QIAGEN Spin/filter column	CDC N2, N3 and NIID 2019-nCoV_N
Westhaus et al., 2021	Composite	Untreated	4/4 (100%)	3.7×10^4	Ultrafiltration	NucleoSpin RNA Virus kit	RdRp from Charité and M gene
		Treated	Detected in supernatant and solid				
Sharif et al., 2021	Grab	Untreated	21/78 (27%)	NS	PEG/dextran separation	Spin star viral nucleic acid kit 1.0 Spin/filter column	ORF lab, N from China, E from Charité

Ampuero et al., 2020	Composite	Untreated	4/4 (100%)	4.8×10^3	Ultracentrifugation	QIAamp® Viral RNA Mini kit Spin/filter column	ORF1ab, N, S
		Treated	3/4 (75%)	1.6×10^2			
Mlejnkova et al., 2020	Composite	Untreated	13/112 (11.6%)	NS	Direct flocculation using beef extract solution and centrifugation	NucliSENS miniMAG Magnetic silica beads	EliGene COVID19 Basic A RT kit
Martin et al., 2020	Composite	Untreated	3/5 (60%)	1.58×10^4	Ultrafiltration	High Pure viral RNA kit	RdRp and E from Charité
Albastaki et al., 2021	Grab	Untreated	829/2900 (29%)	8×10^5	MB Spin Column of DNeasy PowerSoil Kit	MagMax Viral/Pathogen Kit	<i>ORF1ab</i> , N and S
Hasan et al., 2021	Grab	Untreated	85%	3.4×10^4	PEG precipitation Ultrafiltration	ABIOpure Viral DNA/RNA Extraction kits TRIzol Reagent	RdRp
Gonçalves et al., 2021	Composite	Untreated	18/21(86%)	1×10^5	Ultrafiltration	QIAamp® Viral RNA Mini Kit	E and RdRp from Charité
		Treated	13/21(62%)				
Saguti et al., 2021	Composite	Untreated	10/15 (66%)	NS	Nano-Ceram filters- ultracentrifugation	DNeasy Blood and Tissue kit	RdRp

^a PEG polyethylene glycol, ^b ND not detected, ^c NS not specified

Therefore, I aimed to develop a method for enhanced recovery and detection of viral RNA in wastewater. To achieve this, I focused on three main components: 1) simultaneous capture and concentration of viral particles and RNA from both liquid and solid phases, 2) sufficient removal of the sample matrices, particularly RT-qPCR inhibitors while ensuring efficient extraction of viral RNA, and 3) capability of handling large volume of samples. I developed an improved analytical method that can provide consistent and highly efficient concentration of viral particles, extraction of RNA, and removal of inhibitors for RT-qPCR detection, resulting in highly sensitive detection of SARS-CoV-2 RNA in wastewater. The method involves concentration of viral particles and RNA from the whole wastewater sample using electronegative membrane (EM) filtration, followed by viral inactivation and RNA preservation (VIP), magnetic (Mag) capture of RNA, and RT-qPCR detection of the N1 gene of

SARS-CoV-2 (VIP-Mag-RT-qPCR). My improved method, EM-VIP-Mag-RT-qPCR, allows for the concentration of viruses from a large volume of sample, as well as enhanced recovery and detection of RNA of SARS-CoV-2 and variants in wastewater. The EM-VIP-Mag-RT-qPCR method is also inexpensive and broadly accessible, therefore it can be widely used for the detection of viral RNA in wastewater samples containing both high and low concentrations of SARS-CoV-2 viral particles and RNA.

3.2 Experimental

3.2.1 Wastewater Sample Collection

Using appropriate personal protective equipment and sampling equipment, wastewater samples were collected from two wastewater treatment plants (WWTPs) in Calgary and Edmonton, Alberta, Canada. Five hundred milliliters of post-grit raw influent wastewater samples from a 24h composite sampler was collected twice a week from May 2021 to October 2021. All the samples were stored at 4°C after collection and shipped to Dr. Lilly (Xiaoli) Pang's research laboratory on a weekly basis for long term storage at 4°C. I refer to Dr. Pang's laboratory as the reference laboratory in the following discussion as they participate in the Pan Alberta WS program. An aliquot of the same sample was analyzed by Pang's lab using their method^{56,57} and another aliquot was analyzed using my in-house method described in detail below.

3.2.2 Capture of SARS-CoV-2 from Wastewater Samples

An aliquot of 80 mL of wastewater sample was transferred into a sterile DNase free and RNase free conical tube and centrifuged at 1510 g for 30 minutes. This allowed for the separation of the aqueous and solid phase. The resulting supernatant of the aqueous phase was transferred into another DNase and RNase free sterile conical tube and the solid pellet was re-

suspended in beef extract solution (3% weight/volume beef extract in 0.05 mol/L glycine (pH 9.0) at a ratio of 1:5. The pellet suspension was agitated at 800 r/minute for 30 minutes at room temperature on a shaker followed by centrifugation at 1510 g for 10 minutes. The resulting supernatant was transferred into a new tube, neutralized with HCl and then was combined with the aqueous phase. Then MgCl₂ (1 mol/L) was added into each sample to reach the final concentration of 25 mmol/L. The treated wastewater sample was then filtered through an EM using a vacuum filtration set-up. The mixed cellulose ester (MCE) membrane filter had a diameter of 47 mm and a pore size of 0.45 μm.

3.2.3 Extraction of RNA from Wastewater Samples using the VIP Buffer and Concentration onto Magnetic Beads Followed by Direct RT-qPCR Detection

The EMs containing the captured SARS-CoV-2 particles were directly used to extract viral RNA. The in-house developed viral inactivation and preservation (VIP) buffer discussed in the previous chapter was used for RNA extraction. The EMs were vortexed thoroughly in 600 μL of the VIP buffer, placed on a heating block for 10 minutes at 55°C, centrifuged for 2 minutes at 13,000 g, and the final supernatant was transferred to a new tube. This supernatant containing the extracted SARS-CoV-2 RNA was then incubated with the in-house developed magnetic beads mixture. The details on the preparation and optimization of the magnetic beads buffer can be found in the previous chapter. 400 μL of the magnetic beads suspension and 200 μL of 100% ethanol (RNA grade) were added into the extracted RNA supernatant, vortexed until fully mixed, and incubated on a shaker at room temperature for 10 minutes. Samples were then centrifuged to collect the magnetic beads and the resulting beads were washed three times with 0.8 mL of 75% ethanol containing 1.0 mM sodium citrate. The magnetic beads containing the

extracted RNA were air-dried and resuspended in a solution containing 25 μ L of RNase-free water, 4 μ L proteinase K inhibitor, and 1 μ L RNase inhibitor.

The TaqPath 1-Step RT-qPCR Master Mix (Thermo Fisher Scientific) and CDC N1 primer-probes from the 2019-nCoV RUO kit (IDT) were used according to the manufacturers' instructions. The RT-qPCR assay for the N1 segment of the SARS-CoV-2 RNA was optimized as described in the previous chapter. RT-qPCR was performed on a QuantStudio 3 Real-Time PCR System (Applied Biosystems, Thermo Fisher Scientific) using the QuantStudio Design and Analysis Software v1.5.1. The 1/6 portion of the extracted RNA (5 μ L) was used as template in each RT-qPCR reaction. The RT-qPCR standard curve of the N1 gene segment was used to convert the Ct values to viral RNA copies (see previous chapter Figure 2.13). The number of SARS-CoV-2 RNA copies per 100 mL of original wastewater sample was obtained using the following equation: RNA copies/100 mL = RNA copies \times 6 \times 100 mL/80 mL. The purpose of this research was to develop a robust and accessible wastewater protocol with high recovery and sensitivity. Therefore, human fecal controls were not included in this research since the work was not used for clinical case estimates.

3.2.4 Determination of Wastewater Recovery

The recovery experiments were performed using a non-infectious SARS-CoV-2 pseudovirus solution containing both viral particles and free viral RNA (purchased from Sera Care, LGC, Milford, MA, USA). The copy number of total RNA in the solution was determined using the protocol described in the previous chapter. An aliquot of this solution containing 50200 copies of the viral RNA was spiked in two sets of wastewater samples for recovery experiments. In the first set of recovery experiments, three previously determined SARS-CoV-2 negative wastewater samples (1 L each) were pooled together. Aliquots of 80 mL of the pooled negative

samples were used for spiking. In the second set of recovery experiments, six positive wastewater samples containing low SARS-CoV-2 RNA copies were pooled. Aliquots of 80 mL were spiked with the SARS-CoV-2 pseudovirus. The two sets of recovery experiments were repeated twice on different days with triplicate sample aliquots analyzed in each set of repeats. For spiked negative samples, the recovery of SARS-CoV-2 RNA in each sample was calculated as the amount of SARS-CoV-2 RNA measured divided by that of SARS-CoV-2 RNA spiked into the sample. For spiked wastewater samples with low concentrations of SARS-CoV-2 RNA, the amount of previously determined SARS-CoV-2 RNA was subtracted from the total SARS-CoV-2 RNA. This net measured amount was divided by the amount of SARS-CoV-2 RNA spiked into the sample for the recovery value.

3.2.5 Statistical Analysis

GraphPad Prism 10.0.1 was used for Pearson correlation analysis to determine if the Ct values using my method were significantly correlated to the Ct values obtained by the reference lab using their method.

3.3 Results and Discussion

3.3.1 Development of an EM-VIP-Mag-RT-qPCR Method for Enhanced Detection of SARS-CoV-2 in Wastewater

A challenge of analyzing wastewater is the low abundance of target viral particles and RNA as well as the complicated sample matrix that may inhibit RT-qPCR. Therefore, my objective was to efficiently concentrate the viral particles and RNA from wastewater while minimizing co-concentration of the inhibitory matrix. I chose to use filtration with EM for the concentration of viral particles and RNA to achieve cost-effective, fast, and large volume sample processing. A benefit of EM is that co-concentration of inhibitors is minimal, compared to other

wastewater processing methods.⁵⁶ The principle of EM capture is based on the idea that SARS-CoV-2 viral particles and RNA are negatively charged in wastewater. The EM allows small particulate matter and debris smaller than the 0.45 μm pore size to pass through the membrane while capturing viral particles and RNA on the membrane via charge interactions. Adding MgCl_2 allows for Mg^{2+} to serve as salt bridge to facilitate the adsorption of negatively charged viral particle and RNA to the EM.⁵⁷ This technique is widely accessible as only a vacuum filtration set-up is needed and the membranes themselves are not expensive.

I tested two common types of EMs: MCE membrane filters and SPAK gridded mixed cellulose ester membrane filters. I first prepared triplicate spiked samples containing an equivalent of 1941 RNA copies of SARS-CoV-2 pseudovirus solution into deionized water (diH_2O). These spiked samples were analyzed to evaluate the capture of viral particles and RNA on the SPAK and MCE membranes. As shown in Figure 3.1, the MCE membranes captured more spiked SARS-CoV-2 RNA (1823 ± 131 RNA copies), than the SPAK membranes (849 ± 218 RNA copies). To better understand the performance of the membranes with real wastewater samples, I spiked SARS-CoV-2 pseudovirus solution (containing 1941 RNA copies) into the previously confirmed SARS-CoV-2 negative wastewater samples and analyzed the samples in triplicate using both the MCE and SPAK membrane. The MCE membranes again captured more spiked SARS-CoV-2 RNA in wastewater samples than SPAK with recovered RNA copies of 1560 ± 226 and 1063 ± 139 for MCE and SPAK, respectively (Figure 3.1). The resulting wastewater recoveries are 80% and 55% for MCE and SPAK, respectively. Thus, the MCE EM was used for all the subsequent experiments. Furthermore, Ahmed et al. 2020 has used MCE EM to concentrate Murine Hepatitis Virus, a surrogate of SARS-CoV-2, from wastewater and

obtained a recovery of $65\% \pm 23\%$, indicating that EM are appropriate for concentration of viruses from wastewater.²⁷

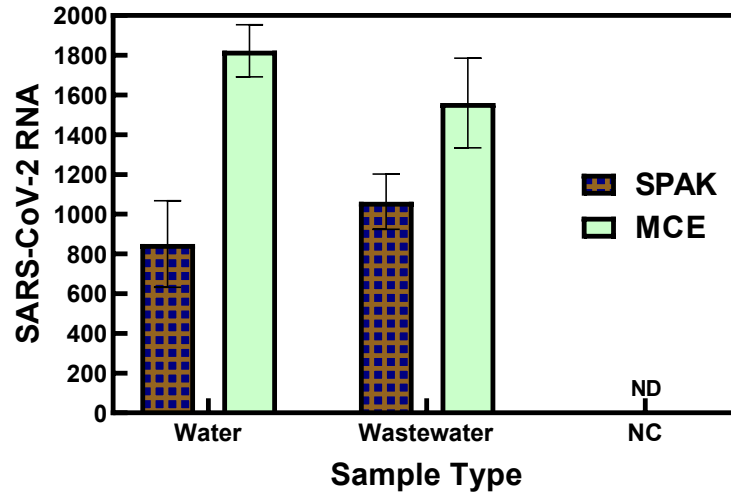


Figure 3.1. Performance analysis of two electronegative membranes (EMs) in deionized water and negative wastewater spiked with 1941 SARS-CoV-2 pseudoviral RNA. The MCE membrane has a better recovery. NC indicates negative control and ND indicates not detected.

To improve the efficiency and reproducibility of the concentration of viral particles and RNA from wastewater samples, I aimed to collect all SARS-CoV-2 viral particles and RNA from both the solid and aqueous phases of the wastewater. To better understand the distribution of SARS-CoV-2 in both phases of wastewater, I separately analyzed the aqueous and solid phases of three representative wastewater samples collected from WWTPs in Calgary and Edmonton. Figure 3.2 presents the RNA copies detected in both the solid and aqueous phases of these samples. These results show that significant amounts of viral RNA were detected in both the solid phase (402 – 159,226 RNA copies/100 mL) and aqueous phase (4,049 – 71,100 RNA copies/100 mL) of the samples (Table 3.2). The detected copies of the viral RNA in the aqueous and solid phases varied between samples even when the samples were collected from the same sewer system. The percentage of SARS-CoV-2 RNA present in the solid phase varied from 1-

23% in the Calgary samples and 24-97% in the Edmonton samples. Three of the Calgary wastewater samples had higher viral RNA concentrations in the aqueous phase than in the solid phase. In the Edmonton wastewater samples, two samples had higher viral RNA concentrations in the solid phase than the aqueous phase. The variable distribution of viral RNA in both solid and aqueous phases demonstrates that discarding either the solid or liquid phase of wastewater can result in large variations, lower recoveries, and falsely decreased or even negative results. Therefore, the use of both the solid and aqueous phase is important to improve recoveries and reduce variations resulting from unpredictable composition of wastewater.

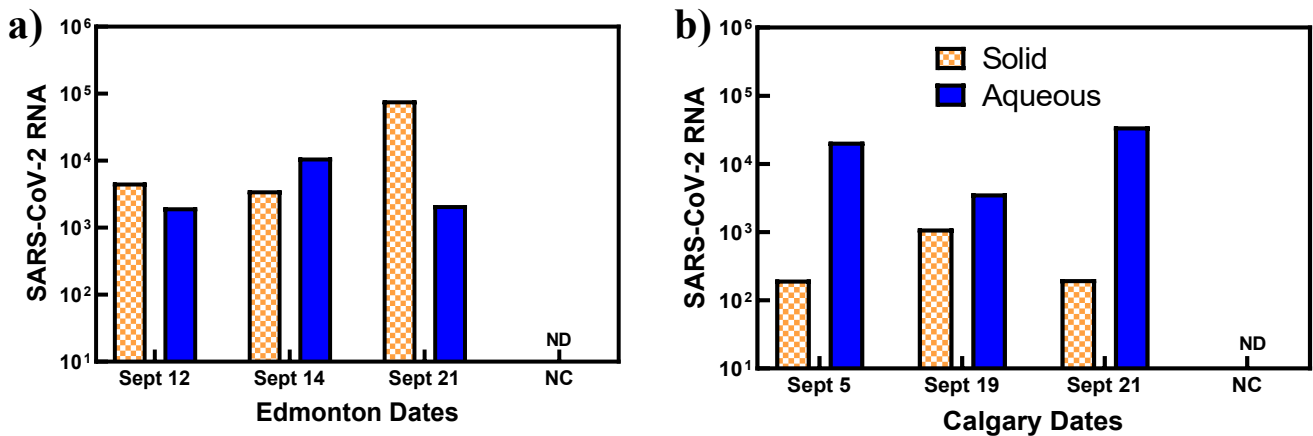


Figure 3.2. Separate analysis of the aqueous and solid phases of wastewater samples collected from two wastewater treatment plants in the cities of Edmonton and Calgary. NC indicates negative control and ND indicates not detectable.

Table 3.2 SARS-CoV-2 RNA copies in the aqueous and solid phase of wastewater samples analyzed separately. Three samples from wastewater treatment plants from Calgary and Edmonton were analyzed (n=6).

Sample	Aqueous Phase RNA Copies/100 mL	Solid Phase RNA Copies/ 100 mL
Calgary		
1	42600	402
2	7400	2270
3	71100	409
Edmonton		
1	4049	9480
2	22268	7209
3	4369	159226

The results in Figure 3.2 and Table 3.1 clarify one of the major contributors to low recovery with large variations in previous WS of SARS-CoV-2 studies, as many of these studies excluded the solid phase and analyzed only the aqueous phase.^{14,18,41,46,60} While discarding solids may reduce inhibitors for the subsequent RT-qPCR analysis, this practice could underestimate the overall SARS-CoV-2 concentrations in wastewater samples. Several studies have demonstrated that SARS-CoV-2 particles could be detected in 2-3 magnitude higher concentrations in solids and sludge portion of some wastewater samples than in the aqueous phase.^{23,26,47,61,62,63} Roldan-Hernandez et al., 2022 have shown persistence of SARS-CoV-2 in solids with a slower rate of decay than in the wastewater influent, further suggesting the importance of including the solid phase which can adsorb the viral particles and RNA.⁶² My results suggest the need for a simple and efficient procedure for the concentration of viral particles and RNA from the entire sample. To achieve highly efficient and reproducible recovery, I designed my method using the 3% beef extract solution to release the viral particles from the solids. The resultant supernatant was then re-combined with the aqueous phase for

subsequent concentration of viral particles and RNA. This approach facilitates the efficient concentration of viral particles and RNA from wastewater samples, reduces loss of viral particles and RNA adsorbed on solids, and minimizes interference of solid matter on subsequent concentration and extraction steps. The overall WS protocol process can be found below.

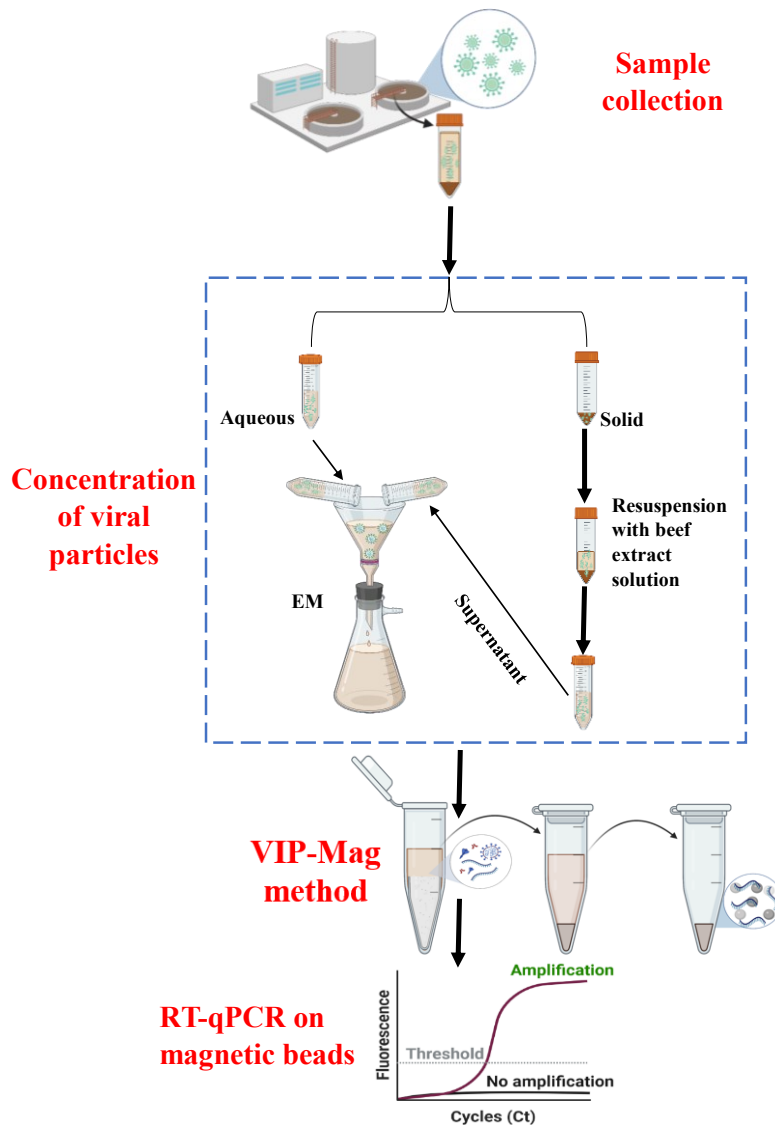


Figure 3.3. Schematic showing steps of wastewater sample processing and analysis, including sample collection, concentration of viral particles and RNA using an electronegative membrane (EM), extraction of RNA onto magnetic beads along with viral inactivation and RNA preservation (VIP-Mag), and direct RT-qPCR detection of RNA on magnetic beads.

3.3.2 VIP-Mag-RT-qPCR for Efficient Removal of RT-qPCR Inhibitors and Ultra-Sensitive In-Situ Amplification on Beads

Detection of SARS-CoV-2 by RT-qPCR is highly impacted by the purity and integrity of the RNA target template extracted. Enzymes involved in RT-qPCR can be partially or completely inhibited by the residual sample matrix components present in the RNA extract, possibly leading to falsely decreased or negative results.^{26,65} Wastewater contains a variety of compounds, such as ions, bile salts, urea, alcohols, and numerous proteins (i.e., collagen, myoglobin, hemoglobin, and RNases). Many of these compounds can inhibit RT-qPCR, whereas the RNases can degrade RNA.¹⁶ I overcame this challenge by designing steps for efficient removal of inhibitors and sufficiently degrading RNases. During the first solid phase separation step, after the viral particles were released into the beef extract solution, the remaining solids were discarded to remove any RT-qPCR inhibitors. Secondly, I used the in-house developed VIP-Mag method, which concentrated pure RNA with high integrity. The VIP buffer, which includes reagents such as 2-ME, guanidinium isothiocyanate, Triton X-100, proteinase K, and glycogen, effectively lysed the SARS-CoV-2 viral particles and denatured RNases.^{66,67} The extracted RNA was then captured on magnetic beads, and any remaining RT-qPCR inhibitors were removed through repeated washing of the beads (Figure 3.3). To optimize the VIP-Mag method for wastewater samples, I optimized the previously developed VIP-Mag method (Chapter 2 of thesis) by increasing the wash steps. I tested two aliquots of six different wastewater samples with one aliquot receiving the standard 2 washes of the magnetic beads and another aliquot receiving 3 washes of the magnetic beads (Figure 3.4). Increasing the washing step from 2 to 3 washes allowed better removal of RT-qPCR inhibitors and increased RNA recovery in previously confirmed authentic positive Edmonton and Calgary wastewater samples.

Finally, after the magnetic beads were washed, RNase inhibitor and proteinase K inhibitor were added to the extracted RNA to minimize any degradation of RNA and prevent RT-qPCR inhibition by proteinase K.

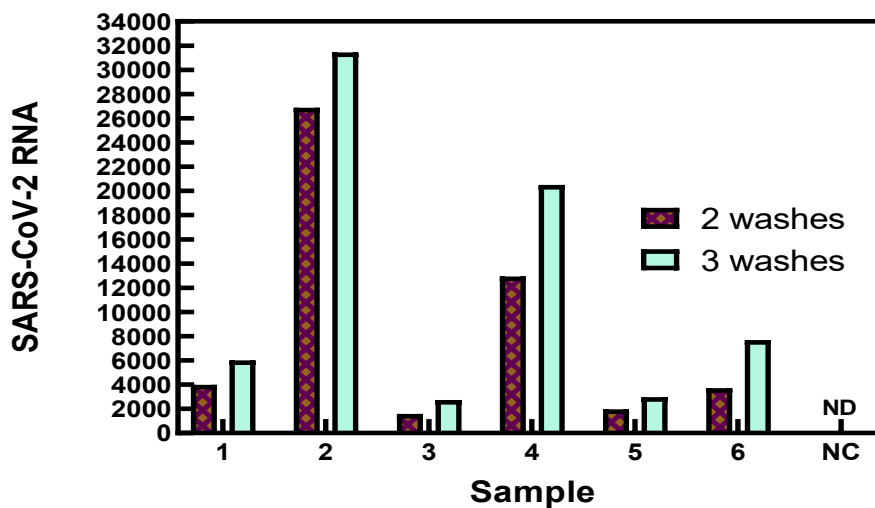


Figure 3.4. Optimization of the previously developed VIP-Mag method for wastewater samples by increasing the wash step from 2 to 3 washes.

To confirm that there was minimal RT-qPCR inhibition, I monitored several wastewater samples. The monitoring of the presence of RT-qPCR inhibitors was performed by analyzing two samples every month from May 2021 to February 2022 alongside regular wastewater sample analysis using the EM-VIP-Mag-RT-qPCR protocol (Figure 3.5). Prior to RT-qPCR analysis, magnetic beads with the captured RNA from wastewater samples were diluted 5x and run simultaneously alongside the corresponding undiluted sample. If RT-qPCR inhibition was present, the 5 times (x) dilution would minimize the inhibition, leading to a lower Ct for positive detections. Table 3.3 shows that the differences in the Ct values (ΔCt) between the 5x diluted and undiluted beads of samples ranged from 0.8 to 2.5. The mean ΔCt was 1.7 ± 0.6 , which is close to the expected ΔCt value of 2.3 from a 5x dilution, suggesting that no apparent inhibitors

are present in the undiluted magnetic beads suspension. These results demonstrate that my VIP-Mag method achieved sufficient removal of RT-qPCR inhibitors.

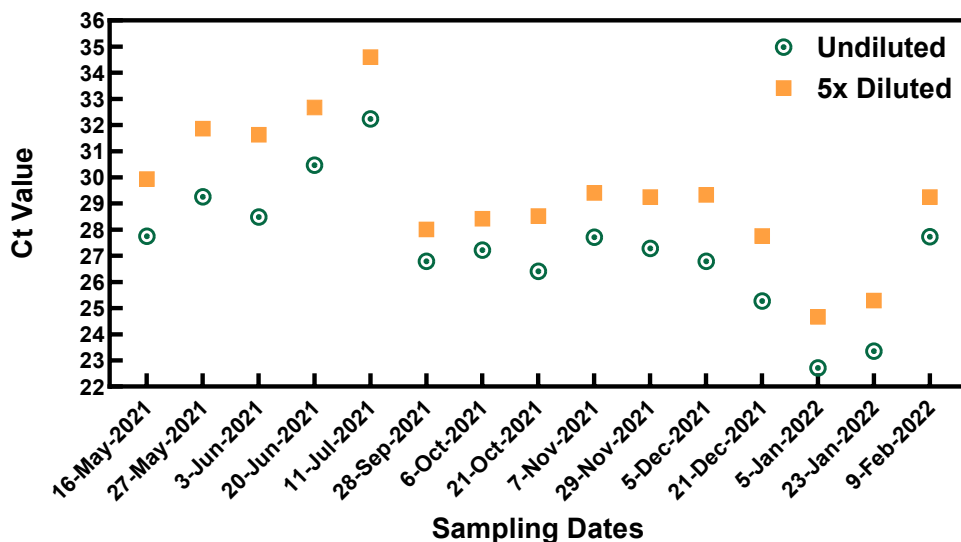


Figure 3.5. Monitoring wastewater samples for the presence of RT-qPCR inhibitors. Two wastewater samples were analyzed every month from May 2021 to February 2022 alongside regular wastewater sample analysis using the EM-VIP-Mag-RT-qPCR protocol.

Table 3.3. 5x dilutions of specific bi-monthly wastewater samples to monitor for sufficient removal of RT-qPCR inhibitors using my EM-VIP-Mag-RT-qPCR method.

Sample Name	Ct Value	Δ Ct Value (5xDiluted-Undiluted)
September 26 th	27.2	1.1
September 26 th 5X	28.3	
September 28 th	26.8	1.2
September 28 th 5X	28.0	
October 6 th	27.2	1.2
October 6 th 5X	28.4	
October 21 st	26.4	2.1
October 21 st 5X	28.5	
November 7 th	27.7	1.7
November 7 th 5X	29.4	
November 29 th	27.3	1.9
November 29 th 5X	29.2	
December 5 th	26.8	2.5
December 5 th 5X	29.3	
December 21 st	25.3	2.5

December 21 st 5X	27.7	
January 5 th	22.7	2.0
January 5 th 5X	24.7	
January 23 rd	23.3	1.9
January 23 rd 5X	25.3	
February 9 th	27.7	1.5
February 9 th 5X	29.2	
February 22 nd	27.8	0.8
February 22 nd 5X	28.6	

3.3.3 Improved RNA Recovery

Having optimized my EM-VIP-Mag-RT-qPCR method and demonstrated sufficient RT-qPCR inhibitor removal, I evaluated the overall recovery of SARS-CoV-2 by analyzing two sets of wastewater samples spiked with SARS-CoV-2 pseudovirus. Prior to these spiking experiments, the two sets of the wastewater samples were confirmed to be negative or positive with low copies of SARS-CoV-2 RNA by the references from Alberta Precision Laboratories (APL). In the first set of recovery experiments using negative wastewater samples, the recovery was $80\% \pm 4\%$ (Figure 3.6). In the second set of recovery experiments using positive samples with low copies of RNA, the recovery was $76\% \pm 4\%$ (Figure 3.6). The second set of experiments using low positive wastewater samples was performed to account for sample-to-sample variation. The recovery was calculated by taking the detected RNA copies and subtracting the RNA copies detected in the corresponding unspiked samples, and then dividing by the spiked amount. These overall recovery results demonstrate that my method constantly provided high recovery of viral RNA in wastewater samples.

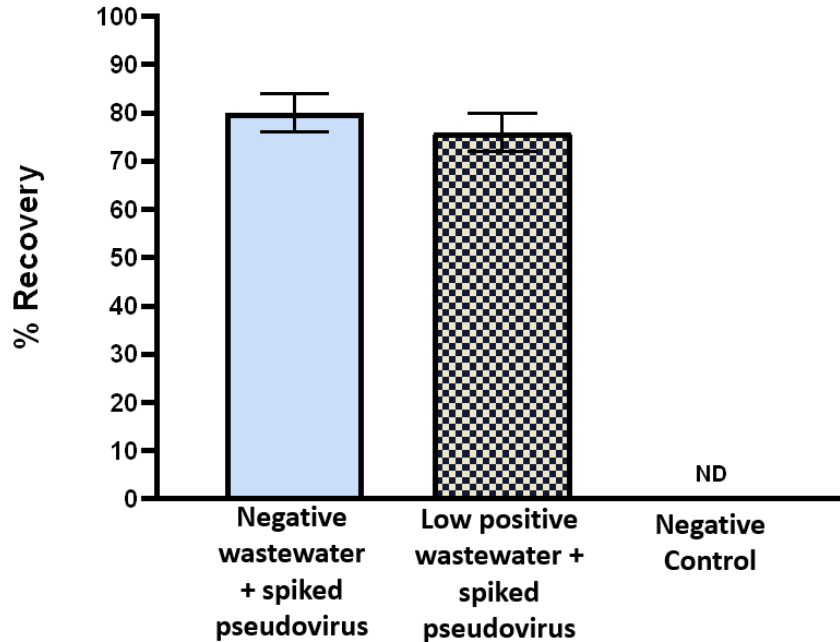


Figure 3.6. Recovery of viral RNA from wastewater samples. RNA of SARS-CoV-2 pseudovirus (10^4 copies) was added to an aliquot of each wastewater matrix; negative wastewater and a low positive wastewater. The N1 gene of SARS-CoV-2 was detected using RT-qPCR. The recovery was 80% \pm 4% and 76% \pm 4% from the analysis of these wastewater samples. The samples were tested in triplicates over three independent experimental days (n= 9). NC indicates negative control and ND indicates not detectable.

The EM-VIP-Mag-RT-qPCR method achieved consistently higher wastewater recovery than previously reported. Several WS of SARS-CoV-2 studies using enveloped surrogate viruses have reported largely variable recoveries ranging from 0.08-66% between studies and even within the same study.¹⁶ Furthermore, my method achieved higher recoveries than those of the previous studies which also used EM for viral particle and RNA concentration.^{24,27,60} The improved recovery provided by the EM-VIP-Mag-RT-qPCR method can be attributed to several strategies I incorporated. To maximize viral particle concentration and minimize RNA loss, I

released and isolated SARS-CoV-2 and RNA from solids using beef extract solution, efficiently extracted and maintained RNA integrity using the VIP buffer, and utilized magnetic beads to concentrate and directly detect RNA without an elution step. Additionally, to minimize co-concentration of RT-qPCR inhibitors, I removed inhibitors by separating the solid and aqueous phase prior to the EM filtration step and used the VIP-Mag method with three wash steps. Thus, I successfully developed a method with enhanced recovery.

3.3.4 Blind Test of Composite Wastewater Samples with Diverse SARS-CoV-2 RNA Concentrations

In a blind inter-laboratory comparison format, I analyzed a set of composite wastewater samples previously collected from a long-term care facility (APL confirmed SARS-CoV-2 negative) and from the Edmonton WWTP (APL confirmed SARS-CoV-2 positive). APL diluted the SARS-CoV-2 positive wastewater sample with the SARS-CoV-2 negative wastewater sample by 10, 100, and 1000 fold. I received the undiluted and diluted composite wastewater samples without prior knowledge of the sample characteristics or their viral RNA concentrations. Composed of wastewater from two sources, these samples appeared to have a very dirty and complex matrix. Due to these conditions, the reference lab was unable to detect SARS-CoV-2 RNA in any of the sample dilutions. However, using my EM-VIP-Mag-RT-qPCR method, I was able to quantify the SARS-CoV-2 RNA concentrations in these wastewater samples (Figure 3.7). My analyses showed that the concentrations of the SARS-CoV-2 RNA ranged from 1.9×10^2 RNA copies/100 mL to 4.1×10^5 RNA copies/100 mL wastewater (Figure 3.7). These results are consistent with the expected dilution factors and the concentrations in the composite wastewater samples, even though this information was blind to me prior to analysis. Furthermore, since the reference lab was unable to detect SARS-CoV-2 RNA in any of the dilutions, this demonstrates

that my method is effective at removing RT-qPCR inhibitors from a dirty and complex wastewater sample and detecting RNA at reasonably accurate concentrations.

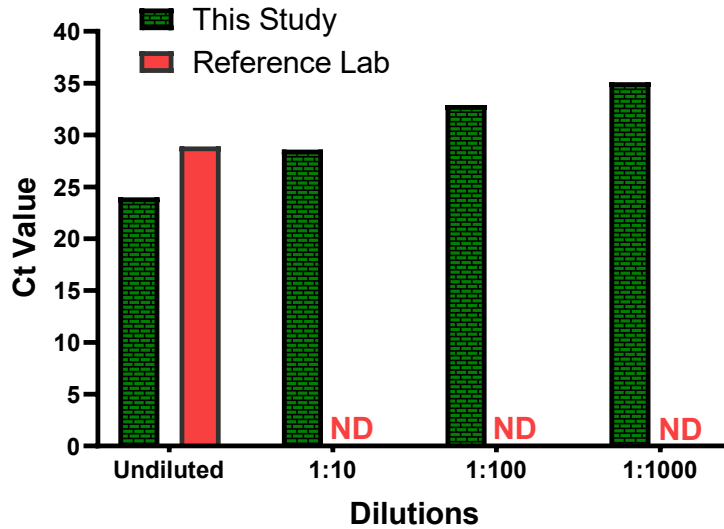


Figure 3.7. Dilution validation study where a previously determined wastewater sample was diluted by a negative wastewater sample by 10, 100, and 1000 times and processed by this study and the reference lab.

Also in a blind inter-laboratory comparison format, I analyzed the composite wastewater sample that APL prepared by diluting 0.1 mL Edmonton WWTP wastewater sample (SARS-CoV-2 positive) with 100 mL long-term care wastewater sample (SARS-CoV-2 negative). My analysis showed that the concentration of SARS-CoV-2 RNA was 190 RNA copies/100 mL of wastewater. For comparison, APL diluted 0.1 mL of the same Edmonton WWTP wastewater sample (SARS-CoV-2 positive) with 100 mL distilled deionized water (ddH₂O) and analyzed this relatively clean sample using APL's routine method. APL detected 10² RNA copies/100 mL of this diluted sample (mostly in ddH₂O). My result of detecting 190 copies of the SARS-CoV-2 RNA copies/100 mL of wastewater agrees with APL's result of detecting 10² RNA copies /100 mL of ddH₂O, which demonstrates the ability of my EM-VIP-Mag-RT-qPCR method for detecting trace and diverse concentrations of SARS-CoV-2 RNA in wastewater.

3.3.5 Detection of SARS-CoV-2 in 120 Wastewater Samples using EM-VIP-Mag-RT-qPCR and Comparison with APL Reference Lab

I successfully applied my EM-VIP-Mag-RT-qPCR method to detect SARS-CoV-2 in wastewater samples collected from two WWTPs in Calgary and Edmonton over a period of ten months (May 2021 to February 2022). Figure 3.8 shows C_t values from the analysis of 120 samples (60 samples from each city) using my EM-VIP-Mag-RT-qPCR method and the results obtained independently by the reference lab (APL) using their method. Pearson correlation between the two sets of C_t values was $r=0.81$ and $p<0.0001$, indicating that my results are significantly correlated with those of the reference lab.

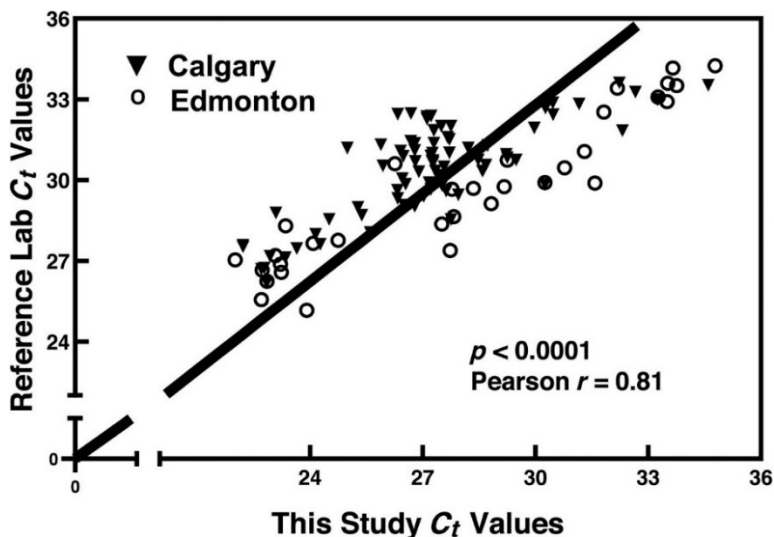


Figure 3.8. Pearson correlation analysis of results obtained using the EM-VIP-Mag-RT-qPCR method with the results provided by the reference laboratory from the analysis of 120 wastewater samples.

Figure 3.9 shows the SARS-CoV-2 RNA concentrations in representative wastewaters collected from Calgary and Edmonton WWTPs and analyzed by me as well as the reference lab using their method. These results show that my EM-VIP-Mag-RT-qPCR method was able to

detect the viral RNA in all 120 wastewater samples, with the lowest concentrations being 2.4×10^2 copies per 100 mL and the highest concentrations being 2.9×10^6 RNA copies/100 mL of wastewater. These results demonstrate excellent sensitivity and the wide dynamic range of my method. a)

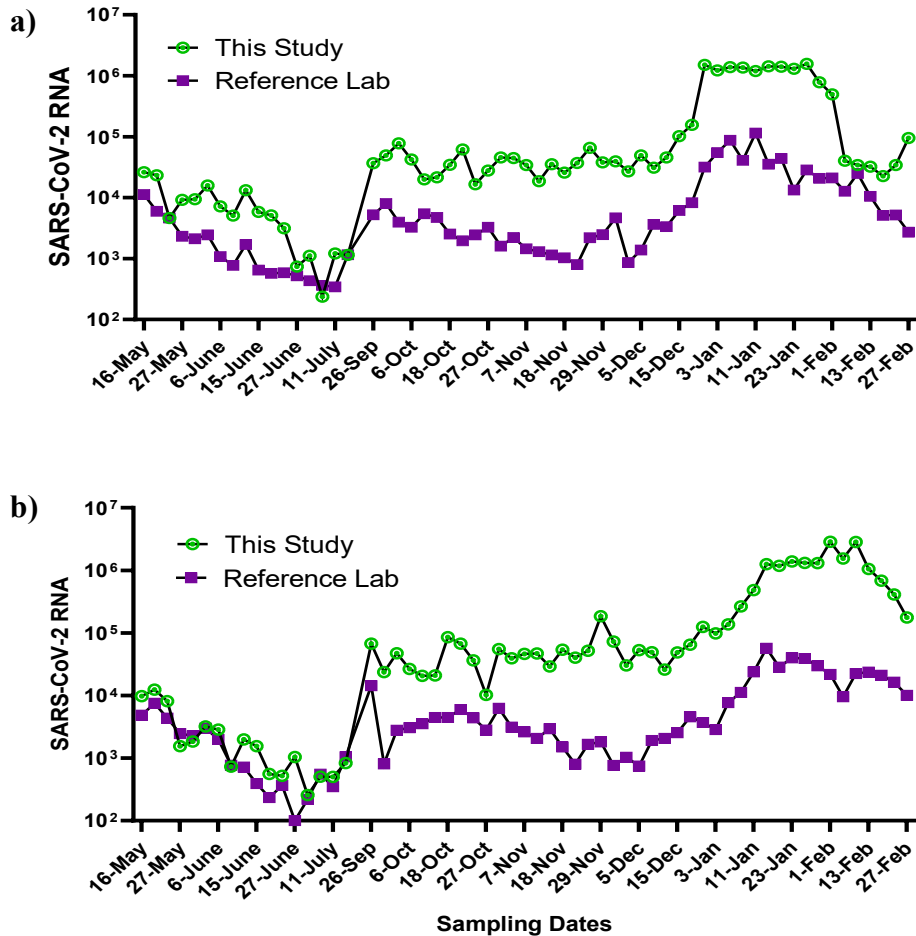


Figure 3.9. 120 wastewater samples analyzed from May 2021 to February 2022. 60 wastewater samples were collected from (a) Calgary and 60 wastewater samples were collected from (b) Edmonton. Overall, there is excellent concordance with the results provided by APL with my WS protocol providing a higher recovery of RNA overall.

In the Calgary and Edmonton samples, both results (mine and APL) show consistent trends of viral loads in wastewater over the sampling months. My method consistently detected higher RNA copies than APL for the Calgary and Edmonton wastewater samples over the

sampling time. These results demonstrate that my WS method is sensitive, reproducible, and capable of providing accurate results. Compared to APL, my enhanced WS protocol has improved SARS-CoV-2 detection due to improvements on three specific steps: (1) viral particle and RNA release from solids, (2) concentration of viral particles and RNA, and (3) RNA extraction. These improvements will be discussed in detail below.

To release viral particles from solids, I separately incubated the solid phase in a beef extract solution, collected the subsequent supernatant containing the released viral particles and RNA, and recombined with the aqueous phase. In the APL method, the whole sample was treated with NaOH to a pH of 9.6-10, vigorously shaken, and centrifuged to collect the supernatant. RNA is unstable in alkaline conditions because bases can easily deprotonate the hydrogen from the hydroxyl group on the 2'-carbon atom.⁶⁸ Moreover, Wurtzer et al., 2020 reported that most of the SARS-CoV-2 RNA present in wastewater is in unprotected forms (i.e., lysed and released from viral particle) rather than in infectious (i.e., culturable and contained in viral particle) or other protected forms.³² The alkaline conditions of the reference lab's sample pretreatment may have degraded some RNA present in the wastewater samples, contributing to the reduced copies of the RNA detected by the APL method.

At the viral particle concentration step, my WS protocol used EM filtration. APL used ultrafiltration with a Centricon Plus-70 centrifugal ultrafilter (30 kDa) to concentrate viral particles. Although ultrafiltration has advantages such as wide availability and fast-processing time, a major disadvantage is co-concentration of RT-qPCR inhibitors, which was reported in a previous study.²⁷ This study compared the recovery efficiency of several WS concentration methods using a SARS-CoV-2 surrogate virus and determined that ultrafiltration using the Centricon Plus-70 ultrafilter had a lower recovery of $28.0 \pm 9.1\%$ compared to EM ($65.7 \pm$

23.8%). This may be due to the higher abundance of co-concentrated RT-qPCR inhibitors by ultrafiltration, which may contribute to the lower copies of RNA detected by APL.

At the RNA extraction step, I used my in-house VIP-Mag method, enabling the direct detection of RNA on magnetic beads concentrated from 80 mL of sample without needing an elution step. In the APL method, viral RNA was extracted using the MagMAX™ Viral RNA Isolation Kit using the automated KingFisher™ Flex Purification System. This is a general use commercial extraction kit used for a variety of samples. Thus, it is not optimized for the complex matrix of wastewater and may not completely eliminate RT-qPCR inhibitors. This kit also requires an elution step. These factors may contribute to inhibition of RT-qPCR amplification and a lower overall recovery. Therefore, my WS protocol is more efficient, reliable, and accurate than commercially available and previously reported WS protocols.

3.4 Conclusion

I successfully developed the EM-VIP-Mag-RT-qPCR method that enhanced the recovery and detection of SARS-CoV-2 in wastewater samples. The main features that contribute to the improvement include recovery of SARS-CoV-2 viral particles and RNA from both solids and aqueous phase, processing with a large volume (80 mL) of wastewater, efficient RNA extraction and preservation using the VIP buffer, removal of sample matrix and inhibitors using magnetic beads, and direct RT-qPCR detection on magnetic beads. This method provides reproducible recovery of (76-80% ± 4%), representing a significant improvement compared to the previous studies (0.96-65.7%). My method uses accessible equipment and reagents and is cost-effective. It can be applied for monitoring of SARS-CoV-2 in wastewater for community surveillance, complementing clinical testing. This method can also be adapted for detection of other pathogens in wastewater.

3.5 References

1. Hrudey, S.E.; Bischel, H.N.; Charrois, J.; Chik, A.H.S.; Conant, B.; Delatolla, R.; et al. Wastewater surveillance for SARS-CoV-2 RNA in Canada. *Facets* **2022**, *7*, 1493-1597.
2. Centers for Disease Control and Prevention. *National Wastewater Surveillance System*, **2020**. Available from: <https://www.cdc.gov/healthywater/surveillance/wastewater-surveillance/wastewater-surveillance.html> (accessed 2022-08-10).
3. International Water Association. *COVID-19 wastewater-based epidemiology*. **2022**, Available from: <https://iwa-network.org/learn/covid-19-wastewater-based-epidemiology/> (accessed 2022-08-10).
4. NCCID (National Collaborating Centre for Infectious Disease). *Public Health Agency of Canada Wastewater surveillance program for COVID-19*, **2022**. Available from: <https://nccid.ca/wastewater-surveillance-for-covid-19/> (accessed 2022-08-10).
5. Canadian Water Network. *COVID-19 wastewater coalition*, **2022**. Available from: <https://cwn-rce.ca/covid-19-wastewater-coalition/> (accessed 2022-8-10).
6. Gupta, S.; Parker, J.; Smits, S.; Underwood, J.; Dolwani, S. Persistent viral shedding of SARS-CoV-2 in faeces – a rapid review. *Colorectal Dis.* **2020**, *22*, 611–620.
7. Wölfel, R.; Corman, V.M.; Guggemos, W.; Seilmaier, M.; Zange, S.; Muller, M.; et al. Virological assessment of hospitalized patients with COVID-2019. *Nature* **2020**, *581*, 465–469.
8. Zhang, W.; Du, R.H.; Li, B.; Zheng, X.S.; Yang, X.L.; Hu, B.; et al. Molecular and serological investigation of 2019-nCoV infected patients: implication of multiple shedding routes. *Emerging Microbes Infect.* **2020**, *9*, 386–389.

9. Karthikeyan, S.; Levy, J.I.; De Hoff, P.; Humphrey, G.; Birmingham, A.; et al. Wastewater sequencing reveals early cryptic SARS-CoV-2 variant transmission. *Nature* **2022**, 609 (7925), 101-108.
10. Vo, V.; Tillett, R.L.; Papp, K.; Shen, S.; Gu, R.; Gorzalski, A.; et al. Use of wastewater surveillance for early detection of Alpha and Epsilon SARS-CoV-2 variants of concern and estimation of overall COVID-19 infection burden. *Sci. Total Environ.* **2022**, 835, 155410.
11. Xie, Y.; Challis, J.K.; Oloye, F.F.; Asadi, M.; Cantin, J.; Brinkmann, M.; et al. RNA in municipal wastewater reveals magnitudes of COVID-19 outbreaks across four waves driven by SARS-CoV-2 variants of concern. *ACS ES&T Water* **2022**, 2 (11), 1852-1862.
12. Le, C. Sensitivity of wastewater surveillance: What is the minimum COVID-19 cases required in population for SARS-CoV-2 RNA to be detected in wastewater? *J. Environ. Sci.* **2023**, 125, 851–853.
13. Li, Q.; Lee, B.E.; Gao, T.; Qiu, Y.; Ellehoj, E.; Yu, J.; et al. Number of COVID-19 cases required in a population to detect SARS-CoV-2 RNA in wastewater in the province of Alberta, Canada: Sensitivity assessment. *J. Environ. Sci.* **2023**, 125, 843–850.
14. Chik, A.H.S.; Glier, M.B.; Servos, M.; Mangat, C.S.; Pang, X.L.; Qiu, Y.; et al. Comparison of approaches to quantify SARS-CoV-2 in wastewater using RT-qPCR: results and implications from a collaborative inter-laboratory study in Canada. *J. Environ. Sci.* **2021**, 107, 218–229.
15. Kantor, R.S.; Nelson, K.L.; Greenwald, H.D.; Kennedy, L.C. Challenges in measuring the recovery of SARS-CoV-2 from wastewater. *Environ. Sci. Technol.* **2021**, 55, 3514–3519.

16. Kumblathan, T.; Liu, Y.; Uppal, G.K.; Hruday, S.E.; Li, X.F. Wastewater-based epidemiology for community monitoring of SARS-CoV-2: Progress and Challenges. *ACS Environ. Au* **2021**, 1, 18–31.
17. Kumblathan, T.; Piroddi, N.; Hruday, S.E.; Li, X.F. Wastewater based surveillance of SARS-CoV-2: challenges and perspective from a Canadian inter-laboratory study. *J. Environ. Sci.* **2022**, 116, 229–232.
18. Pecson, B.M.; Darby, E.; Haas, C.N.; Amha, Y.M.; Bartolo, M.; Danielson, R.; et al. Reproducibility and sensitivity of 36 methods to quantify the SARS-CoV-2 genetic signal in raw wastewater: findings from an interlaboratory methods evaluation in the U.S. *Environ. Sci.: Water Res. Technol.* **2021**, 7, 504–520.
19. Wu, F.; Xiao, A.; Zhang, J.; Gu, X.; Lee, W.L.; Kauffman, K.; et al. SARS-CoV-2 titers in wastewater are higher than expected from clinically confirmed cases. *mSystems* **2020**, 5, e00614-20.
20. Green, H.; Wilder, M.; Middleton, F.A.; Collins, M.; Fenty, A.; Gentile, K.; et al. Quantification of SARS-CoV-2 and cross-assembly phage (crAssphage) from wastewater to monitor coronavirus transmission within communities. *MedRxiv* **2020**. Available from: <https://doi.org/10.1101/2020.05.21.20109181> (accessed 2022-08-10).
21. Sherchan S.P.; Shahin, S.; Ward, L.M.; Tandukar, S.; Aw, T.G.; Schmitz, B.; Ahmed, W.; Kitajima, M. First detection of SARS-CoV-2 RNA in wastewater in North America: A study in Louisiana, USA. *Sci. Total Environ.* **2020**, 743, 140621.
22. Nemudryi, A.; Nemudraia, A.; Wiegand, T.; Surya, K.; Buyukyoruk, M.; Cicha, C.; et al. Temporal detection and phylogenetic assessment of SARS-CoV-2 in municipal wastewater. *Cell Rep. Med.* **2020**, 1 (6), 100098.

23. Peccia, J.; Zulli, A.; Brackney, D.E.; Grubaugh, N.D.; Kaplan, E.H.; Casanovas-Massana, A.; et al. Measurement of SARS-CoV-2 RNA in wastewater tracks community infection dynamics. *Nat. Biotechnol.* **2020**, *38*, 1164–1167.
24. Gonzalez, R.; Curtis, K.; Bivins, A.; Bibby, K.; Weir, M.H., Yetka, K.; et al. COVID-19 surveillance in southeastern Virginia using wastewater based epidemiology. *Water Res.* **2020**, *186*, 116296.
25. Gerrity, D.; Papp, K.; Stoker, M.; Sims, A.; Frehner, W. Early-pandemic wastewater surveillance of SARS-CoV-2 in Southern Nevada: methodology, occurrence, and incidence/prevalence considerations. *Water Res. X.* **2021**, *10*, 100086.
26. Graham, K.E.; Loeb, S.K.; Wolfe, M.K.; Catoe, D.; Sinnott-Armstrong, N.; Kim, S.; et al. SARS-CoV-2 RNA in wastewater settled solids is associated with COVID-19 cases in a large urban Sewershed. *Environ. Sci. Technol.* **2021**, *55*, 488– 498.
27. Ahmed, W.; Bertsch, P.M.; Bivins, A.; Bibby, K.; Farkas, K.; Gathercole, A. Comparison of virus concentration methods for the RT-qPCR-based recovery of murine hepatitis virus, a surrogate for SARS-CoV-2 from untreated wastewater. *Sci. Total Environ.* **2020**, *739*, 139960.
28. Kumar, M.; Patel, A.K.; Shah, A.V.; Raval, J.; Rajpara, N.; Joshi, M.; Joshi, CG. First proof of the capability of wastewater surveillance for COVID-19 in India through detection of genetic material of SARS-CoV-2. *Sci. Total Environ.* **2020**, *746*, 141326.
29. Arora, S.; Nag, A.; Rajpal, A.; Tiwari, S.B.; Sethi, J.; Sutaria, D.; et al. Detection of SARS-CoV-2 RNA in fourteen wastewater treatment systems in Uttarakhand and Rajasthan States of North India. *Water* **2021**, *13* (16), 2265.

30. Medema, G.; Heijnen, L.; Elsinga, G.; Italiaander, R.; Brouwer A. Presence of SARS-Coronavirus-2 in sewage. *Environ. Sci. & Technol. Lett.* **2020**, 7 (7), 511-516.
31. Trottier, J.; Darques, R.; Mouheb, N.A.; Partiot, E.; Bakhache, W.; Deffieu, M.S.; Gaudin R. Post-lockdown detection of SARS-CoV-2 RNA in the wastewater of Montpellier, France. *One Health* **2020**, 10, 100157.
32. Wurtzer, S.; Marechal, V.; Mouchel, J.M.; Maday, Y.; Teyssou, R.; Richard, E.; et al., Evaluation of lockdown effect on SARS-CoV-2 dynamics through viral genome quantification in wastewater, Greater Paris, France, 5 March to 23 April 2020. *Eurosurveillance* **2020**, 25, 2000776.
33. Fongaro, G.; Stoco, P.H.; Souza, D.S.; Grisard, E.C.; Magri, M.E.; Rogovski, P.; et al. SARS-CoV-2 in human sewage in Santa Catarina, Brazil, November 2019. *Sci. Total Environ.* **2021**, 778, 146198.
34. Prado, T.; Fumian, T.M.; Mannarino, C.F.; Maranhão, A.G.; Siqueira, M.M.; Miagostovich, M.P. Preliminary results of SARS-CoV-2 detection in sewerage system in Niterói municipality, Rio de Janeiro, Brazil. *Mem. Inst. Oswaldo Cruz.* **2020**, 115, e200196.
35. Bar-Or, I.; Yaniv, K.; Shagan, M.; Ozer, E.; Erster, O.; Mendelson, E.; et al. Regressing SARS-CoV-2 sewage measurements onto COVID-19 burden in the population: a proof-of-concept for quantitative environmental surveillance. *Public Health Front.* **2022**, 9, 561710.
36. La Rosa, G.; Iaconelli, M.; Mancini, P.; Bonanno Ferraro, G.; Veneri, C.; Bonadonna, L.; et al. First detection of SARS-CoV-2 in untreated wastewaters in Italy. *Sci. Total Environ.* **2020**, 736, 139652.

37. La Rosa, G.; Mancini, P.; Bonanno, F.G.; Veneri, C.; Iaconelli, M.; Bonadonna, L.; et al. SARS-CoV-2 has been circulating in northern Italy since December 2019: evidence from environmental monitoring. *Sci. Total Environ.* **2021**, 750, 141711.
38. Rimoldi, S.G.; Stefani, F.; Gigantiello, A.; Polesello, S.; Comandatore, F.; Mileto, D.; et al. Presence and infectivity of SARS-CoV-2 virus in wastewaters and rivers. *Sci. Total Environ.* **2020**, 744, 140911.
39. Randazzo, W.; Truchado, P.; Cuevas-Ferrando, E.; Simón, P.; Allende, A.; Sánchez, G. SARS-CoV-2 RNA in wastewater anticipated COVID-19 occurrence in a low prevalence area. *Water Res.* **2020a**, 181, 115942.
40. Randazzo, W.; Cuevas-Ferrando, E.; Sanjuán, R.; Domingo-Calap, P.; Sánchez G. Metropolitan wastewater analysis for COVID-19 epidemiological surveillance. *Int. J. Hyg. Environ. Health.* **2020b**, 230, 113621.
41. Balboa, S.; Mauricio-Iglesias, M.; Rodríguez, S.; Martínez Lamas, L.; Vasallo, F.J.; Regueiro, B.; et al. The fate of SARS-CoV-2 in wastewater treatment plants points out the sludge line as a suitable spot for incidence monitoring. *Sci. Total Environ.* **2021**, 772, 145268.
42. Chavarria-Miró, G.; Anfruns-Estrada, E.; Guix, S.; Paraira, M.; Galofré, B.; Sáanchez, G.; et al. Sentinel surveillance of SARS-CoV-2 in wastewater anticipates the occurrence of COVID-19 cases. *MedRxiv.* **2020**. Available from: <https://doi.org/10.1101/2020.06.13.20129627> (accessed 2022-08-10).
43. Kocamemi, B.A.; Kurt, H.; Hacioglu, S.; Yarali, C.; Saatci, A.M.; Pakdemirli, B. First Data-Set on SARS-CoV-2 Detection for Istanbul Wastewaters in Turkey. *MedRxiv.* **2020**. Available from: <https://doi.org/10.1101/2020.05.03.20089417> (accessed 2022-08-10).

44. Haramoto, E.; Malla, B.; Thakali, O.; Kitajima, M. First environmental surveillance for the presence of SARS-CoV-2 RNA in wastewater and river water in Japan. *Sci. Total Environ.* **2020**, *737*, 140405.
45. Kitamura, K.; Sadamasu, K.; Muramatsu, M.; Yoshida, H. Efficient detection of SARS-CoV-2 RNA in the solid fraction of wastewater. *Sci. Total Environ.* **2021**, *763*, 144587.
46. Hata, A.; Hara-Yamamura, H.; Meuchi, Y.; Imai, S.; Honda, R. Detection of SARS-CoV-2 in wastewater in Japan during a COVID-19 outbreak. *Sci. Total Environ.* **2021**, *758*, 143578.
47. Westhaus, S.; Weber, F.A.; Schiwy, S.; Linnemann, V.; Brinkmann, M.; Widera, M.; et al. Detection of SARS-CoV-2 in raw and treated wastewater in Germany—suitability for COVID-19 surveillance and potential transmission risks. *Sci. Total Environ.* **2021**, *751*, 141750.
48. Sharif, S.; Ikram, A.; Khurshid, A.; Salman, M.; Mehmood, N.; Arshad, Y.; et al. Detection of SARS-Coronavirus-2 in wastewater, using the existing environmental surveillance network: an epidemiological gateway to an early warning for COVID-19 in communities. *PLoS ONE* **2021**, *16* (6), e0249568.
49. Ampuero, M.; Valenzuela, S.; Valiente-Echeverría, F.; Soto-Rifo, R.; Barriga, G.P.; Chnaiderman, J.; et al. SARS-CoV-2 detection in sewage in Santiago. Chile - preliminary results. *MedRxiv.* **2020**. Available from: <https://doi.org/10.1101/2020.07.02.20145177> (accessed 2022-08-10).
50. Mlejnkova, H.; Sovova, K.; Vasickova, P.; Ocenaskova, V.; Jasikova, L.; Juranova, E. Preliminary study of Sars-Cov-2 occurrence in wastewater in the Czech Republic. *Int. J. Environ. Res. Public Health.* **2020**, *17*, 5508.

51. Martin, J.; Klapsa, D.; Wilton, T.; Zambon, M.; Bentley, E.; Bujaki, E.; et al. Tracking SARS-CoV-2 in sewage: evidence of changes in virus variant predominance during COVID-19 pandemic. *Viruses* **2020**, *12* (10), E1144.
52. Albastaki, A.; Naji, M.; Lootah, R.; Almeheiri, R.; Almulla, H.; Almarri, I.; et al. First confirmed detection of SARS-COV-2 in untreated municipal and aircraft wastewater in Dubai, UAE: the use of wastewater based epidemiology as an early warning tool to monitor the prevalence of COVID-19. *Sci. Total Environ.* **2021**, *760*, 143350.
53. Hasan, S.W.; Ibrahim, Y.; Daou, M.; Kannout, H.; Jan, N.; Lopes, A.; et al. Detection and quantification of SARS-CoV-2 RNA in wastewater and treated effluents: Surveillance of COVID-19 epidemic in the United Arab Emirates. *Sci. Total Environ.* **2021**, *764*, 142929.
54. Gonçalves, J.; Koritnik, T.; Mioč, V.; Trkov, M.; Bolješič, M.; Berginc, N.; et al. Detection of SARS-CoV-2 RNA in hospital wastewater from a low COVID-19 disease prevalence area. *Sci. Total Environ.* **2021**, *755*, 143226.
55. Saguti, F.; Magnil, E.; Enache, L.; Churqui, M.P.; Johansson, A.; Lumley, D.; et al. Surveillance of wastewater revealed peaks of SARS-CoV-2 preceding those of hospitalized patients with COVID-19. *Water Res.* **2021**, *189*, 116620.
56. Hasing, M.; Yu, J.; Qiu, Y.; Maal-Bared, R.; Bhavanam, S.; Lee, B.; et al. Comparison of detecting and quantitating SARS-CoV-2 in wastewater using moderate-speed centrifuged solids versus an ultrafiltration method. *Water* **2021**, *13*, 2166.
57. Qiu, Y.; Yu, J.; Pabbaraju, K.; Lee, B.E.; Gao, T.; Ashbolt, N.J.; et al. Validating and optimizing the method for molecular detection and quantification of SARS-CoV-2 in wastewater. *Sci. Total Environ.* **2022**, *812*, 151434.

58. Lu, D.; Huang, Z.; Luo, J.; Zhang, X.; Sha, S. Primary concentration: The critical step in implementing the wastewater based epidemiology for the COVID-19 pandemic: A mini-review. *Sci. Total Environ.* **2020**, 747, 141245.
59. Shi, H.; Pasco, E.V.; Tarabara, V.V. Membrane-based methods of virus concentration from water: A review of process parameters and their effects on virus recovery. *Environ. Sci: Water Res. Technol.* **2017**, 3, 778–792.
60. LaTurner, Z.W.; Zong, D.M.; Kalvapalle, P.; Gamas, K.R.; Terwilliger, A.; Crosby, T.; et al. Evaluating recovery, cost, and throughput of different concentration methods for SARS-CoV-2 wastewater-based epidemiology. *Water Res.* **2021**, 197, 117043.
61. D’Aoust, P.M.; Mercier, E.; Montpetit, D.; Jia, J.J.; Alexandrov, I.; Neault, N.; et al. Quantitative analysis of SARS-CoV-2 RNA from wastewater solids in communities with low COVID-19 incidence and prevalence. *Water Res.* **2021**, 188, 116560.
62. Carrillo-Reyes, J.; Barragán-Trinidad, M.; Buitrón, G. Surveillance of SARS-CoV-2 in sewage and wastewater treatment plants in Mexico. *J. Water Process. Eng.* **2021**, 40, 101815.
63. Buonerba, A.; Corpuz, M.V.; Ballesteros, F.; Choo, K.H.; Hasan, S.W.; Korshin, G.V.; et al. Coronavirus in water media: Analysis, fate, disinfection and epidemiological applications. *J. Hazard. Mater.* **2021**, 415, 125580.
64. Roldan-Hernandez, L.; Graham, K.; Duong, D.; Boehm, A. Persistence of endogenous SARS-CoV-2 and pepper mild mottle virus RNA in wastewater settled solids. *ACS ES&T Water* **2022**, 2 (11), 1944-1952.
65. Schrader, C.; Schielke, A.; Ellerbroek, L.; Johne, R. PCR inhibitors—occurrence, properties and removal. *J. Appl. Microbiol.* **2012**, 113 (5), 1014-1026.

66. Liu, Y.; Kumblathan, T.; Feng, W.; Pang, B.; Tao, J.; Xu, J.; et al. On-site viral inactivation and RNA preservation of gargle and saliva samples combined with direct analysis of SARS-CoV-2 RNA on magnetic beads. *ACS Meas. Sci. Au* **2022**, 2, 224–232.
67. Ramón-Núñez, L.A.; Martos, L.; Fernández-Pardo, Á.; Oto, J.; Medina, P.; España, F.; Navarro, S. Comparison of protocols and RNA carriers for plasma miRNA isolation. Unraveling RNA carrier influence on miRNA isolation. *PLoS One* **2017**, 12, e0187005.
68. Lemire, K.A.; Rodriguez, Y.Y.; McIntosh, M.T. Alkaline hydrolysis to remove potentially infectious viral RNA contaminants from DNA. *Viol. J.* **2016**, 13, 1-12.

Chapter Four: Multiplex RT-qPCR Assays for the Early Detection of Variants of Concern (VOCs) in Wastewater*

*This chapter has been published and a portion was modified from Liu, Y.; Kumblathan, T.; Joyce, M.A.; Tyrrell, D.L.; Tipples, G.; Pang, X.; Li, X.F.; Le, X.C. Multiplex Assays Enable Simultaneous Detection and Identification of SARS-CoV-2 Variants of Concern in Clinical and Wastewater Samples. *ACS Meas. Sci. Au*, **2023**, 3, 258–268. Liu Y conceptualized experimental design, performed the multiplex optimization and clinical experiments, data collection and analysis, text, and schematic composition, and revised the primary manuscript. I performed the multiplex optimization and wastewater experiments, data collection and analysis, and helped revise the primary manuscript. Joyce MA, Tyrrell DL, Tipples G, Pang X, Li XF, and Le XC contributed to editing the manuscript.

*This chapter has been published and a portion was modified from Kumblathan, T.; Liu, Y.; Pang, X,L.; Hrudey, S.E.; Le, X.C.; Li, X.F. Quantification and Differentiation of SARS-CoV-2 Variants in Wastewater for Surveillance. *ACS Environ. Health* **2023b**, 1, 203-213. I conceptualized experimental design, performed the experiments, data collection and analysis, text and schematic composition, and revised the overall manuscript. Liu Y contributed to experimental design and manuscript revisions. Pang X, Hrudey SE, Le XC, and Li XF contributed to editing the manuscript.

*The research project, of which this thesis is a part, received research ethics approval from the University of Alberta Research Ethics Board, project name “CL3 Viral Infectivity Models”, No. UAP3885, June 1 2020.

4.1 Introduction

In the previous chapters, I introduced how SARS-CoV-2 can be detected from different sample types such as oral fluids and wastewater. However, SARS-CoV-2 has been rapidly evolving through natural selection mechanisms over the last few years of the pandemic, therefore using the N gene for detection is not sufficient for the detection of newly emerging variants. This is because the naturally selected mutations are in the S protein. The S protein is commonly associated with enhanced viral infectivity and pathogenicity, and the mutations are associated with vaccine-breakthrough or antibody resistance.^{1,2,3} Thus, numerous genetic lineages of SARS-CoV-2 variants containing these naturally selected mutations are emerging continuously.^{1,4} So far, five globally dominant lineages of SARS-CoV-2 have been designated as variants of concern (VOCs) by the World Health Organization (WHO). The WHO proposed labels for these five lineages of SARS-CoV-2 as Alpha (B.1.1.7 and descendant lineage), Beta (B.1.351 and descendant lineage), Gamma (P.1 and descendant lineage), Delta (B.1.617.2 and descendent lineage), and Omicron (B.1.1.529, and sub-lineages).⁵ Compared to the other VOCs, Omicron is a variant family, containing six sub-variants: BA.1, BA.2, BA.3, BA.4 and BA.5, and XBB.⁶ The Omicron family is continuously mutating with new sub-lineages expected to emerge.

Research has revealed the functions of some of the VOC mutations. For example, mutation D614D allows an advantage for enhanced transmissibility and infectivity.^{7,8} Mutation N501Y, located in the receptor-binding domain of the S protein, allows elevated affinity for host receptors.^{9,10} The HV69-70 deletion allows a higher level of infectivity and higher infection severity based on hospitalizations and fatality cases.^{11,12} Mutations K417N/T moderately decreases the affinity of the S protein to host receptors while facilitating immune evasion.¹⁰ Mutation T478K can diminish the neutralizing activity of antibodies.¹³ Mutation P681R can

enhance the cleavage of the S protein to S1 and S2, leading to increased viral replication.¹⁴ Additionally, mutation L452R is unique as it can be used to differentiate Omicron BA.4/5 from other Omicron subvariants.¹⁵

As each VOC carries different mutation combinations in its S protein, the five VOCs have different capabilities on transmission, pathogenicity, and immune evasion. Beta and Gamma are more lethal than Alpha due to the combination of the K417N/T, E484K, and N501Y mutations present.¹⁶ Additionally, the Delta variant caused a significantly increased vaccine breakthrough, and had higher hospital admission and fatalities than Alpha, Beta, and Gamma.^{17,18} On the other hand, the Omicron subvariants have increased vaccine breakthrough, but decreased hospitalization rates and less disease severity.^{19,20} Among the dominant subvariants of Omicron, BA.2 is ~1.5 times more infectious than BA.1, while BA.4 and BA.5 are ~1.4 times more contagious than BA.2.²¹⁻²⁴ At the time of this project, XBB.1.5 and XBB.1.16 were the current circulating variant of interest.¹⁵ New variants are continuously evolving, each with their own unique characteristics.

Therefore, it is critical to have a rapid and inexpensive surveillance method to specifically identify these VOCs and monitor for emerging variants. The detection of SARS-CoV-2 variants is an important component of COVID-19 surveillance. Depending on the stage of the pandemic, detection of SARS-CoV-2 variants has been used for 1) guiding public health contact-tracing investigations with the objective to contain newly detected VOCs in a particular geographic area, 2) the identification of variants to determine likely susceptibility or resistance to antibody treatment, 3) linking with clinical and epidemiological data to better understand disease severity, breakthrough infections, and reinfections associated with particular variants, and 4) surveillance information as one of the many factors in public health policy and strategy

decisions. Uncontrollable outbreaks of these unique VOCs increase the burden on the healthcare system that has already been stretched thin by the COVID-19 pandemic. Clinical surveillance alone is unable to cope with the large number of cases and is unable to fully track SARS-CoV-2 variant emergence and spread because of the limited testing capacity, case participation, and asymptomatic cases. Reports demonstrate that clinical results are intrinsically delayed and are only available 3-9 days after illness onset.²⁵ With the rise of each unique variant, it became apparent that community monitoring of different SARS-CoV-2 variants is necessary. This reality highlights the need for innovative technologies for managing the ongoing pandemic and building preparedness for the future.

The routine surveillance method of sequencing provides the highest resolution of information and is essential for detecting new emerging variants. However, sequencing approaches suffer from long turnaround times, high costs, and are not available in many places due to a lack of resources and expertise. However, complementary “targeted screening” assays can be much faster and enable screening of a higher proportion of COVID-19 positive cases in a community or jurisdiction. The challenge with targeted screening tests is the need to constantly update and optimize targets included in the assays. Alternatively, RT-qPCR is a faster and specific approach to identify a specific VOC through testing the unique mutations present in a specific VOC. So far, several jurisdictions have been relying upon a readily available commercial assay (i.e., TaqPath Thermo Fisher assay) to identify S gene target failures (SGTFs) and rapidly detect potential VOCs. Unfortunately, this can only detect variants containing HV 69-70 deletion such as Alpha and Omicron (BA.1, BA.3, BA.4 and BA.5), and cannot discriminate between them.²⁶ Multiplex RT-qPCR assays, in which several targets can be detected from a single assay, are beneficial for SARS-CoV-2 VOC detection because several

mutations (i.e., HV 69-70, K417N/T, T478K, P681R, L452R) can be used as detection targets. Other advantages of multiplex RT-qPCR assays include saving of resources (samples, reagents, etc.), cost reduction, faster results, and increased precision in results.^{27,28} Although multiplex RT-qPCR assays are a promising solution for the detection of VOCs, an alternative sample to NPS needs to be used to monitor for VOCs in the community on a large scale for reasons discussed in previous chapters.

As mentioned in the previous chapter, WS has been an excellent alternative to monitor the scope of the COVID-19 pandemic in a community and is complementary to clinical testing for guiding public health measurements.²⁹ Studies have shown that SARS-CoV-2 RNA in wastewater can appear 4-10 days prior to clinical PCR test results.²⁹ Many countries have utilized metagenomic sequencing of SARS-CoV-2 RNA from wastewater samples to obtain high resolution sequence information and identify emerging and dominant variants in a specific community.²⁹ Sequencing approaches and variant-specific singleplex RT-qPCR assays have been developed and applied for the identification of variants in wastewater.^{26,30} However, the RNA present in wastewater is at low concentration, fragmented, and contains a mixture of SARS-CoV-2 variants, resulting in tremendous technical challenges with detection and re-assembly of viral genomes from wastewater.²⁹ To identify all the VOCs present in the wastewater, many singleplex RT-qPCR assays are required, which may be expensive, require extensive reagents, and operation time. In contrast, multiplex RT-qPCR assay enables simultaneous detection and differentiation of variants co-circulating in wastewater.

In this chapter, my objective was to develop alternative variant screening assays that can be applied to new targets and new variants in a timely manner. I chose target mutations that confer increased infectivity and evasion of immune response, which favor the survival of new

variants. These mutations are naturally selected and may appear in future SARS-CoV-2 variants.^{1,3} Therefore, these targets used for identification of the current variants have the potential to be used for detection of future variants. It is important to recognize that SARS-CoV-2 variants continue to evolve, but my approach is adaptable in a timely manner for newer targets and variants. My procedure entails capturing SARS-CoV-2 variant viral particles and free RNA from wastewater, effective extraction of RNA and enrichment onto magnetic beads while removing PCR inhibitors and direct multiplex RNA detection on magnetic beads. The ABG and Delta multiplex can detect the Alpha, Beta, Gamma, and Delta variants. The Omicron multiplex assay can detect and differentiate Omicron BA.1, BA.2, BA.4/5, and XBB. The goal of this chapter is to monitor VOCs in WS and compare the trends of these variants in wastewater with the clinical cases provided by Alberta Health Services. My results demonstrate the sensitivity and specificity of my platform and its application for timely WS monitoring of the variants circulating in the community.

4.2 Experimental

4.2.1 Wastewater Sample Collection

Wastewater samples were collected from two wastewater treatment plants (WWTPs) located in Calgary and Edmonton (Alberta, Canada) from May 2021 to March 2023. Five hundred milliliters of post-grit raw influent wastewater samples were collected from 24-hour composite samplers twice a week. All the samples were labelled with date, time, and sampling location, stored at 4°C, and shipped to Dr. Lilly (Xiaoli) Pang's research laboratory (Pan Alberta WS program) on a weekly basis and an aliquot was provided to me for analysis.

4.2.2 SARS-CoV-2 RNA Used for the Development and Validation of Multiplex RT-qPCR Assays

Purified SARS-CoV-2 RNA used for the development and validation of the multiplex RT-qPCR assays were provided by collaborators in the Li Ka Shing Institute of Virology. The purified RNA was prepared from passaged isolates of clinical samples submitted to the Provincial Health Laboratory Alberta Precision Laboratories (APL) who are an accredited clinical laboratory responsible for the province-wide clinical testing of COVID-19. The Global Initiative on Sharing All Influenza Data (GISAID) accession numbers for the sequences of the SARS-CoV-2 VOCs RNAs extracted from clinical nasopharyngeal specimens are listed below in Table 4.1. In brief, the first passage SARS-CoV-2 was made from 50 µL of a de-identified nasopharyngeal sample, which was filtered and incubated with Vero-TMPRSS2 cells. Second passage virus was then made similarly. RNA was extracted using the QIAamp viral RNA mini kit (Qiagen). The purified RNA was diluted and stored in THE RNA Storage Solution (ThermoFisher Scientific (Carlsbad, CA, USA) containing 1.2 U/µL of RNasin® Plus RNase Inhibitor at -80°C to ensure RNA stability.

Table 4.1. GISAID accession numbers for the sequence of the clinical nasopharyngeal specimens used to extract Alpha, Beta, Gamma, Delta, and Omicron (BA.1, BA.2, BA.4, BQ1.1 (derivative of BA.5), and XBB.1) RNA.

SARS-CoV-2 Variants of Concern	GISAID Accession Number
Alpha	EPI_ISL_2164495
Beta	EPI_ISL_2164334
Gamma	EPI_ISL_2166896.2
Delta	EPI_ISL_2477869
Omicron BA.1	EPI_ISL_8595751
Omicron BA.2	EPI_ISL_13215692
Omicron BA.4	EPI_ISL_13725091
Omicron BQ1.1 (BA.5 derivative)	EPI_ISL_16136893
Omicron XBB.1	EPI_ISL_16400048

4.2.3 Wastewater Viral Particle Concentration and RNA Extraction Protocol: EM-VIP-Mag

The wastewater sample analysis was performed similar to as described in Chapter 3. 80 or 200 mL of wastewater sample was centrifuged for the separation of the aqueous and solid phase. The resulting aqueous phase was transferred into another conical tube and the solid pellet was re-suspended in a 3% beef extract solution (pH 9.0). The mixture was agitated and centrifuged. The resulting supernatant was transferred into a new tube, neutralized with HCl, and then combined with the aqueous phase. Afterwards, MgCl₂ (1 mol/L) was added into the resulting mixture to reach the final concentration of 25 mmol/L. The treated wastewater sample was filtered through an EM using a vacuum filtration set-up. The EMs containing the captured SARS-CoV-2 particles were directly used to extract viral RNA using my established VIP-Mag method discussed in Chapters 2 and 3 of this thesis. In this method, the RNA was released using the VIP buffer and the released RNA was extracted and enriched on magnetic beads. The resulting magnetic beads possessing the extracted RNA were air-dried and resuspended in a 30 µL of solution consisting of 25 µL of RNase-free water, 4 µL proteinase K inhibitor, and 1 µL RNase inhibitor. The extracted RNA was stored at -80°C until time of analysis. This entire virus concentration and RNA extraction protocol is referred to as the EM-VIP-Mag method. Details on the development of the EM-VIP-Mag method can be found in Chapters 2 and 3.

4.2.4 Determination of Total SARS-CoV-2 RNA Directly on Magnetic Beads Containing Concentrated Viral RNA via CDC N1 Gene RT-qPCR

Total SARS-CoV-2 RNA was determined using the TaqPath 1-Step RT-qPCR Master Mix (Thermo Fisher Scientific, Waltham, CA, USA) and CDC N1 primer-probes from the 2019-

nCoV RUO kit (IDT, Coralville, IA, USA) according to the manufacturers' instructions. A portion (5 μ L) of the extracted RNA was used as template for each RT-qPCR reaction. The RT-qPCR assay was performed on a QuantStudio™ 3 Real-Time PCR System (Applied Biosystems, Thermo Fisher Scientific) using the QuantStudio™ Design & Analysis Software v1.5.1. A standard curve was used to convert Ct values to viral RNA copies which were then converted to the number of SARS-CoV-2 RNA copies within 100 mL of original wastewater sample.

4.2.5 Singleplex RT-qPCR Assays for the Alpha, Beta, Gamma, and Delta Variants

I first optimized singleplex assays for each VOC. The NEB Luna Universal Probe One-Step RT-qPCR Kit was used to perform all assays. Primers-probe sets for each of the K417N, K417T, T478K, and P681R mutations and the HV69-70 deletion targets were designed using Primer Express 3.0.1 software, and their sequences are summarized below in Table 4.2.

Annealing temperatures and concentrations of primers and probes were optimized for each of the single target assays: HV69-70 deletion and K417N, K417T, T478K, and P681R mutations. For optimization of the primer concentrations, a range of concentrations (100 to 800 nM) of each forward primer were paired with different concentrations of its corresponding reverse primer. Probe concentrations from 50 to 500 nM were tested in the optimization experiments. Each singleplex assay was conducted to test variant RNA containing specific mutations and the wild-type SARS-CoV-2 RNA in parallel at annealing temperatures ranging from 55 to 65°C to find the optimal temperature capable of differentiating mutations from the wild-type sequence. The optimized conditions for each assay are shown below in Table 4.3.

The RT-qPCR reaction mixture (20 μ L of total reaction volume) for each singleplex assay contained 10 μ L of Luna Universal One-Step Reaction Mix (2 \times), 1 μ L of Luna WarmStart

RT Enzyme Mix (20×), optimal concentrations of the corresponding forward primer, reverse primer, and probe for each assay (Table 4.3), and 5 µL of the template (sample). RT-qPCR thermal cycling conditions were as follows: 55 °C for 10 min, 95 °C for 1 min, and 45 cycles of 95 °C for 10 s and 60–64 °C annealing temperature (Table 4.3) for 1 min. All the RT-qPCR assays were performed on a QuantStudio 3 Real-Time PCR System (Applied Biosystems, Thermo Fisher Scientific) using the QuantStudio Design & Analysis Software v1.5.1.

Table 4.2. Primer and probe combinations developed for the detection and discrimination of SARS-CoV-2 variants of concern.

Amplicon & primer name (accession number in GISAID)	Oligo sequence (from 5' to 3')
K417N amplicon (89 bp) (EPI_ISL_16540372)	5' GAGGTGATGAAGTCAGACAAATCGCTCCAGGGC AAACTGGAAATATTGCTGATTATAATTATAAATTACCA GATGATTTTACAGGCTGC
K417T Amplicon (89 bp) (EPI_ISL_16645710)	5' GAGGTGATGAAGTCAGACAAATCGCTCCAGGGCA AACTGGAACGATTGCTGATTATAATTATAAATTACCAG ATGATTTTACAGGCTGC
K417N/T F- primer	5' GAGGTGATGAAGTCAGACAAATCG
K417N/T R-primer	5' GCAGCCTGTAAAATCATCTGGTAA
K417N Probe (G22813T)	5' FAM- CAAACTGGAAA ^t ATTGCTGATT-NFQ-MGB
K417T Probe (A22812C)	5' NED- AACTGGAA ^c GATTGCT-NFQ-MGB
HV69-70 deletion amplicon (74 bp) (EPI_ISL_601443)	5' CCTTTCTTTTCCAATGTTACTTGGTTCCATGCTATCT CTGGGACCAATGGTACTAAGAGGTTTGATAACCCTGT
HV69-70 deletion F-primer	5' CCTTTCTTTTCCAATGTTACTTGGTT
HV69-70 deletion R-primer	5' ACAGGGTTATCAAACCTCTTAGTACCA
HV69-70 deletion Probe (21765-21770 deletion)	5' Yakima-ATGCTATCT/ZEN/CTGGGACCAA- <i>IABkFQ</i>
T478K amplicon (87 bp) (EPI_ISL_16647223)	5' CCTTTTGAGAGAGATATTTCAACTGAAATCTATCA GGCCGGTAGCAAACCTTGTAAATGGTGTGAAGGTTTT AATTGTTACTTTCCT

T478K F-primer	5' CCTTTTGAGAGAGATATTTCAACTGAAAT
T478 K R-primer	5' AGGAAAGTAACAATTAACCTTCAACAC
T478 K probe (C22995A)	5' FAM- CCGGTAGCA ^a ACCTTGTA-NFQ-MGB
P681R amplicon (89 bp) (EPI_ISL_16647223)	5' CCCATTGGTGCAGGTATATGCGCTAGTTATCAGACT CAGACTAATTCTCGTCGGCGGGCACGTAGTGTAGCTA GTCAATCCATCATTGC
P681P F-primer	5' CCCATTGGTGCAGGTATATGC
P681R R-primer	5' GCAATGATGGATTGACTAGCTACACT
P681R probe (C23604G)	5' VIC- AGACTAATTCTC ^g TCGGCG-NFQ-MGB

*Genome position according to GISAID reference strain: hCoV-19/Wuhan/WIV04/2019, (EPI_ISL_402124 in GISAID). The single nucleotide mutations associated with variants of concern are indicated with lower case letters and in red color. F-primer represents forward-primer. R-primer indicates reverse-primer. IABkFQ denotes Iowa black fluorescence quencher. ZEN indicates internal ZEN black quencher. NFQ-MGB is a nonfluorescent quencher-minor groove binder.

Table 4.3. Optimal RT-qPCR conditions for singleplex and multiplex assays for the detection of five targets: HV69-70 deletion, and K417N, K417T, T478K and P681R mutations

Targets	Singleplex RT-qPCR				Assay	Multiplex RT-qPCR			
	F-primer (nM)	R-primer (nM)	Probe (nM)	Annealing T (°C) *		F-primer (nM)	R-primer (nM)	Probe (nM)	Annealing T (°C)
HV69-70 deletion	100	800	250	61	ABG	100	800	250	
K417N	100	800	500	60		100	800	500	61
K417T	100	800	500	60		100	800	500	
T478K	400	800	250	64	Delta	400	800	250	
P681R	200	800	250	60		100	800	250	64

*T represents temperature.

4.2.6 Multiplex RT-qPCR Assays for the Alpha, Beta, and Delta Variants

Next, I optimized the ABG multiplex assay conditions based on the three singleplex assays targeting the HV69-70 deletion, and K417N or K417T mutation (Table 4.3). The ABG multiplex RT-qPCRs (20 µL of total reaction volume) contained 10 µL of Luna Universal One–

Step Reaction Mix (2×), 1 µL of Luna WarmStart RT Enzyme Mix (20×), 100 nM of each forward primer, 800 nM of each reverse primer, 250 nM of probe for the HV69-70 deletion target, 500 nM of each probe for the K417N and K417T mutation targets, and 5 µL of sample. The multiplex RT-qPCR thermal cycling conditions were as follows: 55 °C for 10 minutes, 95 °C for 1 minute, and 45 cycles of 95 °C for 10 seconds and 61 °C annealing temperature for 1 minute. The ABG multiplex RT-qPCR assays were performed on a QuantStudio 3 Real-Time PCR System and data analyzed using the QuantStudio Design & Analysis Software v1.5.1 (Applied Biosystems, Thermo Fisher Scientific). This instrument has four spectral channels, with one channel used for the reference, therefore a maximum of three channels can only be used for a multiplex assay in a single run.

4.2.7 Multiplex RT-qPCR Assays for the Delta Variant

The Delta assay targeting both T478K and P681R mutations was optimized based on the two singleplex assays for these targets. The Delta assay multiplex RT-qPCRs (20 µL of total reaction volume) contained 10 µL of Luna Universal One-Step Reaction Mix (2×), 1 µL of Luna WarmStart RT Enzyme Mix (20×), 400 nM of forward primer for the T478K target, 100 nM of forward primer for the P681R target, 800 nM of each reverse primer, 250 nM of each probe for the T478K and P681R mutation targets, and 5 µL of sample. The multiplex RT-qPCR thermal cycling conditions were as follows: 55 °C for 10 minutes, 95 °C for 1 minute, and 45 cycles of 95 °C for 10 seconds and 64 °C for 1 minute. The Delta assay was conducted on the same instrument as the ABG assay.

4.2.8 Dynamic Range, Efficiency, Analytical Sensitivity, Specificity, and Reproducibility of the ABG and Delta Multiplex RT-qPCR Assays

The dynamic range for these two multiplex RT-qPCR assays was determined by testing 10-fold serial dilutions of quantified pure RNA in triplicate. The log values of the copies of pure SARS-CoV-2 variant RNA were plotted against the corresponding Ct values to generate standard curves (Figures 4.1 and 4.2). The slope of each standard curve was used to calculate the RT-qPCR efficiency of each assay using the following equation: $E = -1 + 10^{(-1/\text{slope})}$, where E represents PCR efficiency. The analytical sensitivity of the two assays was determined by testing twofold serial dilutions of variant RNA. The limit of detection (LOD) for the ABG multiplex RT-qPCR assay was determined by testing Alpha, Beta, and Gamma RNA ranging from 4 to 250 copies/reaction. The LOD of the Delta multiplex RT-qPCR assay was determined by testing Delta RNA ranging from 8 to 250 copies/reaction. In the ABG assay, reactions containing 16–250 copies of RNA were conducted in six replicates, while reactions containing 4 and 8 copies of RNA were performed in 10 replicates. In the Delta assay, reactions containing 32–250 copies of RNA were conducted in six replicates, while reactions containing 8 and 16 copies of RNA were performed in 10 replicates. The LOD was defined as the lowest RNA concentration detected in all of 10 replicates. Ct values over 40 were considered as a non-detectable threshold. The analytical specificity of the ABG and Delta assays was determined by testing $\sim 10^5$ copies of wild-type SARS-CoV-2, Alpha, Beta, Gamma, and Delta RNA individually using the ABG and Delta multiplex RT-qPCR assays.

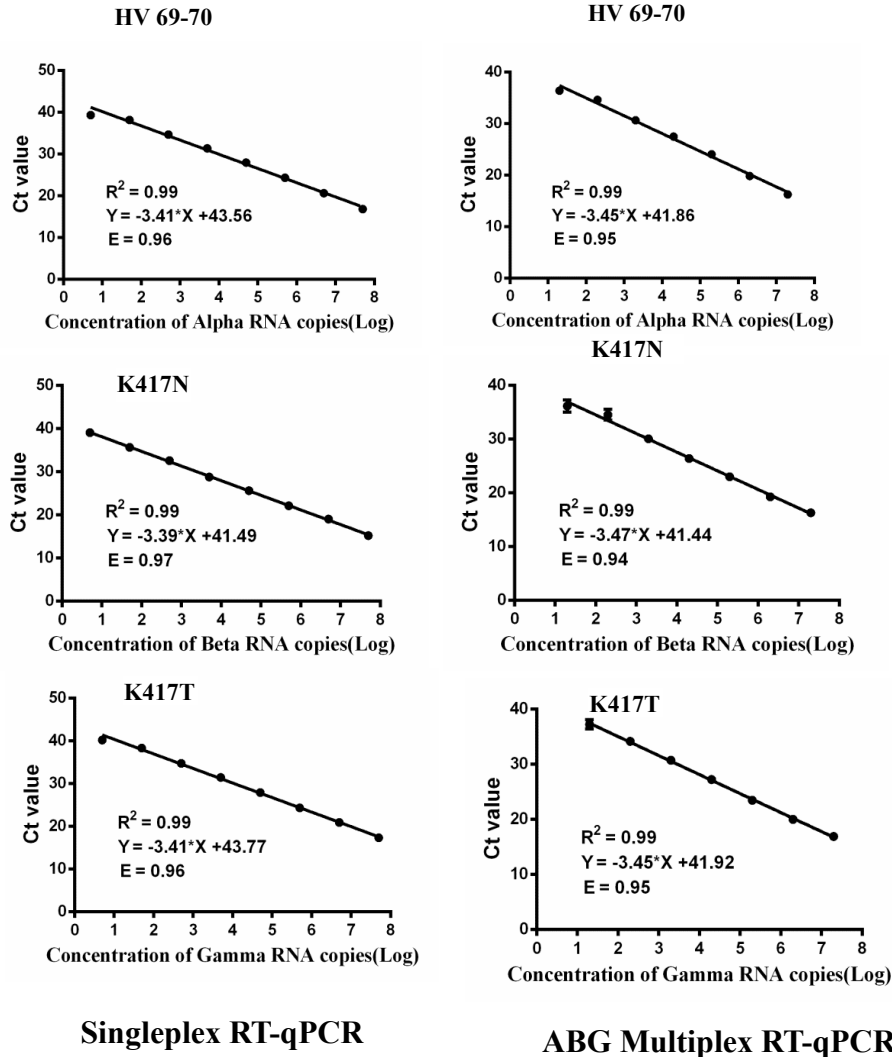


Figure 4.1. Standard curves of targets HV69-70 deletion, and K417N and K417T mutation using singleplex RT-qPCR assays (left figures) and using the ABG multiplex RT-qPCR assay (right figures). E represents PCR efficiency which was calculated using the equation: $E = -1 + 10^{(-1/\text{slope})}$, where slope refers to the slope of the standard curve. This standard curve was used to quantify the amounts of SARS-CoV-2 variant RNA in the samples.

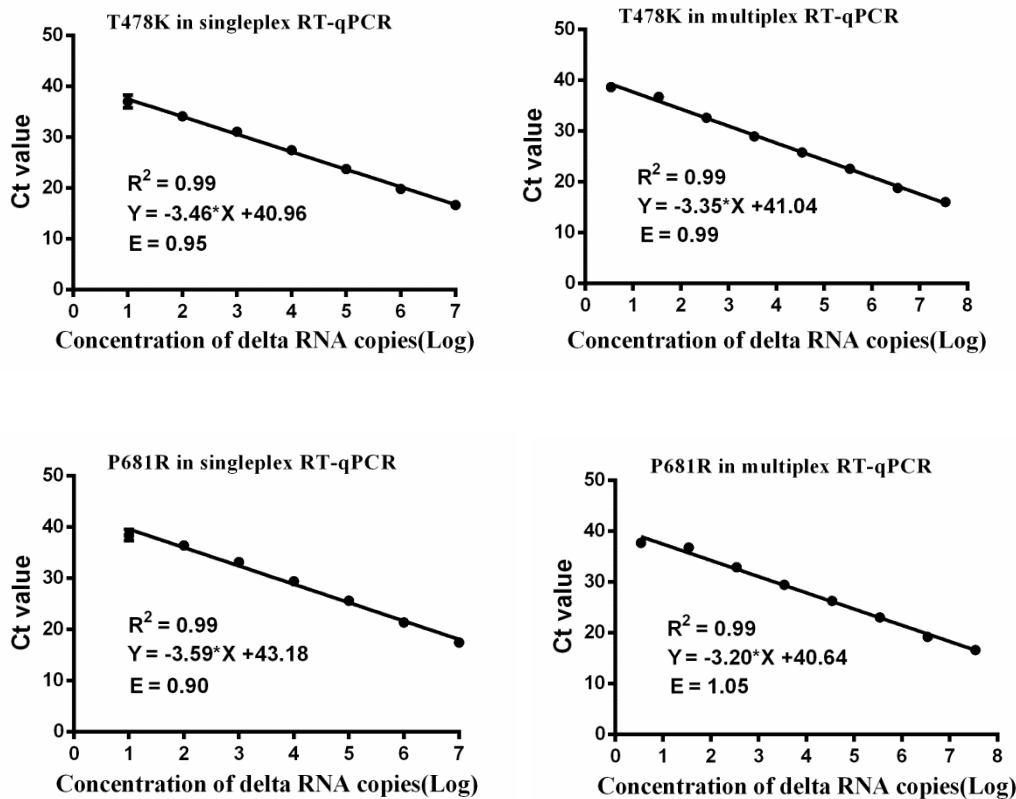


Figure 4.2. Standard curves of targets T478K and P681R using singleplex RT-qPCR assays (left figures) and using the Delta multiplex RT-qPCR assay (right figures). E represents PCR efficiency. This standard curve was used to quantify the amounts of SARS-CoV-2 variant RNA in the samples.

4.2.9 Singleplex RT-qPCR Assays for the Omicron Variants

As SARS-CoV-2 continues to evolve into Omicron and its subvariants, the K417N and T478K mutations reappeared in all the Omicron subvariants while the HV 69-70 deletion reappeared in BA.1/3 and BA.4/5. As a result, I directly adopted the primer-probe of target HV 69-70 deletion and K417N from ABG assay and designed a new primer-probe set for the new target L452R to develop an Omicron triplex RT-qPCR assay. This assay is for detecting and distinguishing the Omicron subvariants. The Primer Express 3.0.1 software was used to design

the sequences of the primer-probe set for the L452R target and all the sequences are summarized below in Table 4.4. The NEB Luna Universal Probe One-Step RT-qPCR kit (New England Biolab, Ipswich, MA, USA) was used for the assay. The forward and reverse primer concentrations were optimized by testing a range of forward primer concentrations (100 nmol/L to 800 nmol/L) paired with different concentrations of the corresponding reverse primer (100 nmol/L to 800 nmol/L). Then the probe concentrations ranging from 50 to 500 nmol/L were tested in the optimization experiments using the optimal concentrations of forward and reverse primers. To find the optimal temperature capable of differentiating L452R mutation from wild-type SARS-CoV-2 sequence, the L452R singleplex assay was used to examine BA.4 variant RNA and wild-type SARS-CoV-2 RNA in parallel at annealing temperatures ranging from 58-62 °C. The optimized conditions for targeting L452R are shown in Table 4.5. Each L452R singleplex RT-qPCR reaction (20 µL total reaction volume) contained 10 µL of Luna Universal One-Step Reaction Mix (2x), 1 µL of Luna WarmStart® RT Enzyme Mix (20x), 400 nmol/L of forward primer, 800 nmol/L of reverse primer, and 250 nmol/L of probe, and 5 µL of the template. RT-qPCR thermal cycling conditions were: 55 °C for 10 minutes, 95 °C for 1 minute, and 45 cycles of 95 °C for 10 seconds and 61°C annealing temperature for 1 minute. This assay was performed on QuantStudio™ 3 Real-Time PCR System.

Table 4.4. Primer and probe combinations developed for the detection and discrimination of SARS-CoV-2 Omicron subvariants.^a

Amplicon & primer name (accession number in GISAID)	Oligo sequence (from 5' to 3')
HV 69-70 deletion amplicon (74 bp) (EPI_ISL_601443)	5' CCTTTCTTTTCCAATGTTACTTGGTTCCATGCTATCTCT GGGACCAATGGTACTAAGAGGTTTGATAACCCTGT
HV 69-70 deletion Forward Primer	5' CCTTTCTTTTCCAATGTTACTTGGTT
HV 69-70 deletion Reverse Primer	5' ACAGGGTTATCAAACCTCTTAGTACCA
HV 69-70 deletion Probe	5'Yakima-ATGCTATCT/ZEN/CTGGGACCAA-IABkFQ
K417N amplicon (89 bp) (EPI_ISL_16540372)	5' GAGGTGATGAAGTCAGACAAATCGCTCCAGGGC AAACTGGAAATATTGCTGATTATAATTATAAATTACCA GATGATTTTACAGGCTGC
K417N Forward Primer	5' GAGGTGATGAAGTCAGACAAATCG
K417N Reverse Primer	5' GCAGCCTGTAAAATCATCTGGTAA
K417N Probe	5' NED- CAAACTGGAAAtATTGCTGATT-NFQ-MGB
L452R amplicon (103bp) (EPI_ISL_15373789)	5' AGCTTGATTCTAAGGTTGGTGGTAATTATAATTACCG GTATAGATTGTTTAGGAAGTCTAATCTCAAACCTTTTG AGAGAGATATTTCAACTGAAATCTATCA
L452R Forward Primer	5'TGATAGATTTTCAAGTTGAAATATCTCTCTCA
L452R Reverse Primer	5' AGCTTGATTCTAAGGTTGGTGGTAAT
L452R Probe	5' FAM-CTAAACAATCTATACcGGTAATT-NFQ-MGB

^a The single nucleotide mutations associated with the corresponding amino acid mutations are indicated with lower case letters. IABkFQ denotes Iowa black fluorescence quencher. ZEN indicates internal ZEN black quencher. NFQ-MGB is the nonfluorescent quencher-minor groove binder.

4.2.10 Triplex RT-qPCR Assay for the Omicron Variants

The Omicron triplex assay conditions were optimized based on three singleplex assays targeting the HV 69-70 deletion, K417N, or L452R mutations (Table 4.5). Each Omicron triplex reaction (20 µL total reaction volume) contained 10 µL of Luna Universal One-Step Reaction

Mix (2x), 1 µL of Luna WarmStart® RT Enzyme Mix (20x), 100 nmol/L, 200nmol/L, and 800 nmol/L of forward primer of the HV 69-70 deletion, K417N, and L452R mutation targets, respectively, 800 nmol/L of each reverse primer, 250 nmol/L of each target probe, and 5 µL of sample (template). The multiplex RT-qPCR thermal cycling conditions were: 55 °C for 10 minutes, 95 °C for 1 minute, and 45 cycles of 95 °C for 10 seconds and 61 °C annealing temperature for 1 minute. This assay was performed on QuantStudio™ 3 Real-Time PCR System.

Table 4.5. Optimal RT-qPCR conditions for the singleplex and Omicron triplex assays for the detection of three targets: HV 69-70 deletion, K417N, and L452R mutations.

Targets	Singleplex RT-qPCR					Triplex RT-qPCR			
	F-primer (nM)	R-primer (nM)	Probe (nM)	Annealing Temperature (°C)	Assay	F-primer (nM)	R-primer (nM)	Probe (nM)	Annealing Temperature (°C)
HV69-70 deletion	100	800	250	61		100	800	250	
K417N	200	800	250	61	Omicron	200	800	250	61
L452R	400	800	250	61		400	800	250	

4.2.11 Dynamic Range, Efficiency, Analytical Sensitivity, and Validation of the Omicron Triplex Assay

I tested serial dilutions of pre-quantified pure Omicron BA.4 RNA from 10⁸ to 10 in triplicate to determine the dynamic ranges of L452R singleplex assay and the Omicron triplex assay. The log values of the quantified pure Omicron BA.4 RNA were plotted against the corresponding Ct values to generate standard curves (Figure 4.3). The slope of each standard curve was used to calculate RT-qPCR efficiency of L452R assay or each target in Omicron triplex assay using the following equation: $E = -1 + 10^{(-1/-slope)}$, where E represents PCR efficiency.

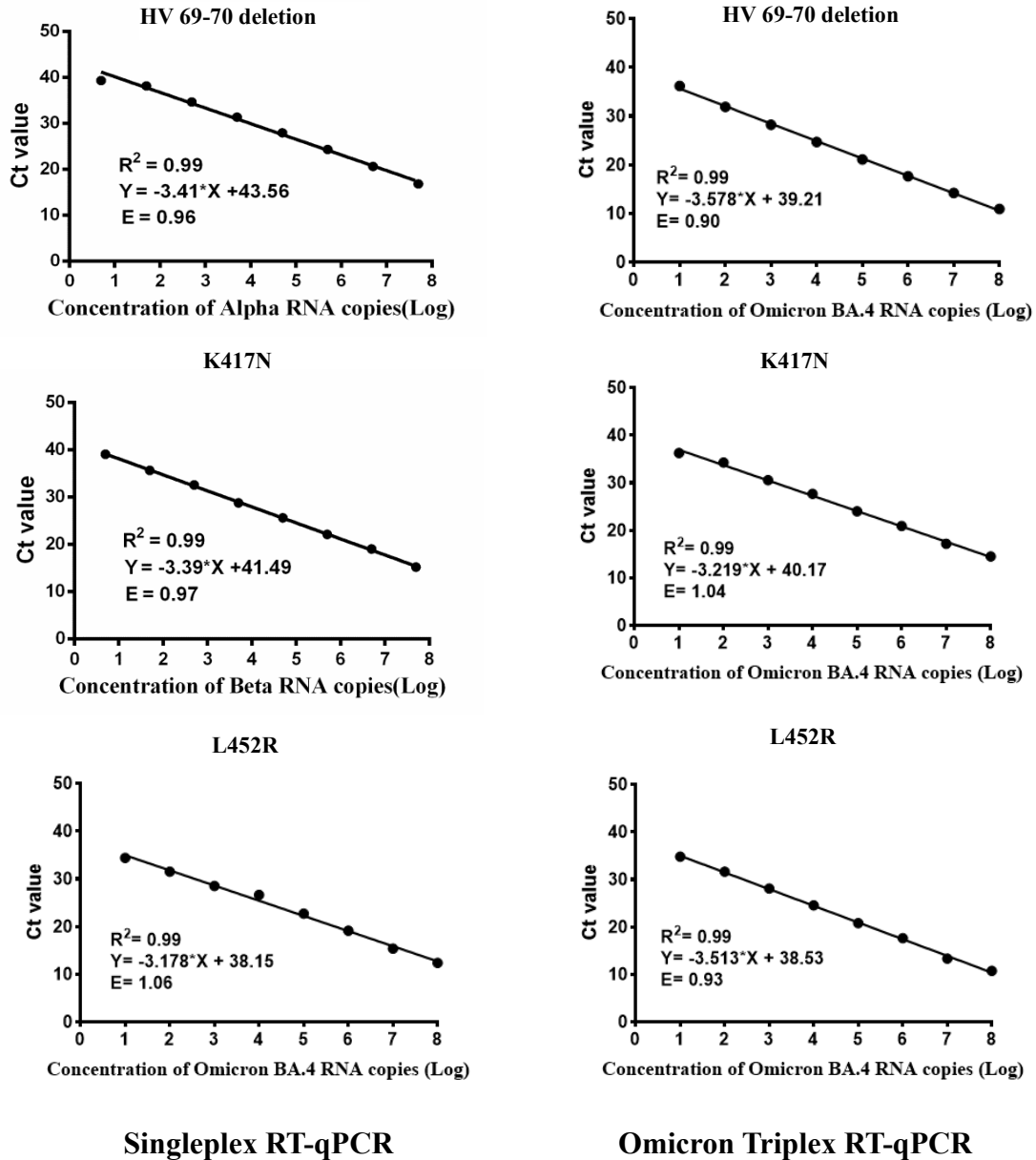


Figure 4.3. Standard curves of targets HV69-70 deletion, K417N, and L452R mutation using singleplex RT-qPCR assays (left) and using the Omicron triplex RT-qPCR assay (right). E represents PCR efficiency which was calculated using the equation $E = -1 + 10^{(-1/\text{slope})}$, where slope refers to the slope of the standard curve. This standard curve was used to quantify the amounts of SARS-CoV-2 variant RNA in the wastewater samples.

The analytical sensitivity for the Omicron triplex assay was determined by testing 2-fold serial dilutions of the Omicron BA.4 RNA from 900 to 3 RNA copies per reaction. The reactions containing 56–900 copies of RNA were conducted in 6 replicates, while reactions containing 3–28 copies of RNA were performed in 10 replicates. The LOD was defined as the lowest RNA concentration detected in all of 10 replicates. Ct values over 40 were considered as a non-detectable threshold. The Omicron assay was validated using Omicron BA.1, BA.2, BA.4, BQ.1.1 (BA.5 derivative), and XBB.1 RNA extracted from passaged isolates originating from clinical samples provided by my collaborators in the Li Ka Shing Institute of Virology. There were no cross-reactions observed among the Omicron sub-lineages in the Omicron triplex assay.

4.2.12 Application of the ABG, Delta, and Omicron Multiplex RT-qPCR Assays for Monitoring SARS-CoV-2 Variants of Concern in Wastewater Samples

I used the ABG, Delta, and Omicron multiplex assays to determine RNA copies of specific VOCs in the RNA extracts of the wastewater samples collected from two wastewater treatment plants in Edmonton and Calgary from May 2021 to March 2023. The wastewater samples were processed using the EM-VIP-Mag approach. In each of the subsequent analyses, an aliquot of 5 μ L of each extract concentrated on magnetic beads was used. First, the total SARS-CoV-2 RNA copies were determined using RT-qPCR assay targeting N1 gene in all samples. The ABG multiplex assay was used to detect RNA of Alpha, Beta, and Gamma variants in wastewater samples collected from May 2021 to July 2021. The Delta assay was used to detect Delta variant in the wastewater samples collected from July 2021 to Jan 2022 and the Omicron assay was used to detect and differentiate the Omicron subvariants in the wastewater samples collected from December 2021 to March 2023.

4.2.13 Application of the ABG and Delta Multiplex RT-qPCR Assays for Investigating Distribution of Variants in Mouse Tissues

In addition to wastewater analysis, another application of the ABG and Delta multiplex assays was for the identification and quantification of specific VOC RNA in tissues of mice. These experiments were in collaboration with the Li Ka Shing Institute of Virology to investigate if specific VOCs prefer specific tissues in mice and whether different routes of infection or transmission impacted these preferences. My collaborators obtained research ethics approval from the University of Alberta Research Ethics Board (project name “CL3 Viral Infectivity Models” No. UAP3885) for this mice study. The collaborators prepared all the tissue samples and extracted the RNA. My role was to analyze the extracted RNA using the multiplex RT-qPCR assays that I developed. An additional singleplex assay called the Wildtype (WT) assay was developed by me for this collaborative project.

For the WT assay, the D614D mutation was used as the target. The Primer Express 3.0.1 software was used to design the sequences of the primer-probe set for the D614D target and all the sequences are summarized below in Table 4.6. The NEB Luna Universal Probe One-Step RT-qPCR kit (New England Biolab, Ipswich, MA, USA) was used for the assay. The forward and reverse primer concentrations were optimized by testing a range of forward primer concentrations (100 nmol/L to 800 nmol/L) paired with different concentrations of the corresponding reverse primer (100 nmol/L to 800 nmol/L). Then the probe concentrations ranging from 50 to 500 nmol/L were tested in the optimization experiments using the optimal concentrations of forward and reverse primers. To find the optimal temperature capable of differentiating the D614D mutation from other mutations, the D614D singleplex assay was used to examine Omicron BA.4 variant RNA and wild-type SARS-CoV-2 RNA in parallel at

annealing temperatures ranging from 58-62 °C. The standard curve of the D616D target was used to quantify WT RNA (Figure 4.4). Each optimized D614D singleplex RT-qPCR reaction (20 µL total reaction volume) contained 10 µL of Luna Universal One-Step Reaction Mix (2x), 1 µL of Luna WarmStart® RT Enzyme Mix (20x), 100 nmol/L of forward primer, 800 nmol/L of reverse primer, and 250 nmol/L of probe, and 5 µL of the template. RT-qPCR thermal cycling conditions were: 55 °C for 10 minutes, 95 °C for 1 minute, and 45 cycles of 95 °C for 10 seconds and 63°C annealing temperature for 1 minute. This assay was performed on QuantStudio™ 3 Real-Time PCR System.

Table 4.6. Primer and probe combinations developed for the detection of SARS-CoV-2 WT

Amplicon & primer and probe name (accession number in GISAID)	Oligo sequence (from 5' to 3')
D614D amplicon (EPI_ISL_402124)	5'CCAGGAACAAATACTTCTAACCAGGTTGCTGTTCTTTATCAGGATGTAACTGCACAGAAGTCCCTGTTGCTATT CATG
D614D Forward Primer	5' CCAGGAACAAATACTTCTAACCAGGT
D614D Reverse Primer	5' CATGAATAGCAACAGGGACTTCTG
D614D MGB probe	5'FAM- TTC TTT ATC AGG ATG TTA ACT GC- MGBNFQ

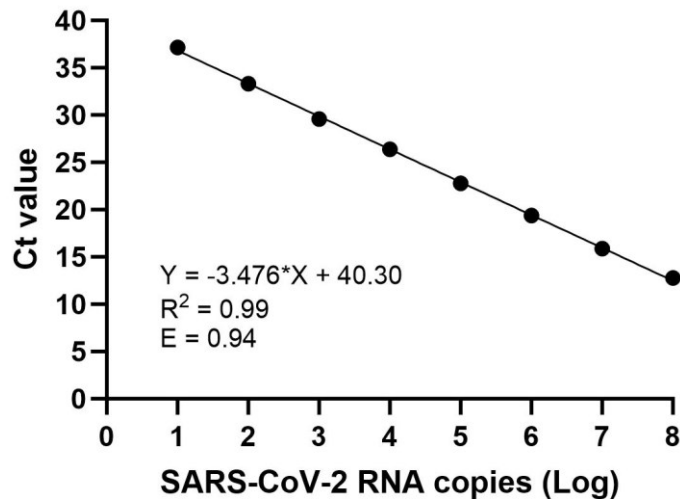


Figure 4.4. Standard curves of target D614D using the singleplex RT-qPCR assay. E represents PCR efficiency which was calculated using the equation $E = -1 + 10^{(-1/\text{slope})}$, where slope refers to the slope of the standard curve. This standard curve was used to quantify the amounts of SARS-CoV-2 variant RNA in the mice samples.

In brief, the VOC were originally isolated from clinical samples (Alberta Precision Laboratory) and passaged using the Vero-TMPRSS2 cells (Japanese Collection of Research Bioresources cell bank). Mice that express the ACE2 receptor in all tissues (K18hACE2 mice, n=12) were infected with a mixture containing each VOC (WT, Alpha, Beta, Gamma, Delta, and Omicron) in 20 μL . The mice were inoculated with a mixture containing equal amounts of each VOC either via the nostrils intranasally (IN) or directly into the lungs via the oropharyngeal (OP) route. Some (n=4) infected mice were also co-housed with un-infected mice to investigate which VOCs resulted in transmission of infection. For the negative control, mice were not infected with any VOC. For the positive control, mice were infected by a single variant at high doses both via the IN and OP routes. Three different doses were used in the experiment: high (2.5×10^4 plaque forming unit (pfu) of each variant, 1.5×10^6 pfu total), medium (5000 pfu of each variant, 3.0×10^4 pfu total), low (833 pfu of each variant, 5000 pfu total). The mice were then euthanized at

various points after infection, tissues extracted, and the isolated RNA was provided to me by the collaborators. The time the mice were euthanized was dependent on the weight change of the mouse after infection (Figure 4.5). For the medium and high inoculation of VOCs, mice were euthanized after 3 days. For low inoculation of VOCs, mice were euthanized after 5 days of infection. Co-housed mice were euthanized 6 days after infection of their house mates (Figure 4.5). In brief, 100 mg of mouse tissue (nasal turbinates, trachea, lung, brain, and heart) was harvested in 1mL TRIzol (Qiagen) and frozen at -80°C until processing. Tissue was disrupted using a FastPrep-24 5G bead beating grinder (MP Biomedicals), according to the specific program recommended for the tissue being homogenized. RNA was extracted from the homogenized tissues using the Direct-zol RNA MiniPrep kit (Zymo Research).

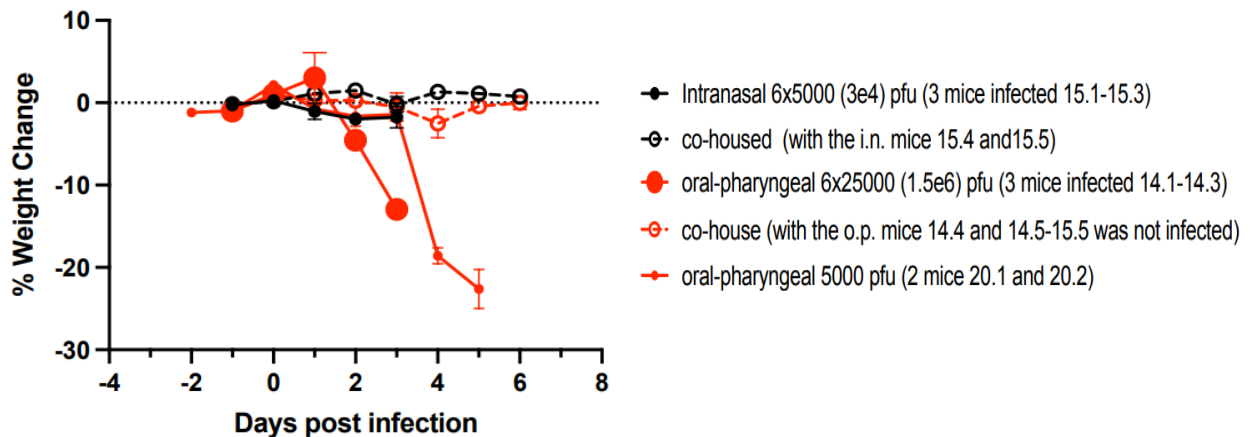


Figure 4.5 Changes in the percentage weight of mice after being infected with different doses of VOC and routes of infection.

The collaborators provided me with 15 μ L of RNA extract for analysis using the ABG and Delta RT-qPCR multiplex assays, as well as WT RT-qPCR singleplex assay. I used 5 μ L of RNA extract for each RT-qPCR assay and the respective standard curves of each RT-qPCR assay was used to quantify RNA copies in each sample. The collaborators used the viral RNA

copy number to estimate the titer number using the formula: RNA copies from PCR / (5 μ L x amount of RNA ng/ μ L in the tissue).

4.3 Results and Discussion

4.3.1 Development and Assessment of ABG and Delta Multiplex Assays

Prior to conducting the multiplex ABG and Delta multiplex RT-qPCR assays, I first optimized the concentration of the primers-probe set for each target in each single target RT-qPCR assay. The optimal concentrations of the primers-probe sets are listed in Table 4.3. I also determined the optimal annealing temperatures, 61 °C for the HV69-70 deletion assay and 60 °C for the K417N and K417T assays, which enabled the discrimination of each mutation from the wild-type sequence of SARS-CoV-2. Under the optimal conditions, the PCR efficiency for the three targets involving the HV69-70 deletion, and K417N and K417T mutations was 96, 97, and 96%, respectively (Figure 4.1). Efficiency in the range of 90–110% is considered excellent performance.^{31,32}

To perform the ABG multiplex RT-qPCR assay in a single tube, I combined the primers and probes of the three targets at optimized concentrations. I further fine-tuned the overall annealing temperature (61 °C) of the ABG assay for maximum discrimination of all the three targets from the wild-type sequence. To evaluate whether the amplification efficiency of three targets in the ABG assay was compromised, I conducted the ABG multiplex assay and three single target assays in parallel. I found that for a wide range of concentrations (10^2 , 10^4 , or 10^6 copies) of Alpha, Beta, and Gamma RNA, the Δ Ct value between singleplex and ABG multiplex assays for each target was less than 1 (Table 4.7). The ABG multiplex assay achieved RT-qPCR efficiency of 94–95% for all three targets in the same reaction tube (Table 4.8, Figure

4.1). These results indicate that having similar amplification efficiencies for all three targets in both singleplex and multiplex assays meets the criteria of optimal performance.³²

Table 4.7. Performance comparison between singleplex and multiplex RT-qPCR assays for the five targets

Target	Template (Copies)	10² (Ct value)	10⁴ (Ct value)	10⁶ (Ct value)
HV 69-70 deletion	Singleplex Ct	34.65	27.92	20.62
	Multiplex (ABG) Ct	34.61	27.48	19.82
	ΔCt value (single Ct - multi Ct)	0.04	0.44	0.8
K417N	Singleplex Ct	34.66	26.77	20.10
	Multiplex (ABG) Ct	34.50	26.40	19.21
	ΔCt value	0.16	0.33	0.89
K417T	Singleplex Ct	33.73	26.90	20.47
	Multiplex (ABG) Ct	34.15	27.21	19.97
	ΔCt value	-0.42	-0.31	0.5
T478K	Singleplex Ct	33.53	26.32	18.99
	Multiplex (delta) Ct	32.72	25.54	18.75
	ΔCt value	0.81	0.78	0.24
P681R	Singleplex Ct	33.78	26.08	19.35
	Multiplex (delta) Ct	32.89	25.99	19.20
	ΔCt value	0.89	0.09	0.15

ΔCt between singleplex and multiplex assays was <1 for all five targets and three template concentrations, suggesting that both the singleplex and multiplex assays perform similarly.

Table 4.8. RT-qPCR efficiencies and limits of detection (LOD) of ABG assay and Delta assay for the detection of SARS-CoV-2 variants of concern

Multiplex RT- qPCR assay	Target	RT-qPCR efficiency (%)	Limit of detection (copies per reaction)
ABG	HV69-70 deletion	95	4
	K417N	94	8
	K417T	95	8
Delta	T478K	99	16
	P681R	105	16

Using the same process, I optimized primer-probe sets and annealing temperature for the targets involving the T478K and P681R mutations (Table 4.3). The PCR amplification efficiency was 95% for the T478K target and 90% for the P681R target in the singleplex format (Figure 4.2). I compared the performance of the Delta multiplex assay for both targets with the corresponding single target assay. I found that the ΔC_t value between singleplex and multiplex assays for each target at identical concentrations (10^2 , 10^4 , or 10^6 copies) was less than 1 (Table 4.7). The efficiency of the Delta multiplex assay for targets T478K and P681R was 99 and 105%, respectively (Table 4.8, Figure 4.2). These results indicate that the performance and conditions of the Delta multiplex assay were optimal.³²

I determined the LOD of both ABG and Delta multiplex assays by analyzing viral RNA of Alpha, Beta, Gamma, and Delta variants. I performed 6–10 replicate analyses using viral RNA, with each reaction containing 4–250 copies of the viral RNA. My results show that as few as 4 copies of RNA of Alpha variant (HV69-70 deletion) were consistently detected in 10 replicate analyses using the ABG assay. Beta (K417N target) and Gamma (K417T target) were consistently detected in all 10 replicate analyses when there were 8 or more copies of viral RNA (Table 4.9). Similarly, the Delta multiplex assay for both T478K and P681R targets provided consistent positive detection in all 10 replicates when there were 16 or more copies of viral RNA (Table 4.9). These results represent LOD of 4, 8, 8, and 16 copies of the viral RNA of Alpha, Beta, Gamma, and Delta variants, respectively.

Table 4.9. Analytical sensitivity of the ABG and Delta multiplex RT-qPCR assay for the detection of the Alpha, Beta, Gamma, and Delta variants of SARS-CoV-2.

RNA	Copies/ reaction	Average Ct (SD) ^a			Detected/tested (%)		
		HV69-70 deletion (Alpha)	K417N (Beta)	K417T (Gamma)	HV69-70 deletion (Alpha)	K417N (Beta)	K417T (Gamma)
Alpha Beta Gamma	250	30.15 (0.36)	32.07 (0.62)	32.47 (0.09)	6/6 (100%)	6/6 (100%)	6/6 (100%)
	125	31.12 (0.18)	32.65 (0.68)	33.81 (0.54)	6/6 (100%)	6/6 (100%)	6/6 (100%)
	62	32.23 (0.08)	33.98 (0.42)	35.30 (0.14)	6/6 (100%)	6/6 (100%)	6/6 (100%)
	31	33.45 (0.39)	34.39 (0.50)	35.38 (0.93)	6/6 (100%)	6/6 (100%)	6/6 (100%)
	16	33.57 (0.13)	35.97 (0.84)	37.82 (0.48)	6/6 (100%)	6/6 (100%)	6/6 (100%)
	8	34.15 (0.67)	37.14 (0.48)	38.55 (0.90)	10/10 (100%)	10/10 (100%)	10/10 (100%)
	4	36.67 (1.1)	37.80 (1.07)	38.91 (0.98)	10/10 (100%)	9/10 (90%)	9/10 (90%)

RNA	Copies/ reaction	Average Ct (SD) ^a		Detected/tested (%)	
		T478K	P681R	T478K	P681R
Delta	250	33.87 (0.24)	34.21 (0.16)	6/6 (100%)	6/6 (100%)
	125	34.70 (0.44)	35.13 (0.47)	6/6 (100%)	6/6 (100%)
	62.5	35.58 (0.69)	36.00 (0.38)	6/6 (100%)	6/6 (100%)
	31	36.10 (0.45)	36.71 (0.52)	6/6 (100%)	6/6 (100%)
	16	36.73 (0.60)	37.05 (0.34)	10/10 (100%)	10/10 (100%)
	8	38.55 (1.00)	38.64 (0.98)	4/10 (40%)	4/10 (40%)

^a SD denotes one standard deviation. The results in **red color** indicate the limit of detection (LOD) for the three targets. The LOD was defined as the lowest RNA copy number detected in all 10 replicates.

I also evaluated the specificity of the ABG multiplex and Delta assays by analyzing RNA of the variants (Alpha, Beta, Gamma, and Delta) and wild-type SARS-CoV-2. The positive signal from the ABG assay was observed only when the specific target corresponding to the Alpha, Beta, or Gamma variant was present. Similarly, the positive signals from the Delta assay for both T478K and P681R mutations were observed only when the RNA of Delta variant was present. These results demonstrate good analytical specificity of both the ABG and Delta multiplex RT-qPCR assays.

4.3.2 Wastewater Surveillance using ABG Multiplex Assay

The ABG multiplex assay was coupled with the EM-VIP-Mag method and was successfully applied for retrospective wastewater analysis. I used the ABG assay to detect the HV 69-70 deletion for Alpha, K417N for Beta, and K417T target for Gamma variants in wastewater samples collected from May 16 to July 18, 2021. As shown in Figure 4.6 below, Alpha was the dominant variant during this period in all the wastewater samples collected from both Calgary and Edmonton. The Alpha RNA copies ranged from 862 copies / 100 mL of wastewater at the start of the sampling period to undetectable near the end of the sampling period.

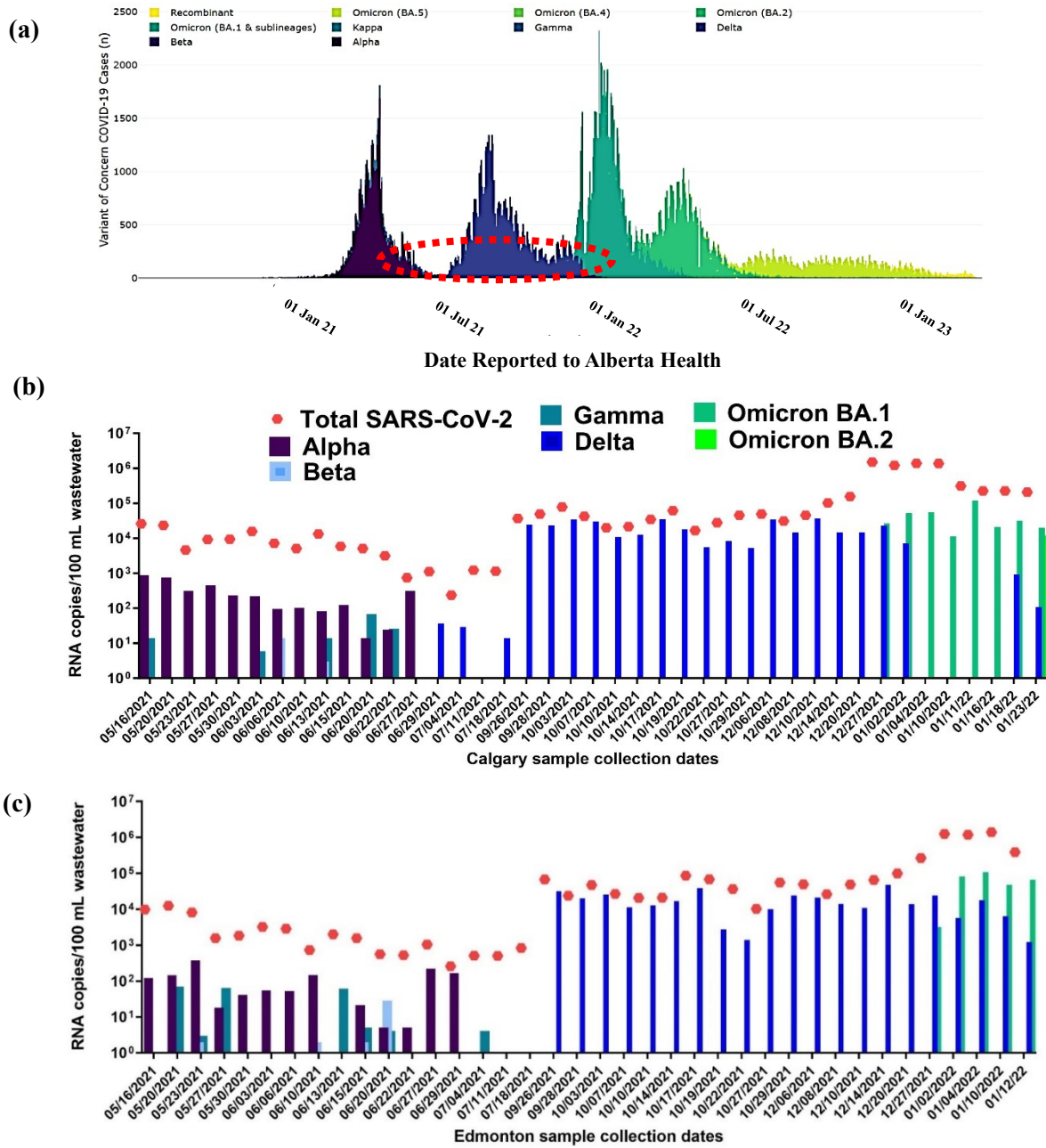


Figure 4.6. (a) Cases of SARS-CoV-2 Variants of Concern reported in Alberta by Alberta Health Services (AHS). Red indicates wastewater sampling period. Detection and monitoring of Alpha, Beta, Gamma, and Delta in (b) Calgary and (c) Edmonton wastewater using multiplex RT-qPCR from May 16th 2021 – January 23rd 2022.

Additionally, I detected lower signals of the Beta and Gamma variants in a few samples consistently for both the Calgary and Edmonton wastewater samples (Figure 4.6 b & c). The relative trend of Alpha, Beta, and Gamma detected in wastewater is in concordance with the trend of clinical cases reported by AHS during the period of wastewater sampling (Figure 4.6 a).³³ Alpha was the variant responsible for most COVID-19 cases while Beta and Gamma variants were responsible for far less COVID-19 cases.

4.3.3 Wastewater Surveillance using Delta Multiplex Assay

Using the Delta multiplex RT-qPCR assay coupled with the EM-VIP-Mag WS protocol, I detected the T478K and P681R mutations in wastewater samples collected from June 29, 2021 to January 23, 2022. Analysis of these wastewater samples demonstrated that the dominant variant was Delta until December 27, 2021 (Figure 4.6). The Delta RNA concentration ranged from 14 to 44884 copies / 100mL in Calgary samples (Figure 4.6 b) and 155 to 44947 copies / 100mL in Edmonton samples (Figure 4.6 c). The last day Delta was detected in the wastewater samples was January 23, 2022 or Calgary (Figure 4.6 b) and January 12, 2022 for Edmonton (Figure 4.6 c). The trend of Delta in wastewater is in concordance with the trend of clinical cases reported by AHS with Delta dominating during the fall months of 2021 and then beginning to disappear in early 2022 when another VOC begins to dominate.³³ As shown in Figure 4.6 a, during the sampling period (May 2021 – July 2021) for testing Alpha, Beta, Gamma, and Delta, the AHS clinically reported cases were minimal. However, I detected all four variants, indicating that my WS platform with the ABG and Delta multiplex assays are sensitive and specific for detecting and identifying SARS-CoV-2 variants in wastewater samples.

4.3.4 Development and Assessment of Omicron Multiplex Assay

Omicron subvariants contain diverse mutation combinations in the S protein of the virus, resulting in diverse infectivity and capability in evading the immune system. To identify the Omicron subvariants, BA.1, BA.2, BA.3, BA.4/5, and XBB, I compared the mutations existing in these six subvariants and chose unique mutations and combinations. For simultaneous identification purposes, I used the minimum number of targets (HV 69-70 deletion, K417N, and L452R mutations) in a single multiplex RT-qPCR assay. Targeting both HV 69-70 deletion and K417N mutation identifies BA.1 and BA.3, while the K417N mutation identifies BA.2 and XBB. Detection of all three targets involving HV 69-70 deletion, K417N, and L452R mutations identifies BA.4 and BA.5. At the time of the project, XBB 1.5 and XBB.1.16 were the dominant subvariants globally and originated from BA.2.⁵ Because BA.2 is no longer circulating in the world, the K417N target allows for detecting XBB.1.5 and XBB.1.16.

Prior to establishing the Omicron triplex RT-qPCR assay, I first optimized the concentration of the primer-probe set to obtain the highest sensitivity for L452R in singleplex RT-qPCR assay. The optimal concentrations of the primer-probe set for L452R assay are summarized in Table 4.5. I also determined the optimal annealing temperatures for L452R assay, which enabled the discrimination of L452R from the wild-type sequence of SARS-CoV-2. The optimal annealing temperature for L452R assay was 61°C. Under the optimized conditions, the efficiency of the L452R singleplex assay was determined to be 106% (Figure 4.3). This efficiency demonstrates that this assay is in the excellent performance range (90-110%).³²

Building on the optimal conditions for the singleplex L452R, HV 69-70, and K417N assays, I established a triplex Omicron assay in a single tube consisting of all the primers and probes of the three targets at optimized concentrations (Table 4.5). The annealing temperature

was set at 61°C for the triplex assay to differentiate the three targets (HV 69-70 deletion, K417N, and L452R) from the wild-type sequence. In parallel experiments, the singleplex and the Omicron triplex assays were performed to evaluate their amplification efficiency. When various concentrations (10^2 , 10^4 , or 10^6 copies) of Omicron BA.4 RNA were amplified, the Δ Ct value between the singleplex and Omicron triplex assays for the targets involving HV 69-70 deletion, K417N, and L452R mutations was less than 1 (Table 4.10). This supports that the amplification efficiency of each target in the triplex assay is consistent with the singleplex assays, even when the primers, probes, and templates of other targets are present in the same tube.³²

Table 4.10. Performance comparison between singleplex and Omicron triplex RT-qPCR assays for the three Omicron assay targets.

Target	Assay ^a	Template (RNA Copies)		
		10 ² (Ct value)	10 ⁴ (Ct value)	10 ⁶ (Ct value)
HV 69-70 deletion	Singleplex Ct	32.5	27.2	19.1
	Triplex Ct	32.1	27.2	19.2
	Δ Ct value	0.4	0.0	0.1
K417N	Singleplex Ct	34.6	29.7	21.8
	Triplex Ct	34.2	30.0	22.7
	Δ Ct value	0.4	0.3	0.9
L452R	Singleplex Ct	33.1	28.4	20.8
	Triplex Ct	32.9	28.3	20.6
	Δ Ct value	0.2	0.1	0.2

^a Δ Ct = Ct from singleplex assay - Ct from triplex assay. Δ Ct value between singleplex and triplex assays was <1 for all three targets and three template concentrations, suggesting that both the singleplex and triplex assays perform similarly.

The Omicron triplex assay achieved RT-qPCR efficiencies of 90%, 104%, and 93% for targets HV 69-70 deletion, K417N, and L452R, respectively (Figure 4.3). I determined the limit of detection (LOD) of the Omicron triplex assay by analyzing a wide range of Omicron BA.4 viral RNA copies (3-900) in 10-6 replicates (Table 4.11). The results in Table 4.11 demonstrate that the Omicron triplex assay can consistently detect positive signals for HV 69-70 deletion,

K417N, and L452R in all 10 replicates when the amount of Omicron BA.4 viral RNA in each reaction was 28 copies or higher. These results demonstrate that the LOD of all three targets (HV 69-70 deletion, K417N, and L452R) is 28 RNA copies per reaction. Additionally, the multiplex assay positively detected the three targets in 50% of the 10 replicates (Table 4.11), when 14 RNA copies were used in the reactions.

Table 4.11. Analytical sensitivity of the Omicron triplex RT-qPCR assay for the detection of the Omicron BA.4.

RNA	Copies/ reaction	Average Ct (Standard Deviation)			Detected/Tested (%)		
		HV69-70 deletion	K417N	L452R	HV69-70 deletion	K417N	L452R
Omicron BA.4	900	33.3 (0.2)	36.7 (0.1)	31.9 (0.1)	6/6 (100%)	6/6 (100%)	6/6 (100%)
	450	34.7 (0.4)	37.7 (0.4)	32.8 (0.5)	6/6 (100%)	6/6 (100%)	6/6 (100%)
	225	35.2 (0.3)	38.0 (0.9)	33.5 (0.5)	6/6 (100%)	6/6 (100%)	6/6 (100%)
	112	36.1 (1.0)	39.2 (1.0)	34.3 (0.7)	6/6 (100%)	6/6 (100%)	6/6 (100%)
	56	37.5 (1.0)	40.9 (0.8)	35.4 (1.1)	6/6 (100%)	6/6 (100%)	6/6 (100%)
	28	39.0 (1.5)	39.9 (0.6)	36.1 (0.7)	10/10 (100%)	10/10 (100%)	10/10 (100%)
	14	40.7 (2.2)	39.8 (0.3)	36.2 (0.7)	7/10 (70%)	5/10 (50%)	8/10 (80%)
	7	39.8 (1.3)	39.8 (0.8)	36.2 (0.5)	5/10 (50%)	3/10 (30%)	7/10 (70%)
	3	39.4 (1.4)	ND	36.3 (0.7)	7/10 (70%)	0/10 (0%)	4/10 (40%)

The results in **bold** indicate the limit of detection (LOD) as 28 copies of RNA per reaction for the three targets. The LOD was defined as the lowest RNA copy number detected in all 10 replicates.

I validated the Omicron triplex assay using RNA extracted from passaged isolates of clinical nasopharyngeal samples, which were identified previously as Omicron BA.1, BA.2, BA.4, BQ 1.1 (BA.5 derivative), and XBB.1 by sequencing. The Omicron assay accurately

identified the variants in each sample provided (Table 4.12). The positive signals of both HV 69-70 deletion and K417N identified variant BA.1 RNA in a sample, while the signal of the K417N target alone identified the BA.2 or XBB.1 RNA target. Positive signals of the three HV 69-70 deletion, K417N, and L452R targets were detected in the samples containing BA.4 or BQ RNA.

Table 4.12. Validation of the Omicron Triplex RT-qPCR assay by examining the RNA of Omicron subvariants (BA.1, BA.2, BA.4, BQ 1.1 (derivative of BA.5), and XBB.1 extracted from passaged isolates of clinical nasopharyngeal swab samples by collaborators at the Li Ka Shing Institute of Virology. These clinical samples were provided by the accredited Alberta Precision Laboratories.

RNA Samples	Ct Values from Omicron Triplex Assay for Each Target			Variant Identified by Omicron Triplex Assay
	HV 69-70 deletion (SD) ^a	K417N (SD)	L452R (SD)	
Omicron BA.1	23.7 (0.2)	21.2 (0.0)	NA	Omicron BA.1
Omicron BA.2	NA	19.5 (0.0)	NA	Omicron BA.2
Omicron BA.4	15.5 (0.1)	20.4 (0.1)	16.1 (0.1)	Omicron BA.4
Omicron BQ1.1 (BA.5)	17.2 (0.1)	21.2 (0.2)	15.5 (0.1)	Omicron BA.5
Omicron XBB.1	NA	19.5 (0.2)	NA	Omicron XBB.1

^a SD denotes one standard deviation. NA indicates no amplification.

Successful detection and discrimination of all six Omicron subvariants in a single assay was a challenge that limited previous studies.³⁴⁻³⁸ My Omicron triplex assay is advantageous because by utilizing three target mutations, all six Omicron subvariants (BA.1/BA.3, BA.2/XBB, and BA.4/BA.5) can be discriminated. Additionally, my triplex assay only requires a commonly available PCR instrument, uses less reagents, and is more versatile and cost effective. Although

the previously reported Omicron pentaplex assay can differentiate BA.1, BA.2, and BA.4/5, this pentaplex assay involving five targets requires a PCR instrument with six different fluorescence channels which is more expensive and not commonly available in most facilities.³⁴ The other Omicron multiplex assays are unable to detect and differentiate all Omicron subvariants. For example, the Δ 143-145 deletion target can only detect BA.1 and BA.3, but cannot detect BA.2, BA.4, or BA.5.³⁵ Using combinations of the HV 69-70 deletion, N501Y, and T478K targets to detect Omicron can broaden the range of Omicron subvariants detected, but this assay is not capable of differentiating BA.1 from BA.4/5.³⁶ Additionally, targeting two mutations in the N gene and the two mutations E484A and S477N in the S gene can detect all Omicron subvariants, but these assays cannot differentiate all the subvariants, because these mutations are shared by all the Omicron subvariants.^{37,38}

4.3.5 Wastewater Surveillance using Omicron Triplex Assay

The Omicron variants started to emerge in December 2021 and the subvariant BA.1 quickly became the dominant variant starting in January 2022. I applied the Omicron triplex RT-qPCR assay to detect and differentiate the six Omicron subvariants BA.1, BA.2, BA.3, BA.4, BA.5 and XBB in wastewater samples from 2021 to 2023. From December 27, 2021 to March 18, 2022, Omicron BA.1 was detected by targeting HV 69-70 deletion and K417N in Calgary wastewater samples with RNA concentrations ranging from 36 to 117850 copies / 100mL (Figure 4.7). In the Edmonton wastewater samples, Omicron BA.1 RNA concentrations ranged from 145 to 109426 copies / 100mL from December 27, 2021 to March 21, 2022 (Figure 4.8). It is important to note that the BA.2 subvariant of Omicron was simultaneously detected in the wastewater samples using the K417N signal. In the Calgary samples, Omicron BA.2 was detected as early as January 23, 2022 and present samples until June 29, 2022 with RNA

concentrations ranging from 1341 to 168842 copies / 100mL (Figure 4.7). In the Edmonton samples, Omicron BA.2 was detected on January 24, 2022 – August 24, 2022 with RNA concentrations ranging from 49 to 294846 copies / 100mL (Figure 4.8).

New subvariants of Omicron continued to emerge and quickly dominated the rest of 2022. Omicron BA.4/5 started being detectable in Calgary May 10, 2022 until March 20, 2023, exhibiting the signals of HV69-70 deletion, K417N, and L452R mutations. The RNA concentration ranged from 1090 – 1743557 copies / 100mL in Calgary (Figure 4.7). In the Edmonton samples, Omicron BA.4/5 started being detectable on May 31, 2022 until March 20, 2023, and the RNA concentration ranged from 1972 – 697871 copies / 100mL (Figure 4.8). The XBB subvariant began to appear in the wastewater samples collected in Calgary and Edmonton on February 27, 2023 and March 6, 2023. The RNA concentration ranged from 13295 – 27233 copies / 100mL and 11134 – 363331 copies / 100mL in Calgary and Edmonton, respectively (Figures 4.7 and 4.8). Although BA.2 and XBB share the same K417N signal for identification in the Omicron triplex assay, since BA.2 has been undetectable both clinically and in wastewater samples in Alberta since September 2022, the K417N signal detected in the February 2023 and onward samples is attributed to the XBB subvariant.

The overall trends of Omicron BA.1, BA.2, BA.4/5, and XBB detected in wastewater in both Calgary and Edmonton are in concordance with the trend of clinical cases reported by AHS during the periods of wastewater sampling (Figure 4.7 a and 4.8 a).³³ Like a previously reported study by Hasing et al., 2023, I also observed the decline of a previously dominant VOC simultaneously with the rise of the next emerging VOC for most of the COVID-19 waves.³⁹ My WS data demonstrates the potential for early detection of specific Omicron sub-lineage RNA in wastewater in the beginning of its appearance in Edmonton and Calgary, when only small

number of clinical cases were reported in all of Canada. For example, the Public Health Agency of Canada only reported around 50 cases of Omicron BA.2 in all of Canada by the end of January 2022.⁴⁰ My Omicron triplex assay detected Omicron BA.2 RNA at 10^4 copies / 100 mL in wastewater in both Edmonton and Calgary as early as January 23, 2022. Furthermore, according to AHS, Omicron BA.2 was declared as the dominant variant circulating in the population as of March 2022. My WS data showed the same trend with a low copy number of Omicron BA.1 in early March 2022, Omicron BA.1 completely disappearing by the end of March 2022, followed by the domination of Omicron BA.2 (Figures 4.7 and 4.8). Additionally, by early May 2022, very low numbers of clinical cases (daily average of less than 20 clinical cases) of Omicron BA.4/5 were being reported by AHS.³³ The Omicron BA.4/5 were detected at RNA concentrations of 10^3 copies / 100mL of wastewater starting on May 10 and May 30, 2022 in Calgary and Edmonton, respectively (Figures 4.7 and 4.8). From July 2022 to March 2023, most wastewater samples were detected to have the BA.4/BA.5 RNA at concentrations higher than 10^5 copies / 100 mL of wastewater (Figures 4.7 and 4.8). The WS data indicates that the actual infection cases are likely higher than the clinical cases reported by AHS (less than ~200 cases/day).³³ The small number of cases being clinically reported may be due to asymptomatic patients, lack of participation of infected patients in clinical PCR testing and more reliance on at home rapid antigen testing that are not reported to AHS. Therefore, to better understand the scope of COVID-19 infections in a community, WS for community biomonitoring can complement clinical testing. The successful monitoring of the Omicron subvariants demonstrates the capabilities of my WS protocol and Omicron triplex assay to offer highly efficient concentration, extraction, and recovery of viral RNA, and sensitive detection and discrimination between all the Omicron subvariants in wastewater.

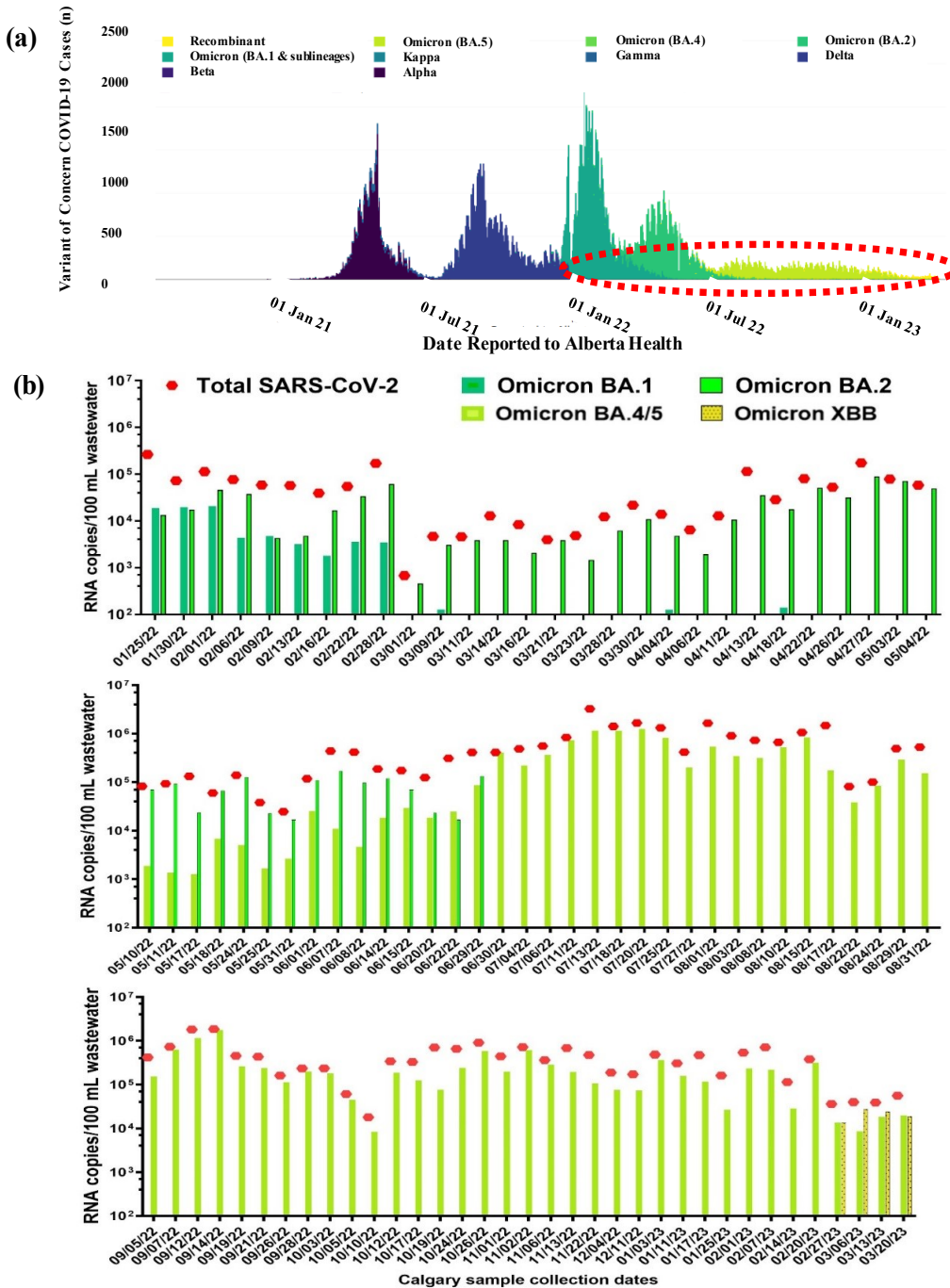


Figure 4.7. (a) Cases of SARS-CoV-2 Variants of Concern reported in Alberta by Alberta Health Services (AHS). Red indicates wastewater sampling period. (b) Detection and monitoring of Omicron sub-lineage in Calgary wastewater using multiplex RT-qPCR from January 25th 2022 – March 20th 2023.

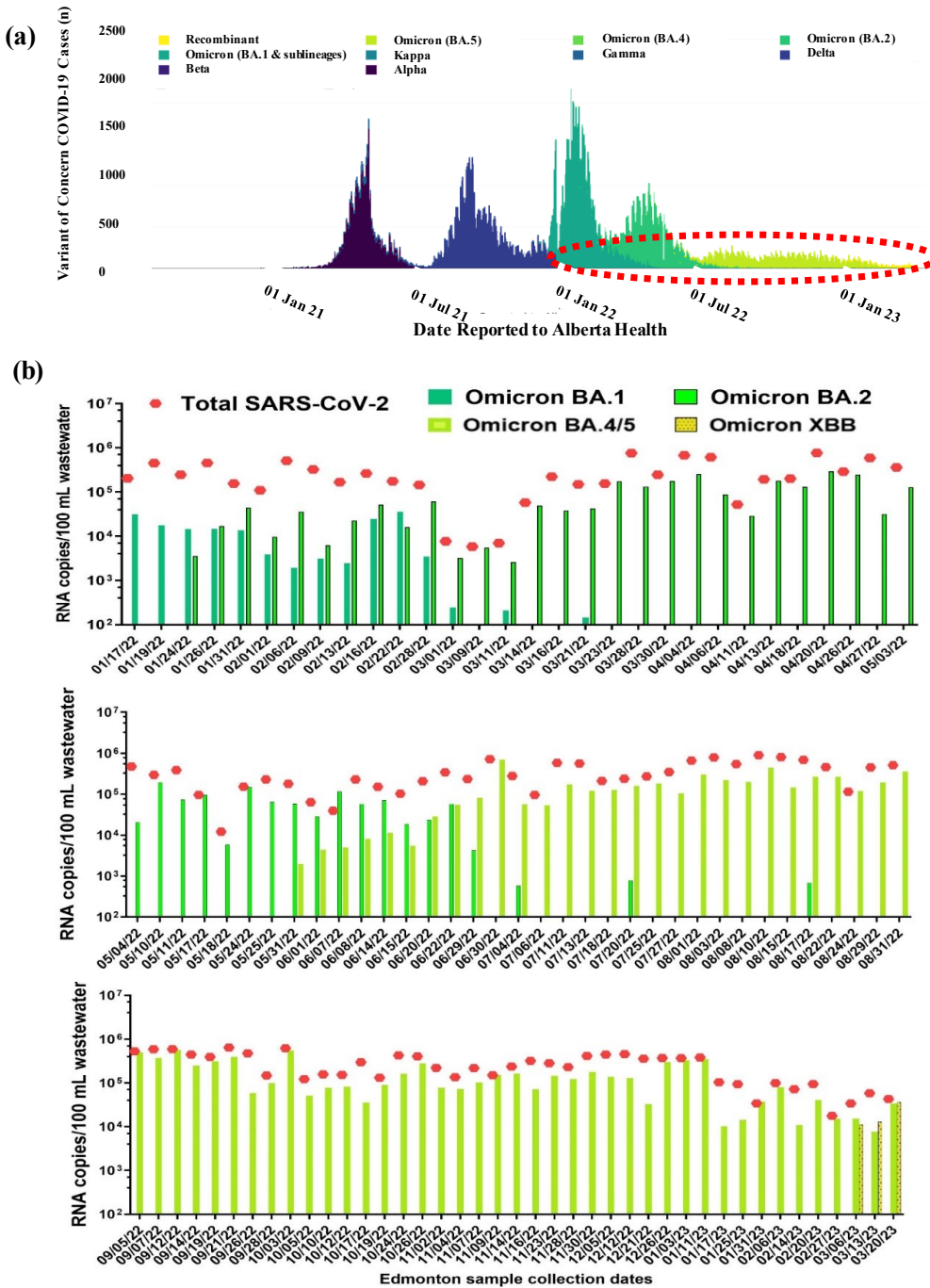


Figure 4.8. (a) Cases of SARS-CoV-2 Variants of Concern reported in Alberta by Alberta Health Services (AHS). Red indicates wastewater sampling period. (b) Detection and monitoring of Omicron sub-lineage in Edmonton wastewater using multiplex RT-qPCR from January 25th 2022 – March 20th 2023.

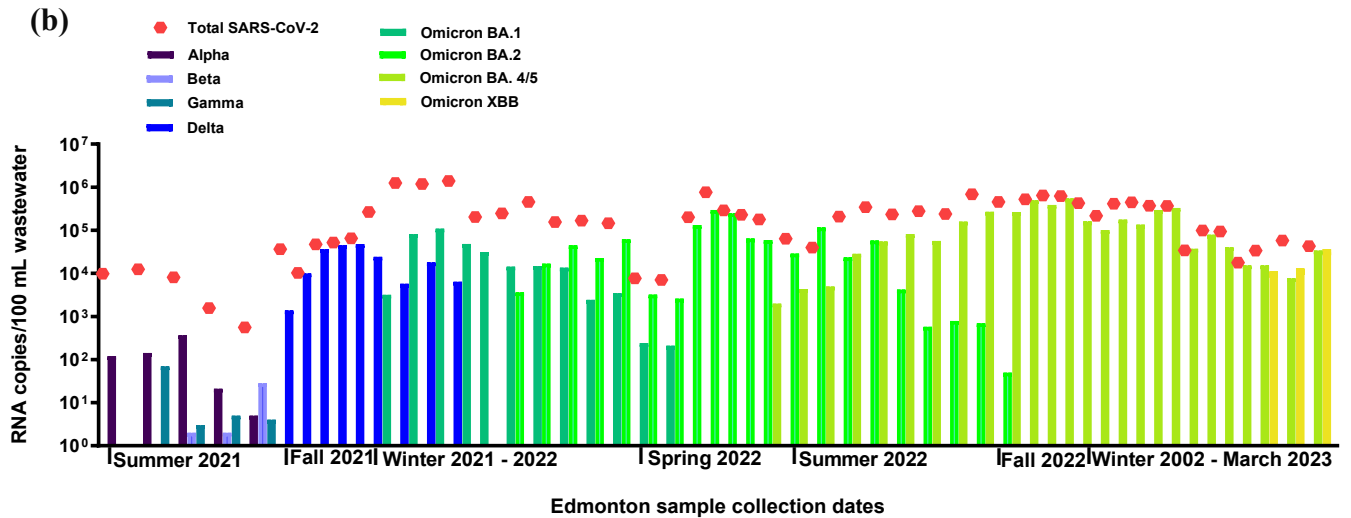
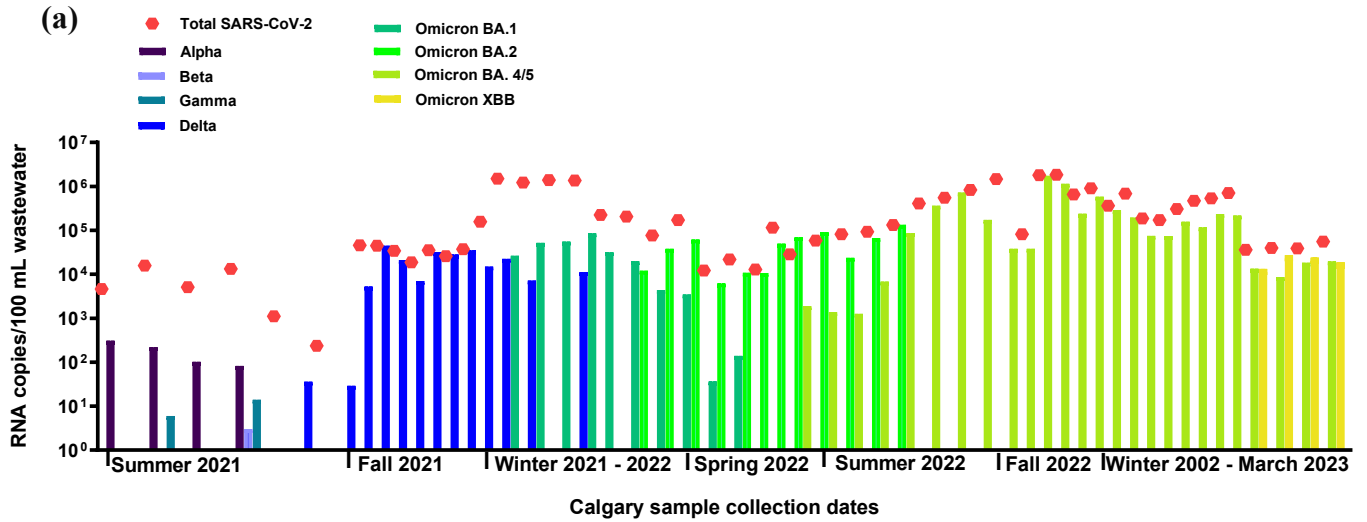


Figure 4.9. Overall detection trend of SARS-CoV-2 Variants of Concern (Alpha, Beta, and Gamma, Delta, and Omicron subvariants) in wastewater samples collected from (a) Calgary and (b) Edmonton, Alberta, Canada from May 2021 to March 2023.

4.3.6 Application of Multiplex Assays for Investigating Distribution of Variants in Mouse Tissues

To further demonstrate the broad applications of the multiplex assays other than for wastewater analysis, I collaborated with the Li Ka Shing Institute of Virology in a project to investigate if VOCs have preference for specific mouse tissues, and whether the route of infection or transmission might affect these preferences. The K18 hACE2 mice was used as a study model because this mouse expresses the human ACE2 receptor in all cells, and thus can be infected by all VOC. The tissues were dissected from individual mice either infected with the VOCs via OP, IN, or co-housed with infected mice. The RNA was then extracted by the collaborators and provided to me for RT-qPCR multiplex detection.

There were two types of controls in the experiments. For the negative control, uninfected mice tissue isolated from the lungs, nasal turbinates, and brains were tested for RNA. The Ct value obtained from these samples was 35 which indicates that all these mice were uninfected at the beginning of the study. For the positive control, mice were infected by a single variant both via the IN and OP routes. The PCR results for these were all positive demonstrating successful infection. The experimental results demonstrate that although all VOCs seem to be capable in their ability to replicate in vivo, there are differences in the distribution of the VOC in specific tissues and depending on the route of infection (Figure 4.10). Firstly, the distribution of VOCs in tissues that are likely to come into direct contact with the primary inoculum was approximately even. For example, the nasal turbinates of the IN inoculated mice as well as the nasal turbinates, oral swabs, and trachea of the OP inoculated mice are expected to be exposed to the primary inoculum. However, the lungs, brain, and heart were not directly exposed to the inoculums, so they were secondary infections, and did not show the same approximately even distribution of

VOCs. Interestingly, although the brains of infected mice did not have an even distribution, there was also no dominant variant. This suggests a possible stochastic infection where the first VOC reaching the brain becomes the dominant infection.

Secondly, transmission of the co-housed mice was evident. Three of the four mice had significant titers. Mouse 14.5 was not likely infected as titers were low in all tissues examined. Alpha is the dominant variant causing transmission in mice which are co-housed, except for mouse 14.4 in which there is no dominant VOC. Based on the observations of this experiment, Beta is slightly more favored in the heart. These observations suggest that variants have differing preferences for different cell types. However, whether this observation is because of changing receptors, other than ACE2 which is present in all mouse tissues, co-receptors in the tissues, or because of other potential mechanistic relationships requires further investigation in the future as this is an ongoing study and concrete conclusions cannot be drawn as of now.

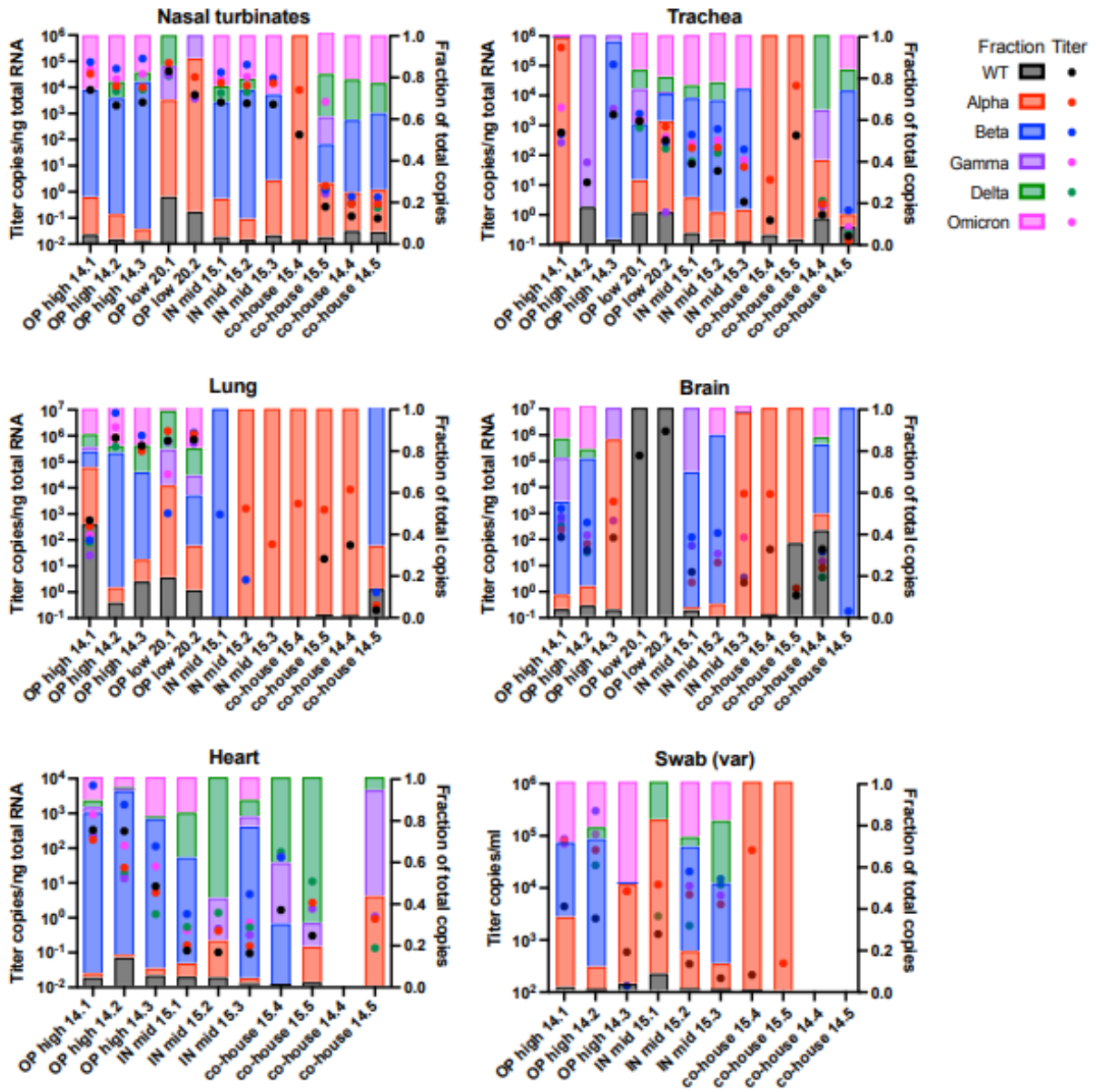


Figure 4.10 Distribution of VOCs found in different mouse tissues after being infected either oropharyngeally (OP), intranasally (IN), or via transmission from an infected mouse (Co-house). The VOC doses used ranged from high (2.5×10^4 pfu of each variant, 1.5×10^6 pfu total), medium (5000 pfu of each variant, 3.0×10^4 pfu total), low (833 pfu of each variant, 5000 pfu total). The mice utilized in the study are numbered as 14.1, 14.2, 14.3, 15.1, 15.3, 15.4, 15.5, 14.4, and 14.5.

4.4 Conclusion

I successfully developed an Omicron triplex RT-qPCR assay capable of identifying and distinguishing the six Omicron subvariants. The Omicron assay coupled with the WS EM-VIP-Mag protocol successfully detected and differentiated Omicron BA.1, BA.2, BA.4/5, and XBB in wastewater samples collected from Calgary and Edmonton from 2022 to 2023. The occurrence of each subvariants detected in wastewater has the same trend as the clinical cases reported by AHS (Figure 4.9). My study is the first of its kind where a single tube RT-qPCR triplex assay detected and identified all the Omicron subvariants in wastewater samples over the course of a year. In my study, the integrated platform of the ABG and Delta multiplex assays also successfully monitored the occurrence trends of specific variants (Alpha, Beta, Gamma, and Delta) of SARS-CoV-2 in wastewater samples from 2021-2022. The successful monitoring of the variants from 2021-2023 demonstrates that the ABG, Delta, and Omicron multiplex assays provide specificity and sensitivity, while the optimized WS EM-VIP-Mag protocol efficiently captures viral particles and RNA in both liquid and solid phases of a wastewater sample with enhanced inhibitor removal and RNA recovery. Clinical testing of SARS-CoV-2 variants is limited, thus, the WS results provide necessary information for guiding public health to implement appropriate measures. The COVID-19 pandemic has shown that SARS-CoV-2 is capable of mutating and evolving at a rapid pace. Therefore, it is possible that new Omicron subvariants or new SARS-CoV-2 variants will continuously emerge. Because my multiplex assays target mutations that are naturally selected and are beneficial for survival, these mutations may re-appear in the future Omicron subvariants or SARS-CoV-2 variants. This platform can be easily adopted for detecting SARS-CoV-2 variants and other viruses. The multiplex assays were also applied for detecting VOC in mouse tissues to investigate routes of

infection and transmission. My wastewater protocol can also be coupled with other RT-qPCR and isothermal detection techniques to detect viral pathogens. The strategies and techniques developed in this study contribute to building capacity for future biomonitoring of community infections.

4.5 References

1. Wang, R.; Chen, J.; Wei, G.W. Mechanisms of SARS-CoV-2 evolution revealing vaccine-resistant mutations in Europe and America. *J. Phys. Chem.* **2021**, 12 (49), 11850-11857.
2. Upadhyay, V.; Lucas, A.; Panja, S.; Miyauchi, R.; Mallela, K.M. Receptor binding, immune escape, and protein stability direct the natural selection of SARS-CoV-2 variants. *J. Biol. Chem.* **2021**, 297 (4), 101208.
3. Chen, J.; Wang, R.; Wang, M.; Wei, G.W. Mutations strengthened SARS-CoV-2 infectivity. *J. Mol. Biol.* **2020**, 432 (19), 5212-5226.
4. Rambaut, A.; Holmes, E.C.; O'Toole, Á.; Hill, V.; McCrone, J.T.; Ruis, C.; du Plessis, L.; Pybus, O.G. A dynamic nomenclature proposal for SARS-CoV-2 lineages to assist genomic epidemiology. *Nat. Microbiol.* **2020**, 5 (11), 1403-1407.
5. World Health Organization (WHO). *Tracking SARS-CoV-2 variants*, **2023**. Available from: <https://www.who.int/en/activities/tracking-SARS-CoV-2-variants> (accessed 2023-06-05).
6. Majumdar, S.; Sarkar, R. Mutational and phylogenetic analyses of the two lineages of the Omicron variant. *J. Med. Virol.* **2022**, 94 (5), 1777-1779.
7. Arora, P.; Pöhlmann, S.; Hoffmann, M. Mutation D614D increases SARS-CoV-2 transmission. *Signal Transduct. Target. Ther.* **2021**, 6 (1), 1-2.
8. Plante, J.A.; Liu, Y.; Liu, J.; Xia, H.; Johnson, B.A.; Lokugamage, K.G.; et al. Spike mutation D614D alters SARS-CoV-2 fitness. *Nature* **2021**, 592 (7852), 116-121.

9. Gu, H.; Chen, Q.; Yang, G.; He, L.; Fan, H.; Deng, Y.Q.; et al. Adaptation of SARS-CoV-2 in BALB/c mice for testing vaccine efficacy. *Science* **2020**, 369 (6511), 1603-1607.
10. Barton, M.I.; MacGowan, S.A.; Kutuzov, M.A.; Dushek, O.; Barton, G.J.; van der Merwe, P.A. Effects of common mutations in the SARS-CoV-2 Spike RBD and its ligand, the human ACE2 receptor on binding affinity and kinetics. *Elife* **2021**, 10, e70658.
11. Meng, B.; Kemp, S.A.; Papa, G.; Datir, R.; Ferreira, I.A.; Marelli, S.; et al. Recurrent emergence of SARS-CoV-2 spike deletion H69/V70 and its role in the Alpha variant B.1.1.7. *Cell Rep.* **2021**, 35 (13), 109292.
12. Brown, K.A.; Gubbay, J.; Hopkins, J.; Patel, S.; Buchan, S.A.; Daneman, N.; Goneau, L.W. S-gene target failure as a marker of variant B.1.1.7 among SARS-CoV-2 isolates in the greater Toronto area, December 2020 to March 2021. *J. Am. Med. Assoc.* **2021**, 325 (20), 2115-2116.
13. Wilhelm, A.; Toptan, T.; Pallas, C.; Wolf, T.; Goetsch, U.; Gottschalk, R.; et al. Antibody-mediated neutralization of authentic SARS-CoV-2 B.1.617 variants harboring L452R and T478K/E484Q. *Viruses* **2021**, 13 (9), 1693.
14. Liu, Y.; Liu, J.; Johnson, B.A.; Xia, H.; Ku, Z.; Schindewolf, C.; et al. Delta spike P681R mutation enhances SARS-CoV-2 fitness over Alpha variant. *Cell Rep.* **2022**, 39 (7), 110829.
15. Tegally, H.; Moir, M.; Everatt, J.; Giovanetti, M.; Scheepers, C.; Wilkinson, E.; et al. Emergence of SARS-CoV-2 omicron lineages BA. 4 and BA. 5 in South Africa. *Nat. Med.* **2022**, 28 (9), 1785-1790.

16. Khan, A.; Zia, T.; Suleman, M.; Khan, T.; Ali, S.S.; Abbasi, A.A.; Mohammad, A.; Wei, D.Q. Higher infectivity of the SARS-CoV-2 new variants is associated with K417N/T, E484K, and N501Y mutants: an insight from structural data. *J. Cell. Physiol.* **2021**, *236* (10), 7045-7057.
17. Christensen, P.A.; Olsen, R.J.; Long, S.W.; Subedi, S.; Davis, J.J.; Hodjat, P.; et al. Delta variants of SARS-CoV-2 cause significantly increased vaccine breakthrough COVID-19 cases in Houston, Texas. *Am. J. Clin. Pathol.* **2021**, *192* (2), 320-331.
18. Twohig, K.A.; Nyberg, T.; Zaidi, A.; Thelwall, S.; Sinnathamby, M.A.; Aliabadi, S.; et al. Hospital admission and emergency care attendance risk for SARS-CoV-2 delta (B.1.617.2) compared with alpha (B.1.1.7) variants of concern: a cohort study. *Lancet Infect. Dis.* **2022**, *22* (1), 35-42.
19. Syed, A.M.; Ciling, A.; Taha, T.Y.; Chen, I.P.; Khalid, M.M.; Sreekumar, B.; et al. Omicron mutations enhance infectivity and reduce antibody neutralization of SARS-CoV-2 virus-like particles. *Proc. Natl. Acad. Sci. U. S. A.* **2022**, *119* (31), p.e2200592119.
20. Zhang, X.; Wu, S.; Wu, B.; Yang, Q.; Chen, A.; Li, Y.; et al. SARS-CoV-2 Omicron strain exhibits potent capabilities for immune evasion and viral entrance. *Sig. Transduct. Target. Ther.* **2021**, *6* (1), 1-3.
21. Chen, J.; Qiu, Y.; Wang, R.; Wei, G.W. Persistent Laplacian projected Omicron BA.4 and BA.5 to become new dominating variants. *Comput. Biol. Med.* **2022**, *151*, 106262.
22. Wang, Q.; Guo, Y.; Iketani, S.; Nair, M.S.; Li, Z.; Mohri, H.; et al. Antibody evasion by SARS-CoV-2 Omicron subvariants BA. 2.12. 1, BA. 4 and BA. 5. *Nature* **2022**, *608* (7923), 603-608.

23. Rahimi, F. and Abadi, A.T.B. Implications of the SARS-CoV-2 subvariants BA. 4 and BA. 5. *Int. J. Surg.* **2022**, 104, p.106806.
24. Chatterjee, S.; Bhattacharya, M.; Nag, S.; Dhama, K.; Chakraborty, C. A Detailed Overview of SARS-CoV-2 Omicron: Its Subvariants, Mutations and Pathophysiology, Clinical Characteristics, Immunological Landscape, Immune Escape, and Therapies. *Viruses* **2023**, 15 (1), 167.
25. Nemudryi, A.; Nemudraia, A.; Wiegand, T.; Surya, K.; Buyukyoruk, M.; Cicha, C.; et al. Temporal detection and phylogenetic assessment of SARS-CoV-2 in municipal wastewater. *Cell Rep. Med.* **2020**, 1 (6), p.100098.
26. Metzger, C.M.; Lienhard, R.; Seth-Smith, H.M.; Roloff, T.; Wegner, F.; Sieber, J.; et al. PCR performance in the SARS-CoV-2 Omicron variant of concern. *Swiss Med. Wkly.* **2021**, 49 (151), w30120.
27. Henegariu, O.; Heerema, N.A.; Dlouhy, S.R.; Vance, G.H.; Vogt, P.H. Multiplex PCR: Critical parameters and step-by-step protocol. *Biotechniques* **1997**, 23 (3), 504–511.
28. Butler, K.S.; Carson, B.D.; Podlevsky, J.D.; Mayes, C.M.; Rowland, J.M.; Campbell, D.; et al. Singleplex, multiplex and pooled sample real-time RT-PCR assays for detection of SARS-CoV-2 in an occupational medicine setting. *Sci. Rep.* **2022**, 12 (1), 17733.
29. Hrudehy, S.E.; Bischel, H.N.; Charrois, J.; Chik, A.H.; Conant, B.; Delatolla, R.; et al. Wastewater surveillance for SARS-CoV-2 RNA in Canada. *Facets* **2022**, 7, 1493-1597.
30. Hubert, C.R.J.; Acosta, N.; Waddell, B.J.; Hasing, M.E.; Qiu, Y.; Fuzzen, M.; et al. Tracking Emergence and Spread of SARS-CoV-2 Omicron Variant in Large and Small Communities by Wastewater Monitoring in Alberta, Canada. *Emerg. Infect. Dis.* **2022**, 28 (9), 1770–1776.

31. Johnson, G.; Nolan, T.; Bustin, S.A. Real-time quantitative PCR, pathogen detection and MIQE, in: Totowa, N.J. (Eds), *PCR Detection of Microbial Pathogens*. Humana Press **2013**, 1-16.
32. Taqman. *TaqMan multiplex PCR optimization user guide*, **2022**. Available from http://assets.thermofisher.com/TFS-Assets/LSG/manuals/taqman_optimization_man.pdf (accessed 2023-03-03).
33. Alberta Health Services (AHS). *COVID-19 Alberta statistics-Interactive aggregate data on COVID-19 cases in Alberta*, **2023**. Available from <https://www.alberta.ca/stats/covid-19-alberta-statistics.htm#variants-of-concern> (accessed 2023-06-05).
34. Stanhope, B.J.; Peterson, B.; Knight, B.; Decadiz, R.N.; Pan, R.; Davis, P.; et al. Development, testing and validation of a SARS-CoV-2 multiplex panel for detection of the five major variants of concern on a portable PCR platform. *Front. Public Health* **2022**, 10, 4676.
35. Wolfe, M.; Hughes, B.; Duong, D.; Chan-Herur, V.; Wigginton, K.R.; White, B.J.; Boehm, A.B. Detection of SARS-CoV-2 variants mu, beta, gamma, lambda, delta, alpha, and omicron in wastewater settled solids using mutation-specific assays is associated with regional detection of variants in clinical samples. *Appl. Environ. Microbiol.* **2022**, 88 (8), e00045-22.
36. Xu, X.; Deng, Y.; Ding, J.; Zheng, X.; Li, S.; Liu, L.; et al. Real-time allelic assays of SARS-CoV-2 variants to enhance sewage surveillance. *Water Res.* **2022**, 220, 118686.
37. Fuzzen, M.; Harper, N.B.; Dhiyebi, H.A.; Srikanthan, N.; Hayat, S.; Bragg, L.M.; et al. An improved method for determining frequency of multiple variants of SARS-CoV-2 in wastewater using qPCR assays. *Sci. Total. Environ.* **2023**, 881, 163292.

38. Tangwangvivat, R.; Wacharapluesadee, S.; Pinyopornpanish, P.; Petcharat, S.; Hearn, S.M.; Thippamom, N.; et al. SARS-CoV-2 Variants Detection Strategies in Wastewater Samples Collected in the Bangkok Metropolitan Region. *Viruses* **2023**, *15* (4), 876.
39. Hasing, M.E.; Lee, B.E.; Gao, T.; Li, Q.; Qiu, Y.; Ellehoj, E.; et al. Wastewater surveillance monitoring of SARS-CoV-2 variants of concern and dynamics of transmission and community burden of COVID-19. *Emerg. Microbes & Infect.* **2023**, *12* (2), 2233638.
40. Public Health Agency of Canada. *COVID-19 epidemiology update: Testing and variants*, **2022**. Available from: <https://health-infobase.canada.ca/covid-19/testing-variants.html#VOC> (accessed on 2022-01-25).

Chapter Five: Advances in Wastewater Analysis Revealing the Co-Circulating Viral Trends of Noroviruses and Omicron Subvariants*

*This chapter has been published and was modified from Kumblathan, T.; Liu, Y.; Crisol, M.; Pang, X.L.; Hruvey, S.E.; Le, X.C.; Li, X.F. Advances in Wastewater Analysis Revealing the Co-Circulating Viral Trends of Noroviruses and Omicron Subvariants. *Sci. Total Environ.* **2024**, 920, 170887. I conceptualized experimental design, performed the experiments, data collection and analysis, text and schematic composition, and revised the overall manuscript. Liu Y contributed to experimental design and manuscript revisions. Crisol M contributed to some multiplex optimization experiments. Pang XL, Hruvey SE, Le XC, and Li XF contributed to editing the manuscript.

5.1 Introduction

As I discussed in my previous chapters, many healthcare resources have been diverted towards diagnosing, treating, and controlling the outbreaks caused by the COVID-19 pandemic over the last few years. However, infections caused by other respiratory viruses, as well as enteric viruses, dramatically increased after the relaxation of COVID-19 public health restrictions.^{1,2} Other viruses can also cause large scale, but more localized outbreaks. Thus, the presence of SARS-CoV-2 with other pathogenic viruses simultaneously in the community, also known as co-circulation, may further increase the burden on healthcare systems. This unique situation calls for the simultaneous monitoring of SARS-CoV-2 variants and other commonly occurring pathogenic viruses, and in particular, WS as a cost-effective approach for understanding the true scale of ongoing outbreaks.

Assessment of the true scale of infections caused by the co-circulation of viruses cannot be dependent on clinical testing alone, especially when newly occurring infections overwhelm clinical testing capacity. WS, when optimized, can be an objective indicator of the amount of a specific virus shed into wastewater, which may be still subject to challenges for interpreting the number of cases, both new and existing.^{3,4} WS is also a proven alternative to detect various substances, pathogens, and antimicrobial resistance markers shed into a common wastewater system.³ The viral levels present in wastewater are closely associated with the corresponding clinical positive rates.⁵ Prior to the COVID-19 pandemic, WS has demonstrated its applicability through applications in monitoring influenza, hepatitis A, and measuring the eradication of poliovirus.^{6,7,8} Because SARS-CoV-2 viral particles are shed into stool, RNA was found to be detectable in wastewater with a 99% probability if there are more than 38 new cases per 100,000 people in the community.⁹ WS has been successfully implemented to monitor SARS-CoV-2

burden at the community level¹⁰⁻¹³ and building level^{14,15,16}. Additionally, WS has been used for the detection, identification, and quantification of emerging variants^{17,18,19} and prediction of COVID-19 hospitalizations.^{20,21} Furthermore, WS of SARS-CoV-2 allows for near real-time monitoring (depending on sample processing time) so that public health officials may be able to obtain early warnings of an imminent disease outbreak and gather information about emerging strains.^{22,23}

In addition to the enveloped viruses, such as SARS-CoV-2, non-enveloped viral pathogens are also commonly found in wastewater, for example, Norovirus (NoV). NoV is classified into 10 genogroups (from GI to GX), with GI and GII most reported in human infections.²⁴ NoV is implicated in ~20% of all cases of diarrhea globally, causing about 699 million infections and up to 200 000 deaths annually.²⁵⁻³⁰ In Alberta, Canada, NoV caused 70% of all acute gastroenteritis (AGE) outbreaks and ~25% of AGE in pediatric patients.^{31,32} An infectious dose as low as 18 viral particles can cause infection.³³ The infection is acquired through the fecal-oral route with individuals displaying symptoms of acute abdominal pain, vomiting, nausea, and diarrhea.^{25,34} Clinical testing often focuses on outbreak investigations and specific patient populations. The true disease burden in the community is unknown. Importantly, no effective treatment or licensed vaccine against NoV is available.²⁸ NoV is shed into human stool, thus it is detectable in the influent of wastewater treatment plants (WWTP). Numerous studies have reported positive correlations between virus levels in wastewater and epidemiological surveillance data.^{29,35-38} Therefore, WS of NoV and other co-circulating viruses can assist public health measures in promoting adherence to infection control activities in the community and institutional settings. Additionally, previous studies have discussed the role of viral interference and competition in viral evolution.^{29,40} For example, almost every virus triggers

an immune interferon response once in the host and most viruses are susceptible to interferons. This can potentially provide a temporary nonspecific immunity in the host which can impact the presence of other viruses.^{39,41} However, due to the limitations of clinical testing, alternative approaches are needed to understand the true impact of co-circulating viruses. Therefore, simultaneous WS of co-circulating viruses such as NoV and SARS-CoV-2 can provide results for assessment of their true impact and presence of NoV and Omicron variants co-circulating in the community.

The co-presence of SARS-CoV-2 Omicron and NoV requires a robust analytical platform for their simultaneous concentration and highly sensitive detection. Previous studies investigating WS of SARS-CoV-2 and NoV using different methods have reported poor viral recoveries.^{29,41-44} WS is further complicated by technical challenges such as RNA fragmentation, dilution effects, complex wastewater matrices, and high abundance of PCR inhibitors.⁴⁴ These two types of viruses also have different surface characteristics, which may have various degrees of influence on viral concentration efficiency and recovery from wastewater samples.

These challenges highlight the need to develop an improved method that can efficiently concentrate and detect both enveloped and non-enveloped viruses in wastewater samples. I previously developed platforms for the detection of SARS-CoV-2 RNA in wastewater (Chapters 3 and 4 of this thesis). The primary objective of the present chapter is to establish a multiplex method enabling simultaneous concentration and sensitive quantification of both NoV (non-enveloped virus) and SARS-CoV-2 Omicron variants (enveloped virus). The new method involves concentration of all structurally different viral particles and components onto an EM, extraction and preservation of RNA using an in-house viral inactivation and preservation (VIP) buffer, RNA enrichment onto magnetic beads (Mag), and direct detection using two multiplex

RT-qPCR assays. Because of the evolution of NoV GI and GII genogroups, previously reported primers and probes for molecular assays cannot detect all GI and GII present in wastewater. Thus, new primers-probe sets must be designed and evaluated in a new duplex RT-qPCR assay to detect and differentiate NoV GI and GII simultaneously in wastewater samples. Finally, integration of the multiplex RT-qPCR assays with the optimized EM-VIP-Mag method for sample processing is critical for the simultaneous quantification of the Omicron variants and NoV (GI and GII) in the same wastewater samples. Monitoring both viral pathogens in wastewater provides an opportunity to explore their temporal occurrence trends and potential relations. This technique and strategy is versatile and could be adaptable for WS of other viruses.

5.2. Experimental

5.2.1 Wastewater Collection from Two Wastewater Treatment Plants (July 2022-June 2023)

Wastewater samples were collected from two WWTPs located in the cities of Calgary and Edmonton (Alberta, Canada) from July 2022 to June 2023. Five hundred milliliters of post-grit raw influent wastewater samples were collected from 24-hour composite samplers three times per week. All the samples were labelled and shipped on ice immediately to Dr. Lilly (Xiaoli) Pang's research laboratory (Pan Alberta WS program) and an aliquot from two samples (total volume of 200 mL) was provided on a weekly basis for analysis. The aliquots were stored at 4°C and analyzed within a week of sampling.

5.2.2 Simultaneous Concentration, Extraction, and Preservation of RNA of Structurally Different Viruses

The concentration of viral particles and extraction of RNA in wastewater samples was performed using my previous protocol with slight modifications (Chapters 3 and 4). Each

wastewater sample (200 mL) was centrifuged for the separation of the aqueous and solid phase. The resulting aqueous phase was transferred into another conical tube and the solid pellet was re-suspended and agitated in a 3% beef extract solution (pH 9.0). After centrifugation, the resulting supernatant was transferred into a new tube and then combined with the aqueous phase. Afterwards, MgCl_2 (1 mol/L) was added into the resulting mixture to reach the final concentration of 25 mmol/L. The treated wastewater sample was filtered through an EM using a vacuum filtration set-up and the SARS-CoV-2 and NoV viral particles were captured on the EM. The large pore size of the EM allowed for small particulate matter and debris to be filtered out of the wastewater sample. The viral particles and RNA are negatively charged in wastewater. By adding the MgCl_2 , the Mg^{2+} served as a salt bridge to facilitate the adsorption of negatively charged viral particles and RNA to the EM. The EMs containing the captured SARS-CoV-2 and NoV were directly used to extract viral RNA with my established VIP-Mag method (Chapter 2). In this method, the RNA was released using the VIP buffer and the released RNA was extracted and enriched on magnetic beads Mag. The resulting magnetic beads possessing the extracted RNA were air-dried and resuspended in a 30 μL of solution consisting of 25 μL of RNase-free water, 4 μL proteinase K inhibitor, and 1 μL RNase inhibitor. The extracted RNA was stored at -80°C until time of analysis.

5.2.3 Determination of the Recovery of Norovirus from Wastewater using a Surrogate (Murine Norovirus)

I used a non-infectious murine norovirus (MNoV) (VIRSeek Murine Norovirus Process Control) as a surrogate of human NoV to evaluate the recovery of NoV from wastewater samples. I first determined the total RNA in the solution provided by the manufacturer. 5 μL of 10^5 viral particles / μL of MNoV solution were directly extracted using the VIP-Mag method.

The extracted RNA was serially diluted and then tested with RT-qPCR to establish a standard curve according to manufacturer's instructions (Figure 5.1). The RT-qPCR reaction (20 μ L of total volume) was performed according to manufacturer's instructions and contained 5 μ L of Basic Mix, 10 μ L of Oligio Mix, and 5 μ L of the extracted RNA. The multiplex RT-qPCR thermal cycling conditions were 50°C for 10 minutes, 95°C for 3 minutes, and 40 cycles of 95°C for 3 seconds and 58°C annealing temperature for 30 seconds. RT-qPCR assays were performed on a QuantStudio™ 3 Real-Time PCR System. Details on the MNoV solution, primers, probes, and thermal cycles conditions can be found in the manufacturer's manual.⁴⁵

In the first set of recovery experiments, multiple previously determined MNoV negative wastewater samples (1 L each) were pooled together. Aliquots of 200 mL of the pooled negative samples were used for spiking. Aliquots of 200 mL were spiked with 5 μ L of MNoV and processed using the EM-VIP-Mag WS protocol. The final wash step was optimized using either 3 times (x), 4x, or 5x wash step. The 4x wash protocol was chosen because the Ct value was better than the 3x wash protocol for the same sample which demonstrates improved PCR inhibitor removal. However, the 5x wash had the same Ct value as the 4x wash, therefore the 4x wash was used for future experiments. The optimized 4x wash protocol was repeated twice on different days with triplicate sample aliquots analyzed in each set of repeats. The recovery experiments were performed three times on separate days with triplicate sample aliquots analyzed in each set of repeats. For the spiked negative samples, the recovery of MNoV RNA in each sample was calculated as the amount of MNoV RNA measured divided by that of MNoV RNA spiked into the sample.

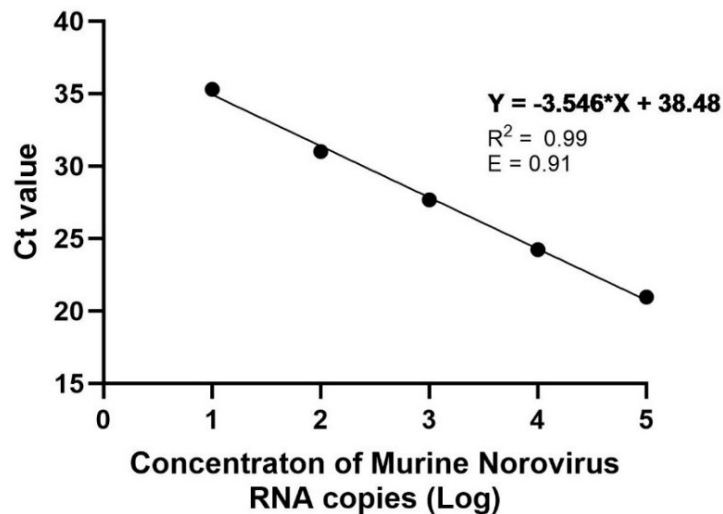


Figure 5.1. Standard curve of Murine Norovirus (MNoV) (VIRSeek Murine Norovirus Process Control). This standard curve was used to calculate MNoV recovery from wastewater samples and thus, to evaluate the recovery of norovirus from wastewater samples.

5.2.4 Norovirus GI and GII Primer, Probe, and Target Sequence Design

The ORF1 and ORF2 junction region is highly conserved among NoV genogroups⁴⁶, thus, this region was selected as the target for NoV GI and GII. Table 5.1 below presents the sequences of the primers and probes used in this study. Specifically, these are the target sequences used in this study: NoV GI GenBank accession no. OP669384.1 and NoV GII GenBank accession no. OP727614.1. The specific primer and probe set of NoV GI and GII were designed using the Primer Express™ Software version 3.0 and specificity was confirmed using NCBI BLAST (Basic Local Alignment Search Tool). There was no formation of non-target secondary structures, and this was confirmed using IDT OligoAnalyzer®.

Table 5.1. Sequences of primers and probes designed to detect NoV GI and GII. Degenerate nucleotide bases are indicated in bolded red text.

Genogroup	Parameter	Sequence
GI	Pf	5' – CGCTGGATGCG N TTCCAT – 3'
	Pr	5' – TCCTTAGACGCCATCATCATTAC – 3'
	Probe	5' VIC-TGGACAGGAGA Y CGC – NFQ-MGB 3'
GII	Pf	5' – ATGTT CAG R T GGATGAG R TTCTC W G A – 3'
	Pr	5' – CGACGCCATCTTCATTCACA – 3'
	Probe	5' FAM-AC D TGGGAGGGCGAT – NFQ-MGB 3'

Abbreviations: NoV = norovirus, Pf = forward primer, Pr = reverse primer, NFQ-MGB = non fluorescence quencher minor groove binding.

N = A/C/G/T, Y = C/T, R = A/G, W = A/T, and D = A/G/T.

5.2.5 Norovirus GI and GII Singleplex RT-qPCR Assay Optimization

I first optimized the NoV GI and GII forward and reverse primer concentrations by testing a range of forward primer concentrations (100 nmol/L to 800 nmol/L) with corresponding reverse primer concentrations (100 nmol/L to 800 nmol/L). Then the concentrations (50 to 500 nmol/L) of NoV GI and GII probes were tested with the forward and reverse primers at their optimized concentrations. Optimal annealing temperature was evaluated by testing temperatures ranging from 55-62°C. Each NoV GI or GII singleplex reaction (20 µL total reaction volume) contained 10 µL of Luna Universal One-Step Reaction Mix (2x), 1 µL of Luna WarmStart® RT Enzyme Mix (20x), 800 nmol/L of forward primer, 800 nmol/L of reverse primer, and 500 nmol/L of probe, and 5 µL of the template. RT-qPCR thermal cycling conditions for both GI and GII singleplex assays were: 55 °C for 10 minutes, 95 °C for 1 minute, and 40 cycles of 95 °C for

10 seconds and 55°C annealing temperature for 1 minute. Both assays were performed on QuantStudio™ 3 Real-Time PCR System.

5.2.6 Norovirus GI and GII Multiplex RT-qPCR Optimization

The conditions of the NoV multiplex assay targeting NoV GI and GII were set based on the optimal conditions of the GI and GII singleplex assays. To achieve high amplification efficiencies for the two targets in multiplex assay, I re-optimized the primer and probe concentrations using the singleplex RT-qPCR optimization techniques. Each NoV multiplex reaction (20 µL total reaction volume) contained 10 µL of Luna Universal One-Step Reaction Mix (2x), 1 µL of Luna WarmStart® RT Enzyme Mix (20x), 400 nmol/L forward primer of GI and GII, 800 nmol/L of each reverse primer, 500 nmol/L each target probe, and 5 µL of sample (template). The multiplex RT-qPCR thermal cycling conditions were: 55 °C for 10 minutes, 95 °C for 1 minute, and 40 cycles of 95 °C for 10 seconds and 55°C annealing temperature for 1 minute. This assay was performed on QuantStudio™ 3 Real-Time PCR System.

5.2.7. Dynamic Range, Efficiency, Analytical Specificity, Sensitivity, and Reproducibility of NoV Multiplex Assay

To test the analytical capabilities of my assay, I purchased the selected NoV GI and GII target sequences (10^{12} copies each) from ThermoFisher Scientific. Serial dilutions of the NoV GI and GII targets from 10^8 to 10^1 were tested in triplicate to determine the dynamic ranges of the singleplex and multiplex assays. The log values of the quantified NoV GI and GII targets were plotted against the corresponding Ct values to generate standard curves as seen below (Figure 5.2). The slope of each standard curve was used to calculate the RT-qPCR efficiency of each GI and GII target in the singleplex and multiplex assays using the following equation: $E = -1 + 10^{(-1/\text{slope})}$, where E represents PCR efficiency. The analytical specificity of the NoV multiplex assay

was validated using RNA isolates of mixed NoV GI/GII, pure NoV GI, and pure NoV GII. The RNA was extracted from clinical stool samples provided by collaborators in the Public Health Laboratory, Alberta Precision Laboratories (APL). MNoV was also tested using the NoV multiplex assay. There were no cross-reactions observed among the NoV genogroups or MNoV in the NoV multiplex assay. The analytical sensitivity and reproducibility for the NoV multiplex assay were determined by testing 2-fold serial dilutions of the NoV GI and GII target from 15 - 75 copies per reaction. The reactions containing 75 copies were conducted in 6 replicates, while the reactions containing 15-50 copies were performed in 10 replicates. The LOD was defined as the lowest concentration detected in all 10 replicates. To prevent possible non-specific amplification between GI and GII after extended amplification cycles, Ct values over 34 were considered as the non-detectable threshold.

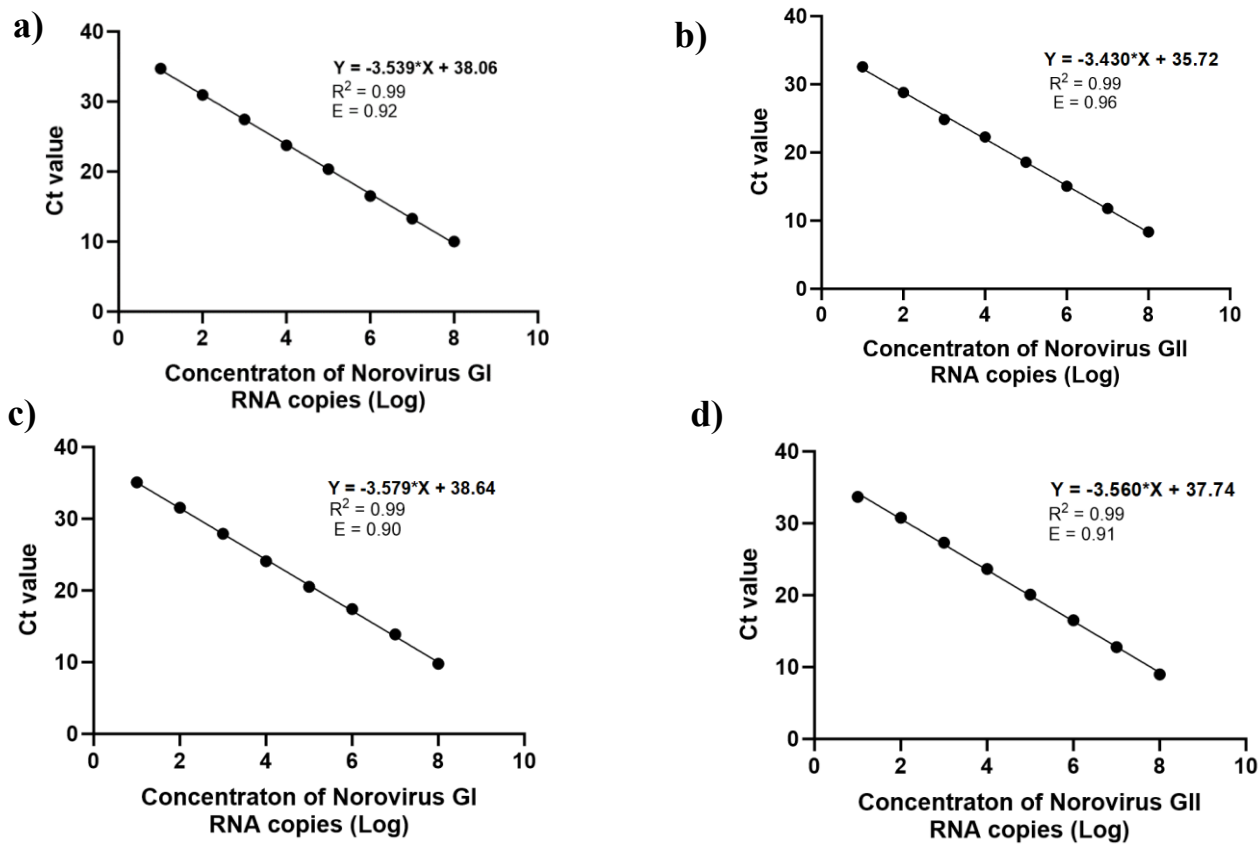


Figure 5.2. Standard curves of targets Norovirus (NoV) GI and GII using singleplex RT-qPCR assays (top) and the multiplex RT-qPCR assay (bottom). This standard curve was used to quantify NoV GI and GII RNA in the wastewater samples.

5.2.8 Application of the Norovirus Multiplex RT-qPCR Assays and Omicron Triplex RT-qPCR Assay for Monitoring Norovirus GI and GII, and Omicron in Wastewater Samples

The NoV multiplex assay was used to determine the RNA copies of NoV GI and GII while the Omicron triplex assay (discussed previously in Chapter 4)¹⁹ targeting the HV 69-70 deletion, and K417Ns and L452R mutation were used to detect and measure the RNA copies of Omicron subvariants in the wastewater samples. The wastewater samples were collected from two WWTPs in Calgary and Edmonton from July 2022 to June 2023 and processed by using the

EM-VIP-Mag-multiplex protocol. An aliquot of 5 μ L of each RNA extract concentrated on magnetic beads was used as the template in the NoV multiplex RT-qPCR reaction and the Omicron triplex reaction, respectively.

5.2.9 Statistical Analysis

GraphPad Prism 10.0.1 was used to create chart figures and determine the slope for efficiency calculations. GraphPad Prism 10.0.1 was also used for Pearson correlation analysis to determine the relationship between the trends of NoV and Omicron subvariants in wastewater.

5.3. Results and Discussion

5.3.1 Simultaneous Capture and Extraction of Norovirus and Omicron from Wastewater Samples

To achieve efficient capture and sensitive detection of both non-enveloped and enveloped viruses from the same wastewater samples, I developed an EM-VIP-Mag-multiplex platform. This platform integrated three steps: 1) efficient capture of viral RNA and particles in a wastewater sample, 2) preservation and extraction of RNA with efficient removal of inhibitors, and 3) direct multiplex RT-qPCR detection of RNA on magnetic beads without the need for elution of RNA. In this chapter, I demonstrated the capability of the EM-VIP-Mag-multiplex platform for detection of non-enveloped NoV (GI and GII) and enveloped Omicron variants as examples of structurally different viruses in the same samples.

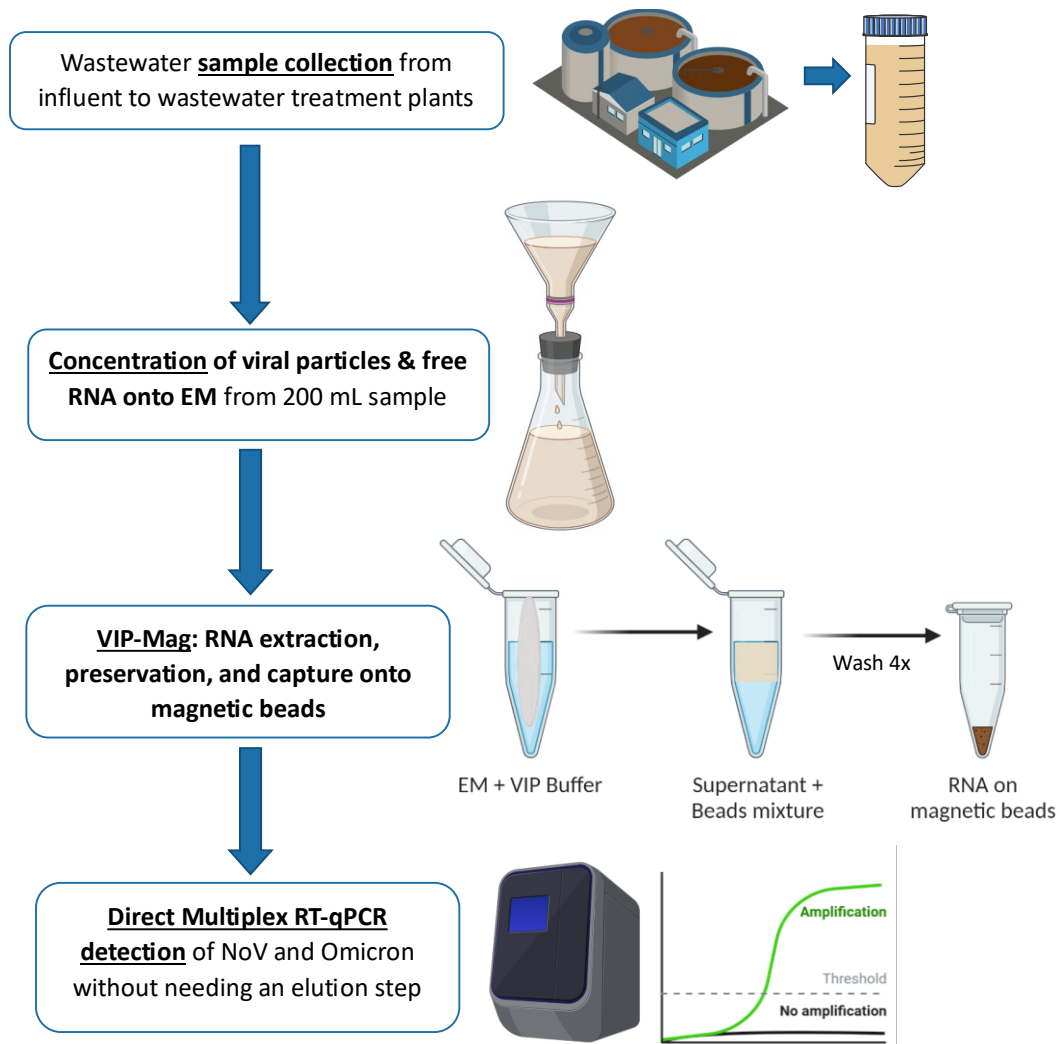


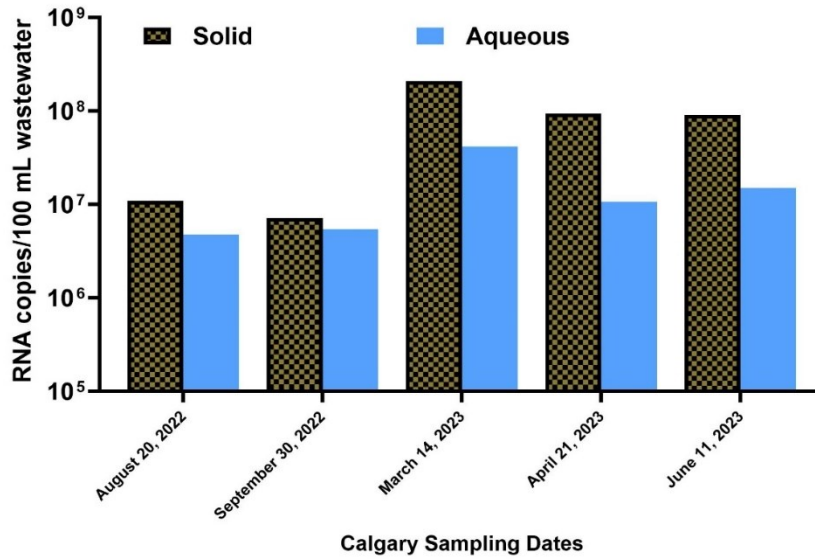
Figure 5.3. Overview of wastewater protocol for Norovirus (NoV) and Omicron from sample collection, concentration of viral particles and RNA using an electronegative membrane (EM), extraction of RNA onto magnetic beads along with the viral inactivation and RNA preservation (VIP) buffer, and direct multiplex RT-qPCR detection of RNA on magnetic beads (Mag).

Figure 5.3 summarizes the simultaneous capture, extraction, and detection of viral RNA of NoV and Omicron from wastewater samples. First, I demonstrated that the EM-VIP-Mag method can provide flexibility and capability for concentrating viral particles from a large volume (200 mL) of wastewater sample. Applying four washes of the RNA on beads effectively

removed inhibitors co-concentrated from the large volume sample. This was followed by direct RT-qPCR multiplex detection of RNA on the magnetic beads without the need for elution. The EM-VIP-Mag-multiplex platform achieved high recovery of $80\pm 4\%$ for an enveloped virus (SARS-CoV-2, discussed in Chapter 3 of this thesis)¹³ and $72\pm 5\%$ for a non-enveloped one (MNoV). This method consistently provides higher recovery compared to other studies that either lack recovery studies or reported inconsistent and lower recoveries of 0-67% for non-enveloped viruses including NoV^{29,42,43} and 0.1-73% for SARS-CoV-2.⁴⁴

Wastewater samples have a variable biphasic composition containing a complex mixture of chemical and biological compounds. Studies have reported that NoV preferentially adsorbs on wastewater solids and suggests that only using the solid phase is sufficient for analysis.^{47,48} To better understand the distribution of NoV viral particles in the solid and aqueous phase of different wastewater samples, I analyzed the solid and aqueous phases separately using ten representative samples of 24h composite wastewater collected from two large WWTPs in Calgary and Edmonton were analyzed throughout the sampling study period. Figures 5.4 (a and b) demonstrate that RNA was present in both the solid and aqueous phases of these samples. The data demonstrates that considerable amounts of NoV RNA were detected in both the solid phase ($9.7 \times 10^5 - 2.1 \times 10^8$ RNA copies/100 mL) and aqueous phase ($3.3 \times 10^6 - 4.2 \times 10^7$ RNA copies/100 mL) of these samples. The RNA abundance varies even when the samples were collected from the same sewer system for both cities during different months. For example, in the Edmonton samples, the August 2022 sample has similar RNA abundance in both the solid and aqueous phase. However, the October 2022 sample has higher RNA abundance in the aqueous phase, whereas the remaining 2023 samples have higher RNA abundance in the solid phase (Figure 5.4 b).

(a)



(b)

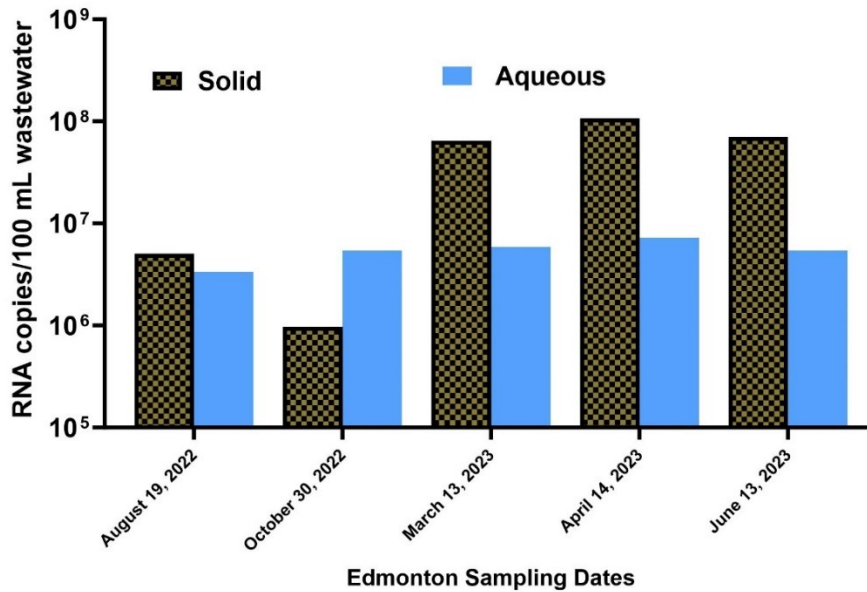


Figure 5.4. Separate analysis of the aqueous and solid phases of ten representative wastewater samples collected from two wastewater treatment plants in the cities of (a) Calgary and (b) Edmonton.

The composition of the wastewater sample depends on several factors such as the flow rate, temperature, precipitation, water quality, pH, and community demographics. Because these factors may be unpredictable, the resulting wastewater composition varies even at the same

sampling location. The percentage of NoV RNA present in the solid phase varied from 57-90% and 15-94% in the Calgary and Edmonton samples, respectively. This observation highlights several important findings. Firstly, both the solid and aqueous phases of wastewater contain significant amounts of RNA. Secondly, the amounts of RNA on the solids and aqueous phases vary from sample to sample even in the same sewer system. Finally, as seen between the Calgary and Edmonton samples, RNA distribution in the solid and aqueous phases vary from system to system (Figure. 5.4 a and b). Analyzing the solid phase alone may be sufficient for determination of viral presence, however analysis of both phases is essential for sensitive detection and estimation of infections. For accurate quantitative purposes, analysis of RNA in both aqueous and solid phases of a wastewater sample is necessary to prevent variations in RNA quantification, to improve recovery, and to reduce false negative or decreased results. The EM-VIP-Mag platform enables simultaneous concentration, preservation, and extraction of RNA of both enveloped and non-enveloped viruses from both the solid and aqueous phase of wastewater.

5.3.2 Development and Assessment of a Multiplex RT-qPCR TaqMan MGB Assay for NoV GI and GII

Several studies have utilized singleplex or multiplex RT-qPCR methods to detect NoV genogroups GI and GII in clinical samples and environmental samples.^{49,50,51} However, the primers and probes published previously are not capable of detecting all the reported strains of GI and GII. This is because as NoV continues to evolve, new strains of GI and GII are emerging. To ensure the detection of all the GI and GII of NoV in the wastewater samples collected from July 2022 to June 2023, I first designed new primers and probes based on all the available sequences belonging to GI and GII in the National Center for Biotechnology (NCBI) database; second, I incorporated degenerate nucleotide codes into the primer and probe sequences.

Degenerate bases in these primers are specified with ambiguity codes that represent alternative nucleotide configurations. Degenerate PCR primers and probes allow for the simultaneous amplification of a heterogeneous population by providing a mixture of PCR primers and probes, each of which anneal to an alternative genogroup found in the NCBI database. To further improve discrimination between GI, GII, and other microbes in wastewater, I incorporated the TaqMan MGB probes for fluorescence detection. The MGB at the 3' end of probes can stabilize probe-target hybrids and provide better discrimination of a single nucleotide mismatch.⁵²

Prior to establishing the NoV multiplex RT-qPCR assay, I optimized several key conditions for the GI and GII singleplex assays. The key factors that were optimized included the concentrations of the primer-probe set and annealing temperatures for GI and GII singleplex assays, as summarized below in Table 5.2. Building upon the optimized singleplex assays, I established the NoV multiplex assay in a single tube consisting of all the primers and probes of the GI and GII targets at the optimized concentrations (Table 5.2).

Table 5.2. Optimized NoV GI and GII singleplex RT-qPCR conditions and NoV multiplex RT-qPCR conditions.

Target	Singleplex RT-qPCR				Multiplex RT-qPCR			
	F-primer (nM)	R-primer (nM)	Probe (nM)	Annealing Temperature (°C)	F-primer (nM)	R-primer (nM)	Probe (nM)	Annealing Temperature (°C)
NoV GI	800	800	500	55	400	800	500	55
NoV GII	400	800	500	55	400	800	500	

Abbreviations: NoV = norovirus, F-primer = forward primer, R-primer = reverse primer

The NoV multiplex RT-qPCR assay was optimized at annealing temperature of 55°C to prevent the formation of nonspecific PCR byproducts and obtain the highest sensitivities. In parallel experiments, I evaluated the amplification efficiency of the singleplex and the NoV multiplex assays for each target. The NoV GI and GII singleplex assays achieved RT-qPCR efficiencies of 92% and 96%, respectively. The NoV multiplex assay achieved RT-qPCR efficiencies of 90% and 91% for targets GI and GII, respectively (Figure 5.1). When varying concentrations (10^2 , 10^4 , or 10^6) of the NoV GI and GII targets were amplified, the ΔCt value between the singleplex and multiplex assays for the GI and GII was less than 1 as shown in Table 5.3 below. This finding supports that the amplification efficiency of each target in the multiplex assay is consistent with the singleplex assays, even when the primers, probes, and templates of other targets are present in the same tube.⁵²

Table 5.3. Performance comparison of singleplex versus multiplex assay for NoV GI and GII.

Target	Template concentration	Ct value (mean) – Singleplex assay	Ct value (mean) – Multiplex assay	ΔCt^a
NoV GI	10^2	29.9	29.8	-0.1
	10^4	22.7	22.1	0.6
	10^6	17.2	16.6	0.6
NoV GII	10^2	30.5	30.4	0.1
	10^4	24.5	25.1	-0.6
	10^6	17.9	18.7	-0.8

^a $\Delta Ct = Ct$ value from singleplex assay – Ct value from triplex assay. $|\Delta Ct|$ value between singleplex and triplex assays was < 1 for both targets and three template concentrations, suggesting that both the singleplex and triplex assays perform similarly.

I validated the analytical specificity of the NoV multiplex assay using RNA extracted from clinical stools samples, which were previously confirmed to be positive for NoV GI and GII by collaborators (Public Health Laboratory, Alberta Precision Laboratories). I received blind RNA samples from collaborators. The NoV multiplex assay correctly identified the RNA in the samples as seen below in (Table 5.4), demonstrating 100% analytical specificity.

Table 5.4. Validation of the NoV multiplex RT-qPCR assay by examining the RNA of Norovirus (NoV) genogroups (GI and GII) isolated from clinical stool samples.

RNA Samples	Ct Values from NoV Multiplex Assay for Each Target		Identification by NoV Multiplex Assay
	GI ORF1-ORF2 junction region (SD) ^a	GII ORF1-ORF2 junction region (SD) ^a	
NoV GI	26.3 (0.0)	NA	NoV GI
NoV GII	NA	29.6 (0.1)	NoV GII
Mixed NoV GI & GII	26.2 (0.2)	30.7 (0.1)	NoV GI & GII
Murine NoV	NA	NA	NA

^a SD denotes one standard deviation. NA indicates no amplification.

I determined the LOD of the NoV multiplex assay by analyzing a wide range of NoV GI and GII target copies (15 - 75) in 6 -10 replicates. The results below in Table 5.5 demonstrate that the NoV multiplex assay can consistently detect positive signals for GI and GII in all 10 replicates, when the target amount in each RT-qPCR reaction was 15 copies or higher. These results demonstrate that the LOD of the GI and GII targets is 15 copies per reaction, which corresponds to Ct values of 33 and 31, respectively. Any signal above a Ct value of 34 is considered as no amplification or considered as non-specific amplification. The use of customized degenerate nucleotide bases and the TaqMan® MGB probes in the current NoV

multiplex assay plays a key role in improving the analytical sensitivity and specificity of my multiplex assay and preventing false negative results.

Table 5.5. Analytical sensitivity of the NoV multiplex RT-qPCR assay for the detection of NoV GI and GII.

RNA	Copies per reaction	Average Ct (Standard Deviation)	Detected/Tested (%)
NoV GI	75	31.0 (0.2)	6/6 (100%)
	50	31.1 (0.3)	10/10 (100%)
	25	31.3 (0.3)	10/10 (100%)
	15	32.1 (0.9)	10/10 (100%)
NoV GII	75	30.2 (0.1)	6/6 (100%)
	50	30.2 (0.0)	10/10 (100%)
	25	30.9 (0.4)	10/10 (100%)
	15	31.3 (1.1)	10/10 (100%)

The results in **bold** indicate the limit of detection (LOD) as 15 copies of RNA per reaction for GI and GII targets. The LOD was defined as the lowest RNA copy number detected in all 10 replicates.

5.3.3 Simultaneous Monitoring of Norovirus and Omicron Subvariants in 94 Wastewater Samples Collected from July 2022 to June 2023

Here I demonstrated the capability of the EM-VIP-Mag-multiplex platform for WS of both enveloped viruses (Omicron) and non-enveloped viruses (Norovirus). I analyzed NoV (GI and GII) and Omicron variants (BA4/5 and XBB) in 94 wastewater samples collected from two large WWTPs in Calgary and Edmonton over a period of a year (July 2022 to June 2023) as seen below in Figure 5.5 and Figure 5.6.

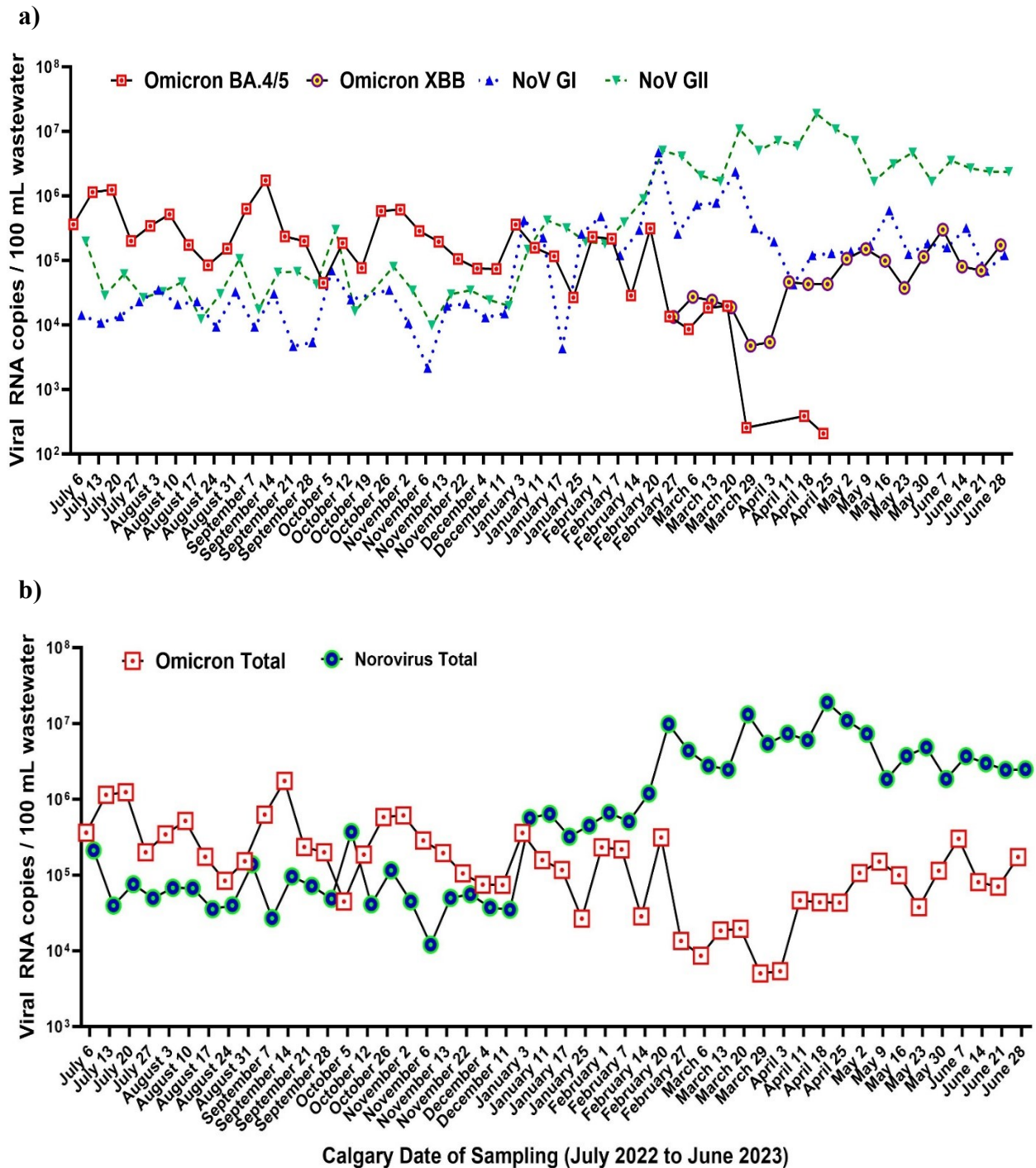


Figure 5.5. Detection and monitoring of wastewater samples collected from Calgary from July 2022 to June 2023. (a) Trends of individual subvariants of Omicron (BA.4/5 and XBB) and genogroups of Norovirus (NoV GI and GII). (b) Total Omicron and Norovirus.

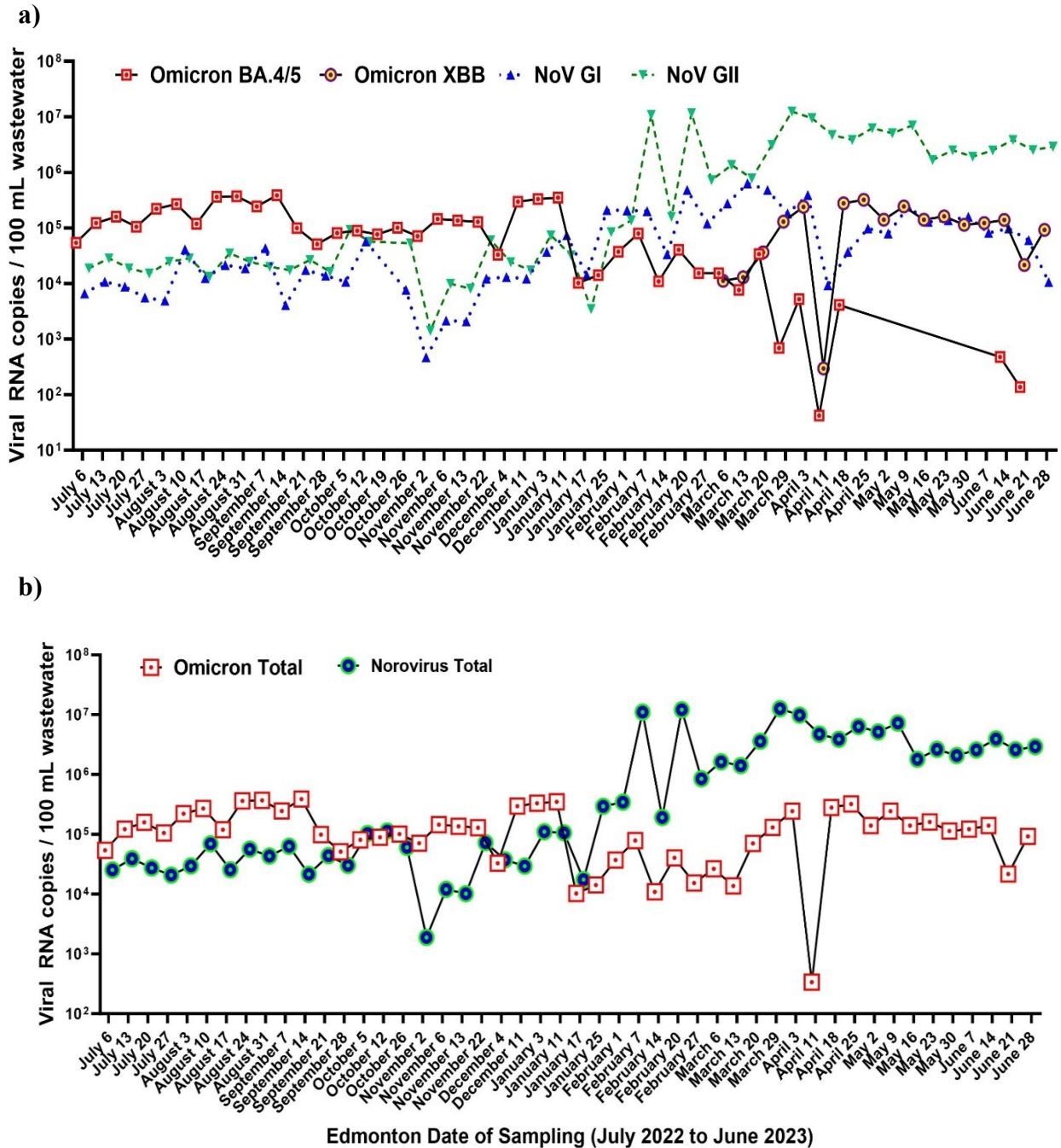


Figure 5.6. Detection and monitoring of wastewater samples collected from Edmonton from July 2022 to June 2023. (a) Trends of individual subvariants of Omicron (BA.4/5 and XBB) and genogroups of Norovirus (NoV GI and GII). (b) Total Omicron and Norovirus.

These RNA results show occurrence trends of NoV GI and GII as well as Omicron variants (BA4/5 and XBB) during July 2022-June 2023 in both systems. In the Calgary wastewater samples, the RNA copies ranged from 4.7×10^3 to 4.7×10^6 copies/100 mL for NoV GI, and from 1.2×10^4 to 1.9×10^7 copies/100 mL for NoV GII (Figure 5.5). Similarly, the RNA copies ranged from 4.7×10^2 to 6.3×10^5 copies/100 mL for NoV GI and from 1.4×10^3 to 1.2×10^7 copies/100 mL for NoV GII in the Edmonton wastewater samples (Figure 5.6).

The NoV RNA levels in the Calgary and Edmonton wastewater were similar. The current RNA levels of NoV GI and GII in Calgary wastewater samples are higher, compared with the 2015 and 2016 Calgary data (2.3×10^2 to 2.0×10^4 copies/100 mL for NoV GI and 2.2×10^3 to 6.2×10^4 copies/100 mL for NoV GII).⁴² The difference in NoV RNA wastewater levels between the two studies may be explained by two factors. First, all mandatory public health restrictions were lifted in Alberta, Canada on June 14, 2022, which may have led to an increase in the spread of common enteric viruses.⁵³ These changes in increased social interaction, decreased personal hygiene practices such as hand washing and sanitation, and increased travel may have led to a surge in various pathogens such as NoV. Second, my WS technique has a substantially greater NoV recovery rate (72%) than the protocol used in the previous study (ranging from 3-21%)⁴², because my study captured RNA from both aqueous and solid phases. The temporal trends of NoV GII RNA started to rise in both the Calgary and Edmonton wastewater samples in January 2023 (Figure 5.5 and Figure 5.6), which is consistent with the trend of NoV GII previously reported in Calgary wastewater⁴² and in southeast Michigan wastewater.³⁸ However, NoV GI exhibits no apparent rise since January 2023 in comparison to NoV GII at both sampling sites. This observation is reasonable given that the majority of NoV clinical cases are caused by NoV GII^{54,55}, and that, in accordance with data provided by the Canadian Food Safety Institute (2023), a

significant increase in NoV outbreaks was reported in the months of January, February, and March 2023 in the province of Alberta.⁵⁶

The majority of wastewater samples from Calgary and Edmonton contained higher levels of NoV GII RNA than GI. This result is in line with other studies that have found that NoV GII is detected at higher concentrations than GI in wastewater samples from all around North America^{38,48} as well as from other regions.^{1,57} Additionally, a study found that over a 1-year period, diarrheic individuals living in southwestern Alberta had a considerably greater prevalence of NoV GII infections than NoV GI infections.⁵⁵ My results also demonstrate the presence of NoV GI and GII RNA at levels $> 10^2$ RNA copies / 100 mL wastewater throughout the summer and fall months demonstrating the occurrence of infections in the communities during these times. This highlights the occurrence of NoV infections in the community throughout the year. This wastewater data can assist public health agencies and encourage communities to follow proper hygiene regulations throughout the year and not just during expected outbreak seasons for the prevention of infections.

SARS-CoV-2 Omicron BA.4/5 and XBB were dominant subvariants circulating during the sampling period from July 2022 to June 2023 in Alberta. I used the Omicron triplex assay that I developed (Chapter 4 of thesis) to detect and differentiate these subvariants present in wastewater samples. The Omicron triplex assay can detect three targets (the HV 69–70 deletion and K417N and L452R mutations). Omicron BA.4/5 was the dominant Omicron subvariant detected in Calgary wastewater samples until February 20th, 2023, exhibiting the signals of HV 69–70 deletion and K417N and L452R mutations. The last day Omicron BA.4/5 was detected in the Calgary wastewater samples was April 25th, 2023. The BA.4/5 RNA concentration in wastewater samples during the sampling period ranged from 2.1×10^2 to 1.7×10^6 copies/100

mL in Calgary (Figure 5.5). The XBB subvariant first appeared on February 27th, 2023, exhibiting the K417N signal. XBB became dominant starting on April 3rd, 2023. The XBB RNA concentration in wastewater samples during the sampling period ranged from 4.7×10^3 to 3.0×10^5 copies/100 mL in Calgary (Figure 5.5). Omicron BA.4/5 was dominant and detected in Edmonton wastewater samples from July 2022 until February 27th, 2023, exhibiting the signals of HV 69–70 deletion and K417N and L452R mutations. The last day Omicron BA.4/5 was detected in the Edmonton wastewater samples was June 21st, 2023. The BA.4/5 RNA concentration in wastewater samples during the sampling period ranged from 41 to 3.9×10^5 copies/100 mL in Edmonton (Figure 5.6). The XBB subvariant first appeared in Edmonton wastewater samples on March 6th, 2023, exhibiting the K417N signal. XBB became the dominant subvariant on March 29th, 2023. The XBB RNA concentration in wastewater samples during the sampling period ranged from 3.0×10^2 to 3.2×10^5 copies/100 mL in Edmonton (Figure 5.6). The overall trends of Omicron BA.4/5 and XBB detected in wastewater in both Calgary and Edmonton are in concordance with the trend of clinical cases reported by Alberta Health Services during the period of wastewater sampling.⁵⁸

Simultaneous monitoring of NoV GI and GII genogroups and SARS-CoV-2 Omicron variants in the same wastewater samples provides an opportunity to compare emergence of these different viruses and potential interactions. No study has observed a potential relationship between the trends of NoV and Omicron variants (BA.4/5 and XBB) in the same wastewater samples or analyzed from two wastewater systems. My results demonstrate that the total Omicron RNA levels are slightly higher than the total NoV RNA levels from the months of July 2022 to December 2022 in both the Calgary and Edmonton wastewater samples. Then the total NoV RNA levels began to dramatically increase on January 3rd and January 17th of 2023 for Calgary and Edmonton,

respectively (Figure 5.5b and Figure 5.6b). The total NoV RNA levels are 1-3 orders of magnitude higher than the total Omicron RNA levels between February 14, 2023 and June 28, 2023 in both cities. Pearson correlation analysis of the RNA levels demonstrates that there is a statistically significant inverse relationship between the presence of total NoV RNA and total Omicron RNA ($p < 0.0001$). Additionally, I also observed a statistically significant inverse relationship between the abundance of NoV GI RNA and Omicron ($p < 0.0004$) and between the abundance of NoV GII RNA and Omicron ($p < 0.0001$) at both sampling sites.

It is important to note that this data does not suggest a direct link between the RNA levels of NoV and Omicron or the presence of a mechanistic relationship. The observation of these trends in these wastewater samples from two WWTPs is intriguing and warrants further investigation into the potential interactions between different viruses. This is supported by studies that SARS-CoV-2 may mediate interferon (INF) release in the gastrointestinal tract and impact the presence of other viruses.⁴¹ Specifically, type III IFN plays a major role in regulating NoV infection and spread by inhibiting persistent viral shedding in stool.⁵⁹ There are also case studies which suggest that SARS-CoV-2 can impact the presence of other viruses in humans and vice versa. For example, in a study done by Stockdale et al. 2023 in India, Hepatitis C commonly co-occurred with SARS-CoV-2 in wastewater samples. The authors suggested that this occurrence is because of the increased expression of entry receptor ACE2 and transmembrane protease serine 2 (TMPRSS2) in hepatocytes which allows enhanced entry of both Hepatitis C and SARS-CoV-2.⁶⁰ Several studies have also investigated the impact of common respiratory viruses (i.e. Influenza, Rhinovirus, Adenovirus) on SARS-CoV-2, and vice versa.^{61,62} Additionally, COVID-19 prevention measures (i.e., hand hygiene, masking, and physical distancing) have had an impact on suppressing the spread of the other pathogens in the years 2020 – 2022.³⁷ In 2023, the majority of the COVID-19

restrictions were globally lifted. The lack of public health measures such as physical distancing and mandatory isolation, reduced personal hygiene practices such as hand washing and sanitation, and increased travel such as that on cruise ships may have led to a surge in various pathogens such as NoV. While my observations suggest a potential relationship between the presence of Omicron and NoV in wastewater, it is unclear whether there are biological interactions between the viruses, requiring future studies. Regardless, my WS platform has demonstrated its adaptability for structurally different viruses and could be used in the future as alternative tools to evaluate population-level viral interferences and biological causation between different viruses, such as SARS-CoV-2 and influenza. Additionally, previous studies have demonstrated the potential of WS for early prediction of disease outbreaks in the community by 2-8 days prior to clinical case reports.^{63,64} With frequent wastewater sampling, rapid wastewater analysis, and appropriate reporting to public health, my WS protocol for NoV and SARS-CoV-2 can be applied for early warning of outbreaks or rise of new viral mutations in the community. Additionally, localized wastewater testing of high-risk groups (i.e. daycares, long-term care facilities) using the established wastewater protocol may also be beneficial for early detection and prevention of disease spread. Therefore, it is important to continue to monitor such clinically significant pathogens in the community and build capacity for future outbreak preparedness.

5.4. Conclusion

The EM-VIP-Mag-multiplex WS platform can efficiently concentrate, extract, and preserve RNA of both enveloped and non-enveloped viral pathogens in wastewater. Combined with the multiplex RT-qPCR assays for NoV and Omicron, my WS platform enables simultaneous quantification and differentiation of NoV GI and GII and Omicron subvariants BA.4/5 and XBB in wastewater samples. The occurrence of NoV GI and GII, as well as Omicron

BA.4/5 and XBB, detected in wastewater matches the trends of clinical cases reported in both cities from July 2022 to June 2023. This chapter has demonstrated that the WS platform is robust and provides highly sensitive detection of different viral pathogens in wastewater. My observations show inverse occurrence trends of NoV and Omicron in wastewater over the course of the sampling period. This raises a hypothesis of potential interactions between NoV and SARS-CoV-2 Omicron variants for future investigation. Because current clinical testing for both NoV and Omicron is limited, WS results provide necessary information for informing the public about disease prevalence and practicing proper prevention measures. The successful detection of structurally different, enveloped and non-enveloped, viral pathogens demonstrates the capability of the WS platform for monitoring various viral pathogens, contributing to the advancement of biomonitoring and surveillance of community infections.

5.5. References

1. Wang, H.; Churqui, M.P.; Tunovic, T.; Enache, L.; Johansson, A.; Lindh, M.; et al. Measures against COVID-19 affected the spread of human enteric viruses in a Swedish community, as found when monitoring wastewater. *Sci. Total Environ.* **2023**, 895, 165012.
2. Zafeiriadou, A.; Kaltsis, L.; Kostakis, M.; Kapes, V.; Thomaidis, N.S.; Markou, A. Wastewater surveillance of the most common circulating respiratory viruses in Athens: The impact of COVID-19 on their seasonality. *Sci. Total Environ.* **2023**, 900, 166136.
3. Choi, P.M.; Tschärke, B.J.; Donner, E.; O'Brien, J.W.; Grant, S.C.; Kaserzon, S.L.; et al. Wastewater-based epidemiology biomarkers: past, present and future. *Trends Analyt. Chem.* **2018**, 105, 453–469.
4. Polo, D.; Quintela-Baluja, M.; Corbishley, A.; Jones, D.L.; Singer, A.C.; Graham, D.W.; Romalde, J.L. Making waves: Wastewater-based epidemiology for COVID-19—approaches and challenges for surveillance and prediction. *Water Res.* **2020**, 186, 116404.
5. Hughes, B.; Duong, D.; White, B.J.; Wigginton, K.R.; Chan, E.M.; Wolfe, M.K.; Boehm, A.B. Respiratory syncytial virus (RSV) RNA in wastewater settled solids reflects RSV clinical positivity rates. *Environ. Technol. Lett.* **2022**, 9, 173-178.
6. Hovi, T.; Shulman, L.M.; Van Der Avoort, H.; Deshpande, J.; Roivainen, M.; De Gourville, E.M. Role of environmental poliovirus surveillance in global polio eradication and beyond. *Epidemiol. Infect.* **2012**, 140, 1–13.
7. Hellmér, M.; Paxéus, N.; Magnius, L.; Enache, L.; Arnholm, B.; Johansson, A.; et al. Detection of pathogenic viruses in sewage provided early warnings of Hepatitis A virus and Norovirus outbreaks. *Appl. Environ. Microbiol.* **2014**, 80, 6771–6781.

8. Dumke, R.; Geissler, M.; Skupin, A.; Helm, B.; Mayer, R.; Schubert, S.; et al. Simultaneous detection of SARS-CoV-2 and Influenza virus in wastewater of two cities in southeastern Germany, January to May 2022. *Int. J. Environ. Res. Public Health* **2022**, *19*, 13374.
9. Li, Q.; Lee, B.E.; Gao, T.; Qiu, Y.; Ellehoj, E.; Yu, J.; et al. Number of COVID-19 cases required in a population to detect SARS-CoV-2 RNA in wastewater in the province of Alberta, Canada: Sensitivity assessment. *J. Environ. Sci.* **2023**, *125*, 843-850.
10. Ahmed, W.; Bivins, A.; Bertsch, P.M.; Bibby, K.; Choi, P.M.; Gyawali, P.; et al. Surveillance of SARS-CoV-2 RNA in wastewater: Methods optimization and quality control are crucial for generating reliable public health information. *Curr. Opin. Environ. Sci. Health* **2020**, *17*, 82-93.
11. Medema, G.; Heijnen, L.; Elsinga, G.; Italiaander, R.; Brouwer, A. Presence of SARS-Coronavirus-2 RNA in sewage and correlation with reported COVID-19 prevalence in the early stage of the epidemic in the Netherlands. *Environ. Technol. Lett.* **2020**, *7*, 511-516.
12. Keshaviah, A.; Diamond, M.B.; Wade, M.J.; Scarpino, S.V.; Ahmed, W.; Amman, F.; et al. Wastewater monitoring can anchor global disease surveillance systems. *Lancet Glob. Health* **2023**, *11*, e976-81.
13. Kumblathan, T.; Liu, Y.; Qiu, Y.; Pang, L.; Hrudehy, S.E.; Le, X.C.; Li, X.F. An efficient method to enhance recovery and detection of SARS-CoV-2 RNA in wastewater. *J. Environ. Sci.* **2023a**, *130*, 139-148.

14. Gibas, C.; Lambirth, K.; Mittal, N.; Juel, M.A.I.; Barua, V.B.; Roppolo, Brazell, L.; et al. Implementing building-level SARS-CoV-2 wastewater surveillance on a university campus. *Sci. Total Environ.* **2021**, 782, 146749.
15. Welling, C.M.; Singleton, D.R.; Haase, S.B.; Browning, C.H.; Stoner, B.R.; Gunsch, C.K.; Grego, S. Predictive values of time-dense SARS-CoV-2 wastewater analysis in university campus buildings. *Sci. Total Environ.* **2022**, 835, 155401.
16. Marin, M.A.L.; Zdenkova, K.; Bartackova, J.; Cermakova, E.; Dostalkova, A.; Demnerova, K.; et al. Monitoring COVID-19 spread in selected Prague's schools based on the presence of SARS-CoV-2 RNA in wastewater. *Sci. Total Environ.* **2023**, 871, 161935.
17. Ahmed, W.; Bivins, A.; Stephens, M.; Metcalfe, S.; Smith, W.J.; Sirikanchana, K.; et al. Occurrence of multiple respiratory viruses in wastewater in Queensland, Australia: Potential for community disease surveillance. *Sci. Total Environ.* **2023**, 864, 161023.
18. Anand, U.; Pal, T.; Zanoletti, A.; Sundaramurthy, S.; Varjani, S.; Rajapaksha, A.U.; et al. The spread of the omicron variant: Identification of knowledge gaps, virus diffusion modelling, and future research needs. *Environ. Res.* **2023**, 225, 115612.
19. Kumblathan, T.; Liu, Y.; Pang, X,L.; Hrudey, S.E.; Le, X.C.; Li, X.F. Quantification and Differentiation of SARS-CoV-2 Variants in Wastewater for Surveillance. *ACS Environ. Health* **2023b**, 1, 203-213.
20. Galani, A.; Aalizadeh, R.; Kostakis, M.; Markou, A.; Alygizakis, N.; Lytras, T.; et al. SARS-CoV-2 wastewater surveillance data can predict hospitalizations and ICU admissions. *Sci. Total Environ.* **2022**, 804, 150151.

21. Schenk, H.; Heidinger, P.; Insam, H.; Kreuzinger, N.; Markt, R.; Nägele, F.; et al.
Prediction of hospitalisations based on wastewater-based SARS-CoV-2 epidemiology.
Sci. Total Environ. **2023**, 873, 162149.
22. Mao, K.; Zhang, K.; Du, W.; Ali, W.; Feng, X.; Zhang, H. The potential of wastewater-based epidemiology as surveillance and early warning of infectious disease outbreaks.
Curr. Opin. Environ. Sci. Health **2020**, 17, 1–7.
23. Hrudey, S.E.; Bischel, H.N.; Charrois, J.; Chik, A.H.; Conant, B.; Delatolla, R.; et al.
Wastewater surveillance for SARS-CoV-2 RNA in Canada. *Facets* **2022**, 7, 1493-1597.
24. Chhabra, P.; de Graaf, M.; Parra, G.I.; Chan, M.C.W.; Green, K.; Martella, V.; et al.
Updated classification of norovirus genogroups and genotypes. *J. Gen. Virol.* **2019**, 100, 1393.
25. Glass, R.I.; Parashar, U.D.; Estes, M.K. Norovirus gastroenteritis. *N. Engl. J. Med.* **2009**, 361, 1776–1785.
26. Pires, S.M.; Fischer-Walker, C.L.; Lanata, C.F.; Devleeschauwer, B.; Hall, A.J.; Kirk, M.D.; et al. Aetiology-specific estimates of the global and regional incidence and mortality of diarrhoeal diseases commonly transmitted through food. *PLoS One* **2015**, 10, e0142927.
27. Lopman, B.A.; Steele, D.; Kirkwood, C.D.; Parashar, U.D. The vast and varied global burden of norovirus: prospects for prevention and control. *PLoS Med.* **2016**, 13, e1001999.
28. Jahun, A.S. and Goodfellow, I.G. Interferon responses to norovirus infections: current and future perspectives. *J. Gen. Virol.* **2021**, 102 (10), 001660.

29. Huang, Y.; Zhou, N.; Zhang, S.; Yi, Y.; Han, Y.; Liu, M.; et al. Norovirus detection in wastewater and its correlation with human gastroenteritis: a systematic review and meta-analysis. *Environ. Sci. Pollut. Res.* **2022**, *29*, 22829–22842.
30. Centers for Disease Control and Prevention (CDC). *Norovirus*, **2023**. Available from: <https://www.cdc.gov/norovirus/index.html> (accessed 2023-08-14).
31. Freedman, S.B.; Xie, J.; Nettel-Aguirre, A.; Lee, B.; Chui, L.; Pang, X.L.; et al. Enteropathogen detection in children with diarrhoea, or vomiting, or both, comparing rectal flocked swabs with stool specimens: an outpatient cohort study. *Lancet Gastroenterol. Hepatol.* **2017**, *2*, 662-669.
32. Pang, X.L.; Preiksaitis, J.K.; Wong, S.; Li, V.; Lee, B.E. Influence of novel norovirus GII.4 variants on gastroenteritis outbreak dynamics in Alberta and the Northern Territories, Canada between 2000 and 2008. *PloS One* **2010**, *5*, e11599.
33. Bányai, K.; Estes, M.K.; Martella, V.; Parashar, U.D. Viral gastroenteritis. *Lancet* **2018**, *392*, 175-186.
34. MacCannell, T.; Umscheid, C.A.; Agarwal, R.K.; Lee, I.; Kuntz, G.; Stevenson, K.B. Healthcare Infection Control Practices Advisory Committee (HICPAC). Guideline for the prevention and control of Norovirus gastroenteritis outbreaks in healthcare settings. *Infect. Control Hosp. Epidemiol.* **2011**, *32*, 939–969.
35. Kazama, S.; Miura, T.; Masago, Y.; Konta, Y.; Tohma, K.; Manaka, T.; et al. Environmental surveillance of Norovirus genogroups I and II for sensitive detection of epidemic variants. *Appl. Environ. Microbiol.* **2017**, *83*, e03406-16.
36. Wang, H.; Neyvaldt, J.; Enache, L.; Sikora, P.; Mattsson, A.; Johansson, A.; et al. Variations among viruses in influent water and effluent water at a wastewater plant over

- one year as assessed by quantitative PCR and metagenomics. *Appl. Environ. Microbiol.* **2020**, 86, e02073-20.
37. Markt, R.; Stillebacher, F.; Nägele, F.; Kammerer, A.; Peer, N.; Payr, M.; et al. Expanding the pathogen panel in wastewater epidemiology to Influenza and Norovirus. *Viruses* **2023**, 15, 263.
38. Ammerman, M.L.; Mullapudi, S.; Gilbert, J.; Figueroa, K.; Cruz, F.P.; Bakker, K.M.; et al. 2023. Norovirus GII wastewater monitoring for epidemiological surveillance. *PLOS Water* **2024**, 3 (1), e0000198.
39. Piret, J. and Boivin, G. Viral interference between respiratory viruses. *Emerg. Infect. Dis.* **2022**, 28, 273-281.
40. Chin, T.; Foxman, E.F.; Watkins, T.A.; Lipsitch, M. What can be learned from viral co-detection studies in human populations. *MedRxiv* **2023**, Available from: <https://doi.org/10.1101/2023.06.17.23291541> (accessed 2023-08-14).
41. Stanifer, M.L.; Guo, C.; Doldan, P.; Boulant, S. Importance of type I and III interferons at respiratory and intestinal barrier surfaces. *Front. Immunol.* **2020**, 11, 608645.
42. Qiu, Y.; Li, Q.; Lee, B.E.; Ruecker, N.J.; Neumann, N.F.; Ashbolt, N.J.; Pang, X. UV inactivation of human infectious viruses at two full-scale wastewater treatment plants in Canada. *Water Res.* **2018**, 147, 73-81.
43. Jahne, M.A.; Brinkman, N.E.; Keely, S.P.; Zimmerman, B.D.; Wheaton, E.A.; Garland, J.L. Droplet digital PCR quantification of norovirus and adenovirus in decentralized wastewater and graywater collections: Implications for onsite reuse. *Water Res.* **2020**, 169, 115213.

44. Kumblathan, T.; Liu, Y.; Uppal, G.K.; Hruday, S.E.; Li, X.F. Wastewater-based epidemiology for community monitoring of SARS-CoV-2: progress and challenges. *ACS Environ. Au* **2021**, *1*, 18-31.
45. VIRSeek Murine Norovirus Process Control, Eurofins GeneScan Technologies. *VIRSeek murine norovirus process control real-time RT-PCR*, **2022**. Available from: https://www.goldstandarddiagnostics.com/pub/media/productattachments/files/MNL_VI_RSeek_MNV_Proc_Ctrl_real_time_RT_PCR_5728200401_5728200801_V4.pdf (accessed 2023-09-28).
46. Kageyama, T.; Kojima, S.; Shinohara, M.; Uchida, K.; Fukushi, S.; Hoshino, F.B.; et al. Broadly reactive and highly sensitive assay for Norwalk-like viruses based on real-time quantitative reverse transcription-PCR. *J. Clin. Microbiol.* **2003**, *41* (4), 1548-1557.
47. Tao, Z.; Wang, Z.; Lin, X.; Wang, S.; Wang, H.; Yoshida, H.; et al. One-year Survey of human enteroviruses from sewage and the factors affecting virus adsorption to the suspended solids. *Sci. Rep.* **2016**, *6*, 31474.
48. Boehm, A.B.; Wolfe, M.K.; White, B.J.; Hughes, B.; Duong, D.; Banaei, N.; Bidwell, A. Human norovirus (HuNoV) GII RNA in wastewater solids at 145 United States wastewater treatment plants: comparison to positivity rates of clinical specimens and modeled estimates of HuNoV GII shedders. *J. Expo. Sci. Environ. Epidemiol.* **2023a**, 1-8.
49. Hoehne, M.; Schreier, E. Detection of Norovirus genogroup I and II by multiplex real-time RT-PCR using a 3'-minor groove binder-DNA probe. *BMC Infect. Dis.* **2006**, *6*, 69.
50. Pang, X.L.; Preiksaitis, J.K.; Lee, B. Multiplex real time RT-PCR for the detection and quantitation of norovirus genogroups I and II in patients with acute gastroenteritis. *J. Clin. Virol.* **2005**, *33*, 168-171.

51. Wolf, S.; Williamson, W.M.; Hewitt, J.; Rivera-Aban, M.; Lin, S.; Ball, A.; et al. Sensitive multiplex real-time reverse transcription-PCR assay for the detection of human and animal Noroviruses in clinical and environmental samples. *Appl. Environ. Microbiol.* **2007**, *73*, 5464–5470.
52. Taqman. *TaqMan multiplex PCR optimization user guide*, **2022**. Available from: https://assets.thermofisher.com/TFSAssets/LSG/manuals/taqman_optimization_man.pdf (accessed 2023-08-14).
53. Alberta Health Services (AHS). *COVID-19 info for Albertans*, **2022**. Available from: <https://www.alberta.ca/coronavirus-info-for-albertans> (accessed 2023-08-14).
54. Nordgren, J.; Matussek, A.; Mattsson, A.; Svensson, L.; Lindgren, P.E. Prevalence of norovirus and factors influencing virus concentrations during one year in a full-scale wastewater treatment plant. *Water Res.* **2009**, *43*, 1117–1125.
55. Leblanc, D.; Inglis, G.D.; Boras, V.F.; Brassard, J.; Houde, A. The prevalence of enteric RNA viruses in stools from diarrheic and non-diarrheic people in southwestern Alberta, Canada. *Arch. Virol.* **2017**, *162*, 117-128.
56. Canadian Food Safety Institute. *Canadian health authorities worried about 2023 Norovirus outbreaks*, **2023**. Available from: <https://news.foodsafety.ca/canadian-health-authorities-worried-about-2023-norovirus-outbreaks> (accessed 2023-08-14).
57. Eftim, S.E.; Hong, T.; Soller, J.; Boehm, A.; Warren, I.; Ichida, A; Nappier, S.P. Occurrence of norovirus in raw sewage—a systematic literature review and meta-analysis. *Water Res.* **2017**, *111*, 366-374.

58. Alberta Health Services (AHS). *COVID-19 Alberta statistics-Interactive aggregate data on COVID-19 cases in Alberta*, **2023**. Available from: <https://www.alberta.ca/stats/covid-19-alberta-statistics.htm#variants-of-concern> (accessed 2023-08-14).
59. Lazear, H.M.; Nice, T.J.; Diamond, M.S. Interferon- λ : immune functions at barrier surfaces and beyond. *Immunity* **2015**, *43*, 15-28.
60. Stockdale, S.R.; Blanchard, A.A.; Nayak, A.; Husain, A.; Nashine, R.; Dudani, H.; et al. RNA-Seq of untreated wastewater to assess COVID-19 and emerging and endemic viruses for public health surveillance. *Lancet Reg. Health Southeast Asia* **2023**, *14*, 100205.
61. Boehm, A.B.; Hughes, B.; Duong, D.; Chan-Herur, V.; Buchman, A.; Wolfe, M.K.; White, B.J. Wastewater concentrations of human influenza, metapneumovirus, parainfluenza, respiratory syncytial virus, rhinovirus, and seasonal coronavirus nucleic-acids during the COVID-19 pandemic: a surveillance study. *The Lancet Microbe* **2023a**, *4*, 340-348.
62. Gentry, Z.; Zhao, L.; Faust, R.A.; David, R.E.; Norton, J.; Xagorarakis, I. Wastewater surveillance beyond COVID-19: a ranking system for communicable disease testing in the tri-county Detroit area, Michigan, USA. *Front. Public Health* **2023**, *11*, 1178515.
63. Nemudryi, A.; Nemudraia, A.; Wiegand, T.; Surya, K.; Buyukyoruk, M.; Cicha, C.; et al. Temporal detection and phylogenetic assessment of SARS-CoV-2 in municipal wastewater. *Cell Rep. Med.* **2020**, *1* (6), p.100098.
64. Peccia, J.; Zulli, A.; Brackney, D.E.; Grubaugh, N.D.; Kaplan, E.H.; Casanovas-Massana, A.; et al. Measurement of SARS-CoV-2 RNA in wastewater tracks community infection dynamics. *Nat. Biotechnol.* **2020**, *38*, 1164–1167.

Chapter Six: Conclusions & Future Perspectives

The COVID-19 outbreak caused unprecedented and detrimental effects on worldwide public health in the last 3 years. A major challenge in preventing the spread of disease was keeping up with the high demand for timely and accurate clinical diagnostic testing. Timely and accurate diagnostic testing is critical to guide quarantine regulations and prevent the spread of disease. However, clinical laboratories were overwhelmed with the sheer number of diagnostic tests required during the pandemic. To address these challenges, diagnostic testing was restricted in many jurisdictions due to regional policies, accessibility issues, and shortages in approved diagnostic resources.^{1,2} These restrictions resulted in limited data available for critical public health decisions. To overcome these challenges, my thesis research focused on alleviating this diagnostic burden by developing alternative approaches and assays to complement the standard clinical testing of SARS-CoV-2. The main goal of my alternative approaches was to use oral fluids as the sample type for clinical testing and wastewater as the sample type for community biomonitoring of SARS-CoV-2. For oral fluids testing of SARS-CoV-2, my objectives were to 1) overcome technical challenges associated with the heterogeneous and viscous matrix of oral fluids, 2) develop a streamlined viral inactivation, RNA extraction, preservation, and subsequent analysis protocol, and 3) apply my oral fluids protocol for testing COVID-19 patient samples. For wastewater testing of SARS-CoV-2, my objectives were to 1) overcome issues of poor sensitivity, recovery, and reproducibility due to the complex wastewater matrix, 2) develop an efficient and accessible wastewater protocol, and 3) apply my wastewater protocol for testing wastewater samples for SARS-CoV-2, VOCs, and other viral pathogens. Overall, the aim of these protocols that I developed was to provide beneficial solutions to challenges and burdens previously faced with the standard clinical testing of SARS-CoV-2.

To alleviate the burden of NPS based testing for clinical testing, I developed a diagnostic assay for the detection of SARS-CoV-2 from oral fluids. My unique VIP-Mag platform is innovative because it allows patients to directly spit into the sample tubes containing my VIP buffer which allows for immediate viral inactivation. This approach is also inexpensive because it enables self-collection of oral fluid samples on site or at home without the need for healthcare professionals or resources that are limited in a pandemic and/or outbreak setting (i.e. swabs, viral transport media). Sample collection is followed by sample analysis which involves simultaneous viral inactivation and RNA preservation, RNA concentration on magnetic beads, and direct RNA detection without the need for elution. All these aspects allow for improved removal of matrix effects and enhanced sensitive detection than previously published protocols on oral fluids detection. For example, compared to the CDC recommended QIAamp Viral RNA Mini Kit, my method is more sensitive, simpler, and cheaper. These innovative strategies of my method will be particularly useful for future applications in pooled sample testing for population surveillance on a larger scale, repeated sampling, and for point of care testing for SARS-CoV-2. For example, future studies can incorporate the VIP-Mag method with an isothermal detection method for colorimetric analysis for the presence of a pathogen. This application is not limited to SARS-CoV-2, but can be applied for other infectious diseases caused by viruses (i.e. Influenza, Norovirus, sexually transmitted viruses, etc.) and bacteria (i.e. Streptococcus, Staphylococcus, etc.). Swift and accurate detection of these infectious pathogens enables enhanced treatment, effective containment, and management of disease transmission within the community.

To complement individual clinical testing with biomonitoring of SARS-CoV-2 in the community, I developed a robust protocol and method for reproducible and sensitive detection of SARS-CoV-2 in wastewater samples. I aimed at overcoming existing problems of low recovery

and poor reproducibility. To achieve this, I developed the EM-VIP-Mag-RT-qPCR method that allows for capturing of viral particles and free RNA from both the solids and aqueous phase of wastewater onto an EM, efficient RNA extraction and preservation using the VIP buffer, removal of wastewater matrix and inhibitors using the Mag beads, followed by direct RT-qPCR detection of RNA on the Mag beads without the need for elution. My WS protocol has several innovative aspects. Firstly, my method has a reproducible recovery of 80%, which is higher than any previously published study. Secondly, my protocol is robust, cost-effective, and utilizes accessible equipment. This provides a solution to the rising concern for future implementation of WS where sample collection and reagents are currently considered expensive. There is also a lack of facilities equipped with necessary instrumentation for wastewater analysis.³ The features of my WS protocol supports progress towards accessible laboratory methods which can be used for future applications. For example, future studies can use strategies from my WS method to develop portable laboratory kits which allow for on-site wastewater sample collection and analysis. This can allow for faster and cheaper surveillance of more localized areas such as high risk and vulnerable communities (i.e. long-term care facilities, hospitals, academic institutions, etc.). Therefore, the strategies and techniques developed in this chapter contribute to building the capacity for future biomonitoring of community infections.

To expand the capacity of wastewater monitoring of the rapidly emerging SARS-CoV-2 VOCs, I developed several multiplex RT-qPCR assays for sensitive quantification of Alpha, Beta, Gamma, Delta, and Omicron sub-variants BA.1, BA.2, BA.4/5, and XBB. My multiplex assays provide advanced approaches to monitoring for SARS-CoV-2 mutations. Firstly, unlike sequencing approaches which can be timely, expensive, inaccessible, and laborious, my multiplex assays present an alternative development approach for variant assays that can detect

new variants in an efficient and accessible manner. My multiplex assays target unique mutations or combinations of mutations that benefit the survival of variants. These mutations are naturally selected and may appear in newly emerging variants. Therefore, by utilizing combinations of naturally selected mutations, I can efficiently identify new variants circulating in the community early on. Secondly, I coupled these multiplex RT-qPCR assays with the WS EM-VIP-Mag protocol and successfully identified and quantified VOCs from wastewater samples collected from Edmonton and Calgary from 2021 to 2023. This innovative application of my method allowed me to successfully monitor the trends of these VOCs in wastewater and match these trends with the AHS clinical data. As expected with the innovative design of using naturally selected mutations in my assays, I was successfully able to detect some VOCs earlier in the community via wastewater than what had been clinically reported using NPS based individual diagnostic testing. Using combinations of these target mutations, my WS platform can be easily adapted for future applications in detecting newly emerging SARS-CoV-2 variants or for application with other viral pathogens. For example, future studies can develop wastewater-based target screening assays with panels of naturally selected mutations of clinically significant viruses which can be used to supplement sequencing approaches. By doing so, essential information regarding new strains or outbreaks of pathogens can be reported in advance allowing for public health officials to implement quarantine policies in a timely manner to prevent the spread of disease.

Lastly, to establish a universal platform for the detection of various co-occurring viruses, I developed a platform which can efficiently concentrate, extract, and preserve RNA of both enveloped (SARS-CoV-2) and non-enveloped (NoV) viral pathogens in wastewater. My approach has several novelties because I developed a new WS platform which allowed for

simultaneous quantification and differentiation of both NoV GI and GII and Omicron subvariants. Firstly, compared to the previously published protocols which faced challenges associated with poor recoveries and RT-qPCR inhibition, my WS platform has high recovery and sensitive detection of different viral pathogens in wastewater. Secondly, as both NoV and SARS-CoV-2 clinical testing is limited, my WS results provide necessary information about disease prevalence in the community. I successfully demonstrated that the occurrence of NoV GI and GII, as well as Omicron BA.4/5 and XBB, detected in wastewater matched the trends of clinical cases in two major Canadian cities from 2022-2023. Additionally, to my knowledge, my study was the first to report observations showing an inverse occurrence trend between NoV and Omicron in wastewater over the course of the sampling period. Using similar strategies, the WS EM-VIP-Mag-multiplex protocol can be adapted for applications in detecting various structurally different viral pathogens simultaneously. For example, future studies can develop panels for structurally different viruses that can contribute to the expansion of future wastewater surveillance of clinically significant pathogens. The simultaneous monitoring of these pathogens allows for the opportunity to assess the true impact and presence of these viruses co-circulating in the community.

My research findings, as demonstrated in the previous chapters, have made important contributions to fundamentals and applications in bioanalytical techniques for the detection of viruses in clinical and wastewater samples. Firstly, the formulation for the VIP and Mag buffers is unique and effective. For the VIP buffer, I used reagents (Triton X-100 and buffer RLT which contains guanidinium isothiocyanate) which provide enhanced inactivation of SARS-CoV-2 and extraction of RNA. To prevent degradation of RNA by RNases and preserve the extracted RNA, I added 2-ME and proteinase K to denature proteins and any inhibitory material in the sample.

The Mag beads buffer is then directly added, and the extracted RNA is captured onto the magnetic beads and washed to further remove any inhibitory material. The magnetic beads are resuspended in proteinase K inhibitor, glycogen to improve recovery of RNA, as well as water, and then directly input into the RT-qPCR reaction without the need for an elution step. My protocol reduces the number of reagents used and simplifies technical protocols. The VIP-Mag method also has broad sample applicability, as seen in the use for both clinical (oral fluids) and environmental (wastewater) samples. These comprehensive features of my VIP-MAG method help to relieve cost, time, and resource burdens in healthcare and diagnostic laboratory settings. Clinical laboratories, research laboratories, or industry laboratories can all benefit from these features. Secondly, during the COVID-19 pandemic, the application of WS for SARS-CoV-2 significantly expanded.⁴ However, because of the poor recoveries and lack of standardization of methods, there was an urgent need for improved protocols.⁵ My WS protocol (EM-VIP-Mag RT-qPCR) is the first of its kind which has high recovery and reproducibility, as well as adaptability, for both enveloped and non-enveloped viruses. Thirdly, I was able to demonstrate that my WS protocol along with multiplex RT-qPCR assays can monitor for naturally selected mutations on a community level. These multiplex assays have also been useful for several virology studies. Through collaboration, I demonstrated that the SARS-CoV-2 VOCs may exhibit preferences for distinct mice tissues. These findings are useful for the advancement of SARS-CoV-2 immune response and therapy development studies. Finally, I demonstrated the adaptability of the techniques I have developed for other co-circulating viruses, such as NoV. Several studies have already discussed the impact of viral interference and competition in viral evolution.^{6,7} Viral infections can trigger an interferon response in the host which can provide a nonspecific immunity and impact the presence of other viruses.^{7,8} Therefore, understanding the trends of co-

circulating viruses will deepen the insight into the mechanistic relationships underlying viral infections in the community.

Overall, I have successfully addressed my hypothesis and developed an integrated method of viral inactivation, RNA release and preservation, and subsequent direct detection in a simplified protocol which can provide sensitive detection of different viral pathogens in clinical and wastewater samples. However, there are certain challenges I faced in my research. A limitation of my multiplex assays is that three multiplex assays are required to identify nine SARS-CoV-2 VOCs. This is because the standard RT-qPCR instrument has four spectral channels, with a reference channel and a maximum of three other channels for the multiplex targets in a single run. However, with the evolving nature of SARS-CoV-2, only the Omicron triplex assay is needed in the future as combinations of the naturally selected target mutations in this assay can be used to identify future variants. Other challenges related to my techniques were also shared by other emerging technologies, particularly in the field of wastewater analysis. These challenges encompassed delayed sampling, delivery, and analysis, as well as complexities arising from a complex matrix, the presence of RT-qPCR inhibitors, and the absence of standardized procedures, normalization, and robust quality controls.^{9,10} I overcame several of these challenges using EM-VIP-Mag-RT-qPCR as discussed previously, but completely eliminating these challenges is difficult. Regardless of these challenges, there have been exciting new advancements and applications in the field of wastewater analysis. For example, several studies have begun to monitor wastewater for simultaneous and broader surveillance of several viruses (respiratory, enteroviruses, sexually transmitted viruses, hepatitis), as well as for possible explanations for co-circulating viral trends.¹¹⁻¹⁴ Other studies have also begun to use wastewater as a method of community surveillance of antimicrobials and drug resistant markers.^{15,16,17} In

response to the need for reliable sources and sharing of wastewater data for accurate surveillance, studies have also begun to develop robust and meaningful open datasets for environmental public health surveillance of SARS-CoV-2.^{18,19} In summary, my research strategies and discoveries, along with these novel approaches, offer possibilities for robust and reliable platforms which can enhance the ability to monitor community infections, including SARS-CoV-2, and beyond.

References

1. Michael-Kordatou, I.; Karaolia, P.; Fatta-Kassinos, D. Sewage analysis as a tool for the COVID-19 pandemic response and management: the urgent need for optimized protocols for SARS-CoV-2 detection and quantification. *J. Environ. Chem. Eng.* **2020**, *8* (5), 104306.
2. Silverman, J. D.; Hupert, N.; Washburne, A. D. Using influenza surveillance networks to estimate state-specific prevalence of SARS-CoV-2 in the United States. *Sci. Transl. Med.* **2020**, *12*, eabc1126.
3. Levy, J.I.; Andersen, K.G.; Knight, R.; Karthikeyan, S. Wastewater surveillance for public health. *Science* **2023**, *379* (6627), 26-27.
4. Hrudehy, S. E.; Bischel, H. N.; Charrois, J.; Chik, A.H.S.; Conant, B.; Delatolla, R. Wastewater surveillance for SARS-CoV-2 RNA in Canada. *Facets* **2022**, *7*, 1493–1597.
5. Chik, A. H.; Glier, M. B.; Servos, M.; Mangat, C. S.; Pang, X. L.; Qiu, Y.; et al. Comparison of approaches to quantify SARS-CoV-2 in wastewater using RT-qPCR: Results and implications from a collaborative inter-laboratory study in Canada. *J. Environ. Sci.* **2021**, *107*, 218– 229.
6. Chin, T.; Foxman, E.F.; Watkins, T.A.; Lipsitch, M. What can be learned from viral co-detection studies in human populations. *MedRxiv* **2023**, Available from: <https://doi.org/10.1101/2023.06.17.23291541> (accessed 2023-08-14).
7. Piret, J. and Boivin, G. Viral interference between respiratory viruses. *Emerg. Infect. Dis.* **2022**, *28*, 273-281.

8. Stanifer, M.L.; Guo, C.; Doldan, P.; Boulant, S. Importance of type I and III interferons at respiratory and intestinal barrier surfaces. *Front. Immunol.* **2020**, *11*, 608645.
9. Ahmed, W.; Simpson, S.L.; Bertsch, P.M.; Bibby, K.; Bivins, A.; Blackall, L.L.; et al. Minimizing errors in RT-PCR detection and quantification of SARS-CoV-2 RNA for wastewater surveillance. *Sci. Total Environ.* **2022**, *805*, 149877.
10. Kallem, P.; Hegab, H.M.; Alsafar, H.; Hasan, S.W.; Banat, F. SARS-CoV-2 detection and inactivation in water and wastewater: review on analytical methods, limitations and future research recommendations. *Emerg. Microbes & Infect.* **2023**, *12* (2), 2222850.
11. Ahmed, W.; Bivins, A.; Stephens, M.; Metcalfe, S.; Smith, W.J.; Sirikanchana, K.; et al. Occurrence of multiple respiratory viruses in wastewater in Queensland, Australia: Potential for community disease surveillance. *Sci. Total Environ.* **2023**, *864*, 161023.
12. Boehm, A.B.; Hughes, B.; Duong, D.; Chan-Herur, V.; Buchman, A.; Wolfe, M.K.; White, B.J. Wastewater concentrations of human influenza, metapneumovirus, parainfluenza, respiratory syncytial virus, rhinovirus, and seasonal coronavirus nucleic-acids during the COVID-19 pandemic: a surveillance study. *Lancet Microbe* **2023**, *4* (5), e340-8.
13. Gentry, Z.; Zhao, L.; Faust, R.A.; David, R.E.; Norton, J.; Xagorarakis, I. Wastewater surveillance beyond COVID-19: a ranking system for communicable disease testing in the tri-county Detroit area, Michigan, USA. *Public Health Front.* **2023**, *11*, 1178515.
14. Stockdale, S.R.; Blanchard, A.A.; Nayak, A.; Husain, A.; Nashine, R.; Dudani, H.; et al. RNA-Seq of untreated wastewater to assess COVID-19 and emerging and endemic viruses for public health surveillance. *Lancet Reg. Health Southeast Asia.* **2023**, *14*, 100205.

15. Baba, H.; Kuroda, M.; Sekizuka, T.; Kanamori, H. Highly sensitive detection of antimicrobial resistance genes in hospital wastewater using the multiplex hybrid capture target enrichment. *Msphere* **2023**, 8 (4), e00100-23.
16. Li, J.; Shimko, K.M.; He, C.; Patterson, B.; Bade, R.; Shiels, R.; Mueller, J.F.; et al. Direct injection liquid chromatography-tandem mass spectrometry as a sensitive and high-throughput method for the quantitative surveillance of antimicrobials in wastewater. *Sci. Total Environ.* **2023**, 900, 165825.
17. Sambaza, S.S.; Naicker N. Contribution of wastewater to Antimicrobial Resistance-A Review article. *J. Glob. Antimicrob. Resist.* **2023**, 34, 23-29.
18. National Academies of Sciences, Engineering, and Medicine. *Applying Lessons Learned from COVID-19 Research and Development to Future Epidemics: Proceedings of a Workshop.* **2023**, Available from: <https://doi.org/10.17226/27194> (accessed 2024-01-08).
19. Therrien, J.D.; Thomson, M.; Sion, E.S.; Lee, I.; Maere, T.; Nicolai, N.; et al. A comprehensive, open-source data model for wastewater-based epidemiology. *Water Sci. Technol.* **2024**, 89 (1), 1-9.

Bibliography

Adams G. A beginner's guide to RT-PCR, qPCR and RT-qPCR. *Biochem.* **2020**, 42 (3), 48-53.

Ahmed, W.; Bertsch, P.M.; Bibby, K.; Haramoto, E.; Hewitt, J.; Huygens, F.; et al. Decay of SARS-CoV-2 and surrogate murine hepatitis virus RNA in untreated wastewater to inform application in wastewater-based epidemiology. *Environ. Res. J.* **2020a**, 191, 110092.

Ahmed, W.; Bertsch, P.M.; Bivins, A.; Bibby, K.; Farkas, K.; Gathercole, A. Comparison of virus concentration methods for the RT-qPCR-based recovery of murine hepatitis virus, a surrogate for SARS-CoV-2 from untreated wastewater. *Sci. Total Environ.* **2020b**, 739, 139960.

Ahmed, W.; Bivins, A.; Bertsch, P.M.; Bibby, K.; Choi, P.M.; Farkas, K.; et al. Surveillance of SARS-CoV-2 RNA in wastewater: Methods optimization and quality control are crucial for generating reliable public health information. *Curr. Opin. Environ. Sci. Health.* **2020c**, 17, 82–93.

Ahmed, W.; Simpson, S.L.; Bertsch, P.M.; Bibby, K.; Bivins, A.; Blackall, L.L.; et al. Minimizing errors in RT-PCR detection and quantification of SARS-CoV-2 RNA for wastewater surveillance. *Sci. Total Environ.* **2022**, 805, 149877.

Ahmed, W.; Bivins, A.; Stephens, M.; Metcalfe, S.; Smith, W.J.; Sirikanachana, K.; et al. Occurrence of multiple respiratory viruses in wastewater in Queensland, Australia: Potential for community disease surveillance. *Sci. Total Environ.* **2023**, 864, 161023.

Aita, A.; Basso, D.; Cattelan, A.M.; Fioretto, P.; Navaglia, F.; Barbaro, F.; et al. SARS-CoV-2 identification and IgA antibodies in saliva: One sample two tests approach for diagnosis. *Clinica Chimica Acta.* **2020**, 510, 717-722.

Albastaki, A.; Naji, M.; Lootah, R.; Almeheiri, R.; Almulla, H.; Almarri, I.; et al. First confirmed detection of SARS-COV-2 in untreated municipal and aircraft wastewater in Dubai, UAE: the use of wastewater based epidemiology as an early warning tool to monitor the prevalence of COVID-19. *Sci. Total Environ.* **2021**, 760, 143350.

Alberta Health Services. *Covid-19 Alberta Statistics. Variants of Concern*, **2022**. Available from: <https://www.alberta.ca/stats/covid-19-alberta-statistics.htm#variants-of-concern> (accessed 2022-08-10).

Alberta Health Services (AHS). *COVID-19 info for Albertans*, **2022**. Available from: <https://www.alberta.ca/coronavirus-info-for-albertans> (accessed 2023-08-14).

Alberta Health Services (AHS). *COVID-19 Alberta statistics-Interactive aggregate data on COVID-19 cases in Alberta*, **2023**. Available from: <https://www.alberta.ca/stats/covid-19-alberta-statistics.htm#variants-of-concern> (accessed 2023-08-14).

Ali, N.; Rampazzo, R.D.; Costa, A.D.; Krieger, M.A. Current nucleic acid extraction methods and their implications to point-of-care diagnostics. *Biomed Res. Int.* **2017**, 2017.

Altawalah, H.; AlHuraish, F.; Alkandari, W.A.; Ezzikouri, S. Saliva specimens for detection of severe acute respiratory syndrome coronavirus 2 in Kuwait: A cross-sectional study. *J. Clin. Virol.* **2020**, 132, 104652.

Ammerman, M.L.; Mullapudi, S.; Gilbert, J.; Figueroa, K.; Cruz, F.P.; Bakker, K.M.; et al. 2023. Norovirus GII wastewater monitoring for epidemiological surveillance. *PLOS Water* **2024**, 3 (1), e0000198.

Ampuero, M.; Valenzuela, S.; Valiente-Echeverría, F.; Soto-Rifo, R.; Barriga, G.P.; Chnaiderman, J.; et al. SARS-CoV-2 detection in sewage in Santiago. Chile - preliminary results.

MedRxiv. **2020**. Available from: <https://doi.org/10.1101/2020.07.02.20145177> (accessed 2022-08-10).

Anand, U.; Pal, T.; Zanoletti, A.; Sundaramurthy, S.; Varjani, S.; Rajapaksha, A.U.; et al. The spread of the omicron variant: Identification of knowledge gaps, virus diffusion modelling, and future research needs. *Environ. Res.* **2023**, *225*, 115612.

Andreasen, D.; Fog, J.U.; Biggs, W.; Salomon, J.; Dahslveen, I.K.; Baker, A.; Mouritzen, P. Improved microRNA quantification in total RNA from clinical samples. *Methods* **2010**, *50*, S6– S9.

Andrews, B.A.; Asenjo, J.A. Enzymatic lysis and disruption of microbial cells. *Trends Biotechnol.* **1987**, *5* (10), 273-277.

Arora, P.; Pöhlmann, S.; Hoffmann, M. Mutation D614D increases SARS-CoV-2 transmission. *Signal Transduct. Target. Ther.* **2021**, *6* (1), 1-2.

Arora, S.; Nag, A.; Rajpal, A.; Tiwari, S.B.; Sethi, J.; Sutaria, D.; et al. Detection of SARS-CoV-2 RNA in fourteen wastewater treatment systems in Uttarakhand and Rajasthan States of North India. *Water* **2021**, *13* (16), 2265.

Atieh, M.A.; Guirguis, M.; Alsabeeha, N.H. Cannon RD. The diagnostic accuracy of saliva testing for SARS-CoV-2: a systematic review and meta-analysis. *Oral Dis.* **2022**, *28*, 2347-2361.

Azzi, L.; Maurino, V.; Baj, A.; Dani, M.; d’Aiuto, A.; Fasano, M.; et al. Diagnostic salivary tests for SARS-CoV-2. *J. Dent. Res.* **2021**, *100* (2), 115-123.

Baba, H.; Kuroda, M.; Sekizuka, T.; Kanamori, H. Highly sensitive detection of antimicrobial resistance genes in hospital wastewater using the multiplex hybrid capture target enrichment. *Msphere* **2023**, *8* (4), e00100-23.

Balboa, S.; Mauricio-Iglesias, M.; Rodríguez, S.; Martínez Lamas, L.; Vasallo, F.J.; Regueiro, B.; et al. The fate of SARS-CoV-2 in wastewater treatment plants points out the sludge line as a suitable spot for incidence monitoring. *Sci. Total Environ.* **2021**, 772, 145268.

Bányai, K.; Estes, M.K.; Martella, V.; Parashar, U.D. Viral gastroenteritis. *Lancet* **2018**, 392, 175-186.

Barat, B.; Das, S.; De Giorgi, V.; Henderson, D.K.; Kopka, S.; Lau, A.F.; et al. Pooled saliva specimens for SARS-CoV-2 testing. *J. Clin. Microbiol.* **2021**, 59 (3), e02486-20.

Bar-Or, I.; Yaniv, K.; Shagan, M.; Ozer, E.; Erster, O.; Mendelson, E.; et al. Regressing SARS-CoV-2 sewage measurements onto COVID-19 burden in the population: a proof-of-concept for quantitative environmental surveillance. *Public Health Front.* **2022**, 9, 561710.

Barril, P. A.; Pianciola, L. A.; Mazzeo, M.; Ousset, M. J.; Jaureguiberry, M. V.; Alessandrello, M.; et al. Evaluation of viral concentration methods for SARS-CoV-2 recovery from wastewaters. *Sci. Total Environ.* **2021**, 756, 144105.

Barton, M.I.; MacGowan, S.A.; Kutuzov, M.A.; Dushek, O.; Barton, G.J.; van der Merwe, P.A. Effects of common mutations in the SARS-CoV-2 Spike RBD and its ligand, the human ACE2 receptor on binding affinity and kinetics. *Elife* **2021**, 10, e70658.

Bastos, M.L.; Perlman-Arrow, S.; Menzies, D.; Campbell, J.R. The sensitivity and costs of testing for SARS-CoV-2 infection with saliva versus nasopharyngeal swabs: a systematic review and meta-analysis. *Ann. Intern. Med.* **2021**, 174 (4), 501-510.

Betancourt, W.Q.; Schmitz, B. W.; Innes, G.K.; Prasek, S. M.; Brown, K.M.; Stark, E. R.; et al. COVID-19 containment on a college campus via wastewater-based epidemiology, targeted clinical testing and an intervention. *Sci. Total Environ.* **2021**, 779, 146408.

Bessetti, J. An introduction to PCR inhibitors. *J. Microbiol. Methods* **2007**, 28, 159– 167.

Bivins, A.; North, D.; Ahmad, A.; Ahmed, W.; Alm, E.; Been, F.; et al. Wastewater-based epidemiology: global collaborative to maximize contributions in the fight against COVID-19.

Environ. Sci. Technol. **2020**, 54 (13), 7754–7757.

Bloomfield, V. A. DNA condensation by multivalent cations. *Biopolymers* **1997**, 44, 269–282.

Blow, J.A.; Dohm, D.J.; Negley, D.L.; Mores, C.N. Virus inactivation by nucleic acid extraction reagents. *J. Virol. Methods.* **2004**, 119 (2), 195-198.

Boehm, A.B.; Wolfe, M.K.; White, B.J.; Hughes, B.; Duong, D.; Banaei, N.; Bidwell, A. Human norovirus (HuNoV) GII RNA in wastewater solids at 145 United States wastewater treatment plants: comparison to positivity rates of clinical specimens and modeled estimates of HuNoV GII shedders. *J. Expo. Sci. Environ. Epidemiol.* **2023a**, 1-8.

Boehm, A.B.; Hughes, B.; Duong, D.; Chan-Herur, V.; Buchman, A.; Wolfe, M.K.; White, B.J. Wastewater concentrations of human influenza, metapneumovirus, parainfluenza, respiratory syncytial virus, rhinovirus, and seasonal coronavirus nucleic-acids during the COVID-19 pandemic: a surveillance study. *The Lancet Microbe* **2023b**, 4, 340-348.

Bokelmann, L.; Nickel, O.; Maricic, T.; Pääbo, S.; Meyer, M.; Borte, S.; Riesenberger, S. Point-of-care bulk testing for SARS-CoV-2 by combining hybridization capture with improved colorimetric LAMP. *Nat. Commun.* **2021**, 12 (1), 1-8.

Brown, K.A.; Gubbay, J.; Hopkins, J.; Patel, S.; Buchan, S.A.; Daneman, N.; Goneau, L.W. S-gene target failure as a marker of variant B.1.1.7 among SARS-CoV-2 isolates in the greater Toronto area, December 2020 to March 2021. *J. Am. Med. Assoc.* **2021**, 325 (20), 2115-2116.

Buonerba, A.; Corpuz, M.V.; Ballesteros, F.; Choo, K.H.; Hasan, S.W.; Korshin, G.V.; et al. Coronavirus in water media: Analysis, fate, disinfection and epidemiological applications. *J. Hazard. Mater.* **2021**, 415, 125580.

Bustin, S. Absolute quantification of mRNA using real-time reverse transcription polymerase chain reaction assays. *J. Mol. Endocrinol.* **2000**, 25, 169–193.

Bustin, S.; Dhillon, H.S.; Kirvell, S.; Greenwood, C.; Parker, M.; Shipley, G.L.; Nolan, T. Variability of the Reverse Transcription Step: Practical Implications. *Clin. Chem.* **2015**, 61, 202–212.

Bustin, S.A.; Nolan, T. RT-qPCR testing of SARS-CoV-2: a primer. *Int. J. Mol. Sci.* **2020**, 21 (8), 3004.

Butler-Laporte, G.; Lawandi, A.; Schiller, I.; Yao, M.; Dendukuri, N.; McDonald, E.G.; Lee, T.C. Comparison of saliva and nasopharyngeal swab nucleic acid amplification testing for detection of SARS-CoV-2: a systematic review and meta-analysis. *JAMA Intern. Med.* **2021**, 181 (3), 353-360.

Butler, K.S.; Carson, B.D.; Podlevsky, J.D.; Mayes, C.M.; Rowland, J.M.; Campbell, D.; et al. Singleplex, multiplex and pooled sample real-time RT-PCR assays for detection of SARS-CoV-2 in an occupational medicine setting. *Sci. Rep.* **2022**, 12 (1), 17733.

Califf, R.M. Biomarker definitions and their applications. *Exp. Biol. Med.* **2018**, 243 (3), 213-221.

Canadian Food Safety Institute. *Canadian health authorities worried about 2023 Norovirus outbreaks*, **2023**. Available from: <https://news.foodsafety.ca/canadian-health-authorities-worried-about-2023-norovirus-outbreaks> (accessed 2023-08-14).

Canadian Water Network. *COVID-19 wastewater coalition*, **2022**. Available from: <https://cwn-rce.ca/covid-19-wastewater-coalition/> (accessed 2022-8-10).

Carrillo-Reyes, J.; Barragán-Trinidad, M.; Buitrón, G. Surveillance of SARS-CoV-2 in sewage and wastewater treatment plants in Mexico. *J. Water Process. Eng.* **2021**, 40, 101815.

Centers for Disease Control and Prevention. *Interim Guidelines for Collecting and Handling of Clinical Specimens for COVID-19 Testing*, **2022**, Available from: <https://www.cdc.gov/coronavirus/2019-ncov/lab/guidelines-clinical-specimens.html#:~:text=Store%20respiratory%20specimens%20at%20,70%C2%B0C%20or%20below.> (accessed 2023-09-08).

Centers for Disease Control and Prevention. *National Wastewater Surveillance System*, **2020**. Available from: <https://www.cdc.gov/healthywater/surveillance/wastewater-surveillance/wastewater-surveillance.html> (accessed 2022-08-10).

Centers for Disease Control and Prevention (CDC). *Norovirus*, **2023**. Available from: <https://www.cdc.gov/norovirus/index.html> (accessed 2023-08-14)

Centers for Disease Control and Prevention. *Symptom-based strategy to discontinue isolation for persons with COVID-19*, **2020**. Available from <https://stacks.cdc.gov/view/cdc/88537> (accessed 2023-09-08).

Chan, J.F.; Yuan, S.; Kok, K.H.; To, K.K.; Chu, H.; Yang, J.; et al. A familial cluster of pneumonia associated with the 2019 novel coronavirus indicating person-to-person transmission: a study of a family cluster. *Lancet.* **2020a**, 395 (10223), 514-523.

Chan, J.F.W.; Yip, C.C.Y.; To, K.K.W.; Tang, T.H.C.; Wong, S.C.Y.; Leung, K.H.; et al. Improved molecular diagnosis of COVID-19 by the novel, highly sensitive and specific COVID-

19-RdRp/Hel real-time reverse transcription-polymerase chain reaction assay validated in vitro and with clinical specimens. *J. Clin. Microbiol.* **2020b**, 58 (5), 10-128.

Chatterjee, S.; Bhattacharya, M.; Nag, S.; Dhama, K.; Chakraborty, C. A Detailed Overview of SARS-CoV-2 Omicron: Its Subvariants, Mutations and Pathophysiology, Clinical Characteristics, Immunological Landscape, Immune Escape, and Therapies. *Viruses* **2023**, 15 (1), 167.

Chau, N.V.; Lam, V.T.; Dung, N.T.; Yen, L.M.; Minh, N.N.; Ngoc, N.M.; et al. The natural history and transmission potential of asymptomatic severe acute respiratory syndrome coronavirus 2 infection. *Clin. Infect. Dis.* **2020**, 71 (10), 2679.

Chavarria-Miró, G.; Anfruns-Estrada, E.; Guix, S.; Paraira, M.; Galofré, B.; Sáanchez, G.; et al. Sentinel surveillance of SARS-CoV-2 in wastewater anticipates the occurrence of COVID-19 cases. *MedRxiv.* **2020**. Available from: <https://doi.org/10.1101/2020.06.13.20129627> (accessed 2022-08-10).

Chen, J.; Wang, R.; Wang, M.; Wei, G.W. Mutations strengthened SARS-CoV-2 infectivity. *J. Mol. Biol.* **2020**, 432 (19), 5212-5226.

Chen, J.; Qiu, Y.; Wang, R.; Wei, G.W. Persistent Laplacian projected Omicron BA.4 and BA.5 to become new dominating variants. *Comput. Biol. Med.* **2022**, 151, 106262.

Cheng, C.; Jia, J.L.; Ran, S.Y. Polyethylene glycol and divalent salt-induced DNA reentrant condensation revealed by single molecule measurements. *Soft Matter* **2015**, 11 (19), 3927–3935.

Chhabra, P.; de Graaf, M.; Parra, G.I.; Chan, M.C.W.; Green, K.; Martella, V.; et al. Updated classification of norovirus genogroups and genotypes. *J. Gen. Virol.* **2019**, 100, 1393.

Chik, A.H.; Glier, M.B.; Servos, M.; Mangat, C.S.; Pang, X.L.; Qiu, Y.; D’Aoust, P.M.; et al. Comparison of approaches to quantify SARS-CoV-2 in wastewater using RT-qPCR: Results and implications from a collaborative inter-laboratory study in Canada. *J. Environ. Sci.* **2021**, *107*, 218–229.

Chin, A.W.H.; Poon, L.L.M. Stability of SARS-CoV-2 indifferent environmental conditions—Authors’ reply. *Lancet Microbe* **2020**, *1* (4), e146.

Chin, T.; Foxman, E.F.; Watkins, T.A.; Lipsitch, M. What can be learned from viral co-detection studies in human populations. *MedRxiv* **2023**, Available from: <https://doi.org/10.1101/2023.06.17.23291541> (accessed 2023-08-14).

Choi, P.M.; Tscharke, B.J.; Donner, E.; O’Brien, J.W.; Grant, S.C.; Kaserzon, S.L.; et al. Wastewater-based epidemiology biomarkers: past, present and future. *Trends Analyt. Chem.* **2018**, *105*, 453–469.

Chong, C.Y.; Kam, K.Q.; Li, J.; Maiwald, M.; Loo, L.H.; Nadua, K.D.; et al. Saliva is not a useful diagnostic specimen in children with coronavirus disease 2019 (COVID-19). *Clin. Infect. Dis.* **2021**, *73* (9), e3144-5.

Christensen, P.A.; Olsen, R.J.; Long, S.W.; Subedi, S.; Davis, J.J.; Hodjat, P.; et al. Delta variants of SARS-CoV-2 cause significantly increased vaccine breakthrough COVID-19 cases in Houston, Texas. *Am. J. Clin. Pathol.* **2021**, *192* (2), 320-331.

Cleary, B.; Hay, J.A.; Blumenstiel, B.; Harden, M.; Cipicchio, M.; Bezney, J.; et al. Using viral load and epidemic dynamics to optimize pooled testing in resource-constrained settings. *Sci. Transl. Med.* **2021**, *13*, eabf1568.

Corman, V.M.; Landt, O.; Kaiser, M.; Molenkamp, R.; Meijer, A.; Chu, D.K.; et al. Detection of 2019 novel coronavirus (2019-nCoV) by real-time RT-PCR. *Euro Surveill.* **2020**, *25*, 2000045.

Coronaviridae Study Group of the International Committee on Taxonomy of Viruses (CSG of ICTV). The species Severe acute respiratory syndrome-related coronavirus: classifying 2019-nCoV and naming it SARS-CoV-2. *Nat. Microbiol.* **2020**, *5*, 536–554.

Da Costa Fernandes, P.A.; da Conceicao Ferreira, F.A.; Morais, O.M.; Ramos, C.M.; Fernandes, É.M.; da Rocha, S.A.; et al. Performance of saliva as a specimen to detect SARS-CoV-2. *J. Clin. Virol.* **2021**, *142*, 104913.

D'Aoust, P.M.; Mercier, E.; Montpetit, D.; Jia, J.J.; Alexandrov, I.; Neault, N.; et al. Quantitative analysis of SARS-CoV-2 RNA from wastewater solids in communities with low COVID-19 incidence and prevalence. *Water Res.* **2021**, *188*, 116560.

D'Cruz, R.J.; Currier, A.W.; Sampson, V.B. Laboratory testing methods for novel severe acute respiratory syndrome-coronavirus-2 (SARS-CoV-2). *Front. Cell Dev. Biol.* **2020**, *8*, 468.

Deka, S.; Kalita, D. Effectiveness of sample pooling strategies for SARS-CoV-2 mass screening by RT-PCR: A scoping review. *J. Lab. Physicians* **2020**, *12*, 212–218.

De Paula Eduardo, F.; Bezinelli, L.M.; de Araujo, C.A.; Moraes, J.V.; Birbrair, A.; Pinho, J.R.; et al. Self-collected unstimulated saliva, oral swab, and nasopharyngeal swab specimens in the detection of SARS-CoV-2. *Clin. Oral Investig.* **2022**, *26* (2), 1561-1567.

Dheda, K.; Huggett, J.; Bustin, S.; Johnson, M.A.; Rook, G.; Zumla, A. Validation of housekeeping genes for normalizing RNA expression in real-time PCR. *Biotechniques* **2004**, *37*, 112–119.

Diamond, A.D.; Hsu, J.T. Protein partitioning in PEG/dextran aqueous two-phase systems. *AIChE J.* **1990**, *36* (7), 1017–1024.

Dinnes, J.; Sharma, P.; Berhane, S.; van Wyk, S.S.; Nyaaba, N.; Domen, J.; et al. Rapid, point-of-care antigen tests for diagnosis of SARS-CoV-2 infection. *Cochrane Database Syst. Rev.* **2022**, (7).

Dogan, O.A.; Kose, B.; Agaoglu, N.B.; Yildiz, J.; Alkurt, G.; Demirkol, Y.K.; et al. Does sampling saliva increase detection of SARS-CoV-2 by RT-PCR? Comparing saliva with oropharyngeal swabs. *J. Virol. Methods.* **2021**, *290*, 114049.

Dumke, R.; de la Cruz Barron, M.; Oertel, R.; Helm, B.; Kallies, R.; Berendonk, T. U.; et al. Evaluation of two methods to concentrate SARS-CoV-2 from untreated wastewater. *Pathogens* **2021**, *10*, 195.

Dumke, R.; Geissler, M.; Skupin, A.; Helm, B.; Mayer, R.; Schubert, S.; et al. Simultaneous detection of SARS-CoV-2 and Influenza virus in wastewater of two cities in southeastern Germany, January to May 2022. *Int. J. Environ. Res. Public Health* **2022**, *19*, 13374.

Eftim, S.E.; Hong, T.; Soller, J.; Boehm, A.; Warren, I.; Ichida, A; Nappier, S.P. Occurrence of norovirus in raw sewage—a systematic literature review and meta-analysis. *Water Res.* **2017**, *111*, 366-374.

Ellwanger, J.H.; Chies, J.A. Zoonotic spillover: Understanding basic aspects for better prevention. *Genet. Mol. Biol.* **2021**, *44*.

Elveborg, S.; Monteil, V.M.; Mirazimi, A. Methods of inactivation of highly pathogenic viruses for molecular, serology or vaccine development purposes. *Pathogens.* **2022**, *11* (2), 271.

Fakhruddin, K.S.; Haiat, A.; Ngo, H.C.; Panduwawala, C.; Chang, J.W.; Samaranyake, L.P. Severe acute respiratory syndrome coronavirus-2 (SARS-CoV-2) viral positivity and their burden in saliva of asymptomatic carriers—a systematic review and meta-analysis. *Acta Odontol. Scand.* **2022**, 80 (3), 182-190.

FDA-NIH Biomarker Working Group. *BEST (Biomarkers, EndpointS, and other Tools) Resource*, 2016. Available from www.ncbi.nlm.nih.gov/books/NBK326791/ (accessed 2023-09-08).

Fernández-González, M.; Agulló, V.; de la Rica, A.; Infante, A.; Carvajal, M.; García, J.A.; et al. Performance of saliva specimens for the molecular detection of SARS-CoV-2 in the community setting: does sample collection method matter? *J. Clin. Microbiol.* **2021**, 59 (4), 10-128.

Feng, W.; Newbigging, A.M.; Le, C.; Pang, B.; Peng, H.; Cao, Y.; et al. Molecular diagnosis of COVID-19: challenges and research needs. *Anal. Chem.* **2020**, 92 (15), 10196-10209.

Fomsgaard, A. S.; Rosenstjerne, M. W. An alternative workflow for molecular detection of SARS-CoV-2 – escape from the NA extraction kit-shortage, Copenhagen, Denmark, March 2020. *Euro. Surveill.* **2020**, 25 (14), 2000398.

Fongaro, G.; Stoco, P.H.; Souza, D.S.; Grisard, E.C.; Magri, M.E.; Rogovski, P.; et al. SARS-CoV-2 in human sewage in Santa Catarina, Brazil, November 2019. *Sci. Total Environ.* **2021**, 778, 146198.

Fontana, L.; Villamagna, A.H.; Sikka, M.K.; McGregor, J.C. Understanding viral shedding of SARS-CoV-2: review of current literature. *Infect. Control Hosp. Epidemiol.* **2021**, 42, 659– 668.

Freedman, S.B.; Xie, J.; Nettel-Aguirre, A.; Lee, B.; Chui, L.; Pang, X.L.; et al. Enteropathogen detection in children with diarrhoea, or vomiting, or both, comparing rectal flocced swabs with stool specimens: an outpatient cohort study. *Lancet Gastroenterol. Hepatol.* **2017**, *2*, 662-669.

Fuzzen, M.; Harper, N.B.; Dhiyebi, H.A.; Srikanthan, N.; Hayat, S.; Bragg, L.M.; et al. An improved method for determining frequency of multiple variants of SARS-CoV-2 in wastewater using qPCR assays. *Sci. Total Environ.* **2023**, *881*, 163292.

Gadkar, V.J.; Goldfarb, D.M.; Al-Rawahi, G.N.; Srigley, J.A.; Smailus, D.E.; Coope, R.J.; et al. Extraction-free clinical detection of SARS-CoV-2 virus from saline gargle samples using Hamilton STARlet liquid handler. *Sci. Rep.* **2023**, *13* (1), 4241.

Galani, A.; Aalizadeh, R.; Kostakis, M.; Markou, A.; Alygizakis, N.; Lytras, T.; et al. SARS-CoV-2 wastewater surveillance data can predict hospitalizations and ICU admissions. *Sci. Total Environ.* **2022**, *804*, 150151.

Gentry, Z.; Zhao, L.; Faust, R.A.; David, R.E.; Norton, J.; Xagorarakis, I. Wastewater surveillance beyond COVID-19: a ranking system for communicable disease testing in the tri-county Detroit area, Michigan, USA. *Front. Public Health* **2023**, *11*, 1178515.

Gerrity, D.; Papp, K.; Stoker, M.; Sims, A.; Frehner, W. Early-pandemic wastewater surveillance of SARS-CoV-2 in Southern Nevada: methodology, occurrence, and incidence/prevalence considerations. *Water Res. X.* **2021**, *10*, 100086.

Giacobbo, A.; Rodrigues, M.A.S.; Zoppas Ferreira, J.; Bernardes, A.M.; de Pinho, M.N.; et al. A critical review on SARS-CoV-2 infectivity in water and wastewater. What do we know? *Sci. Total Environ.* **2021**, *774*, 145721.

Gibas, C.; Lambirth, K.; Mittal, N.; Juel, M. A.; Barua, V. B.; Brazell, L. R.; et al. Implementing building-level SARS-CoV-2 wastewater surveillance on a university campus. *Sci. Total Environ.* **2021**, 782, 146749.

Glass, R.I.; Parashar, U.D.; Estes, M.K. Norovirus gastroenteritis. *N. Engl. J. Med.* **2009**, 361, 1776–1785.

Goldfarb, D.M.; Tilley, P.; Al-Rawahi, G.N.; Srigley, J.A.; Ford, G.; Pedersen, H.; et al. Self-collected saline gargle samples as an alternative to health care worker-collected nasopharyngeal swabs for COVID-19 diagnosis in outpatients. *J. Clin. Microbiol.* **2021**, 59, e02427.

Gonçalves, J.; Koritnik, T.; Mioč, V.; Trkov, M.; Bolješič, M.; Berginc, N.; et al. Detection of SARS-CoV-2 RNA in hospital wastewater from a low COVID-19 disease prevalence area. *Sci. Total Environ.* **2021**, 755, 143226.

Gonzalez, R.; Curtis, K.; Bivins, A.; Bibby, K.; Weir, M. H.; Yetka, K.; et al. COVID-19 surveillance in southeastern Virginia using wastewater-based epidemiology. *Water Res.* **2020**, 186, 116296.

Gorkhali, R.; Koirala, P.; Rijal, S.; Mainali, A.; Baral, A.; Bhattarai, H.K. Structure and function of major SARS-CoV-2 and SARS-CoV proteins. *Bioinform. Biol. Insights.* **2021**, 15, 11779322211025876.

Graham, K.E.; Loeb, S.K.; Wolfe, M.K.; Catoe, D.; Sinnott-Armstrong, N.; Kim, S.; et al. SARS-CoV-2 RNA in wastewater settled solids is associated with COVID-19 cases in a large urban Sewershed. *Environ. Sci. Technol.* **2021**, 55, 488–498.

Green, H.; Wilder, M.; Middleton, F.A.; Collins, M.; Fenty, A.; Gentile, K.; et al. Quantification of SARS-CoV-2 and cross-assembly phage (crAssphage) from wastewater to

monitor coronavirus transmission within communities. *MedRxiv* **2020**. Available from: <https://doi.org/10.1101/2020.05.21.20109181> (accessed 2022-08-10).

Griesemer, S.B.; Van Slyke, G.; Ehrbar, D.; Strle, K.; Yildirim, T.; Centurioni, D.A.; et al. Evaluation of specimen types and saliva stabilization solutions for SARS-CoV-2 testing. *J. Clin. Microbiol.* **2021**, *59*, e01418.

Grobe, N.; Cherif, A.; Wang, X.; Dong, Z.; Kotanko, P. Sample pooling: burden or solution? *Clin. Microbiol. Infect.* **2021**, *27*, 1212– 1220.

Gu, H.; Chen, Q.; Yang, G.; He, L.; Fan, H.; Deng, Y.Q.; et al. Adaptation of SARS-CoV-2 in BALB/c mice for testing vaccine efficacy. *Science* **2020**, *369* (6511), 1603-1607.

Gupta, S.; Parker, J.; Smits, S.; Underwood, J.; Dolwani, S. Persistent viral shedding of SARS-CoV-2 in faeces – a rapid review. *Colorectal Dis.* **2020**, *22*, 611–620.

Hall, E.W.; Luisi, N.; Zlotorzynska, M.; Wilde, G.; Sullivan, P.; Sanchez, T.; Bradley, H.; Siegler, A. J. Willingness to use home collection methods to provide specimens for SARS-CoV-2/COVID-19 research: survey study. *J. Med. Internet Res.* **2020**, *22*, e19471.

Hamming, I.; Timens, W.; Bulthuis, M.L.; Lely, A.T.; Navis, G.V.; van Goor, H. Tissue distribution of ACE2 protein, the functional receptor for SARS coronavirus. A first step in understanding SARS pathogenesis. *J. Pathol.* **2004**, *203* (2), 631-637.

Haramoto, E.; Malla, B.; Thakali, O.; Kitajima, M. First environmental surveillance for the presence of SARS-CoV-2 RNA in wastewater and river water in Japan. *Sci. Total Environ.* **2020**, *737*, 140405.

Harrison, A.G.; Lin, T.; Wang, P. Mechanisms of SARS-CoV-2 transmission and pathogenesis. *Trends Immunol.* **2020**, *41* (12), 1100-1115.

Hasan, S.W.; Ibrahim, Y.; Daou, M.; Kannout, H.; Jan, N.; Lopes, A.; et al. Detection and quantification of SARS-CoV-2 RNA in wastewater and treated effluents: Surveillance of COVID-19 epidemic in the United Arab Emirates. *Sci. Total Environ.* **2021**, 764, 142929.

Hasing, M.; Yu, J.; Qiu, Y.; Maal-Bared, R.; Bhavanam, S.; Lee, B.; et al. Comparison of detecting and quantitating SARS-CoV-2 in wastewater using moderate-speed centrifuged solids versus an ultrafiltration method. *Water* **2021**, 13, 2166.

Hasing, M.E.; Lee, B.E.; Gao, T.; Li, Q.; Qiu, Y.; Ellehoj, E.; et al. Wastewater surveillance monitoring of SARS-CoV-2 variants of concern and dynamics of transmission and community burden of COVID-19. *Emerg. Microbes & Infect.* **2023**, 12 (2), 2233638.

Hata, A.; Hara-Yamamura, H.; Meuchi, Y.; Imai, S.; Honda, R. Detection of SARS-CoV-2 in wastewater in Japan during a COVID-19 outbreak. *Sci. Total Environ.* **2021**, 758, 143578.

Hellmér, M.; Paxéus, N.; Magnus, L.; Enache, L.; Arnholm, B.; Johansson, A.; et al. Detection of pathogenic viruses in sewage provided early warnings of Hepatitis A virus and Norovirus outbreaks. *Appl. Environ. Microbiol.* **2014**, 80, 6771–6781.

Henegariu, O.; Heerema, N.A.; Dlouhy, S.R.; Vance, G.H.; Vogt, P.H. Multiplex PCR: Critical parameters and step-by-step protocol. *Biotechniques* **1997**, 23 (3), 504–511.

Herrera, L.A.; Hidalgo-Miranda, A.; Reynoso-Noverón, N.; Meneses-García, A.A.; Mendoza-Vargas, A.; Reyes-Grajeda, J.; et al. Saliva is a reliable and accessible source for the detection of SARS-CoV-2. *Int J. Infect. Dis.* **2021**, 105, 83-90.

Hoehne, M.; Schreier, E. Detection of Norovirus genogroup I and II by multiplex real-time RT-PCR using a 3'-minor groove binder-DNA probe. *BMC Infect. Dis.* **2006**, 6, 69.

Hoffmann, M.; Kleine-Weber, H.; Schroeder, S.; Krüger, N.; Herrler, T.; Erichsen, S.; et al. SARS-CoV-2 cell entry depends on ACE2 and TMPRSS2 and is blocked by a clinically proven protease inhibitor. *Cell* **2020**, 181 (2), 271-280.

Hokajärvi, A.M.; Rytönen, A.; Tiwari, A.; Kauppinen, A.; Oikarinen, S.; Lehto, K.M.; et al. The detection and stability of the SARS-CoV-2 RNA biomarkers in wastewater influent in Helsinki, Finland. *Sci. Total Environ.* **2021**, 770, 145274.

Holland, R. L. What Makes a Good Biomarker? *Adv. Precis. Med.* **2016**, 1, 66.

Hoofnagle, A.N.; Wener, M.H. The fundamental flaws of immunoassays and potential solutions using tandem mass spectrometry. *J. Immunol. Methods.* **2009**, 347, 3-11.

Hovi, T.; Shulman, L.M.; Van Der Avoort, H.; Deshpande, J.; Roivainen, M.; De Gourville, E.M. Role of environmental poliovirus surveillance in global polio eradication and beyond. *Epidemiol. Infect.* **2012**, 140, 1–13.

Hrudey, S.E.; Bischel, H.N.; Charrois, J.; Chik, A.H.S.; Conant, B.; Delatolla, R.; et al. Wastewater surveillance for SARS-CoV-2 RNA in Canada. *Facets* **2022**, 7, 1493-1597.

Huang, C.; Wang, Y.; Li, X.; Ren, L.; Zhao, J.; Hu, Y.; et al. Clinical features of patients infected with 2019 novel coronavirus in Wuhan, China. *Lancet* **2020**, 395 (10223), 497-506.

Huang, N.; Pérez, P.; Kato, T.; Mikami, Y.; Okuda, K.; Gilmore, R.C.; et al. SARS-CoV-2 infection of the oral cavity and saliva. *Nat. Med.* **2021**, 27 (5), 892-903.

Huang, Y.; Zhou, N.; Zhang, S.; Yi, Y.; Han, Y.; Liu, M.; et al. Norovirus detection in wastewater and its correlation with human gastroenteritis: a systematic review and meta-analysis. *Environ. Sci. Pollut. Res.* **2022**, 29, 22829–22842.

Hubert, C.R.J.; Acosta, N.; Waddell, B.J.; Hasing, M.E.; Qiu, Y.; Fuzzen, M.; et al. Tracking Emergence and Spread of SARS-CoV-2 Omicron Variant in Large and Small

Communities by Wastewater Monitoring in Alberta, Canada. *Emerg. Infect. Dis.* **2022**, 28 (9), 1770–1776.

Hughes, B.; Duong, D.; White, B.J.; Wigginton, K.R.; Chan, E.M.; Wolfe, M.K.; Boehm, A.B. Respiratory syncytial virus (RSV) RNA in wastewater settled solids reflects RSV clinical positivity rates. *Environ. Technol. Lett.* **2022**, 9, 173-178.

International Committee on Taxonomy of Viruses Executive Committee. The new scope of virus taxonomy: partitioning the virosphere into 15 hierarchical ranks. *Nat. Microbiol.* **2020**, 5, 668–674.

International Water Association. *COVID-19 wastewater-based epidemiology*. **2022**, Available from: <https://iwa-network.org/learn/covid-19-wastewater-based-epidemiology/> (accessed 2022-08-10).

Jahne, M.A.; Brinkman, N.E.; Keely, S.P.; Zimmerman, B.D.; Wheaton, E.A.; Garland, J.L. Droplet digital PCR quantification of norovirus and adenovirus in decentralized wastewater and graywater collections: Implications for onsite reuse. *Water Res.* **2020**, 169, 115213.

Jahun, A.S. and Goodfellow, I.G. Interferon responses to norovirus infections: current and future perspectives. *J. Gen. Virol.* **2021**, 102 (10), 001660.

Jamal, A.J.; Mozafarihashjin, M.; Coomes, E.; Powis, J.; Li, A.X.; Paterson, A.; et al. Sensitivity of nasopharyngeal swabs and saliva for the detection of severe acute respiratory syndrome coronavirus 2. *Clin. Infect. Dis.* **2021**, 72 (6), 1064-1066.

Johnson, G.; Nolan, T.; Bustin, S.A. Real-time quantitative PCR, pathogen detection and MIQE, in: Totowa, N.J. (Eds), *PCR Detection of Microbial Pathogens*. Humana Press **2013**, 1-16.

Joung, J.; Ladha, A.; Saito, M.; Kim, N.G.; Woolley, A.E.; Segel, M.; et al. Detection of SARS-CoV-2 with SHERLOCK one-pot testing. *N. Engl. J. Med.* **2020**, 383, 1492–1494.

Joyce, G. F. Nucleic acid enzymes: playing with a fuller deck. *Proc. Natl. Acad. Sci. U.S.A.* **1998**, 95, 5845–5847.

Kageyama, T.; Kojima, S.; Shinohara, M.; Uchida, K.; Fukushi, S.; Hoshino, F.B.; et al. 2003. Broadly reactive and highly sensitive assay for Norwalk-like viruses based on real-time quantitative reverse transcription-PCR. *J. Clin. Microbiol.* **2003**, 41 (4), 1548-1557.

Kallem, P.; Hegab, H.M.; Alsafar, H.; Hasan, S.W.; Banat, F. SARS-CoV-2 detection and inactivation in water and wastewater: review on analytical methods, limitations and future research recommendations. *Emerg. Microbes & Infect.* **2023**, 12 (2), 2222850.

Kandel, C.E.; Young, M.; Serbanescu, M.A.; Powis, J.E.; Bulir, D.; Callahan, J.; et al. Detection of severe acute respiratory coronavirus virus 2 (SARS-CoV-2) in outpatients: A multicenter comparison of self-collected saline gargle, oral swab, and combined oral-anterior nasal swab to a provider collected nasopharyngeal swab. *Infect. Control Hosp. Epidemiol.* **2021**, 42, 1340–1344.

Kantor, R.S.; Nelson, K.L.; Greenwald, H.D.; Kennedy, L.C. Challenges in measuring the recovery of SARS-CoV-2 from wastewater. *Environ. Sci. Technol.* **2021**, 55, 3514–3519.

Karthikeyan, S.; Levy, J.I.; De Hoff, P.; Humphrey, G.; Birmingham, A.; et al. Wastewater sequencing reveals early cryptic SARS-CoV-2 variant transmission. *Nature* **2022**, 609 (7925), 101-108.

Kazama, S.; Miura, T.; Masago, Y.; Konta, Y.; Tohma, K.; Manaka, T.; et al. Environmental surveillance of Norovirus genogroups I and II for sensitive detection of epidemic variants. *Appl. Environ. Microbiol.* **2017**, 83, e03406-16.

Keshaviah, A.; Diamond, M.B.; Wade, M.J.; Scarpino, S.V.; Ahmed, W.; Amman, F.; et al. Wastewater monitoring can anchor global disease surveillance systems. *Lancet Glob. Health* **2023**, *11*, e976-81.

Kevadiya, B.D.; Machhi, J.; Herskovitz, J.; Oleynikov, M.D.; Blomberg, W.R.; Bajwa, N.; et al. Diagnostics for SARS-CoV-2 infections. *Nat. Mater.* **2021**, *20* (5), 593-605.

Kellner, M.J.; Ross, J.J.; Schnabl, J.; Dekens, M.P.; Heinen, R.; Grishkovskaya, I.; et al. A rapid, highly sensitive and open-access SARS-CoV-2 detection assay for laboratory and home testing. *Front. Mol. Biosci.* **2022**, *9*, 801309.

Khan, A.; Zia, T.; Suleman, M.; Khan, T.; Ali, S.S.; Abbasi, A.A.; Mohammad, A.; Wei, D.Q. Higher infectivity of the SARS-CoV-2 new variants is associated with K417N/T, E484K, and N501Y mutants: an insight from structural data. *J. Cell. Physiol.* **2021**, *236* (10), 7045-7057.

Khiabani, K.; Amirzade-Iranaq, M.H. Are saliva and deep throat sputum as reliable as common respiratory specimens for SARS-CoV-2 detection? A systematic review and meta-analysis. *Am. J. Infect. Control.* **2021**, *49* (9), 1165-1176.

Khurshid, Z.; Zohaib, S.; Najeeb, S.; Zafar, M.; Slowey, P.; Almas, K. Human saliva collection devices for proteomics: an update. *Int. J. Mol. Sci.* **2016**, *17*, 846.

Kitamura, K.; Sadamasu, K.; Muramatsu, M.; Yoshida, H. Efficient detection of SARS-CoV-2 RNA in the solid fraction of wastewater. *Sci. Total Environ.* **2021**, *763*, 144587.

Kocamemi, B.A.; Kurt, H.; Hacıoglu, S.; Yarali, C.; Saatci, A.M.; Pakdemirli, B. First Data-Set on SARS-CoV-2 Detection for Istanbul Wastewaters in Turkey. *MedRxiv.* **2020**. Available from: <https://doi.org/10.1101/2020.05.03.20089417> (accessed 2022-08-10).

Kohmer, N.; Eckermann, L.; Böddinghaus, B.; Götsch, U.; Berger, A.; Herrmann, E.; et al. Self-collected samples to detect SARS-CoV-2: direct comparison of Saliva, Tongue Swab, Nasal Swab, chewed cotton pads and gargle lavage. *J. Clin. Med.* **2021**, *10* (24), 5751.

Kojima, N.; Turner, F.; Slepnev, V.; Bacelar, A.; Deming, L.; Kodeboyina, S.; Klausner, J. D. Self-collected oral fluid and nasal swabs demonstrate comparable sensitivity to clinician collected nasopharyngeal swabs for coronavirus disease 2019 detection. *Clin. Infect. Dis.* **2021**, *73*, e3106– e3109.

Kralik, P.; Ricchi, M. A basic guide to real time PCR in microbial diagnostics: definitions, parameters, and everything. *Front. Microbiol.* **2017**, *8*,108.

Ku, C.W.; Shivani, D.; Kwan, J.Q.; Loy, S.L.; Erwin, C.; Ko, K.K.; et al. Validation of self-collected buccal swab and saliva as a diagnostic tool for COVID-19. *Int. J. Infect. Dis.* **2021**, *104*, 255-261.

Kucirka, L.M.; Lauer, S.A.; Laeyendecker, O.; Boon, D.; Lessler, J. Variation in false-negative rate of reverse transcriptase polymerase chain reaction–based SARS-CoV-2 tests by time since exposure. *Ann. Intern. Med.* **2020**, *173*, 262– 267.

Kumar, M.; Patel, A.K.; Shah, A.V.; Raval, J.; Rajpara, N.; Joshi, M.; Joshi, CG. First proof of the capability of wastewater surveillance for COVID-19 in India through detection of genetic material of SARS-CoV-2. *Sci. Total Environ.* **2020**, *746*, 141326.

Kumblathan, T.; Liu, Y.; Uppal, G.K.; Hrudey, S.E.; Li, X.F. Wastewater-based epidemiology for community monitoring of SARS-CoV-2: Progress and Challenges. *ACS Environ. Au* **2021**, *1*, 18–31.

Kumblathan, T.; Piroddi, N.; Hrudehy, S.E.; Li, X.F. Wastewater based surveillance of SARS-CoV-2: challenges and perspective from a Canadian inter-laboratory study. *J. Environ. Sci.* **2022**, 116, 229–232.

Kumblathan, T.; Liu, Y.; Qiu, Y.; Pang, L.; Hrudehy, S.E.; Le, X.C.; Li, X.F. An efficient method to enhance recovery and detection of SARS-CoV-2 RNA in wastewater. *J. Environ. Sci.* **2023a**, 130, 139-148.

Kumblathan, T.; Liu, Y.; Pang, X.L.; Hrudehy, S.E.; Le, X.C.; Li, X.F. Quantification and Differentiation of SARS-CoV-2 Variants in Wastewater for Surveillance. *ACS Environ. Health* **2023b**, 1, 203-213.

Kumblathan, T.; Liu, Y.; Crisol, M.; Pang, X.L.; Hrudehy, S.E.; Le, X.C.; Li, X.F. Advances in Wastewater Analysis Revealing the Co-Circulating Viral Trends of Noroviruses and Omicron Subvariants. *Sci. Total Environ.* **2024**, 920, 170887.

Lalli, M.A.; Langmade, J.S.; Chen, X.; Fronick, C.C.; Sawyer, C.S.; Burcea, L.C.; et al. Rapid and extraction-free detection of SARS-CoV-2 from saliva by colorimetric reverse-transcription loop-mediated isothermal amplification. *Clin. Chem.* **2021**, 67 (2), 415-424.

Landry, M.L.; Criscuolo, J.; Peaper, D.R. Challenges in use of saliva for detection of SARS CoV-2 RNA in symptomatic outpatients. *J. Clin. Virol.* **2020**, 130, 104567.

La Rosa, G.; Iaconelli, M.; Mancini, P.; Bonanno Ferraro, G.; Veneri, C.; Bonadonna, L.; et al. First detection of SARS-CoV-2 in untreated wastewaters in Italy. *Sci. Total Environ.* **2020**, 736, 139652.

La Rosa, G.; Mancini, P.; Bonanno, F.G.; Veneri, C.; Iaconelli, M.; Bonadonna, L.; et al. SARS-CoV-2 has been circulating in northern Italy since December 2019: evidence from environmental monitoring. *Sci. Total Environ.* **2021**, 750, 141711.

LaTurner, Z.W.; Zong, D.M.; Kalvapalle, P.; Gamas, K.R.; Terwilliger, A.; Crosby, T.; et al. Evaluating recovery, cost, and throughput of different concentration methods for SARS-CoV-2 wastewater-based epidemiology. *Water Res.* **2021**, *197*, 117043.

Lazear, H.M.; Nice, T.J.; Diamond, M.S. Interferon- λ : immune functions at barrier surfaces and beyond. *Immunity* **2015**, *43*, 15-28.

Le, C. Sensitivity of wastewater surveillance: What is the minimum COVID-19 cases required in population for SARS-CoV-2 RNA to be detected in wastewater? *J. Environ. Sci.* **2023**, *125*, 851–853.

Leblanc, D.; Inglis, G.D.; Boras, V.F.; Brassard, J.; Houde, A. The prevalence of enteric RNA viruses in stools from diarrheic and non-diarrheic people in southwestern Alberta, Canada. *Arch. Virol.* **2017**, *162*, 117-128.

Lee, R.A.; Herigon, J.C.; Benedetti, A.; Pollock, N.R.; Denkinger, C.M. Performance of saliva, oropharyngeal swabs, and nasal swabs for SARS-CoV-2 molecular detection: A systematic review and meta-analysis. *J. Clin. Microbiol.* **2021**, *59*, e02881.

Lemire, K.A.; Rodriguez, Y.Y.; McIntosh, M.T. Alkaline hydrolysis to remove potentially infectious viral RNA contaminants from DNA. *Virol. J.* **2016**, *13*, 1-12.

Lequin, R. M. Enzyme immunoassay (EIA)/Enzyme-linked immunosorbent assay (ELISA). *Clin. Chem.* **2005**, *51*, 2415–2418.

Lever, M.A.; Torti, A.; Eickenbusch, P.; Michaud, A.B.; SantlTemkiv, T.; Jorgensen, B.B. A modular method for the extraction of DNA and RNA, and the separation of DNA pools from diverse environmental sample types. *Front. Microbiol.* **2015**, *6*, 476.

Levy, J.I.; Andersen, K.G.; Knight, R.; Karthikeyan, S. Wastewater surveillance for public health. *Science* **2023**, *379* (6627), 26-27.

Li, J.; Shimko, K.M.; He, C.; Patterson, B.; Bade, R.; Shiels, R.; Mueller, J.F.; et al. Direct injection liquid chromatography-tandem mass spectrometry as a sensitive and high-throughput method for the quantitative surveillance of antimicrobials in wastewater. *Sci. Total Environ.* **2023**, 900, 165825.

Li, Q.; Guan, X.; Wu, P.; Wang, X.; Zhou, L.; Tong, Y.; et al. Early transmission dynamics in Wuhan, China, of novel coronavirus–infected pneumonia. *N. Engl. J. Med.* **2020**, 382 (13), 1199-1207.

Li, Q.; Lee, B.E.; Gao, T.; Qiu, Y.; Ellehoj, E.; Yu, J.; et al. Number of COVID-19 cases required in a population to detect SARS-CoV-2 RNA in wastewater in the province of Alberta, Canada: Sensitivity assessment. *J. Environ. Sci.* **2023**, 125, 843–850.

Li, Z.; Bruce, J.L.; Cohen, B.; Cunningham, C.V.; Jack, W.E.; Kunin, K.; et al. Development and implementation of a simple and rapid extraction-free saliva SARS-CoV-2 RT-LAMP workflow for workplace surveillance. *PLoS One.* **2022**, 17 (5), 0268692.

Lippi, G.; Simundic, A.M. The EFLM strategy for harmonization of the preanalytical phase. *Clin. Chem. Lab. Med.* **2018**, 56, 1660–1666.

Liu, Y.; Liu, J.; Johnson, B.A.; Xia, H.; Ku, Z.; Schindewolf, C.; et al. Delta spike P681R mutation enhances SARS-CoV-2 fitness over Alpha variant. *Cell Rep.* **2022**, 39 (7), 110829.

Liu, Y.; Kumblathan, T.; Feng, W.; Pang, B.; Tao, J.; Xu, J.; et al. On-site viral inactivation and RNA preservation of gargle and saliva samples combined with direct analysis of SARS-CoV-2 RNA on magnetic beads. *ACS Meas. Sci. Au* **2022**, 2, 224–232.

Liu, Y.; Kumblathan, T.; Tao, J.; Xu, J.; Feng, W.; Xiao, H.; et al. Recent advances in RNA sample preparation techniques for the detection of SARS-CoV-2 in saliva and gargle. *Trends Anal. Chem.* **2023**, 165, 117107.

Liu, Y.; Kumblathan, T.; Joyce, M.A.; Tyrrell, D.L.; Tipples, G.; Pang, X.; Li, X.F.; Le, X.C. Multiplex Assays Enable Simultaneous Detection and Identification of SARS-CoV-2 Variants of Concern in Clinical and Wastewater Samples. *ACS Meas. Sci. Au*, **2023**, 3, 258–268.

Loeffelholz, M.J.; Tang, Y.W. Laboratory diagnosis of emerging human coronavirus infections - the state of the art. *Emerging Microbes Infect.* **2020**, 9 (1), 747– 756.

Lopes, J.I.; da Costa Silva, C.A.; Cunha R.G.; Soares, A.M.; Lopes, M.E.; da Conceição Neto, O.C.; et al. A large cohort study of SARS-CoV-2 detection in saliva: A non-invasive alternative diagnostic test for patients with bleeding disorders. *Viruses* **2021**, 13 (12), 2361.

Lopman, B.A.; Steele, D.; Kirkwood, C.D.; Parashar, U.D. The vast and varied global burden of norovirus: prospects for prevention and control. *PLoS Med.* **2016**, 13, e1001999.

Lu, D.; Huang, Z.; Luo, J.; Zhang, X.; Sha, S. Primary concentration: The critical step in implementing the wastewater based epidemiology for the COVID-19 pandemic: A mini-review. *Sci. Total Environ.* **2020**, 747, 141245.

Lu, R.; Zhao, X.; Li, J.; Niu, P.; Yang, B.; Wu, H.; et al. Genomic characterization and epidemiology of 2019 novel coronavirus: implications for virus origins and receptor binding. *Lancet* **2020**, 395 (10224), 565-574.

MacCannell, T.; Umscheid, C.A.; Agarwal, R.K.; Lee, I.; Kuntz, G.; Stevenson, K.B. Healthcare Infection Control Practices Advisory Committee (HICPAC). Guideline for the prevention and control of Norovirus gastroenteritis outbreaks in healthcare settings. *Infect. Control Hosp. Epidemiol.* **2011**, 32, 939–969.

Majumdar, S.; Sarkar, R. Mutational and phylogenetic analyses of the two lineages of the Omicron variant. *J. Med. Virol.* **2022**, 94 (5), 1777-1779.

Mak, G.C.; Cheng, P.K.; Lau, S.S.; Wong, K.K.; Lau, C.S.; Lam, E.T.; et al. Evaluation of rapid antigen test for detection of SARS-CoV-2 virus. *J. Clin. Virol.* **2020**, *129*, 104500.

Mao, K.; Zhang, K.; Du, W.; Ali, W.; Feng, X.; Zhang, H. The potential of wastewater-based epidemiology as surveillance and early warning of infectious disease outbreaks. *Curr. Opin. Environ. Sci. Health* **2020**, *17*, 1–7.

Mao, R.; Qiu, Y.; He, J.S.; Tan, J.Y.; Li, X.H.; Liang, J.; et al. Manifestations and prognosis of gastrointestinal and liver involvement in patients with COVID-19: a systematic review and meta-analysis. *Lancet Gastroenterol. Hepatol.* **2020**, *5* (7), 667-678.

Marin, M.A.L.; Zdenkova, K.; Bartackova, J.; Cermakova, E.; Dostalkova, A.; Demnerova, K.; et al. Monitoring COVID-19 spread in selected Prague's schools based on the presence of SARS-CoV-2 RNA in wastewater. *Sci. Total Environ.* **2023**, *871*, 161935.

Martin, J.; Klapsa, D.; Wilton, T.; Zambon, M.; Bentley, E.; Bujaki, E.; et al. Tracking SARS-CoV-2 in sewage: evidence of changes in virus variant predominance during COVID-19 pandemic. *Viruses* **2020**, *12* (10), E1144.

Markt, R.; Stillebacher, F.; Nägele, F.; Kammerer, A.; Peer, N.; Payr, M.; et al. Expanding the pathogen panel in wastewater epidemiology to Influenza and Norovirus. *Viruses* **2023**, *15*, 263.

Medema, G.; Heijnen, L.; Elsinga, G.; Italiaander, R.; Brouwer A. Presence of SARS-Coronavirus-2 in sewage. *Environ. Sci. & Technol. Lett.* **2020**, *7* (7), 511-516.

Meng, B.; Kemp, S.A.; Papa, G.; Datir, R.; Ferreira, I.A.; Marelli, S.; et al. Recurrent emergence of SARS-CoV-2 spike deletion H69/V70 and its role in the Alpha variant B. 1.1. 7. *Cell Rep.* **2021**, *35* (13), 109292.

Metzger, C.M.; Lienhard, R.; Seth-Smith, H.M.; Roloff, T.; Wegner, F.; Sieber, J.; et al. PCR performance in the SARS-CoV-2 Omicron variant of concern. *Swiss Med. Wkly.* **2021**, 49 (151), w30120.

Michael-Kordatou, I.; Karaolia, P.; Fatta-Kassinos, D. Sewage analysis as a tool for the COVID-19 pandemic response and management: the urgent need for optimized protocols for SARS-CoV-2 detection and quantification. *J. Environ. Chem. Eng.* **2020**, 8 (5), 104306.

Minchin, S.; Lodge, J. Understanding biochemistry: structure and function of nucleic acids. *Essays Biochem.* **2019**, 63 (4), 433-456.

Mlejnkova, H.; Sovova, K.; Vasickova, P.; Ocenaskova, V.; Jasikova, L.; Juranova, E. Preliminary study of Sars-Cov-2 occurrence in wastewater in the Czech Republic. *Int. J. Environ. Res. Public Health.* **2020**, 17, 5508.

Mohammadi, A.; Esmailzadeh, E.; Li, Y.; Bosch, R.J.; Li, J.Z. SARS-CoV-2 detection in different respiratory sites: A systematic review and meta-analysis. *EBioMedicine* **2020**, 59, 102903.

Moreno-Contreras, J.; Espinoza, M.A.; Sandoval-Jaime, C.; Cantú-Cuevas, M.A.; Barón-Olivares, H.; Ortiz-Orozco, O.D.; et al. Saliva sampling and its direct lysis, an excellent option to increase the number of SARS-CoV-2 diagnostic tests in settings with supply shortages. *J. Clin. Microbiol.* **2020**, 58, e01659.

Mukhra, R.; Krishan, K.; Kanchan, T. Possible modes of transmission of Novel coronavirus SARS-CoV-2: a review. *Acta Biomed.* **2020**, 91 (3), e2020036.

Mullis, K.; Faloona, F.; Saiki, R.; Horn, G.; Erlich, H.; Scharf, S. Specific enzymatic amplification of DNA in vitro: The polymerase chain reaction. *Symp. Quant. Boil.* **1986**, 51, 263–273.

Murakami, M.; Hata, A.; Honda, R.; Watanabe, T. Wastewater-based epidemiology can overcome representativeness and stigma issues related to COVID-19. *Environ. Sci. Technol.* **2020**, 54 (9), 5311.

Myers, T.W.; Gelfand, D.H. Reverse transcription and DNA amplification by a *Thermus thermophilus* DNA polymerase. *Biochemistry.* **1991**, 30, 7661–7666.

National Academies of Sciences, Engineering, and Medicine. *Applying Lessons Learned from COVID-19 Research and Development to Future Epidemics: Proceedings of a Workshop.* **2023**, Available from: <https://doi.org/10.17226/27194> (accessed 2024-01-08).

NCCID (National Collaborating Centre for Infectious Disease). *Public Health Agency of Canada Wastewater surveillance program for COVID-19*, **2022**. Available from: <https://nccid.ca/wastewater-surveillance-for-covid-19/> (accessed 2022-08-10).

Nemudryi, A.; Nemudraia, A.; Wiegand, T.; Surya, K.; Buyukyoruk, M.; Cicha, C.; et al. Temporal detection and phylogenetic assessment of SARS-CoV-2 in municipal wastewater. *Cell Rep. Med.* **2020**, 1 (6), 100098.

Nordgren, J.; Matussek, A.; Mattsson, A.; Svensson, L.; Lindgren, P.E. Prevalence of norovirus and factors influencing virus concentrations during one year in a full-scale wastewater treatment plant. *Water Res.* **2009**, 43, 1117–1125.

Ott, I.M.; Strine, M.S.; Watkins, A.E.; Boot, M.; Kalinich, C.C.; Harden, C.A.; et al. Stability of SARS-CoV-2 RNA in non-supplemented saliva. *Emerging Infect. Dis.* **2021**, 27, 1146– 1150.

Pan, Y.; Long, L.; Zhang, D.; Yuan, T.; Cui, S.; Yang, P.; Wang, Q.; Ren, S. Potential false-negative nucleic acid testing results for severe acute respiratory syndrome coronavirus 2 from thermal inactivation of samples with low viral loads. *Clin. Chem.* **2020**, 66 (6), 794– 801.

Pang, X.L.; Preiksaitis, J.K.; Lee, B. Multiplex real time RT-PCR for the detection and quantitation of norovirus genogroups I and II in patients with acute gastroenteritis. *J. Clin. Virol.* **2005**, 33, 168–171.

Pang, X.L.; Preiksaitis, J.K.; Wong, S.; Li, V.; Lee, B.E. Influence of novel norovirus GII. 4 variants on gastroenteritis outbreak dynamics in Alberta and the Northern Territories, Canada between 2000 and 2008. *PloS One* **2010**, 5, e11599.

Pastorino, B.; Touret, F.; Gilles, M.; Luciani, L.; de Lamballerie, X.; Charrel, R.N. Evaluation of chemical protocols for inactivating SARS-CoV-2 infectious samples. *Viruses* **2020**, 12, 624.

Patterson, E.I.; Prince, T.; Anderson, E.R.; Casas-Sanchez, A.; Smith, S.L.; Cansado-Utrilla, C.; et al. Methods of inactivation of SARS-CoV-2 for downstream biological assays. *J. Infect. Dis.* **2020**, 222, 1462– 1467.

Payne S. Introduction to RNA viruses. *Viruses* **2017**, 97–105.

Peccia, J.; Zulli, A.; Brackney, D.E.; Grubaugh, N.D.; Kaplan, E. H.; Casanovas-Massana, A.; et al. Measurement of SARS-CoV-2 RNA in wastewater tracks community infection dynamics. *Nat. Biotechnol.* **2020**, 38 (10), 1164–1167.

Pecson, B.M.; Darby, E.; Haas, C.N.; Amha, Y.M.; Bartolo, M.; Danielson, R.; et al. Reproducibility and sensitivity of 36 methods to quantify the SARS-CoV-2 genetic signal in raw wastewater: findings from an interlaboratory methods evaluation in the U.S. *Environ. Sci.: Water Res. Technol.* **2021**, 7, 504–520.

Peiris, J.S.; Lai, S.T.; Poon, L.L.; Guan, Y.; Yam, L.Y.; Lim, W.; et al. Coronavirus as a possible cause of severe acute respiratory syndrome. *Lancet* **2003**, 361 (9366), 1319-1325.

Pellett, P.E.; Mitra, S.; Holland, T.C. Basics of virology. *Handb. Clin. Neurol.* **2014**, 123, 45-66.

Pérez-Cataluña, A.; Cuevas-Ferrando, E.; Randazzo, W.; Falcó, I.; Allende, A.; Sánchez, G. Comparing analytical methods to detect SARS-CoV-2 in wastewater. *Sci. Total Environ.* **2021**, 758, 143870.

Pijuan-Galito, S.; Tarantini, F.S.; Tomlin, H.; Jenkins, H.; Thompson, J.L.; Scales, D.; et al. Saliva for COVID-19 testing: Simple but useless or an undervalued resource? *Front. Virol.* **2021**, 1, 29.

Pires, S.M.; Fischer-Walker, C.L.; Lanata, C.F.; Devleeschauwer, B.; Hall, A.J.; Kirk, M.D.; et al. Aetiology-specific estimates of the global and regional incidence and mortality of diarrhoeal diseases commonly transmitted through food. *PloS One* **2015**, 10, e0142927.

Piret, J. and Boivin, G. Viral interference between respiratory viruses. *Emerg. Infect. Dis.* **2022**, 28, 273-281.

Plante, J.A.; Liu, Y.; Liu, J.; Xia, H.; Johnson, B.A.; Lokugamage, K.G.; et al. Spike mutation D614D alters SARS-CoV-2 fitness. *Nature* **2021**, 592 (7852), 116-121.

Polo, D.; Quintela-Baluja, M.; Corbishley, A.; Jones, D.L.; Singer, A.C.; Graham, D.W.; Romalde, J.L. Making waves: Wastewater-based epidemiology for COVID-19—approaches and challenges for surveillance and prediction. *Water Res.* **2020**, 186, 116404.

Poukka, E.; Mäkelä, H.; Hagberg, L.; Vo, T.; Nohynek, H.; Ikonen, N.; Liitsola, K.; et al. Detection of SARS-CoV-2 infection in gargle, spit, and sputum specimens. *Microbiol. Spectr.* **2021**, 9 (1), e00035-21.

Prado, T.; Fumian, T.M.; Mannarino, C.F.; Maranhão, A.G.; Siqueira, M.M.; Miagostovich, M.P. Preliminary results of SARS-CoV-2 detection in sewerage system in Niterói municipality, Rio de Janeiro, Brazil. *Mem. Inst. Oswaldo Cruz.* **2020**, 115, e200196.

Prasad, B.V.; Schmid, M.F. Principles of virus structural organization. *Adv. Exp. Med. Biol.* **2012**, 724, 17-47.

Public Health Agency of Canada. *COVID-19 epidemiology update: Testing and variants*, **2022**. Available from: <https://health-infobase.canada.ca/covid-19/testing-variants.html#VOC> (accessed on 2022-01-25).

Qiu, Y.; Li, Q.; Lee, B.E.; Ruecker, N.J.; Neumann, N.F.; Ashbolt, N.J.; Pang, X. UV inactivation of human infectious viruses at two full-scale wastewater treatment plants in Canada. *Water Res.* **2018**, 147, 73-81.

Qiu, Y.; Yu, J.; Pabbaraju, K.; Lee, B.E.; Gao, T.; Ashbolt, N.J.; et al. Validating and optimizing the method for molecular detection and quantification of SARS-CoV-2 in wastewater. *Sci. Total Environ.* **2022**, 812, 151434.

Rahimi, F. and Abadi, A.T.B. Implications of the SARS-CoV-2 subvariants BA. 4 and BA. 5. *Int. J. Surg.* **2022**, 104, p.106806.

Rajh, E.; Šket, T.; Praznik, A.; Sušjan, P.; Šmid, A.; Urbančič, D.; et al. Robust saliva-based RNA extraction-free one-step nucleic acid amplification test for mass SARS-CoV-2 monitoring. *Molecules.* **2021**, 26 (21), 6617.

Rambaut, A.; Holmes, E.C.; O'Toole, Á.; Hill, V.; McCrone, J.T.; Ruis, C.; du Plessis, L.; Pybus, O.G. A dynamic nomenclature proposal for SARS-CoV-2 lineages to assist genomic epidemiology. *Nat. Microbiol.* **2020**, 5 (11), 1403-1407.

Ramón-Núñez, L.A.; Martos, L.; Fernández-Pardo, Á.; Oto, J.; Medina, P.; España, F.; Navarro, S. Comparison of protocols and RNA carriers for plasma miRNA isolation. Unraveling RNA carrier influence on miRNA isolation. *PLoS One* **2017**, *12*, e0187005.

Randazzo, W.; Truchado, P.; Cuevas-Ferrando, E.; Simón, P.; Allende, A.; Sánchez, G. SARS-CoV-2 RNA in wastewater anticipated COVID-19 occurrence in a low prevalence area. *Water Res.* **2020a**, *181*, 115942.

Randazzo, W.; Cuevas-Ferrando, E.; Sanjuán, R.; Domingo-Calap, P.; Sánchez G. Metropolitan wastewater analysis for COVID-19 epidemiological surveillance. *Int. J. Hyg. Environ. Health.* **2020b**, *230*, 113621.

Ranoa, D.; Holland, R.; Alnaji, F.G.; Green, K.; Wang, L.; Brooke, C.; et al. Saliva-based molecular testing for SARS-CoV-2 that bypasses RNA extraction. *Biorxiv* **2020**. Available from: <https://doi.org/10.1101/2020.06.18.159434> (accessed 2021-12-10).

Rao, M.; Rashid, F.A.; Sabri, F.S.; Jamil, N.N.; Zain, R.; Hashim, R.; et al. Comparing nasopharyngeal swab and early morning saliva for the identification of severe acute respiratory syndrome coronavirus 2 (SARS-CoV-2). *Clin. Infect. Dis.* **2021**, *72* (9), 352-356.

Richardson, S.; Hirsch, J.S.; Narasimhan, M.; Crawford, J.M.; McGinn, T.; Davidson, K.W.; et al. Presenting characteristics, comorbidities, and outcomes among 5700 patients hospitalized with COVID-19 in the New York City area. *J. Am. Med. Assoc.* **2020**, *323* (20), 2052-2059.

Rimoldi, S.G.; Stefani, F.; Gigantiello, A.; Polesello, S.; Comandatore, F.; Mileto, D.; et al. Presence and infectivity of SARS-CoV-2 virus in wastewaters and rivers. *Sci. Total Environ.* **2020**, *744*, 140911.

Roldan-Hernandez, L.; Graham, K.; Duong, D.; Boehm, A. Persistence of endogenous SARS-CoV-2 and pepper mild mottle virus RNA in wastewater settled solids. *ACS ES&T Water* **2022**, 2 (11), 1944-1952.

Saah, A.J. and Hoover, D.R. "Sensitivity" and "specificity" reconsidered: the meaning of these terms in analytical and diagnostic settings. *Ann Intern Med.* **1997**, 126 (1), 91-94.

Safiabadi Tali, S.H.; LeBlanc, J.J.; Sadiq, Z.; Oyewunmi, O.D.; Camargo, C.; Nikpour, B.; et al. Tools and techniques for severe acute respiratory syndrome coronavirus 2 (SARS-CoV-2)/COVID-19 detection. *Clin. Microbiol. Rev.* **2021**, 34 (3).

Saguti, F.; Magnil, E.; Enache, L.; Churqui, M.P.; Johansson, A.; Lumley, D.; et al. Surveillance of wastewater revealed peaks of SARS-CoV-2 preceding those of hospitalized patients with COVID-19. *Water Res.* **2021**, 189, 116620.

Sambaza, S.S.; Naicker N. Contribution of wastewater to Antimicrobial Resistance-A Review article. *J. Glob. Antimicrob. Resist.* **2023**, 34, 23-29.

Schenk, H.; Heidinger, P.; Insam, H.; Kreuzinger, N.; Markt, R.; Nägele, F.; et al. Prediction of hospitalisations based on wastewater-based SARS-CoV-2 epidemiology. *Sci. Total Environ.* **2023**, 873, 162149.

Schoeber, J.P.; Schlaghecke, J.M.; Meuwissen, B.M.; van Heertum, M.; van den Brule, A.J.; Loonen, A.J. Comprehensive analytical and clinical evaluation of a RNA extraction-free saliva-based molecular assay for SARS-CoV-2. *Plos One.* **2022**, 17 (5), e0268082.

Schrader, C.; Schielke, A.; Ellerbroek, L.; Johne, R. PCR inhibitors—occurrence, properties and removal. *J. Appl. Microbiol.* **2012**, 113 (5), 1014-1026.

Schulte, P.A.; Weissman, D.N.; Luckhaupt, S.E.; de Perio, M.A.; Piacentino, J.D.; Radonovich, L.J.; et al. Considerations for pooled testing of employees for SARS-CoV-2. *J. Occup. Environ. Med.* **2021**, *63*, 1–9.

Sharif, S.; Ikram, A.; Khurshid, A.; Salman, M.; Mehmood, N.; Arshad, Y.; et al. Detection of SARS-Coronavirus-2 in wastewater, using the existing environmental surveillance network: an epidemiological gateway to an early warning for COVID-19 in communities. *PLoS ONE* **2021**, *16* (6), e0249568.

Shehadul Islam, M.; Aryasomayajula, A.; Selvaganapathy, P.R. A review on macroscale and microscale cell lysis methods. *Micromachines (Basel)*. **2017**, *8* (3), 83.

Sherchan S.P.; Shahin, S.; Ward, L.M.; Tandukar, S.; Aw, T.G.; Schmitz, B.; Ahmed, W.; Kitajima, M. First detection of SARS-CoV-2 RNA in wastewater in North America: A study in Louisiana, USA. *Sci. Total Environ.* **2020**, *743*, 140621.

Shi, H.; Bressan, R. RNA extraction. *Methods Mol. Biol.* **2006**, *323*, 345-348.

Shi, H.; Pasco, E.V.; Tarabara, V.V. Membrane-based methods of virus concentration from water: A review of process parameters and their effects on virus recovery. *Environ. Sci: Water Res. Technol.* **2017**, *3*, 778–792.

Silverman, J.D.; Hupert, N.; Washburne, A.D. Using influenza surveillance networks to estimate state-specific prevalence of SARS-CoV-2 in the United States. *Sci. Transl. Med.* **2020**, *12*, eabc1126.

Stanhope, B.J.; Peterson, B.; Knight, B.; Decadiz, R.N.; Pan, R.; Davis, P.; et al. Development, testing and validation of a SARS-CoV-2 multiplex panel for detection of the five major variants of concern on a portable PCR platform. *Front. Public Health* **2022**, *10*, 4676.

Stanifer, M.L.; Guo, C.; Doldan, P.; Boulant, S. Importance of type I and III interferons at respiratory and intestinal barrier surfaces. *Front. Immunol.* **2020**, *11*, 608645.

Stockdale, S.R.; Blanchard, A.A.; Nayak, A.; Husain, A.; Nashine, R.; Dudani, H.; et al. RNA-Seq of untreated wastewater to assess COVID-19 and emerging and endemic viruses for public health surveillance. *Lancet Reg. Health Southeast Asia* **2023**, *14*, 100205.

Swift, A.; Heale, R.; Twycross, A. What are sensitivity and specificity? *Evid. Based Nurs.* **2020**, *23*, 2-4.

Svec, D.; Tichopad, A.; Novosadova, V.; Pfaffl, M.W.; Kubista, M. How good is a PCR efficiency estimate: Recommendations for precise and robust qPCR efficiency assessments. *Biomol. Detect. Quantif.* **2015**, *3*, 9-16.

Syed, A.M.; Ciling, A.; Taha, T.Y.; Chen, I.P.; Khalid, M.M.; Sreekumar, B.; et al. Omicron mutations enhance infectivity and reduce antibody neutralization of SARS-CoV-2 virus-like particles. *Proc. Natl. Acad. Sci. U. S. A.* **2022**, *119* (31), p.e2200592119.

Takeuchi, O.; Akira, S. Innate immunity to virus infection. *Immunol. Rev.* **2009**, *227* (1), 75-86.

Tan, S.H.; Allicock, O.; Armstrong-Hough, M.; Wyllie, A.L. Saliva as a gold-standard sample for SARS-CoV-2 detection. *Lancet Respir. Med.* **2021**, *9* (6), 562-564.

Tang, J.W.; Tambyah, P.A.; Hui, D.S. Emergence of a new SARS-CoV-2 variant in the UK. *J. Infect.* **2021**, *82* (4), e27–e28.

Tangwangvivat, R.; Wacharapluesadee, S.; Pinyopornpanish, P.; Petcharat, S.; Hearn, S.M.; Thippamom, N.; et al. SARS-CoV-2 Variants Detection Strategies in Wastewater Samples Collected in the Bangkok Metropolitan Region. *Viruses* **2023**, *15* (4), 876.

Tao, Z.; Wang, Z.; Lin, X.; Wang, S.; Wang, H.; Yoshida, H.; et al. One-year Survey of human enteroviruses from sewage and the factors affecting virus adsorption to the suspended solids. *Sci. Rep.* **2016**, 6, 31474.

Taqman. *TaqMan multiplex PCR optimization user guide*, **2022**. Available from: https://assets.thermofisher.com/TFSAssets/LSG/manuals/taqman_optimization_man.pdf (accessed 2023-08-14).

Tegally, H.; Moir, M.; Everatt, J.; Giovanetti, M.; Scheepers, C.; Wilkinson, E.; et al. Emergence of SARS-CoV-2 omicron lineages BA. 4 and BA. 5 in South Africa. *Nat. Med.* **2022**, 28 (9), 1785-1790.

Teo, A.K.; Choudhury, Y.; Tan, I.B.; Cher, C.Y.; Chew, S.H.; Wan, Z.Y.; et al. Saliva is more sensitive than nasopharyngeal or nasal swabs for diagnosis of asymptomatic and mild COVID-19 infection. *Sci. Rep.* **2021**, 11 (1), 3134.

Therrien, J.D.; Thomson, M.; Sion, E.S.; Lee, I.; Maere, T.; Nicolai, N.; et al. A comprehensive, open-source data model for wastewater-based epidemiology. *Water Sci. Technol.* **2024**, 89 (1), 1-9.

Tilley, P.; Gadkar, V.; Goldfarb, D.M.; Young, V.; Watson, N.; Al-Rawahi, G.N.; et al. Gargle-Direct: Extraction-free detection of SARS-CoV-2 using real-time PCR (RT-qPCR) of saline gargle rinse samples. *MedRxiv* **2021**. Available from: <https://doi.org/10.1101/2020.10.09.20203430> (accessed 2021-12-10).

Trottier, J.; Darques, R.; Mouheb, N.A.; Partiot, E.; Bakhache, W.; Deffieu, M.S.; Gaudin R. Post-lockdown detection of SARS-CoV-2 RNA in the wastewater of Montpellier, France. *One Health* **2020**, 10, 100157.

Tsang, N.N.; So, H.C.; Cowling, B.J.; Leung, G.M.; Ip, D.K. Performance of saline and water gargling for SARS-CoV-2 reverse transcriptase PCR testing: a systematic review and meta-analysis. *Eur. Respir. J.* **2022**, 31 (165), 220014.

Twohig, K.A.; Nyberg, T.; Zaidi, A.; Thelwall, S.; Sinnathamby, M.A.; Aliabadi, S.; et al. Hospital admission and emergency care attendance risk for SARS-CoV-2 delta (B.1.617.2) compared with alpha (B.1.1.7) variants of concern: a cohort study. *Lancet Infect. Dis.* **2022**, 22 (1), 35-42.

Udugama, B.; Kadhiresan, P.; Kozlowski, H.N.; Malekjahani, A.; Osborne, M.; Li, V.Y.; et al. Diagnosing COVID-19: the disease and tools for detection. *ACS Nano.* **2020**, 14 (4), 3822-3835.

Upadhyay, V.; Lucas, A.; Panja, S.; Miyauchi, R.; Mallela, K.M. Receptor binding, immune escape, and protein stability direct the natural selection of SARS-CoV-2 variants. *J. Biol. Chem.* **2021**, 297 (4), 101208.

VIRSeek Murine Norovirus Process Control, Eurofins GeneScan Technologies. *VIRSeek murine norovirus process control real-time RT-PCR*, **2022**. Available from: https://www.goldstandarddiagnostics.com/pub/media/productattachments/files/MNL_VIRSeek_MNV_Proc_Ctrl_real_time_RT_PCR_5728200401_5728200801_V4.pdf (accessed 2023-09-28).

Vo, V.; Tillett, R.L.; Papp, K.; Shen, S.; Gu, R.; Gorzalski, A.; et al. Use of wastewater surveillance for early detection of Alpha and Epsilon SARS-CoV-2 variants of concern and estimation of overall COVID-19 infection burden. *Sci. Total Environ.* **2022**, 835, 155410.

Vogels, C.B.F.; Watkins, A.E.; Harden, C.A.; Brackney, D.E.; Shafer, J.; Wang, J.; et al. SalivaDirect: A simplified and flexible platform to enhance SARS-CoV-2 testing capacity. *Med.* **2021**, *2*, 263–280.

Wang, D.; Hu, B.; Hu, C.; Zhu, F.; Liu, X.; Zhang, J.; et al. Clinical characteristics of 138 hospitalized patients with 2019 novel coronavirus–infected pneumonia in Wuhan, China. *J. Am. Med. Assoc.* **2020**, *323* (11), 1061-1069.

Wang, H.; Neyvaldt, J.; Enache, L.; Sikora, P.; Mattsson, A.; Johansson, A.; et al. Variations among viruses in influent water and effluent water at a wastewater plant over one year as assessed by quantitative PCR and metagenomics. *Appl. Environ. Microbiol.* **2020**, *86*, e02073-20.

Wang, H.; Churqui, M.P.; Tunovic, T.; Enache, L.; Johansson, A.; Lindh, M.; et al. Measures against COVID-19 affected the spread of human enteric viruses in a Swedish community, as found when monitoring wastewater. *Sci. Total Environ.* **2023**, *895*, 165012.

Wang, P.; Casner, R.G.; Nair, M.S.; Wang, M.; Yu, J.; Cerutti, G.; et al. Increased resistance of SARS-CoV-2 variant P. 1 to antibody neutralization. *Cell Host Microbe.* **2021**, *29* (5), 747–751.

Wang, R.; Chen, J.; Wei, G.W. Mechanisms of SARS-CoV-2 evolution revealing vaccine-resistant mutations in Europe and America. *J. Phys. Chem.* **2021**, *12* (49), 11850-11857.

Wang, W.K.; Chen, S.Y.; Liu, I.J.; Chen, Y.C.; Chen, H.L.; Yang, C.F.; et al. Detection of SARS-associated coronavirus in throat wash and saliva in early diagnosis. *Emerging Infect. Dis.* **2004**, *10*, 1213–1219.

Wang, W.; Xu, Y.; Gao, R.; Lu, R.; Han, K.; Wu, G.; Tan, W. Detection of SARS-CoV-2 in different types of clinical specimens. *J. Am. Med. Assoc.* **2020**, 323 (18), 1843– 1844.

Wang, Y.; Kang, H.; Liu, X.; Tong, Z.-H. Combination of RT-qPCR testing and clinical features for diagnosis of COVID-19 facilitates management of SARS-CoV-2 outbreak. *J. Med. Virol.* **2020**, 92, 538–539.

Wang, Q.; Guo, Y.; Iketani, S.; Nair, M.S.; Li, Z.; Mohri, H.; et al. Antibody evasion by SARS-CoV-2 Omicron subvariants BA. 2.12. 1, BA. 4 and BA. 5. *Nature* **2022**, 608 (7923), 603-608.

Welch, S.R.; Davies, K.A.; Buczkowski, H.; Hettiarachchi, N.; Green, N.; Arnold, U.; et al. Analysis of inactivation of SARS-CoV-2 by specimen transport media, nucleic acid extraction reagents, detergents, and fixatives. *J. Clin. Microbiol.* **2020**, 58, e01713.

Welling, C.M.; Singleton, D.R.; Haase, S.B.; Browning, C.H.; Stoner, B.R.; Gunsch, C.K.; Grego, S. Predictive values of time-dense SARS-CoV-2 wastewater analysis in university campus buildings. *Sci. Total Environ.* **2022**, 835, 155401.

Westhaus, S.; Weber, F. A.; Schiwy, S.; Linnemann, V.; Brinkmann, M.; Widera, M.; et al. Detection of SARS-CoV-2 in raw and treated wastewater in Germany—suitability for COVID-19 surveillance and potential transmission risks. *Sci. Total Environ.* **2021**, 751, 141750.

Wiersinga, W.J.; Rhodes, A.; Cheng, A.C.; Peacock, S.J.; Prescott, H.C. Pathophysiology, transmission, diagnosis, and treatment of coronavirus disease 2019 (COVID-19): a review. *J. Am. Med. Assoc.* **2020**, 324 (8), 782-793.

Wigginton, K. R.; Boehm, A. B. Environmental engineers and scientists have important roles to play in stemming outbreaks and pandemics caused by enveloped viruses. *Environ. Sci. Technol.* **2020**, 54, 3736–3739.

Wigginton, K. R.; Boehm, A. B. Environmental Engineers and Scientists Have Important Roles to Play in Stemming Outbreaks and Pandemics Caused by Enveloped Viruses. *Environ. Sci. Technol.* **2020**, *54*, 3736–3739.

Wilhelm, A.; Toptan, T.; Pallas, C.; Wolf, T.; Goetsch, U.; Gottschalk, R.; et al. Antibody-mediated neutralization of authentic SARS-CoV-2 B.1.617 variants harboring L452R and T478K/E484Q. *Viruses* **2021**, *13* (9), 1693.

Willeit, P.; Krause, R.; Lamprecht, B.; Berghold, A.; Hanson, B.; Stelzl, E.; et al. Prevalence of RT-qPCR-detected SARS-CoV-2 infection at schools: First results from the Austrian School-SARS-CoV-2 prospective cohort study. *Lancet Reg. Health Eur.* **2021**, *5*, 100086.

Williams, E.; Bond, K.; Zhang, B.; Putland, M.; Williamson, D.A. Saliva as a noninvasive specimen for detection of SARS-CoV-2. *J. Clin. Microbiol.* **2020**, *58* (8), 10-128.

Wolf, S.; Williamson, W.M.; Hewitt, J.; Rivera-Aban, M.; Lin, S.; Ball, A.; et al. Sensitive multiplex real-time reverse transcription-PCR assay for the detection of human and animal Noroviruses in clinical and environmental samples. *Appl. Environ. Microbiol.* **2007**, *73*, 5464–5470.

Wolfe, M.; Hughes, B.; Duong, D.; Chan-Herur, V.; Wigginton, K.R.; White, B.J.; Boehm, A.B. Detection of SARS-CoV-2 variants mu, beta, gamma, lambda, delta, alpha, and omicron in wastewater settled solids using mutation-specific assays is associated with regional detection of variants in clinical samples. *Appl. Environ. Microbiol.* **2022**, *88* (8), e00045-22.

Wölfel, R.; Corman, V. M.; Guggemos, W.; Seilmaier, M.; Zange, S.; Müller, M. A.; et al. Virological assessment of hospitalized patients with COVID-2019. *Nature* **2020**, *581*, 465–469.

World Health Organization. *Coronavirus (COVID-19) Dashboard*, **2023**. Available from: <https://covid19.who.int/> (accessed 2023-09-06).

World Health Organization. *Laboratory Testing for Coronavirus Disease (COVID-19) in Suspected Human Cases: Interim Guidance*. **2020**, Available from: <https://apps.who.int/iris/handle/10665/331501> (accessed 2020-05-08).

World Health Organization (WHO). *Tracking SARS-CoV-2 variants*, **2023**. Available from: <https://www.who.int/en/activities/tracking-SARS-CoV-2-variants> (accessed 2023-06-05).

Wu, F.; Xiao, A.; Zhang, J.; Gu, X.; Lee, W.L.; Kauffman, K.; et al. SARS-CoV-2 titers in wastewater are higher than expected from clinically confirmed cases. *mSystems* **2020**, 5 (4), e00614-20.

Wu, F.; Xiao, A.; Zhang, J.; Moniz, K.; Endo, N.; Armas, F.; et al. SARS-CoV-2 titers in wastewater foreshadow dynamics and clinical presentation of new COVID-19 cases. *Sci. Total Environ.* **2022**, 805, 150121.

Wurtzer, S.; Marechal, V.; Mouchel, J.M.; Maday, Y.; Teyssou, R.; Richard, E.; et al. Evaluation of lockdown effect on SARS-CoV-2 dynamics through viral genome quantification in wastewater, Greater Paris, France, 5 March to 23 April 2020. *Eurosurveillance.* **2020**, 25 (50), 2000776.

Wyllie, A.L.; Fournier, J.; Casanovas-Massana, A.; Campbell, M.; Tokuyama, M.; Vijayakumar, P.; et al. Saliva or nasopharyngeal swab specimens for detection of SARS-CoV-2. *N. Engl. J. Med.* **2020**, 383 (13), 1283-6.

Xiao, F.; Tang, M.; Zheng, X.; Liu, Y.; Li, X.; Shan, H. Evidence for Gastrointestinal Infection of SARS-CoV-2. *Gastroenterology.* **2020**, 158 (6), 1831–1833.

Xiao, H.; Hu, J.; Huang, C.; Feng, W.; Liu, Y.; Kumblathan, T.; et al. CRISPR techniques and potential for the detection and discrimination of SARS-CoV-2 variants of concern. *Trends Anal. Chem.* **2023**, 161, 117000.

Xie, Y.; Challis, J.K.; Oloye, F.F.; Asadi, M.; Cantin, J.; Brinkmann, M.; et al. RNA in municipal wastewater reveals magnitudes of COVID-19 outbreaks across four waves driven by SARS-CoV-2 variants of concern. *ACS ES&T Water* **2022**, 2 (11), 1852-1862.

Xu, X.; Deng, Y.; Ding, J.; Zheng, X.; Li, S.; Liu, L.; et al. Real-time allelic assays of SARS-CoV-2 variants to enhance sewage surveillance. *Water Res.* **2022**, 220, 118686.

Yang, Q.; Meyerson, N.R.; Clark, S.K.; Paige, C.L.; Fattor, W.T.; Gilchrist, A.R.; et al. Saliva Two Step for rapid detection of asymptomatic SARS-CoV-2 carriers. *Elife* **2021**, 10, e65113.

Yao, L.; Zhu, W.; Shi, J.; Xu, T.; Qu, G.; Zhou, W.; et al. Detection of coronavirus in environmental surveillance and risk monitoring for pandemic control. *Chem. Soc. Rev.* **2021**, 50, 3656–3676.

Zafeiriadou, A.; Kaltsis, L.; Kostakis, M.; Kapes, V.; Thomaidis, N.S.; Markou, A. Wastewater surveillance of the most common circulating respiratory viruses in Athens: The impact of COVID-19 on their seasonality. *Sci. Total Environ.* **2023**, 900, 166136.

Zhang, W.; Du, R.H.; Li, B.; Zheng, X. S.; Yang, X.L.; Hu, B.; et al. Molecular and serological investigation of 2019-nCoV infected patients: implication of multiple shedding routes. *Emerg. Microbes Infect.* **2020**, 9 (1), 386–389.

Zhang, Y.Z.; Holmes, E.C. A genomic perspective on the origin and emergence of SARS-CoV-2. *Cell* **202**, 181 (2), 223-227.

Zhang, X.; Wu, S.; Wu, B.; Yang, Q.; Chen, A.; Li, Y.; et al. SARS-CoV-2 Omicron strain exhibits potent capabilities for immune evasion and viral entrance. *Sig. Transduct. Target. Ther.* **2021**, 6 (1), 1-3.

Zhong, M.; Lin, B.; Pathak, J.L.; Gao, H.; Young, A.J.; Wang, X.; et al. ACE2 and furin expressions in oral epithelial cells possibly facilitate COVID-19 infection via respiratory and fecal–oral routes. *Front. Med.* **2020**, 7, 580796.

Zhou, D.; Dejnirattisai, W.; Supasa, P.; Liu, C.; Mentzer, A.J.; Ginn, H.M.; et al. Evidence of escape of SARS-CoV-2 variant B. 1.351 from natural and vaccine-induced sera. *Cell.* **2021**, 184 (9), 2348–2361.

Zhou, P.; Yang, X.L.; Wang, X.G.; Hu, B.; Zhang, L.; Zhang, W.; et al. A pneumonia outbreak associated with a new coronavirus of probable bat origin. *Nature* **2020**, 579 (7798), 270-273.

Zou, L.; Ruan, F.; Huang, M.; Liang, L.; Huang, H.; Hong, Z.; et al. SARS-CoV-2 viral load in upper respiratory specimens of infected patients. *N. Engl. J. Med.* **2020**, 382 (12), 1177– 1179.